DEVELOPMENT OF COMPOSITE STATE CONVERGENCE SCHEMES FOR TELEOPERATION SYSTEMS

by

Muhammad Usman Asad

Submitted in partial fulfillment of the requirements
for the degree of Doctor of Philosophy

at

Dalhousie University
Halifax, Nova Scotia
August 2023

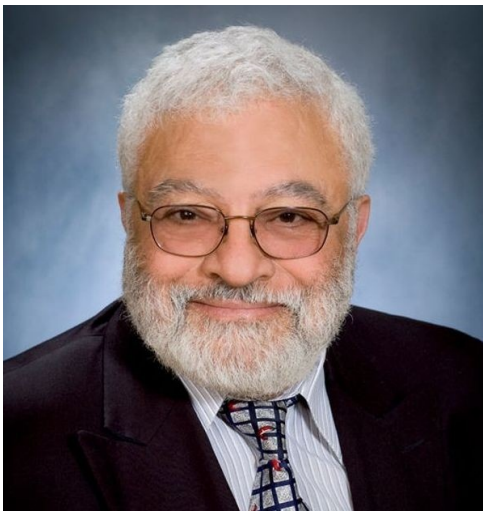

To the loving memories of my former committee member

Dr. Mohamed E. El-Hawary (Fellow IEEE)

Table of Contents

List of Tables

List of Figures

Abstract

A teleoperation system extends the human capability to operate in a remote environment. Humans use this framework to work in hazardous conditions using remotely operated robotic systems. In recent years, teleoperated systems have shown great potential in space, underwater, military, industry, robotic-assisted surgery, and mining applications. In case of manipulation tasks, a teleoperation system is required to be bilateral to execute the task remotely in the presence of time delays. A bilateral teleoperation system is comprised of five elements namely human operator, master robot, communication channel, slave robot, and environment. The control objective in a bilateral teleoperation operation system is defined as the position and force tracking error reduction, which can be achieved using an array of control techniques. This thesis concerns the development of a class of state convergence architectures to develop bilateral control systems. State convergence belongs to a family of model-based control architectures for establishing bilateral communication between the master and slave robots in a teleoperation system. The method provides a systematic procedure to determine the control gains in an elegant way. Originally developed for linear teleoperation systems with small time delays, the method has been extended to nonlinear systems with time-varying delays. However, reliance on the model parameters and a higher number of communication channels remain a limiting factor for the wide adoption of this bilateral control architecture. This thesis addresses these limitations and proposes enhancements in the existing state convergence control architectures to deal with parameter uncertainties and reduce the number of communication channels. The former task is achieved using extended state and nonlinear disturbance observers while the latter objective is accomplished by introducing composite variables. The extension of the proposed bilateral control architectures to the case of multilateral teleoperation systems is also covered. Resultantly, families of robust state convergence control architectures and composite state convergence control architectures are obtained. While constructing the improved control architectures, the elegancy of the state convergence design procedure is retained. To validate the proposed control architectures, simulations, and semi-real-time experiments are conducted in MATLAB/Simulink/QUARC environment using the geomagic haptic device on a single-degree-of-freedom time-delayed teleoperation system. In order to perform semi-real-time experiments, a haptic device is operated along the x-axis to generate a time-varying force for the teleoperation system running inside the computer's Simulink/MATLAB environment. The Simulink model is designed such that the reflected force, as generated by the proposed controller, is also directed to the haptic device and felt by the operator. In this way, the loop is closed around the operator, and the operator can feel the slave's interaction with the environment.

List of Abbreviations

ASP	Adaptive smith predictors
ATS	Asymmetric teleoperation system
CA	Control architecture
CSC	Composite state convergence
C_m	Stabilizing gain for the master
C_s	Stabilizing gain for the slave
D_{m1}, D_{m2}	Fuzzy implemental gains for master
D_{s1}, D_{s2}	Fuzzy implemental gains for slave
DOBs	Disturbance observers
ELA	Extended Lawrence architecture
F_{hk}	Force Exerted by k^{th} operator on k^{th} master system
F_m	Force applied by the human operator to drive the master system
F_m^k	Force exerted by the k^{th} operator
G_2	Influence of the operator's force on the slave system
g_{mk}^1	Environmental force
g_{s1}^k	Influence of the k^{th} operator's force on the slave system
G_{slk}	Effect of k^{th} operator's force in l^{th} slave system
IEAOB	Improved extended active observers
K_{mke}	Stabilizing extended gain for k^{th} master system

K_{sle}	Stabilizing extended gain for l^{th} slave system
k_{m1}	Stabilizing gain for position state of master system
k_{m2}	Stabilizing gain for velocity state of master system
k_{s1}	Stabilizing gain for position state of slave system
k_{s2}	Stabilizing gain for velocity state of slave system
k_m	Feedback gain of the master composite system
k_s	Feedback gain of the slave composite system
k_s^1	Stabilizing gain for the slave system
L_{mke}	Extended state observer's gain for k^{th} master system
L_{ske}	Extended state observer's gain for l^{th} slave system
L_{se}	Slave observer gain
L_{me}	master observer gain
MMT	Model Mediated Teleoperation
MPC	Model predictive control
MM/SS	Multi-master/single-slave
NN	Neural Network
NDOBs	Nonlinear disturbance observers
PEB	Position-error-based architecture
PDC	Parallel distributed compensation
RBFNN	Radial base forward neural network
R_m	Force feedback gain vector

R_s	Effect of master's motion in slave
R_{mkl}	Effect of motion of l^{th} slave system in k^{th} master system
R_{slk}	Effect of motion of k^{th} master system in l^{th} slave system
r_{m1}	Gain carries the slave's position to the master system
r_{m2}	Gain carries the slave's velocity to the master system
r_{s1}	Gain carries the master's position to the slave system
r_{s2}	Gain carries the master's position to the slave system
r_m	Scaler that feeds motion of slave back to the master system
r_s	Scaler that feeds motion of master back to the slave system
r_{s1}^k	Motion of k^{th} master system onto the slave system
r_{mk}^1	Motion of slave system onto k^{th} master system
SC	State convergence
SISO	Single input single output
SMC	Sliding mode control
s_m	Composite variable for master system
s_s	Composite variable for slave system
s_m^k	Composite variable of k^{th} master system
s_s^1	Composite variable of the slave system
TDPC	Time domain passivity control
TS	Takagi-sugeno
T	Time-delay of communication channel

T_{mk}^{1}	Time delay from the slave to the k^{th} master system
T_{s1}^{k}	Time delay from the k^{th} master system to the slave system
WV/S	Wave variable and scattering transformation

Acknowledgements

First, I would like to thank Almighty ALLAH for His countless blessings for completing this dissertation.

Then, I would like to especially thank my research supervisor Dr. Jason Gu for his guidance, suggestions, financial support, and providing an educational experience in the Robotics Lab for Biomedical, Rehabilitation, and Assistive technologies that I could not have found anywhere else. I also want to thank him for his encouragement throughout the course of my Ph.D. I will always feel privileged to be on his Ph.D. students list.

I am grateful to my former supervisory committee member, Dr. Mohamed E. El-Hawary, for his deep insights and suggestions. He taught me Fuzzy Systems as part of my Ph.D. coursework. I am also thankful to my committee members, Dr. Timothy Little and Dr. William Phillips, for their time, support, expertise and feedback on my research.

I would also like to thank our collaborator, Dr. Valentina. Emilia. Balas, Dr. Marius Balas, Dr. Umar Farooq, Dr. Rajeeb Dey, Dr. Athar Hanif, Dr. Ghulam Abbas, Dr. Nabanita Adhikary, Dr. Rupak Datta, and Dr. Irfan.A. Khan for their support.

I also want to thank my lab colleagues, Mr. Xu Zhang (MA.Sc) and Mr. Koceila Cherfouh (MA.Sc), for being so supportive in the Robotics lab.

I also want to thank my departmental administrator, Tamara Cantrill, for providing all the administrative support I need as an international graduate student. I also like to thank Nicole Smith, Ola Hamid, and Liz Joyce for being so supportive and helpful during my stay as an ECE student.

I want to thank Mr. Oliver Zhang from QUANSER for providing me with the required licenses to support my research work. Moreover, I am also thankful to Mr. Peter Jones, P.Eng, for allowing me to work on QUANSER QUBE 2 SERVO and DC motor dial hardware setups in his lab to conduct my experimental work.

I would also like to thank Mr. Tyler Seize and Ms. Emma Gu for helping build the

3D models in Solidworks and PCB designs for the 1-DoF haptic paddle, DC Position control, and DC speed control hardware setups.

A bundle of thanks to Dalhousie University for honoring me with the ECED-FGS publications awards for three consecutive years 2019, 2020, and 2021.

Above all, I am thankful to my family for their support and encouragement all along the way. Lastly, I would also like to thank Canada for granting me an opportunity to study.

Chapter 1

Introduction

Teleoperation Systems attract a significant amount of interest from engineering and healthcare researchers. In the Canadian healthcare system, robot-assisted surgery is becoming popular in recent times and has many benefits for patients and our healthcare system. Nova Scotia's healthcare professionals are able to conduct their first spinal robotic surgery in Canada using Medtronic's MAZOR™ X Stealth Edition. The surgeons are able to perform spinal surgeries through an innovative robotic arm that offers unparalleled accuracy and consistency leading to less pain, less damage to healthy tissues and structures, shorter recovery times, and fewer complications. Moving further, Nova Scotia Health's QEII Health Sciences Centre installed the Mako SmartRobotics system the second surgical robot of its kind in Canada to perform arthroplasty surgeries. Surgeons generate motion commands through an innovative robotic arm to perform hip and knee surgeries and offer unprecedented precision for the placement of a joint implant [120]. There are numerous applications of teleoperation, ranging from repairing nuclear plants, exploring underwater marine environments, space exploration, surgical operations, and monitoring industrial tasks [6], [5], [121], [79], [29], [30], [76], [102], [163], [139]. Some of the teleoperation systems are shown in Figure 1.1.

Bilateral teleoperation systems have become increasingly popular and used in diverse telerobotic applications due to their sense of telepresence. Recently, multilateral teleoperation systems beyond the bilateral one can be used in telerobotic applications where more than one robotic device is involved in performing the task. Instead of using one hand, two hands can help to perform a task using the cooperative manipulation technique. This thesis explores novel control techniques based on state convergence methods to control linear and nonlinear bilateral teleoperation systems and extend to a multilateral teleoperation framework.

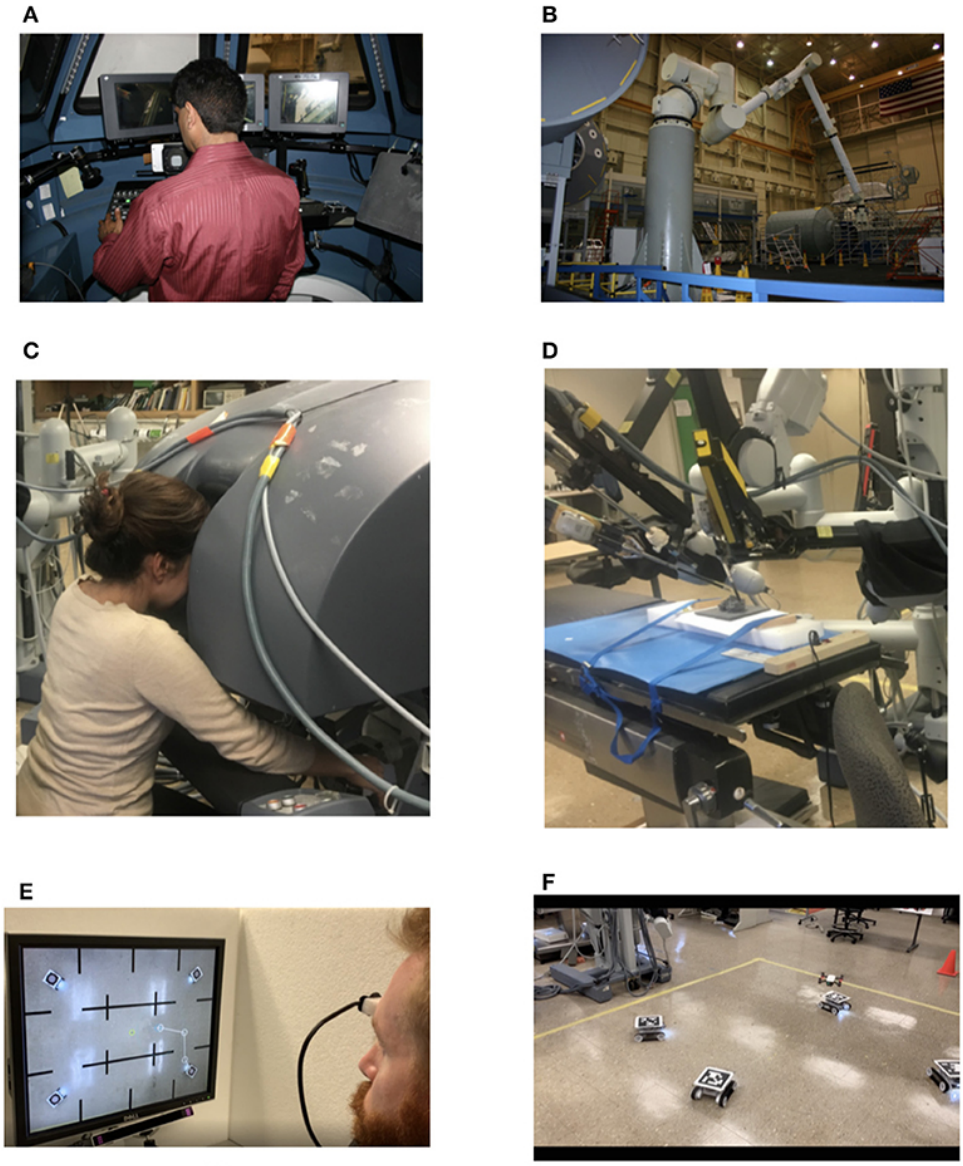

Figure 1.1: Different applications of teleoperation. (A) Operator of a space robot arm, (B) the space robot arm [80]. (C) telesurgery with a research da Vinci surgical system [136], surgeon side. (D) remote patient side, (E) ground robot control with aerial view [116] —operator controls ground robots using eye-tracking and (F) the ground robots [116].

1.1 Thesis Contributions

The contribution of this thesis can be classified into two parts. The first three chapters include improved versions of state convergence architectures for bilateral and multilateral teleoperation systems while the rest of the chapters include reduced complexity versions of state convergence architectures for bilateral and multilateral teleoperation systems. The following contributions are reported in this thesis:

1. Improved version of the bilateral state convergence architecture has been proposed to counter the effect of parametric uncertainties using disturbance observers.

2. Improved version of the bilateral state convergence architecture has been proposed based on TS fuzzy models to counter TS fuzzy model approximation errors and parametric uncertainties using disturbance observers.

3. Improved version of the multilateral state convergence architecture has been proposed to deal with parametric uncertainties using disturbance observers

4. A novel composite state convergence architecture with a reduced number of communication channels has been proposed for bilateral teleoperation.

5. A composite state convergence architecture has been proposed with a feedback linearization scheme for nonlinear bilateral teleoperation.

6. An enhanced version of bilateral composite state convergence architecture has been proposed to counter parametric uncertainties through disturbance observers.

7. Extended the composite state convergence control architecture to multil-master/single slave (MMSS) control architecture.

8. Proposed a composite state convergence controller for teleoperating a multi-degree-of-freedom manipulator.

9. A composite state convergence architecture with a reduced number of communication channels has been proposed for multilateral teleoperation.

10. An enhanced version of multilateral composite state convergence architecture has been proposed to counter the effect of parametric uncertainties through disturbance observers.

1.2 Thesis Outline

The thesis is organized into eleven chapters. The current chapter presents an overview of teleoperation systems and their contributions. The remainder of the thesis is organized as follows:

Chapter 2: Literature Review
This chapter briefly presents various techniques available to control teleoperation systems. The state convergence method and composite state convergence method are presented in detail, as the rest of the thesis is based on this method.

Chapter 3: An Enhanced State Convergence Architecture Incorporating Disturbance Observer for Bilateral Teleoperation Systems

This chapter will address the limitations of the SC method and propose an extended state observer in the existing state convergence architecture. It will compensate for the modeling inaccuracies by treating them as a disturbance and provide estimates of the master and slave states. This study has been published in the International Journal of Advanced Robotic Systems, vol. 16, no. 5, 2019.

Chapter 4 : Disturbance observer-supported fuzzy-model-based controller with application to bilateral teleoperation systems

This chapter presents a nonlinear disturbance observer that has been integrated with a numerator-denominator type TS fuzzy PDC controller to robustify the closed loop regulation performance against the lumped parametric uncertainties and model approximation error. This work has been published in the Journal of Intelligent and Fuzzy Systems, vol. 43, no. 2, pp. 1911-1919, 2022.

Chapter 5: Disturbance Observer-Based Extended State Convergence Architecture for Multilateral Teleoperation Systems

This chapter presents an improved version of extended state convergence architecture through the use of disturbance observers. MATLAB simulations as well as experimental results, prove the validity of the proposed architecture in establishing multilateral communication between k-master and l-slave systems. To the best of the authors' knowledge, robustness improvement of extended state convergence architecture has not been reported in the literature. This work has been published in the International Journal of Robotics and Automation, ACTA PRESS, Canada vol 37, no. 6, pp. 1-10,

2023.

Chapter 6: A Composite State Convergence Scheme for Bilateral Teleoperation Systems

The chapter will discuss a novel composite state convergence scheme that will reduce the complexity of the state convergence algorithm. This chapter is published in IEEE/CAA Journal of Automatica Sinica, vol. 6, no. 5, pp. 1166-1178, September 2019.

Chapter 7: A Composite State Convergence Scheme for a Non-Linear Telerobotic Systems

This chapter is an extension of chapter 6, in which channel simplification of state convergence controller is accomplished, and here we have considered the case of a nonlinear telerobotic system. This chapter is published in Acta Polytechnica Hungarica Vol. 16, no. 10, pp. 157-172, 2019.

Chapter 8: A Composite State Convergence Architecture for Multi-Degrees-of-Freedom System

This chapter is devoted to exploring the applicability of the composite state convergence scheme for a multi-degrees-of-freedom bilateral teleoperation system. To validate the proposed extension, simulations are performed in MATLAB/Simulink environment on two-link manipulators with time delay in the communication channel. This chapter is published in the 7th IFAC International Conference on Advances in Control and Optimization of Dynamical Systems (ACODS 2022), vol. 55, Issue. 1, pp. 126-130, 2022.

Chapter 9 : Disturbance Observer Supported Three-Channel Composite State Convergence Architecture

This chapter will present an improved version of extended state convergence architecture through the use of disturbance observers. To the best of the authors' knowledge, robustness improvement of extended state convergence architecture has not been reported in the literature. This chapter is published in the International Journal of Robotics and Automation (IJRA), ACTA PRESS, Canada, pp 316-324, Issue Jan 2021.

Chapter 10 : A Multi-Master-Single-Slave Composite State Convergence Architecture

This chapter explores the possibility of extending the transparent bilateral state convergence architecture to accommodate multiple systems. In addition, we want to keep the channel complexity at a minimum when multiple systems are communicating. The proposed work is validated through MATLAB simulation by considering a single-degree-of-freedom tri-master-single-slave system. This chapter is published in Communication and Control for Robotic Systems. Smart Innovation, Systems, and Technologies, vol 229, Aug 2021 Springer, Singapore.

Chapter 11 : A Generalized Composite State Convergence Architecture for Multilateral Teleoperation Systems

This chapter aims to generalize the composite state convergence scheme so that l-slave systems can follow the weighted motion of k-master systems. To validate the findings, simulations and semi-real-time experiments are performed in MATLAB/Simulink/QUARC environment by considering different configurations of teleoperation systems. This chapter is published in Studies in Informatics and Control, vol. 30, no. 2, pp. 33-42, 2021.

Chapter 12 : An Improved Composite State Convergence Architecture with Disturbance Compensation for Multilateral Teleoperation Systems

This chapter expands the capability of the composite state convergence scheme to accommodate any number of master and slave systems. It proposes a disturbance observer-based composite state convergence architecture where k-master systems can cooperatively control l-slave systems in the presence of uncertainties. MATLAB simulations are performed and experimental results are obtained using Quanser's Qube-Servo systems in QUARC/Simulink environment. This chapter is published in Studies in Informatics and Control, vol. 31, no. 3, pp. 43-52, 2022.

Chapter 13 : Conclusions and Future Work

This chapter will include the summary of the research work presented in Chapters 3 through 12. In addition, future work directions are also provided.

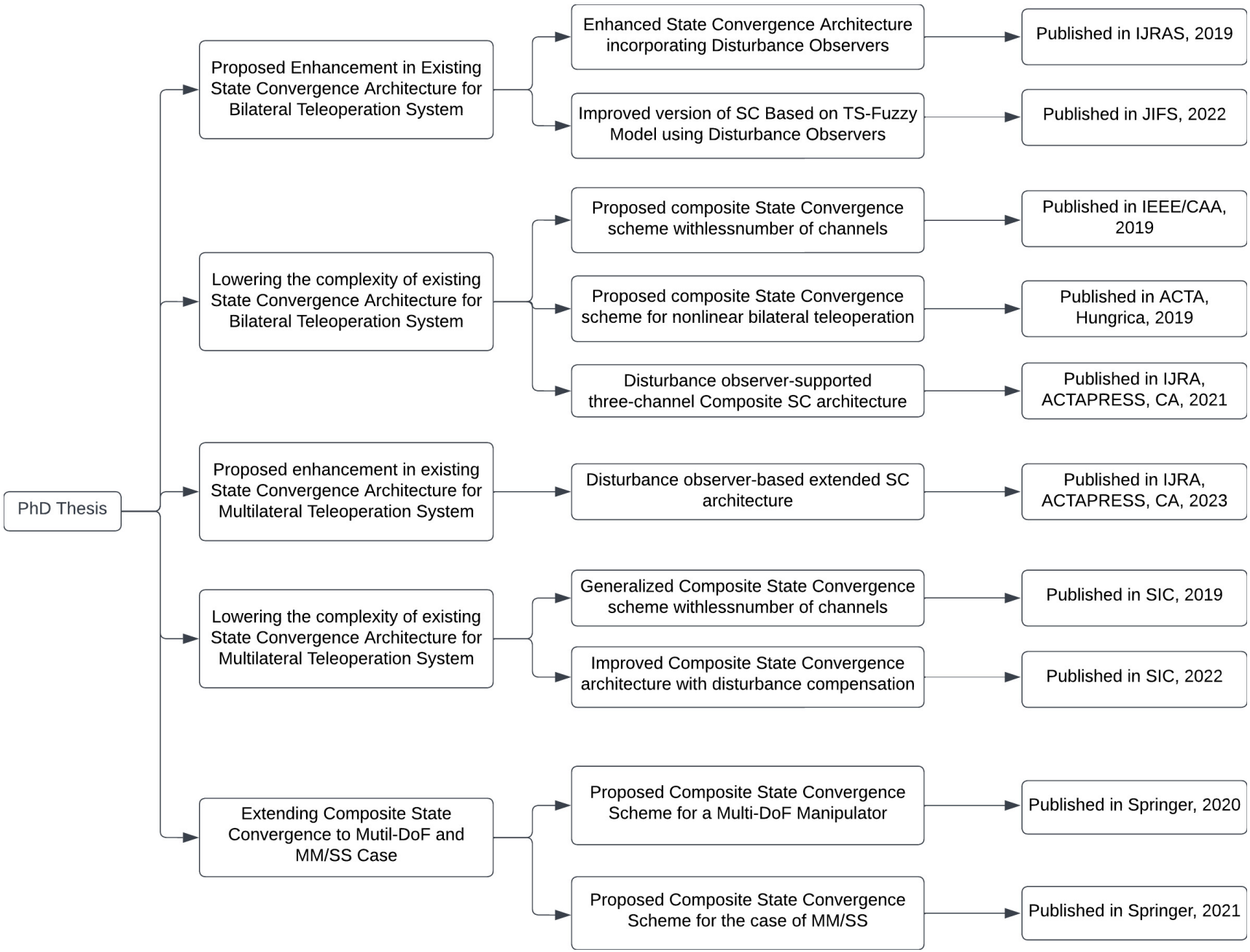

Figure 1.2: Ph.D. thesis contributions flow chart

Chapter 2

Literature Review

2.1 Teleoperation System

Teleoperation systems were invented in the mid-1940s by Geortz to enable humans to manipulate dangerous tasks remotely in hazardous environments via robotic manipulators with enhanced safety at a lower cost or better accuracy as shown in the Figure 2.1. However, the remote environment has uncertain and unknown factors that could degrade any teleoperation system's performance. Thus human intervention becomes necessary to prevent damage, reduce task completion time, to enhance the performance and sense of telepresence. It will improve the user's ability to perform complex tasks. The human-in-the-loop system is known as a teleoperator and has found a wide range of applications ranging from medical and entertainment to large-scale industries [41], [179], [105], [185], [77], [20], [162], [151], [106], [61], [16], [182], [87], [152], [181], [100], [60], [62], [7], [49], [131], [66], [98], [4], [19], [59]. A teleoperation system generally consists of five components: an operator sends the motion commands to operate the remote task via a master hand controller. A communication channel (wired/wireless) is used to transmit those motion commands to a slave robot that will perform the task in a remote environment. In a unilateral teleoperation system, the slave is unable to send the information back to the master; however, if the slave robot can send the force and position signal back to the operator and the operator is kinesthetically coupled to the environment and flow of information is bidirectional, then the teleoperation system is called bilateral. In both cases, the slave robot is placed at a distant location and exchanges information over a communication channel which can cause delays and instability in the whole teleoperation system. Furthermore, a teleoperation system can be classified as either bilateral or multilateral depending upon the number of the robotic system involved in executing the required task. Thus, the prime objective of any teleoperation system is to ensure stability and accuracy in performing the task in the presence of time delays and force -feedback from the environment [56].

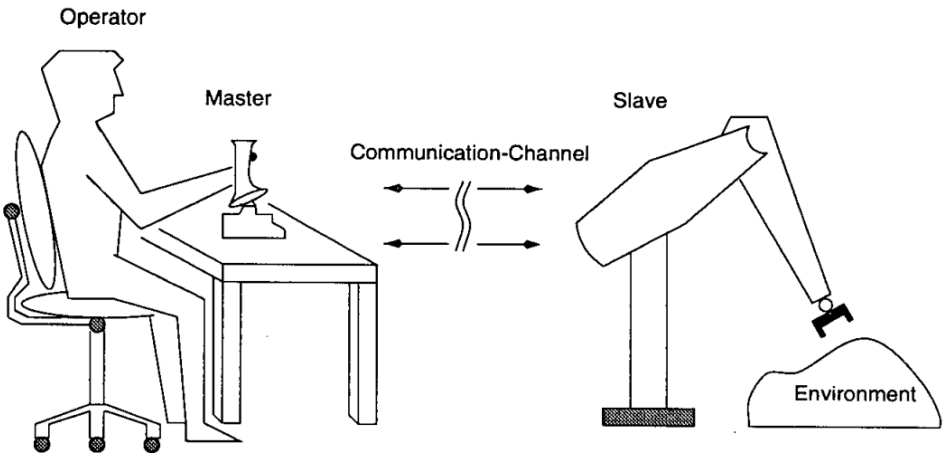

Figure 2.1: Schematic of a teleoperation system [56]

Performance Measures in Teleoperation System

The prime goal of any bilateral teleoperation system is to maintain stability under all circumstances to accomplish a desired performance. Many researchers have employed various techniques to investigate the issue of stability of bilateral teleoperation systems [57], [138], [134], [48], [3], [47], [129], such as Lyapunov theory [173], passivity based tools [115], [122], Nyquist criterion, routh-hurwitz criterion [67] and Root Locus. Like stability, transparency or telepresence is another major goal in the design process of teleoperation systems. It will help the operator better understand the remote environment in the presence of uncertainties and time delays. [88], [135] or in other words it can be interpreted as precise rendering of the remote environment to the operator side to fulfills the prime objective of teleoperation. However, there are certain limitation on achieving the transparency, for instance, system hardware, required bandwidth, master and slave workspace issues, motion scaling and time-delays in the communication channel. According to Lawrence, transparency can be defined as impedance, a quantity that could map input velocity to the output force of the system [28].

2.2 Control Architectures for Bilateral Teleoperation Systems

Various bilateral control architectures have been proposed in the literature to design a stable and transparent teleoperation system. These architectures can be categorized based on the number and type of signals (position, velocity, and/or force) of both master and slave sides exchanged over communication channels. Therefore, different sets of signals resulted in two, three, and four-channel architectures.

Two-Channel Architecture In two-channel architecture, only one signal is sent via the communication channel to the slave side and vice versa. Based on the type of signal which is being exchanged between the master and slave side, it has been classified into four further categories.

1. **Position-Position Architecture**
   In this architecture, position signals of master and slave are transmitted across a communication channel, and Geortz first implemented it in the 50's [43]. One of its variants is position error-based architecture (PEB) which transmits the function of the position states of both master and slave over communication channel [118]. In addition, both ends have their local position tracking controller, which ensures that the slave will track the master manipulator [88]. Some other well-known bilateral teleoperation algorithms based on position-error-based architecture (PEB) are proposed by [15], [119]. The key benefit of these approaches is to provide the system with a sense of force feedback without requiring any force sensor. Similarly, a slave tracking error can be used as feedback to the master instead of any force measurement signal. In an ideal case, there would be no tracking error transmitted to the master side because the slave is able to track the master perfectly, and hence no environmental forces are perceived on the master's side. However, in real-time, the slave tracking error would grow because of its contact with the environment. This error is translated as a force acting on the slave manipulator to the operator side.

   Transparency analyses of position-position architecture are performed by [88] and [103] to identify the shortcomings of this approach. The findings show that it does not provide a high degree of transparency even when the slave is in free motion. Thus, the operator still feels the additional inertia in the system that is not present. [103] found that force tracking is non-ideal when the slave is in contact with the environment, which brings a sense of sluggishness to the system. Hence, the drawback of this architecture is that it exhibits poor performance at hard contact.

2. **Position-Force Architecture**
   In this architecture, the environmental contact force is sent to the master as shown in Figure 2.2, and discussed by many researchers [18], [50], [176], [183].

   In [52], an impedance controller is used to transmit the reflected forces from

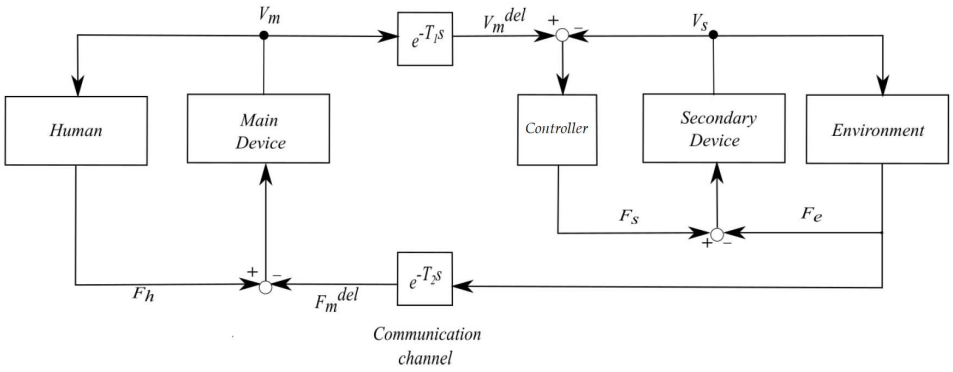

Figure 2.2: Schematic of position-force architecture [156]

the slave to the master manipulator. To perform the trajectory tracking tasks, the slave is provided with all the master states information, such as position, velocity, and acceleration. The control objective for the master manipulator is to provide a desired closed-loop impedance and apply the reflected force. Considering the case of free motion, there will be no additional inertial effects felt on the operator; hence, it provides a better sense of telepresence [103]. In [88], stability analysis is performed and notes that the feedback loop gain is proportional to environmental stiffness. It means when a slave makes contact with stiff surfaces, the system experience oscillations, which can be minimized by reducing the force-feedback gain. Acquiring force feedback requires force sensors which can complicate implementation, for instance, additional hardware resources and increased cost [118]. In addition, stability is often an issue in this architecture due to noisy force sensor measurement, which is addressed using feedback linearization technique to guarantee the stability of a nonlinear teleoperation system [174], [189].

3. **Force-Force Architecture**
   This architecture was first introduced [46] in which only the forces of master and slave are transmitted across a communication channel. The framework lacks coordination between master and slave positions due to the absence of position feedback [88].

4. **Force-Position Architecture**
   This architecture is used for haptic simulation systems and rarely implemented on real-time systems [54].

Three-Channel Architectures

As discussed earlier, two-channel architectures are preferred due to their simplicity [53]; however, not all two-channel CA are transparent, and achieving the necessary trade-off between stability and transparency is difficult. The three-channel control architecture (3CH CA) has been proposed in the literature, aiming to provide increased robustness against time delays with increased transparency [158]. In addition, 3-CH CA offers better optimal transparency than four-channel architecture in the presence of time delays [117], [34]. In [128], transparency of 3CH CA is improved under time delays by eliminating one of the position channels rather than the force channels. In [157], a type of 3CH CA has been tested for multiple robot configurations, known as a multilateral teleoperation system. In [1], authors presented analyses of all the 3CH CA presented in [53], [55] based on passivity-absolute stability and impedance bandwidth. It showed that it is impossible to guarantee the absolute stability of any of the 3CH CA for all sets of frequencies. Furthermore, a comparison of 3CH CA with two-channel architecture is also reported in the literature [40], [140]. The 3CH CA has been classified into four categories.

1. **Position-Position Force Control Architecture (P-PF)**
   This architecture has already been used in medical application [11]. It is proved experimentally that it has better fidelity [10] over P-P and P-F CA. The architecture structure is shown in Figure 2.3. In [13], the author performed absolute stability and transparency analyses using different teleoperator parameters on P-PF architectures as shown in Figure 2.3 (a).

2. **Force-Position Force Control Architecture (F-PF)**
   In [13], the author did analyses in terms of absolute stability margin and transparency for the first time. This architecture, as shown in Figure 2.3 (b), can be derived from the Extended Lawrence architecture (ELA) by setting the force feedforward controller on the master side to zero, i.e., $C_1 = 0$. The author carried out some simulation studies to visualize the characteristics of F-PF CA. It turns out that this CA has a low stability margin, and the presence of time delays and efforts to improve the stability margins will reduce the system's transparency.

3. **Position-Force Position Control Architecture (P-FP)**

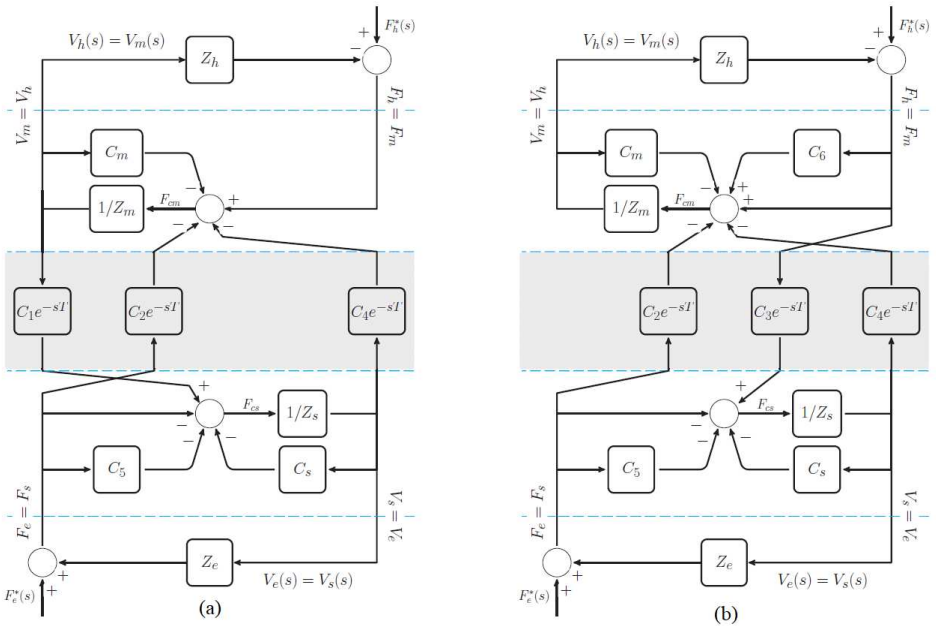

Figure 2.3: 3-ch architecture: (a) P-PF architecture (b) F-PF architecture [13]

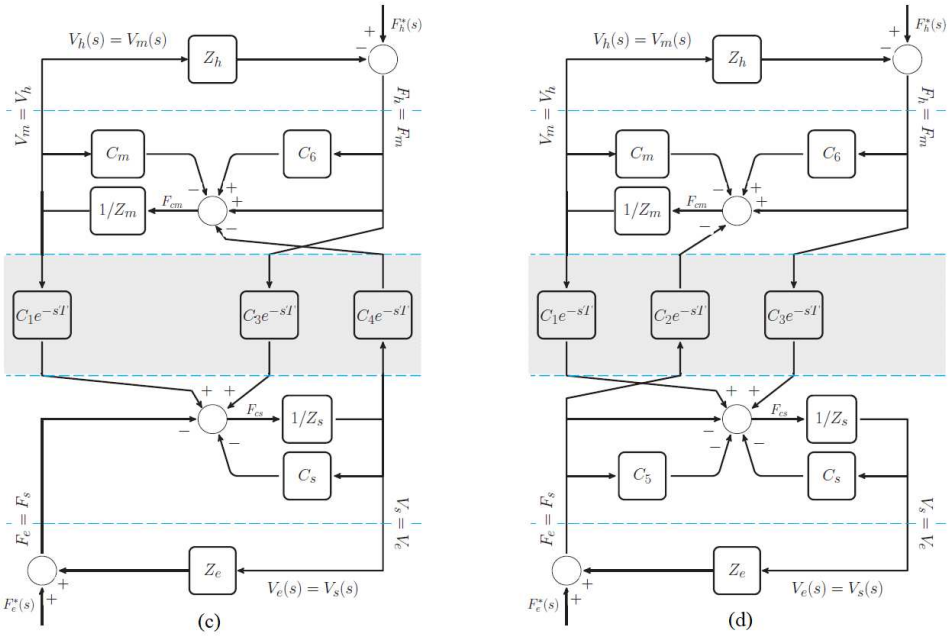

Figure 2.4: 3-ch architecture: (c) P-FP architecture (d) P-FF architecture [13]

This architecture is discussed in [53]. It is a special case deduced from optimized Extended Lawrence architecture (ELA) by applying $C_6 = -1$ as shown in Figure 2.5. In [13], the author considered impedance-impedance type master-slave network for performing the absolute stability and transparency analyses. In addition, the study aims to test three-channel architecture on the surgical application, which normally requires low impedance and negligible time delay. This architecture suffers from low stability and performance measure.

4. **Position-Force Force Control Architecture (P-FF)**
   This architecture is derived from Extended Lawrence architecture (ELA) [53] by setting force feedback gain (slave to master) $C_4 = 0$ as shown in Figure 2.5. This architecture seems to have a satisfactory performance in terms of stability and transparency, which is very close to 4-CH [13].

Four-Channel Architecture

In any teleoperation system, stability and transparency are vital in bringing safety and improving users' telepresence. However, the presence of a communication time delay will make it challenging to achieve precise position tracking and high-fidelity force feedback. In literature, various techniques using four-channel architecture as shown in Figure 2.5, such as time domain passivity control [93], [130], [94], sliding mode control (SMC) [99], [165] and disturbance-observer-based sliding mode control [153], are developed in the presence of time-varying delays, uncertainties, and external disturbances in order to achieve good performance for bilateral teleoperation systems. Furthermore, the four-channel architecture is also implemented to control the multilateral teleoperation to handle dangerous, unknown, and complicated tasks remotely under time-varying delays in the communication channel. A novel framework is proposed in [23], [85] to meet the demands of communication among multiple masters and slave robots.

Control Schemes to deal with Time Delay

A number of control schemes have been proposed in the literature that used either two-channel or four-channel architectures as a baseline to counter time-varying delays, model parameters, and environmental uncertainties, etc.

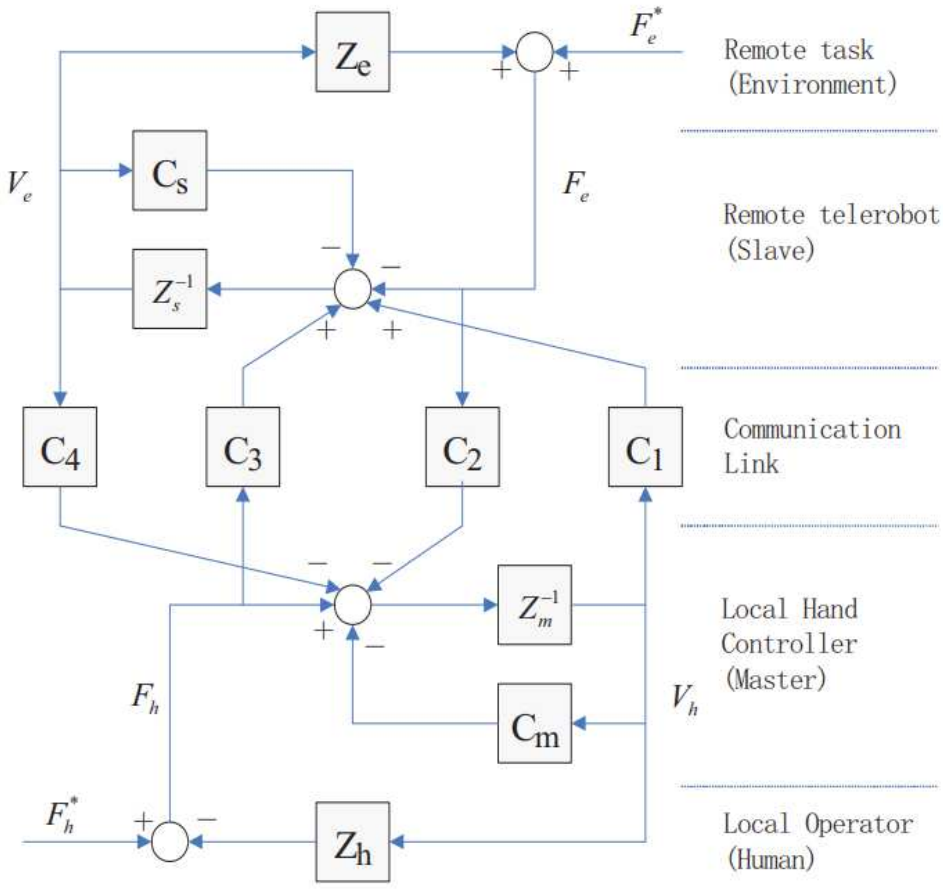

Figure 2.5: Four-channel lawrence architecture [88]

Time-Domain Passivity Based Control Schemes

In [130], the author proposed an extended version of the time-domain passivity framework using four-channel architecture. The controller can stabilize the teleoperation system for constant time delays and in the presence of data loss. The approach offers better performance in terms of transparency and other existing time-domain passivity architectures. In [149], a new wave-based time-domain passivity approach is applied to a non-linear four-channel control architecture. This new wave transformation will help to enhance transparency while maintaining stability in the presence of time-varying delays. The proposed scheme is validated on a 3-DOF teleoperation system. In [177], a time-domain passivity approach is proposed for a bilateral teleoperation system to deal with the instabilities caused by time delays in the communication channel. In [150], the authors used a neural network to propose a new 4-CH wave-based time-domain passivity control scheme to address the nonlinear uncertainties related to the system's dynamic model. The neural network estimates and eliminates those uncertainties in the presence of time-varying delays to improve the position and torque tracking performances. In [27], a study is proposed to minimize the chattering phenomenon due to time-domain passivity architecture. The authors introduced a non-zero velocity threshold which will use adaptive damping of the TDPA to mitigate the chattering while maintaining stability. The proposed method is validated on a time-delayed bilateral teleoperation system. The signal flow diagram of TDPC is shown in Figure 2.6.

Prediction-Based Control Schemes

The concept of prediction-based control in bilateral teleoperation was proposed in 1957 to deal with delays in a chemical plant. The main idea behind the smith controllers is to build a local model on the master side based on the response from the slave and the environment. The predictive model will help to identify the remote object, taking out the negative effects of time delay. The basic concept of prediction control is shown in Figure 2.7.

In most cases, prediction-based control schemes have been designed to reconstruct the slave robot and remote environment to help model the plant on the master side. Various types of predictors have been used to identify the model of the master robot. Some of the popular methods include the smith predictor [145], Kalman filters, linear predictors [141], adaptive linear predictors, passivity-based predictive control [125],

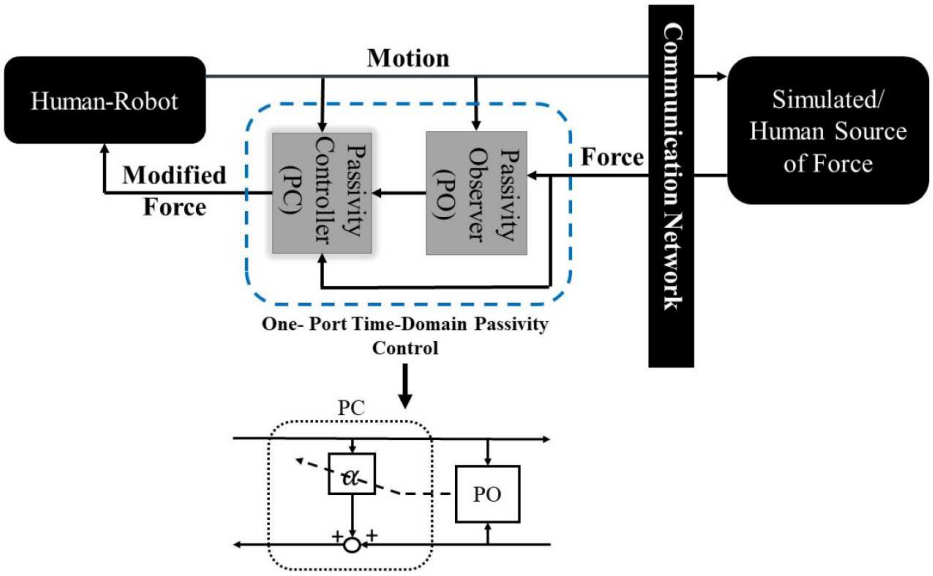

Figure 2.6: Time-domain passivity control [108]

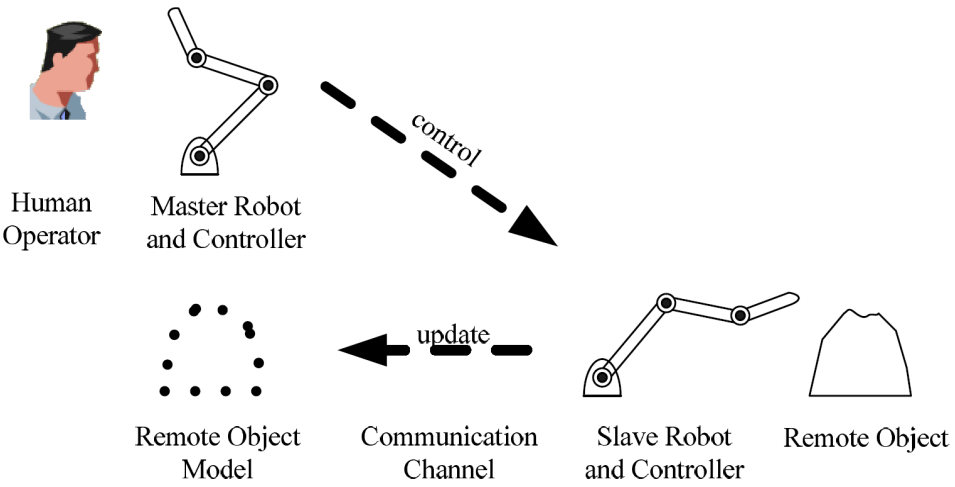

Figure 2.7: Concept of prediction based control scheme [188]

[111], model predictive control [95] and neural network estimation [58]. Other papers in the literature predict other parts of the system, such as states of the master robot [45], operator input [146], or environment [180] only. There is also a growing interest in combining passivity-based control with prediction-based control. Using predictive control will improve transparency, and wave variables ensure the system's stability [168], [137], [25].

Disturbance Observer-Based Control

Disturbance observers (DOBs) have gained popularity in recent years to improve the system stability and transparency in telerobotic applications [44], [8], [9], [127], [81], [114]. Parametric and model uncertainties and nonlinearities can severely compromise the system stability, which must be guaranteed at any cost. In addition, disturbance rejection capability is of critical importance while designing any teleoperation system to counter the unknown disturbance. A promising approach would be to use nonlinear disturbance observers (NDOBs) to suppress those effects. The general structure of the DOBs is shown in Figure 2.8.

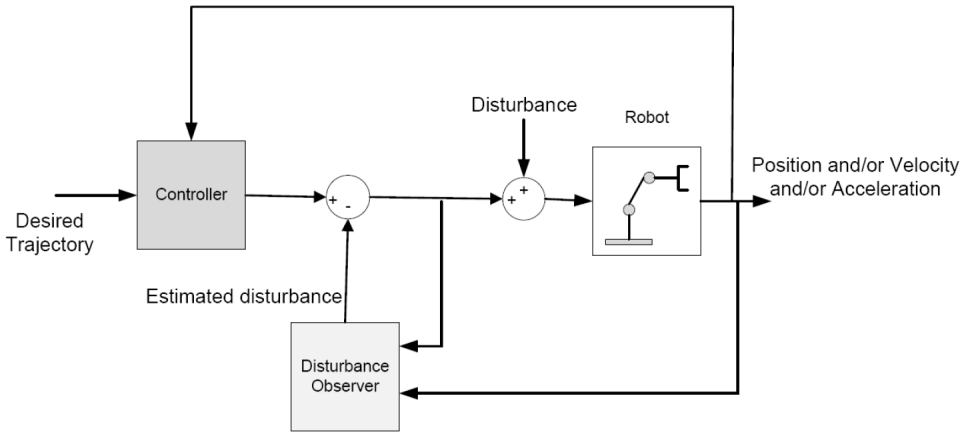

Figure 2.8: Schematic of disturbance observer based control [109]

In [51], [154] a sliding mode control is combined with a disturbance observer for trajectory tracking application of surgical manipulator. The proposed scheme will compensate for the disturbances arising from uncertainties of the dynamic model, frictional forces, and external interaction forces in the control law and eventually enhances the robustness of the system. In [22], authors developed a new robust adaptive nonlinear teleoperation system using an improved extended active observer (IEAOB), adaptive Smith predictor (ASP), and sliding mode control to mitigate the time-delays and model uncertainties. The proposed scheme showed robustness against

robot inertial parameter variations, friction, unmodeled dynamics, and measurement noise. In [187], authors designed a bilateral controller for nonlinear teleoperation systems to deal with external disturbances. This new composite nonlinear bilateral control method is proposed to regulate the nonlinear feedback and compensate for feed-forward disturbances in position and force-tracking error dynamics.

Model-Based Control Design

In the literature, various control schemes used the concept based on master and slave robot model dynamics. The controllers were built for teleoperation applications through this method including identified delayed data in their equation. It is a different strategy a s compared to prediction-based control in which time delay is completely ignored to preserve stability. The main challenge is to accurately identify the model of the system despite external disturbances, frictions, payload variations, and parametric uncertainties. The desired outcome of the controller heavily depends on accurate model identification. A linear dynamic model of the system can be written as follow in Eq 2.1: [188]

$$\begin{aligned} M_m\ddot{x}_m + B_m\dot{x}_m + K_m x_m + f_{fm} &= f_h + f_{mc} \\ M_s\ddot{x}_s + B_s\dot{x}_s + K_s x_s + f_{fs} &= f_e + f_{sc} \end{aligned} \tag{2.1}$$

where M, B, K are system mass, viscous, and spring coefficient, x, $\dot{x}$ and $\ddot{x}$ are the robot end effector's position, velocity, and acceleration. The nonlinear model can be expressed using Lagrange's equation as follows in Eq 2.2:

$$\begin{aligned} D_m\left(x_m\right)\ddot{x}_m + C_m\left(x_m\dot{x}_m\right)\dot{x}_m + G_m\left(x_m\right) + f_{fm} &= f_h + f_{mc} \\ D_s\left(x_s\right)\ddot{x}_s + C_s\left(x_s,\dot{x}_s\right)\dot{x}_s + G_s\left(x_s\right) + f_{fs} &= f_e + f_{sc} \end{aligned} \tag{2.2}$$

where D is the moment of inertia, C is centripetal forces and Coriolis forces, and G is the gravitational forces. The subscript m in the model represents the master and subscript s represents the slave robot linear model.

Impedance Control

Impedance control is a typical model-based control technique in which trajectory tracking is desired to a contact force while considering the robot dynamics. Researchers have combined impedance control with sliding mode control to enhance

robustness. In sliding mode control, a first-order sliding mode surface $S = \dot{e} + e\lambda$ is defined for telerobotic applications. The system slide along the designed surface by first approaching it and then staying on it once it is reached. $\dot{e}$ here represents the error rate between master and slave robots. Several researchers have contributed to the development of controllers in [124], [26], [90], [91], [92]. Matching impedance is another form of impedance control used to improve system transparency, as discussed in [96], [142].

H_∞ Based Control

A telerobotic system in real-time will always be exposed to unknown external disturbances such as noise from the sensors, etc. Eventually, these disturbances could destabilize the system even if the robot model is well-identified with corresponding parameters. Scholars have developed some robust control to compensate for those unpredictable external sources of disturbances by using H_∞ optimal control, as reported in the literature [39], [143], [78].

Model Predictive Control (MPC)

Researchers have merged model-based control with predictive control and developed a very powerful tool known as model-predictive control(MPC) [22], [95], [178], [172], [78]. In this method, the robot's internal dynamics are heavily involved. In [144], the authors proposed a modified version of the model predictive control scheme to improve the robustness of the bilateral control system in the presence of time delays. Lyapunov's method is also used to prove the system stability, as in the case of model base control.

2.3 State Convergence Architecture

State Convergence architecture presents an elegant and simple model-based control technique to design controllers for bilateral teleoperation systems. This method uses state space formulation of the master and slave robot, allowing the slave to follow the master in the presence of communication time delays. This method can also assign desired dynamics behavior of the teleoperation systems. This scheme is originally used for linear systems with either no time delay or minimal time delays. Despite these limitations, the SC method is worth investigating due to its simplicity, modeling easiness, and achieving desired dynamic behavior [73], [72], [71], [17]. Furthermore, the SC method is also used to control the nonlinear teleoperation system. The literature has also addressed various techniques such as Lyapunov theory [65], [70], [63], [64], adaptive control theory [97], feedback linearization techniques [70], fuzzy logic, and

neuro-fuzzy techniques [164], [169] to control the nonlinear-teleoperation-system using SC method.

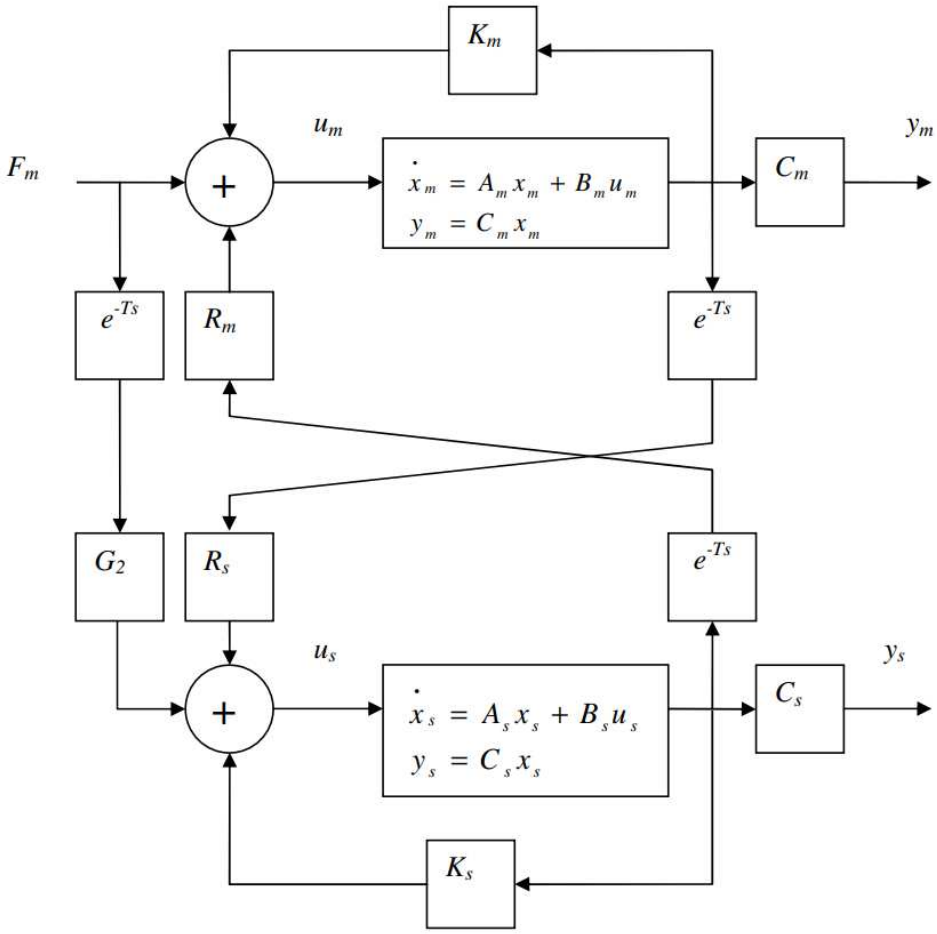

Figure 2.9: State convergence control architecture [72]

Figure 2.9 shows the state convergence architecture. Operator force is provided to the slave manipulator through the matrices G_2 and R_s, which are unknown parameters. Slave tries to mimic the master motion commands while interacting with the environment. The model of the remote environment consists of stiffness k_e and viscous friction b_e. The reaction forces from the slave F_s and force feedback gain k_f are transmitted back to the master via the R_m matrix. R_m is known due to the prior knowledge of the remote environmental parameters. The stabilizing gains K_m and K_s of the master and slave robot are unknown parameters. The $3n+1$ unknown parameters are to be determined through a solution of a set of following design equations [73], which will help assign desired dynamic behavior of the teleoperation system.

$$
\begin{aligned}
&B_1 - B_2 = 0, A_{11} - A_{21} + A_{12} - A_{22} = 0 \\
&|sI - (A_{11} + A_{12})|\,|sI - (A_{22} - A_{12})| = |sI + P||sI + Q|
\end{aligned}
\tag{2.3}
$$

where matrics P and Q are the desired slave and error poles while other entries are as follow [36]:

$$
\begin{aligned}
&A_{11} = A_s + B_s K_s, A_{12} = B_s R_s, A_{21} = B_m R_m, A_{22} = A_m + B_m K_m \\
&B_1 = B_s G_2, B_2 = B_m
\end{aligned}
\tag{2.4}
$$

Considering small time delays in the communication channel, the matrix entries in Eq 2.4 are replaced as:

$$
\begin{aligned}
&A_{11} = S\left(A_s + B_s K_s - T B_s R_s B_m R_m\right), A_{12} = S\left(B_s R_s - T B_s R_s \left(A_m + B_m K_m\right)\right) \\
&A_{21} = M\left(B_m R_m - T B_m R_m \left(A_s + B_s K_s\right)\right), A_{22} = M\left(A_m + B_m K_m - T B_m R_m B_s R_s\right) \\
&B_1 = S\left(B_s G_2 - T B_s R_s B_m\right), B_2 = M\left(B_m - T B_m R_m B_s G_2\right)
\end{aligned}
\tag{2.5}
$$

Where matrices S and M can be determined as:

$$
S = \left(I - T^2 B_m R_m B_s R_s\right)^{-1}, M = \left(I - T^2 B_s R_s B_m R_m\right)^{-1} \tag{2.6}
$$

Variants of State Convergence Architecture

Transparency Optimized SC Method : Transparency-optimized state convergence is developed to enhance the transparency of bilateral teleoperation systems in the presence of time delay. The modified version of state convergence aims to reflect full environmental forces to the operator and achieve desired dynamic behaviour simultaneously, which is a bit challenging. This problem is rectified by limiting the allowable range of time delay and closed loop behaviour [36]. The block diagram of the transparency-optimized state convergence is shown in Figure 2.10.

SC Method for Unknown Environments: The state convergence method initially used a known environmental model to compute the telerobotic system's control gains. In [68], the authors proposed a modified version of the state convergence architecture

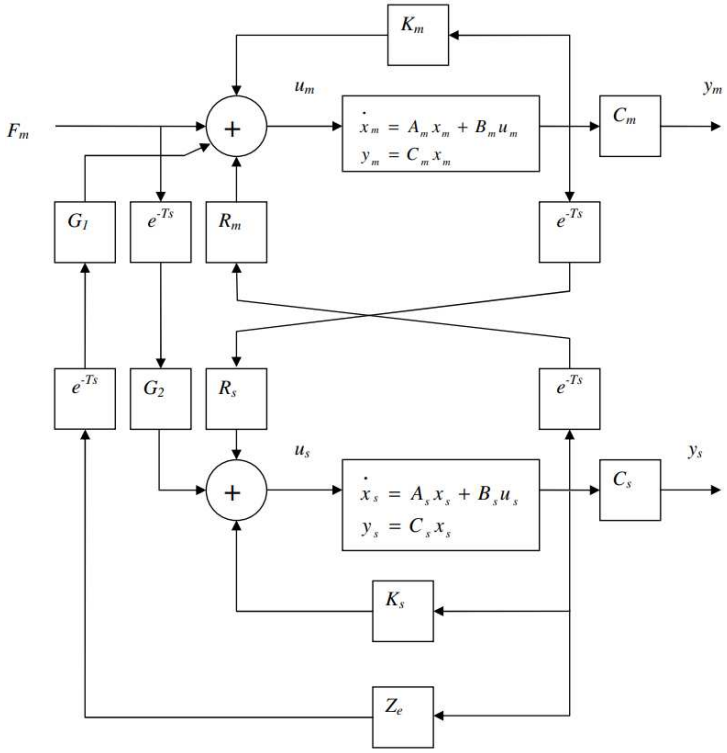

Figure 2.10: Transparency-optimized standard state convergence control architecture [72]

to address the limitation of using it when the environment's model or parameters are unknown. In this version, $3n + 2$ control gains are needed to control a telerobotic system modeled by a pair of nth order linear differential equations. The detailed design procedure to compute the gains is refereed to [73], [68]. The modified version is shown in Figure 2.11.

Fuzzy-based SC Methodology: In [37], a Takagi-Sugeno (TS) fuzzy model is used to design a state convergence (SC) based bilateral controller for a nonlinear teleoperation system. In this method, master and slave systems are represented by TS fuzzy models. The use of appropriate fuzzy control law makes it capable enough to control and impose the desired dynamic behaviour of the teleoperation system in the presence and absence of communication delays using state convergence. The proposed scheme as shown in Figure 2.12 is validated in MATLAB and compared with the existing linear scheme. Using this scheme, there is no need to design a Lyapunov function to prove the system's stability.

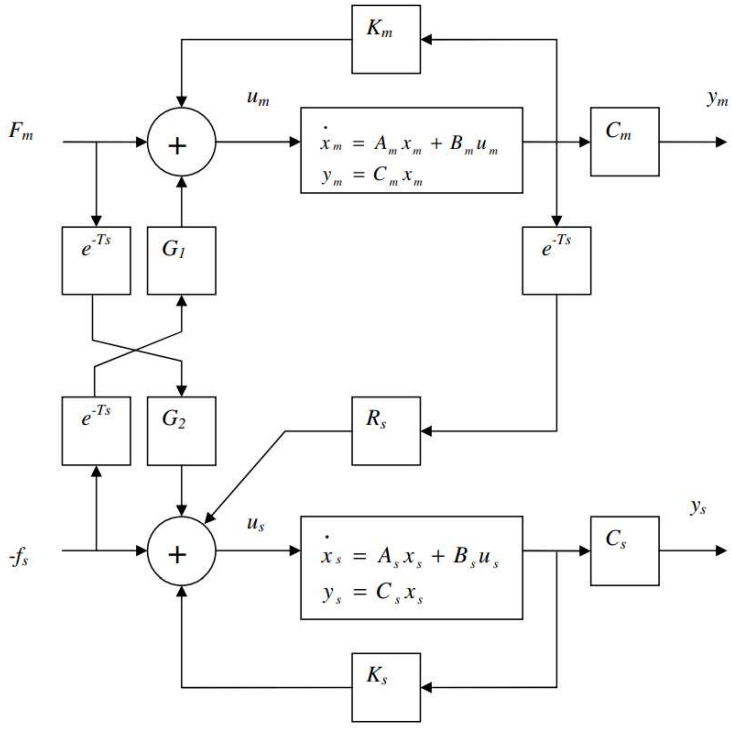

Figure 2.11: State convergence control architecture for unknown environments [68]

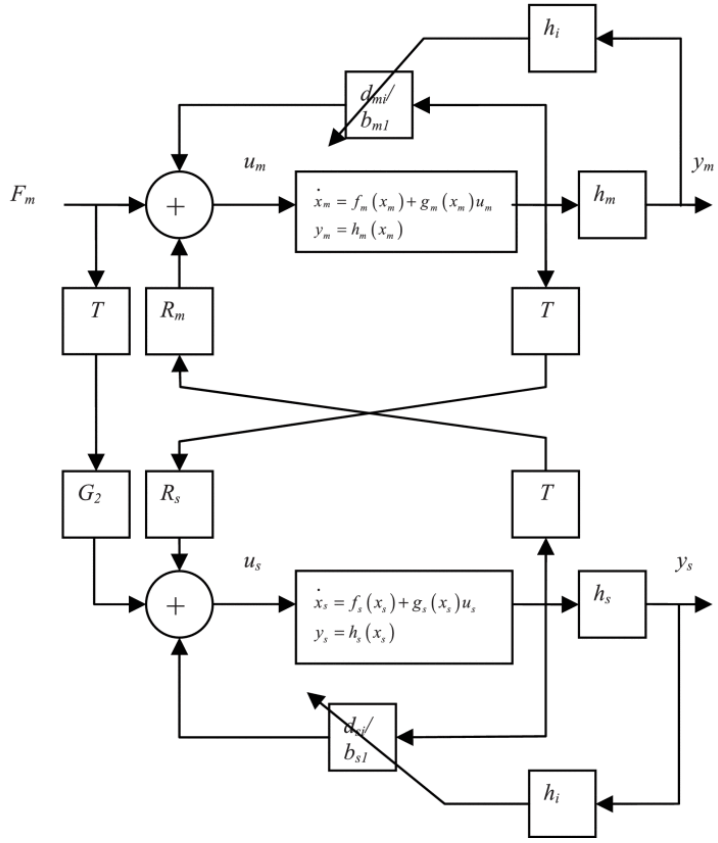

Figure 2.12: SC scheme for bilateral control of a nonlinear teleoperation system using TS fuzzy models [37]

2.4 Control Architectures for Multilateral Teleoperation System

The literature on bilateral teleoperation systems is rich, and many researchers have investigated several algorithms and architectures to address and improve such systems' stability, transparency, and performance measures. The extended versions of these existing architectures to cover the case of multilateral teleoperation systems have also been reported in the literature. A passivity control scheme based on the wave variable method [42] has been extended to control dual master/single slave system [21] to perform a therapeutic task. It empowers the therapist to perform remote therapy for patients located at distant locations. In another study [82], the wave variable approach is used to control the multilateral teleoperation system. In this control scheme, the authors proposed an architecture with a wave node that connects multiple wave variables transmission lines and a formulation to realize the wave node. In addition, wave integral error feedback is used to compensate for the position drift due to time-varying delays. In [24], [155], a novel multilateral teleoperation framework is proposed to control n number of slaves through n number of masters remotely. A time-delay compensator is built using the wave transform method and four-channel architecture to handle the communication among multiple masters and slaves in the presence of time-varying delays. Furthermore, the time-domain passivity concept primarily used for bilateral teleoperation systems is extended to control multilateral teleoperation systems [84], [12], [133] such as multi-master/single slave (MM/SS) [101], dual-master/dual-slave [32], and multi-master/multi-slave (MM/MS) teleoperation systems [126]. The use of disturbances observers to estimate the environmental forces is proposed in [107].In [107], the concept of model decomposition is used to design a multilateral teleoperation system. A position and force control of master and slave is integrated into the acceleration dimension based on the disturbance observer. This type of control is very important in human adaptive mechatronics. In [83], a novel control design is proposed for a multilateral teleoperation system to solve the problem of motion integration of different DOF and structure through the use of spatial mode coordinate systems. In [167], a novel passive four-channel architecture (PFCA) is designed to ensure the system's stability independent of time delay. The scheme is tested on dual-master/single-slave and single-master/dual-slave systems. Similarly, other techniques such as H_∞ optimization, adaptive control [184], sliding mode control [166] and intelligent control [148] are used to control multilateral teleoperation systems.

Extension of SC Architecture For Multilateral Systems:
An alpha-modified version of the standard state convergence architecture is developed for a single-master/single-slave teleoperation system. This method is then extended to control a multi-master/multi-slave teleoperation system as shown in Figure 2.13. The proposed multilateral controller is able to control k -master/l -slave nth order teleoperation system and requires the solution of $n(k+l)+(n+1)kl$ design equations. The controller gains will ensure the synchronization of k-master and l-slave systems in a desired dynamic way [38].

2.5 Summary

In this chapter, various control schemes and architectures for bilateral and multilateral teleoperation systems have been presented. Initially, various control architectures were discussed to give an overview of all the available architectures to control the time-delay and delay-free teleoperation system. Control schemes such as time-domain passivity-based approaches and predictive control, adaptive control, etc., were discussed. Shortly after describing these control schemes, a concept of disturbance observer-based control was introduced to counter parametric uncertainties and unknown disturbances while designing a stable teleoperation system. Model-based control designs were also presented and analyzed the stability of the system considering the master and slave robot model dynamics. This approach's major challenge is accurately identifying the system's model. Other approaches are also presented, such as impedance, robustness, and model predictive control. Control schemes related to the multilateral teleoperation framework are also introduced. Finally, the state convergence method, a novel architecture to control a bilateral teleoperation system, is discussed. Some variants are also developed to enhance transparency and extend their capability when the environment's model or parameters of the bilateral teleoperation systems are unknown. Table 2.1 and Table 2.2 compare different model-based and model-free control architectures for bilateral teleoperation systems.

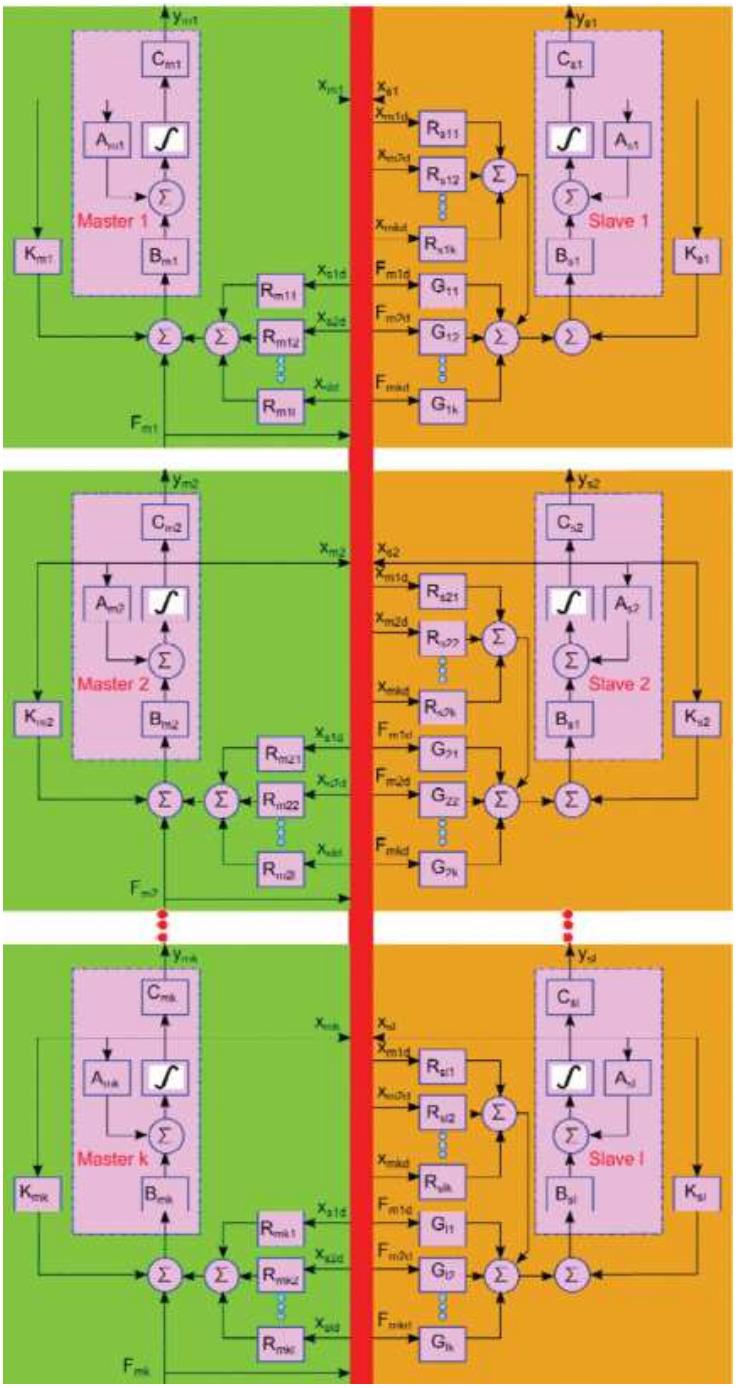

Figure 2.13: Proposed extended state convergence architecture for k -master/ l -slave systems [38]

Table 2.1: Model-based teleoperation control approaches [147]

Model-based Control Scheme				
Criteria	WV/S	TDPA/C	MMT	SC
Input variables/ information transmitted	Force and velocity signals are linearly transformed wave-variables (u and v) [112]	Velocity, force, and required amount of energy dissipated [132]	Position, velocity, acceleration, force, and remote environment parameters [171]	Operators force, position, and velocity signals [73]
Feedback signals	Force feedback signal for force rendering [42]	Exchange of energy between the two end ports [132]	Non-delayed force feedback signal [170]	Position and velocity signals
Model type	Differential equation-based models are used	Discrete models wherein the energy flow is computed in real-time	Transfer function, multi DOF models	Linear state-space model
Effects of model errors	Presence of wave reflections decreases the usefulness of this approach	If the observation period is longer than the width of time intervals, then the data set becomes very large	Due to complex modeling environments and confined resolution of sensors	Difficult to get the exact model of the system
Stability under time-delay case	Passive for fixed time delay [112], energy dissipated from time-varying gains [89]	Passivity is regulated by PO/PC union	When the estimated model matches the remote environment structure [171]	Small time delays can affect the system's stability [68]
Performance criteria in the presence of time delay	Performance deteriorated due to large time delays	Transparency under time-varying delay is affected by a passive leak	Improved performance guaranteed due to locally updated models	Pre-assigned performance by user

Model-based Control Schemes				
Criteria	WV/S	TDPA/C	MMT	SC
Robot Dynamics	Independent of master and slave model parameters and delay size.	Depends on the tuning of damping parameters	User-centered dynamics	Modeling uncertainties are improved using disturbance observers
Position Convergence	Position tracking improved using the Lyapunov method	Achieved when all the system parameters are known	Greatly affected due to model mismatch	Achieved using control gains computed through design equations

Table 2.2: Model-free teleoperation control approaches [147]

Model-free Control		
Criteria	NN-based	Fuzzy-based
Input variables	Variables such as (Position, velocity, and acceleration) are weights $\bar{v}_j$ from the hidden layer to the output layer [153]	Vector space ($\vec{x} = [x_1 \dots x_n]^T$) also called linguistic variables
Feedback signals	Estimated environment values $\widehat{W}_e$	Environment/slave displacement, velocity, and acceleration
Model type	Mathematical model of neurons in $y(t) = \sigma\left(\sum_{j=1}^{n} v_j x_j(t) + v_0\right)$ [56]	Human reasoning/ linguistic rules (if-then)
Effects of model errors	RBFNN method takes care of system uncertainties, tracking errors and force feedback errors [153]	System errors are reduced by introducing adaptive neural methods
Stability under time-delay case	NN-based controllers are robust to external disturbances and unmodeled dynamics [171]	Membership functions are used to maintain system stability under unknown time-delay [123]
Performance criteria in the presence of time delay	Transparency is affected due to the time-varying nature of environmental dynamics	Affected by time-delay
Robot Dynamics	Used to approximate unknown system/robot dynamics along with environment dynamics	Modelling issues are improved in Type-2 fuzzy models
Position Convergence	Desired slave and master position is converged using slave trajectory creator	With the help of adaptive laws, position convergence is achieved [153]

Chapter 3

An Enhanced State Convergence Architecture Incorporating Disturbance Observer for Bilateral Teleoperation Systems

In order to bilaterally control an n^{th}-order teleoperation system modeled on state space, state convergence methodology provides an elegant way to design control gains through a solution of $3n+1$ equations. These design conditions are obtained by allowing the master-slave error to evolve as an autonomous system and assigning the desired dynamic behavior to the slave and error systems. The controller, thus obtained, ensures the motion synchronization of master and slave systems with adjustable force reflection to the operator. Although simple to design and easy to implement, the state convergence method suffers from its dependence on model parameters. Thus, the controller's performance may degrade in the presence of parametric uncertainties. To address this limitation, we propose to integrate an extended state observer in the existing state convergence architecture, which will compensate for the modeling inaccuracies by treating them as a disturbance and providing the estimates of the master and slave states. These estimated states are then used to construct the bilateral controller, which is designed by following the method of state convergence. In this case, $2n + 2$ additional design equations are required to be solved to fix the observer gains. To validate the proposed enhancement in the state convergence architecture, simulations, and semi-real-time experiments are performed in MATLAB/Simulink environment on a single-degree-of-freedom teleoperation system.

3.1 Review of State Convergence Architecture

State convergence architecture [73], shown in Figure 3.1, establishes a bilateral connection between the master and slave systems which can be represented by n^{th} order linear differential equation and modeled on state space as:

$$\begin{aligned} \dot{x}_z &= A_z x_z + B_z u_z \\ y_z &= C_z x_z \end{aligned} \tag{3.1}$$

where, subscript 'z' is to be replaced with 'm' for the master system and with 's' for the slave system. Various matrix entries in Eq (3.2) are given as:

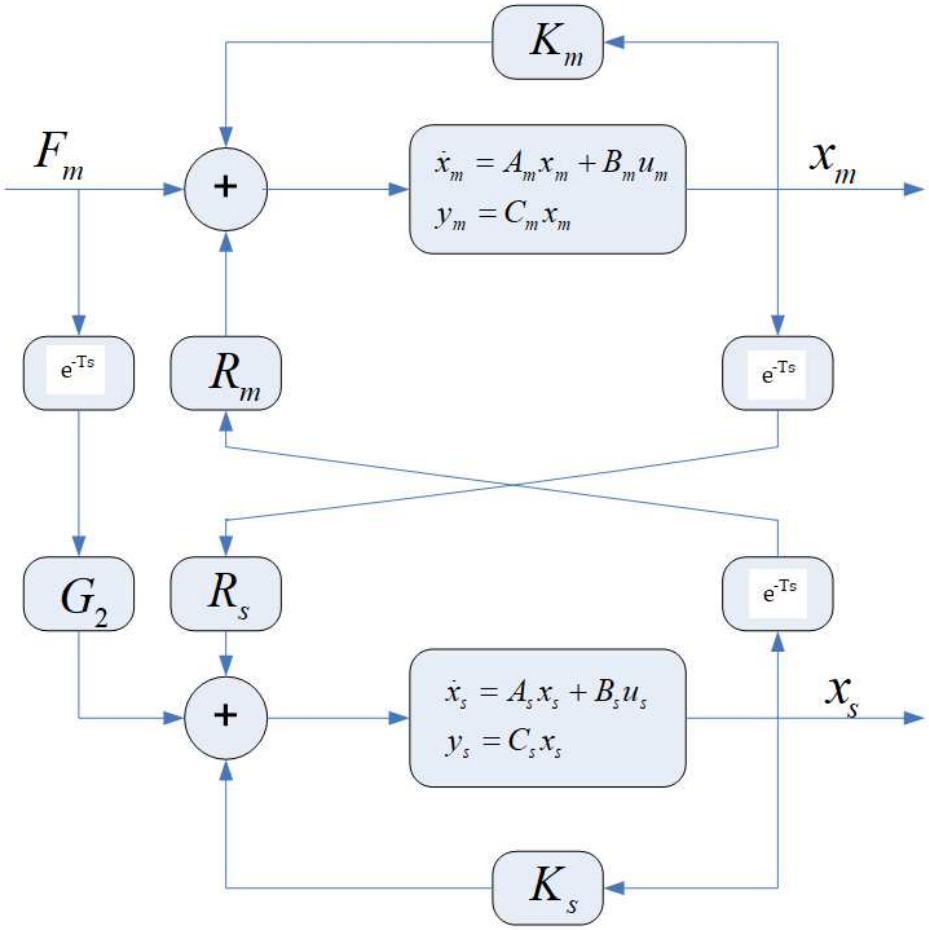

Figure 3.1: State convergence architecture [73]

$$A_z = \begin{bmatrix} 0 & 1 & 0 & \cdots & 0 \\ 0 & 0 & 1 & \cdots & 0 \\ & & \vdots & & \\ 0 & 0 & 0 & \cdots & 1 \\ -a_{z0} & -a_{z1} & -a_{z2} & \cdots & -a_{zn-1} \end{bmatrix}, B_z = \begin{bmatrix} 0 \\ 0 \\ \vdots \\ 0 \\ b_{z0} \end{bmatrix}$$
$$C_z = \begin{bmatrix} 1 & 0 & 0 & \cdots & 0 \end{bmatrix} \tag{3.2}$$

Various parameters forming the state convergence architecture are defined as: $K_m = \begin{bmatrix} k_{m1} & k_{m2} & \cdots & k_{mn} \end{bmatrix}$is the feedback stabilizing controller for master system, $K_s =$

$\begin{bmatrix} k_{s1}^* + k_e & k_{s2}^* + b_e & \cdots & k_{sn} \end{bmatrix}$is the feedback stabilizing controller for the slave system which also includes the stiffness (k_e) and damping (b_e) terms of the environment to counter the environmental force, $R_m = \begin{bmatrix} k_f k_e & k_f b_e & \cdots & 0 \end{bmatrix}$transfers the scaled effect of slave's motion to the master system as the slave interacts with the environment where scaling is achieved through the force feedback gain (k_f), $R_s = \begin{bmatrix} r_{s1} & r_{s2} & \cdots & r_{sn} \end{bmatrix}$transfers the effect of master's motion to the slave system, and $G_2$is the force transmission gain from the master to the slave system when the operator exerts a force (F_m) to move the master system. Of these parameters, G_2, K_m, K_s, R_s are unknown and found through a solution of $3n+1$ design conditions, as described in appendix A.

Remark 3.1. *State convergence scheme employs the model parameters in Eq (3.2) for the design of control gains. In practice, parametric uncertainties cannot be avoided and may degrade the performance of the controller. The effect of these uncertainties has been numerically evaluated on the performance of the state convergence controller in [73], [160]. It is found that the bilateral controller is quite robust to more than 50% variations in the model parameters. However, the effect of these parametric uncertainties has not been explicitly considered during the design phase of the scheme which has motivated us to perform this study. Note that operator and environment force estimation will not be undertaken in this study.*

3.2 Proposed Enhanced State Convergence Architecture

In order to deal with uncertainties, we propose an enhanced version of the state convergence architecture, shown in Figure 3.2, where extended state observers are used to estimate the uncertainties present in the master and slave systems. These observers also provide estimates of the master and slave systems' states. The disturbance and state estimates are then used to form the bilateral control law. We proceed by considering the following nonlinear model of the master ($z = m$) and slave ($z = s$) systems:

$$\begin{aligned} \dot{x}_{z1} &= x_{z2} \\ \dot{x}_{z2} &= x_{z3} \\ &\vdots \\ \dot{x}_{zn} &= f_z(x_z) + b_z u_z \\ y_z &= x_{z1} \end{aligned} \tag{3.3}$$

$$
\begin{aligned}
\dot{x}_{ze1} &= x_{ze2} \\
\dot{x}_{ze2} &= x_{ze3} \\
&\vdots \\
\dot{x}_{zen} &= x_{ze(n+1)} + b_z u_z \\
\dot{x}_{ze(n+1)} &= h_z \\
y_z &= x_{ze1}
\end{aligned}
\tag{3.4}
$$

In Eq (3.3), f_z is considered to be completely unknown and will be estimated by using the disturbance observer along with other systems' states. To this end, we first rewrite Eq (3.3) by considering the disturbance $d_z = f_z$ as an additional $n{+}1^{th}$ state. Note the slight change of notation in Eq (3.4) where subscript 'e' is added to denote the extended system. Further, the time derivative of the disturbance also appears in Eq (3.10) i.e., $h_z = \dot{d}_z$. Before further development, we write systems in Eq (3.3) and Eq (3.4) in compact form as in Eq (3.5) and Eq (3.6):

$$
\begin{aligned}
\dot{x}_z &= A_z x_z + B_z u_z + E_z d_z \\
y_z &= C_z x_z
\end{aligned}
\tag{3.5}
$$

$$
\begin{aligned}
\dot{x}_{ze} &= A_{ze} x_{ze} + B_{ze} u_{ze} + E_{ze} h_z \\
y_z &= C_{ze} x_{ze}
\end{aligned}
\tag{3.6}
$$

where,

$$
A_z = \begin{bmatrix} 0 & 1 & 0 & \cdots & 0 \\ 0 & 0 & 1 & \cdots & 0 \\ & & \vdots & & \\ 0 & 0 & 0 & \cdots & 1 \\ 0 & 0 & 0 & \cdots & 0 \end{bmatrix}, B_z = \begin{bmatrix} 0 \\ 0 \\ \vdots \\ 0 \\ b_z \end{bmatrix}, E_z = \begin{bmatrix} 0 \\ 0 \\ \vdots \\ 0 \\ 1 \end{bmatrix} C_z = \begin{bmatrix} 1 & 0 & 0 & \cdots & 0 \end{bmatrix}
\tag{3.7}
$$

$$
\begin{aligned}
A_{ze} &= \begin{bmatrix} 0 & 1 & 0 & \cdots & 0 & 0 \\ 0 & 0 & 1 & \cdots & 0 & 0 \\ & & & \vdots & & \\ 0 & 0 & 0 & \cdots & 1 & 0 \\ 0 & 0 & 0 & \cdots & 0 & 1 \\ 0 & 0 & 0 & \cdots & 0 & 0 \end{bmatrix}, B_{ze} = \begin{bmatrix} 0 \\ 0 \\ \vdots \\ 0 \\ b_z \\ 0 \end{bmatrix}, E_{ze} = \begin{bmatrix} 0 \\ 0 \\ \vdots \\ 0 \\ 0 \\ 1 \end{bmatrix} \\
C_{ze} &= \begin{bmatrix} 1 & 0 & 0 & \cdots & 0 & 0 \end{bmatrix}
\end{aligned}
\tag{3.8}
$$

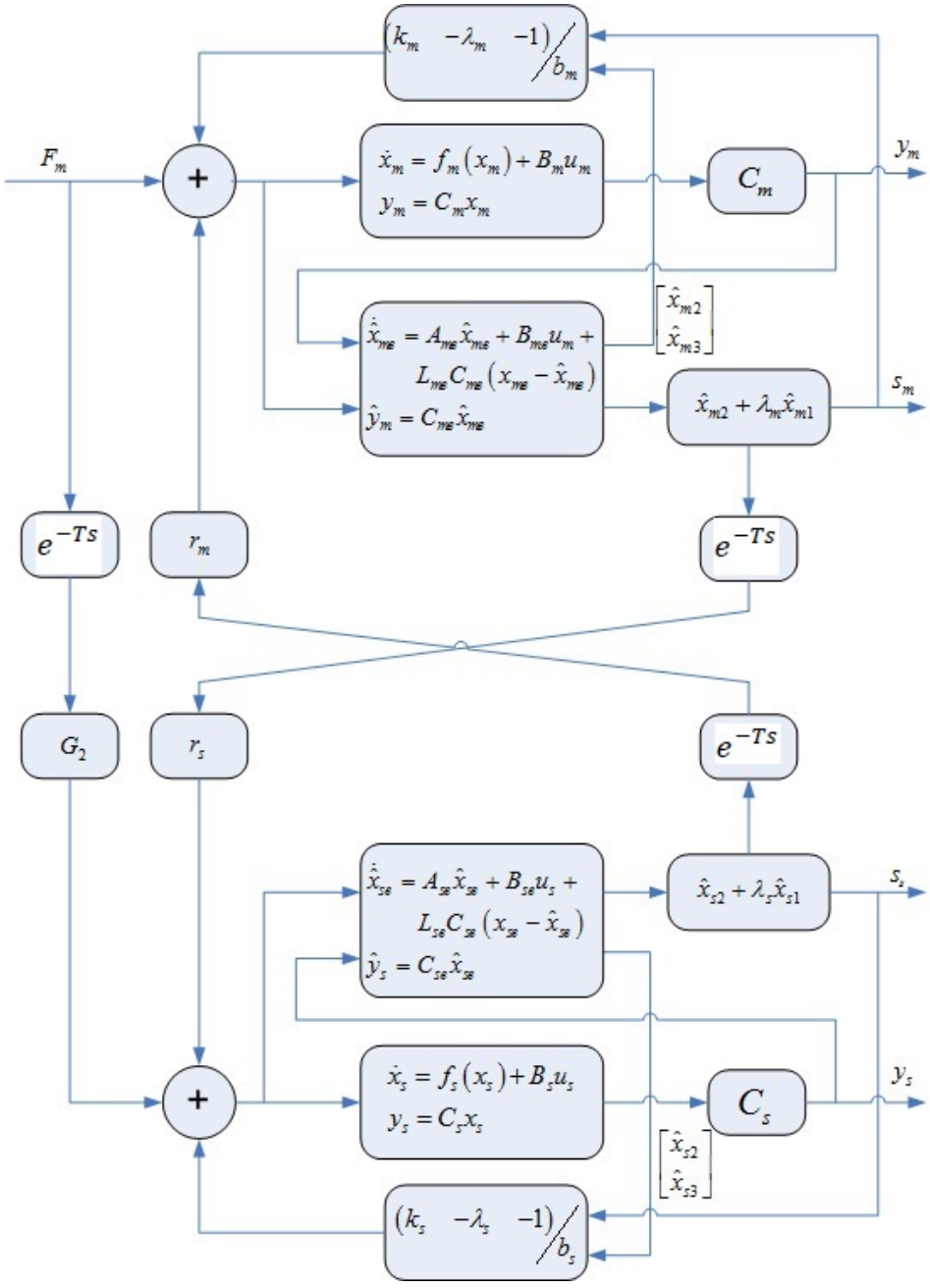

Figure 3.2: State convergence architecture incorporating disturbance observer

Considering the virtual extended system of Eq (3.6), we construct the real extended observer as:

$$\begin{aligned}\dot{\hat{x}}_{ze} &= A_{ze}\hat{x}_{ze} + B_{ze}u_z + L_{ze}C_{ze}\left(x_{ze} - \hat{x}_{ze}\right)\\ \hat{y}_z &= C_{ze}\hat{x}_{ze}\end{aligned} \tag{3.9}$$

In Eq (3.9), $\hat{x}_{ze}$ are the estimated states and L_{ze} is the observer gain given as $L_{ze} = \begin{bmatrix} l_{ze1} & l_{ze2} & l_{ze3} & \cdots & l_{zen} & l_{ze(n+1)} \end{bmatrix}^T$. Let us define the observer error for the master and slave system as:

$$e_{zo} = x_{ze} - \hat{x}_{ze} \tag{3.10}$$

Observer error dynamics can now be written using Eq (3.6), Eq (3.9) and Eq (3.10) as:

$$\dot{e}_{zo} = \left(A_{ze} - L_{ze}C_{ze}\right)e_{zo} + E_{ze}h_z \tag{3.11}$$

We now construct the bilateral state convergence controller using estimated states as:

$$u_m = -\frac{1}{b_m}\hat{x}_{me(n+1)} + K_m\hat{x}_m + R_m\hat{x}_s\left(t - T\right) + F_m \tag{3.12}$$

$$u_s = -\frac{1}{b_s}\hat{x}_{se(n+1)} + K_s\hat{x}_s + R_s\hat{x}_m\left(t - T\right) + G_2F_m\left(t - T\right) \tag{3.13}$$

By plugging Eq (3.12), Eq (3.13) in Eq (3.5) and using Eq (3.10), Eq (3.11) and noting ${}^{B_z}/_{b_z} = E_z$, closed loop augmented slave-master system is found to be:

$$\begin{bmatrix} I & A_{12\ell} \\ A_{2l} & I \end{bmatrix}\begin{bmatrix} \dot{x}_x \\ \dot{x}_m \end{bmatrix} = \begin{bmatrix} A_{11\alpha} & A_{12\alpha} \\ A_{21\alpha} & A_{22\alpha} \end{bmatrix}\begin{bmatrix} x_x \\ x_m \end{bmatrix} + \begin{bmatrix} A_{1e} & A_{12e} \\ A_{2ke} & A_{22e} \end{bmatrix}\begin{bmatrix} e_{ma} \\ e_{m\infty} \end{bmatrix} + \begin{bmatrix} 0 & A_{12\hbar} \\ A_{21\hbar} & 0 \end{bmatrix}\begin{bmatrix} h \\ h \\ h \end{bmatrix} + \begin{bmatrix} B_1 \\ B_2 \end{bmatrix}F_m \tag{3.14}$$

where, $A_{11a} = A_s + B_sK_s$, $A_{12a} = B_sR_s$, $A_{21a} = B_mR_m$, $A_{22a}= A_m + B_mK_m$,
$A_{11e} = -\begin{pmatrix} B_sK_s & -E_s \end{pmatrix}$, $A_{12e} = \begin{pmatrix} TB_sR_s & 0 \end{pmatrix}(A_{me} - L_{me}C_{me}) - \begin{pmatrix} B_sR_s & 0 \end{pmatrix}$,
$A_{21e} = \begin{pmatrix} TB_mR_m & 0 \end{pmatrix}(A_{se} - L_{se}C_{se}) - \begin{pmatrix} B_mR_m & 0 \end{pmatrix}$, $A_{22e} = -\begin{pmatrix} B_mK_m & -E_m \end{pmatrix}$,

$A_{12t} = TB_sR_s$, $A_{21t} = TB_mR_m$, $A_{12h} = \begin{pmatrix} TB_sR_s & 0 \end{pmatrix} E_{me}$,
$A_{21h} = \begin{pmatrix} TB_mR_m & 0 \end{pmatrix} E_{se}$, $B_1 = B_sG_2$, and $B_2 = B_m$.

By pre-multiplying Eq (3.14) by the inverse of matrix$\begin{bmatrix} I & A_{12t} \\ A_{21t} & I \end{bmatrix}$ and combining the resulting expression with the observer dynamics in Eq (3.11), we have:

$$\begin{bmatrix} \dot{x}_s \\ \dot{x}_m \\ \dot{e}_{so} \\ \dot{e}_{mo} \end{bmatrix} = \begin{bmatrix} A_{11} & A_{12} & A_{13} & A_{14} \\ A_{21} & A_{22} & A_{23} & A_{24} \\ 0 & 0 & A_{34} & 0 \\ 0 & 0 & 0 & A_{44} \end{bmatrix} \begin{bmatrix} x_s \\ x_m \\ e_{so} \\ e_{mo} \end{bmatrix} + \begin{bmatrix} B_{11} \\ B_{21} \\ 0 \\ 0 \end{bmatrix} F_m + \begin{bmatrix} E_{11} & E_{12} \\ E_{21} & E_{22} \\ E_{31} & 0 \\ 0 & E_{42} \end{bmatrix} \begin{bmatrix} h_s \\ h_m \end{bmatrix} \tag{3.15}$$

$A_{11} = A_{i1}A_{11a} + A_{i2}A_{21a}$, $A_{12} = A_{i1}A_{12a} + A_{i2}A_{22a}$, $A_{13} = A_{i1}A_{11e} + A_{i2}A_{21e}$, $A_{14} = A_{i1}A_{12e} + A_{i2}A_{22e}$, $A_{21} = A_{i3}A_{11a} + A_{i4}A_{12a}$, $A_{22} = A_{i3}A_{12a} + A_{i4}A_{22a}$, $A_{23} = A_{i3}A_{11e} + A_{i4}A_{21e}$, $A_{24} = A_{i3}A_{12e} + A_{i4}A_{22e}$, $A_{34} = A_{se} - L_{se}C_{se}$, $A_{44} = A_{me} - L_{me}C_{me}$, $B_{11} = A_{i1}B_1 + A_{i2}B_2$, $B_{21} = A_{i3}B_1 + A_{i4}B_2$, $E_{11} = A_{i2}A_{21h}$, $E_{12} = A_{i1}A_{12h}$, $E_{21} = A_{i4}A_{21h}$, $E_{22} = A_{i3}A_{12h}$, $E_{31} = E_{se}$, $E_{42} = E_{me}$, $A_{i1} = I + A_{12t}\Xi A_{21t}$, $A_{i2} = -A_{12t}\Xi$, $A_{i3} = -\Xi A_{21t}$, $A_{i4} = \Xi$, $\Xi = (I - A_{21t}A_{12t})^{-1}$. Following the method of state convergence, we replace the master system in (3.15) with the slave-master error system. To achieve this, we introduce the following linear transformation:

$$\begin{bmatrix} x_s \\ x_e \\ e_{so} \\ e_{mo} \end{bmatrix} = \begin{bmatrix} I & 0 & 0 & 0 \\ I & -I & 0 & 0 \\ 0 & 0 & I & 0 \\ 0 & 0 & 0 & I \end{bmatrix} \begin{bmatrix} x_s \\ x_m \\ e_{so} \\ e_{mo} \end{bmatrix} \tag{3.16}$$

The time derivative of Eq (3.16) in combination with Eq (3.15) yields the following augmented system:

$$\begin{bmatrix} \dot{x}_s \\ \dot{x}_e \\ \dot{e}_{so} \\ \dot{e}_{mo} \end{bmatrix} = \begin{bmatrix} \tilde{A}_{11} & \tilde{A}_{12} & \tilde{A}_{13} & \tilde{A}_{14} \\ \tilde{A}_{21} & \tilde{A}_{22} & \tilde{A}_{23} & \tilde{A}_{24} \\ 0 & 0 & \tilde{A}_{34} & 0 \\ 0 & 0 & 0 & \tilde{A}_{44} \end{bmatrix} \begin{bmatrix} x_s \\ x_e \\ e_{so} \\ e_{mo} \end{bmatrix} + \begin{bmatrix} \tilde{B}_{11} \\ \tilde{B}_{21} \\ 0 \\ 0 \end{bmatrix} F_m + \begin{bmatrix} \tilde{E}_{11} & \tilde{E}_{12} \\ \tilde{E}_{21} & \tilde{E}_{12} \\ \tilde{E}_{31} & 0 \\ 0 & \tilde{E}_{42} \end{bmatrix} \begin{bmatrix} h_s \\ h_m \end{bmatrix} \tag{3.17}$$

where$\tilde{A}_{11} = A_{11} + A_{12}$,$\tilde{A}_{12} = -A_{12}$,$\tilde{A}_{13} = A_{13}$,$\tilde{A}_{14}$= A_{14},$\tilde{A}_{21} = A_{11} - A_{21} + A_{12} - A_{22}$,$\tilde{A}_{22} = -A_{12} + A_{22}$,$\tilde{A}_{23} = A_{13} - A_{23}$,$\tilde{A}_{24} = A_{14} - A_{24}$,$\tilde{A}_{33} = A_{33}$,$\tilde{A}_{44} = A_{44}$,$\tilde{B}_{11} = B_{11}$,$\tilde{B}_{21} = B_{11} - B_{21}$,$\tilde{E}_{11} = E_{11}$,$\tilde{E}_{12} = E_{12}$,$\tilde{E}_{21} = E_{11} - E_{21}$,$\tilde{E}_{22} = E_{12} - E_{22}$,$\tilde{E}_{31} = E_{31}$,$\tilde{E}_{42} = E_{42}$. By eliminating the effect of the slave system's states and operator's force on the error system in Eq (3.17), we obtain the following n+1 design conditions:

$$\tilde{A}_{21} = 0, \tilde{B}_{21} = 0 \tag{3.18}$$

Note that the effect of observers' errors is ignored on the slave-master error system as fast dynamic behavior will be assigned to the observers. Further, the effect of disturbance terms is not considered in the design phase which can be associated with the slow varying nature of the disturbance [74], [75]. Now, by comparing the characteristic polynomial of the augmented system in Eq (3.17) with the desired polynomials, we have:

$$\begin{aligned}
\left| sI - \tilde{A}_{11} \right| &= s^n + p_{n-1}s^{n-1} + ... + p_1 s + p_0 \\
\left| sI - \tilde{A}_{22} \right| &= s^n + q_{n-1}s^{n-1} + ... + q_1 s + q_0 \\
\left| sI - \tilde{A}_{34} \right| &= s^n + r_{n-1}s^{n-1} + ... + r_1 s + r_0 \\
\left| sI - \tilde{A}_{44} \right| &= s^n + w_{n-1}s^{n-1} + ... + w_1 s + w_0
\end{aligned} \tag{3.19}$$

In Eq (3.19), p_i, q_i, r_i, w_i are coefficients of the desired polynomials for the slave, error, slave observer and master observer systems, respectively. Eq (3.18) and Eq (3.19) form together a set of $5n$+3 design conditions which can be solved to find $3n$+1 unknown controller gains (G_2, K_m, K_s, R_s) and $2n$+2 unknown observer (L_{se}, L_{me}) gains of the enhanced state convergence scheme.

3.3 Simulation Results

In order to validate the proposed disturbance observer-based state convergence controller, we perform simulations in MATLAB/Simulink environment by considering a single-degree-of-freedom master and slave systems as:

$$\begin{aligned}
\dot{x}_{z1} &= x_{z2} \\
\dot{x}_{z2} &= f_z\left(x_z\right) + u_z \\
f_z &= -a_{z1}\sin\left(x_{z1}\right) - a_{z2}x_{z2} + \left(b_z - 1\right)u_z
\end{aligned} \tag{3.20}$$

Thus, we have the following model for the design phase:

$$A_z = \begin{bmatrix} 0 & 1 \\ 0 & 0 \end{bmatrix}, B_z = \begin{bmatrix} 0 \\ 1 \end{bmatrix}, A_{ze} = \begin{bmatrix} 0 & 1 & 0 \\ 0 & 0 & 1 \\ 0 & 0 & 0 \end{bmatrix}, B_{ze} = \begin{bmatrix} 0 \\ 1 \\ 0 \end{bmatrix} \tag{3.21}$$

We assume various parameters of the teleoperation system as [73]:

$$\begin{aligned} &a_{m1} = 1, a_{m2} = 7.1429 \\ &a_{s1} = 0.5, a_{s2} = 6.25 \\ &b_m = 0.2656, b_s = 0.2729, T = 0.2s \\ &k_f = 1, k_e = 20Nm/rad, b_e = 0.1Nms/rad \end{aligned} \tag{3.22}$$

Further, we select the coefficients of polynomials in Eq (3.19) as:

$$\begin{aligned} &p_0 = 2, p_1 = 15 \\ &q_0 = 64, q_1 = 16 \\ &r_0 = w_0 = 27000 \\ &r_1 = w_1 = 2700 \\ &r_2 = w_2 = 90 \end{aligned} \tag{3.23}$$

Now, by solving the design conditions [175] and [113], we obtain the controller and observer gains as:

$$\begin{aligned} &G_2 = 1.3436, K_m = \begin{bmatrix} -40.40 & -11.40 \end{bmatrix}, K_s = \begin{bmatrix} -15.4079 & -20.7101 \end{bmatrix} \\ &R_s = \begin{bmatrix} 7.9981 & 1.8524 \end{bmatrix}, L_{me} = L_{se} = \begin{bmatrix} 90 & 2700 & 27000 \end{bmatrix}^T \end{aligned} \tag{3.24}$$

Note that control gains K_s in Eq (3.24) contains the environment information also, as pointed out in section 3.1. In the absence of such information, a steady-state error will exist between the master and slave positions as the slave interacts with the environment. We now perform simulations of a time-delayed nonlinear teleoperation system under the control gains of Eq (3.24), and the results are depicted in Figure 3.3, Figure 3.4, Figure 3.5. It can be seen that disturbance is well-estimated by the observer, and the slave is following the master system. In addition, environmental

force is also reflected to the operator whose amount can be adjusted through the coefficient p_0.

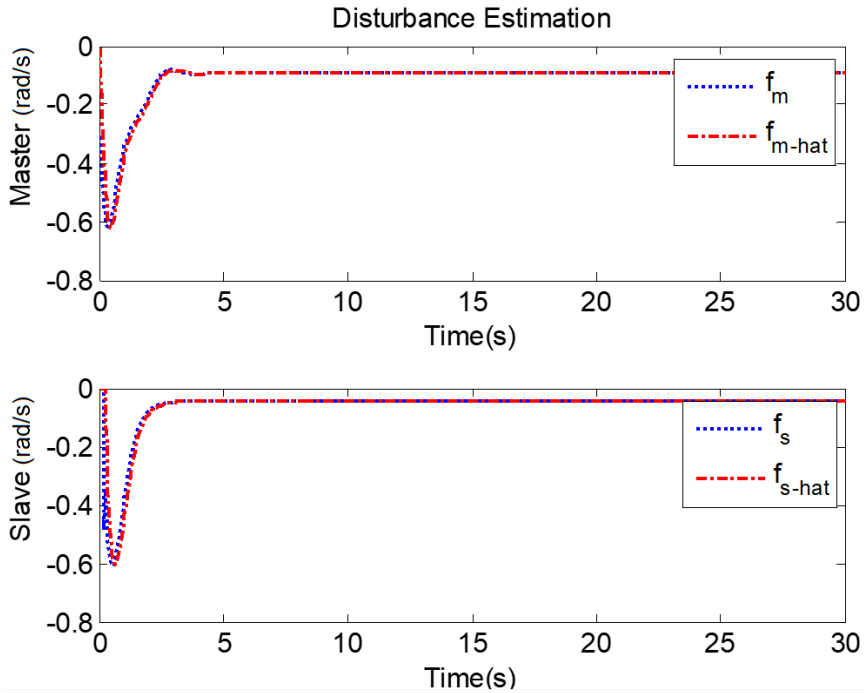

Figure 3.3: Disturbance estimation

Comparison of Proposed Scheme with RBFNN

In order to show some advantage of the proposed scheme, a comparison has been made with a recently proposed tele-controller based on radial basis function neural network (RBFNN) [35]. For the sake of completeness, we mention the RBFNN based control laws here:

$$\begin{aligned} u_z &= l_z s_z + \hat{W}_z h_z\left(x_z\right) + \eta_z sgn\left(s_z\right) - \tau_z, z = m, s \\ s_z &= \dot{e}_z + k_z e_z, z = m, s \\ \dot{\hat{W}}_z &= \tfrac{1}{\delta_z} s_z h_z\left(x_z\right), z = m, s \end{aligned} \tag{3.25}$$

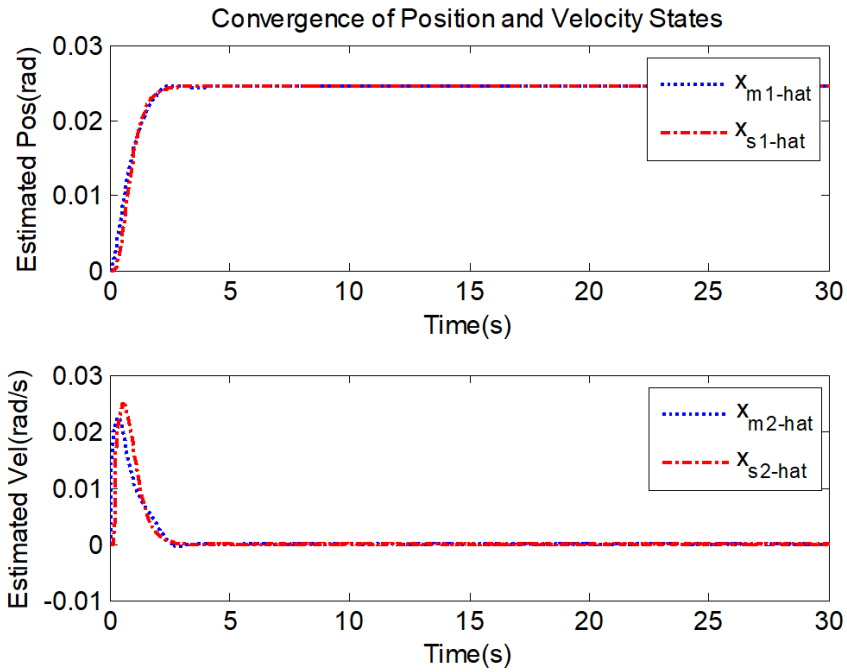

Figure 3.4: Estimated position and velocity states

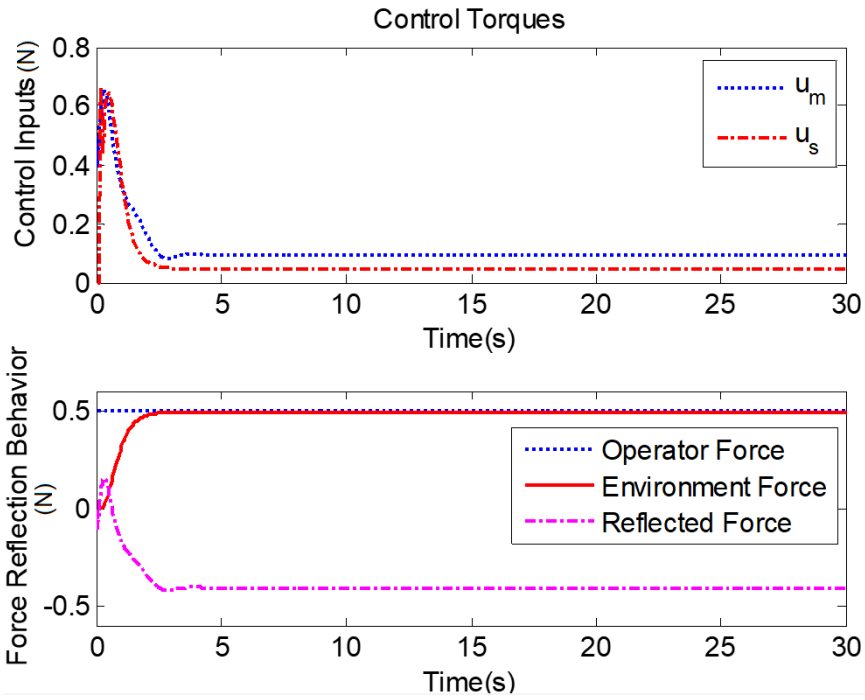

Figure 3.5: Control input torques and force reflection behavior

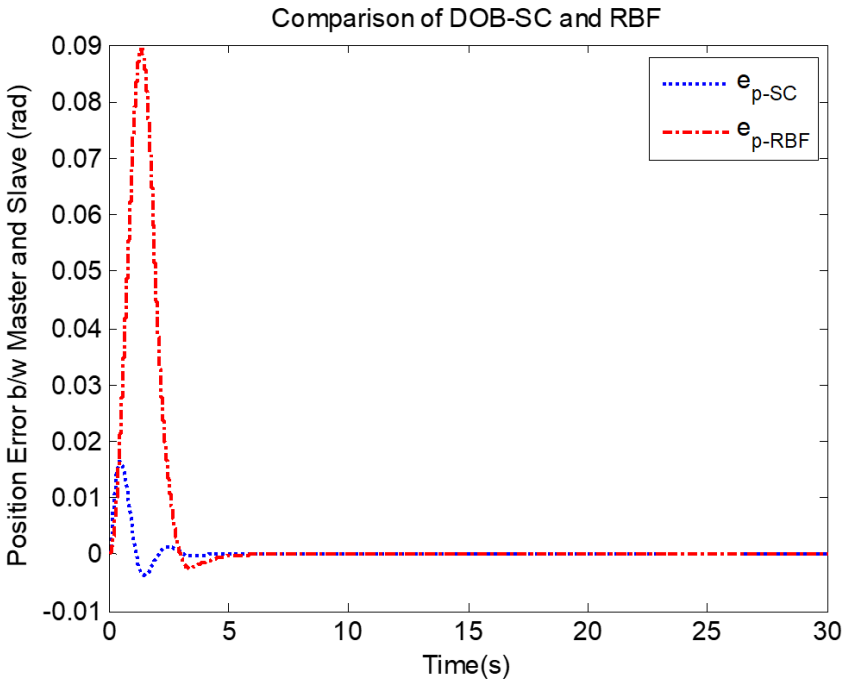

Figure 3.6: Comparison of proposed scheme and RBFNN

By using different parameters of RBFNN controllers as:

$$\begin{aligned}
&\eta_m = \eta_s = 0.25, \\
&\delta_m = \delta_m = 0.05, \\
&l_m = l_s = 15, k_m = k_s = 15, \\
&\tau_f = 0.025, sat = \pm 0.05, n = 5 \\
&b_j = 0.5, C_i = -1 : 0.5 : 1 \\
&M_r = 1, C_r = 4, G_r = 4,
\end{aligned} \tag{3.26}$$

We simulate the same time-delayed telerobotic system under the control of Eq (3.25). Various states recorded in Figure 3.6 depict the position error between the master and slave systems yielded by both the proposed and RBFNN controllers. It can be seen that the proposed controller offers better transient performance as compared to the RBFNN controller for the same final master position. However, the proposed controller is only valid for constant time delays.

3.4 Experimental Results

Finally, we perform some semi-real-time experiments in QUARC/Simulink environment using the geomagic haptic device. To this end, the haptic device is operated along the x-axis to generate a varying time force for the teleoperation system running in the Simulink environment. This force is governed by the relation $F_m(t) = k_{op}(x_{op}(t) - x_0)$. Here, the scaling factor is assumed to be $k_{op} = 5$ while the operator's position (x_{op}) lies in the range $[0.1, 0.2]$ which corresponds to the motion of the link between points '2' and '8' on the cardboard, as shown in Figure 3.7 and Figure 3.8. The proposed controller parameters are presented in Table 3.1.

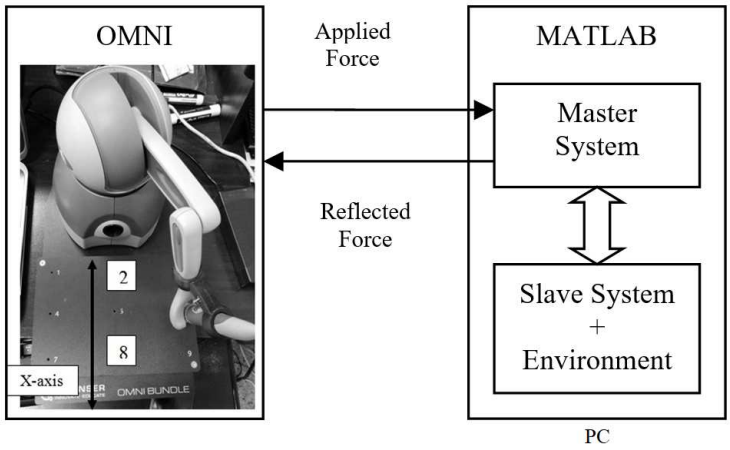

Figure 3.7: Experimental framework: layout

Further, the Simulink model is designed such that the reflected force, as generated by the proposed controller, is also directed to the haptic device. In this way, the loop is closed around the operator as he will be able to feel the slave's interaction with the environment. Now, by using the control gains of Eq (3.24), the nonlinear time-delayed teleoperation system is run under the control of the haptic device, and the results are shown in Figure 3.9, Figure 3.10 and Figure 3.11.

It can be seen that the observer has remained successful in estimating the disturbance and the observer-based controller has established the convergence of master and slave states. Further, environmental force is also felt by the operator. These results suggest that the proposed methodology has indeed enhanced the capability of state convergence architecture to deal with uncertain nonlinear teleoperation systems.

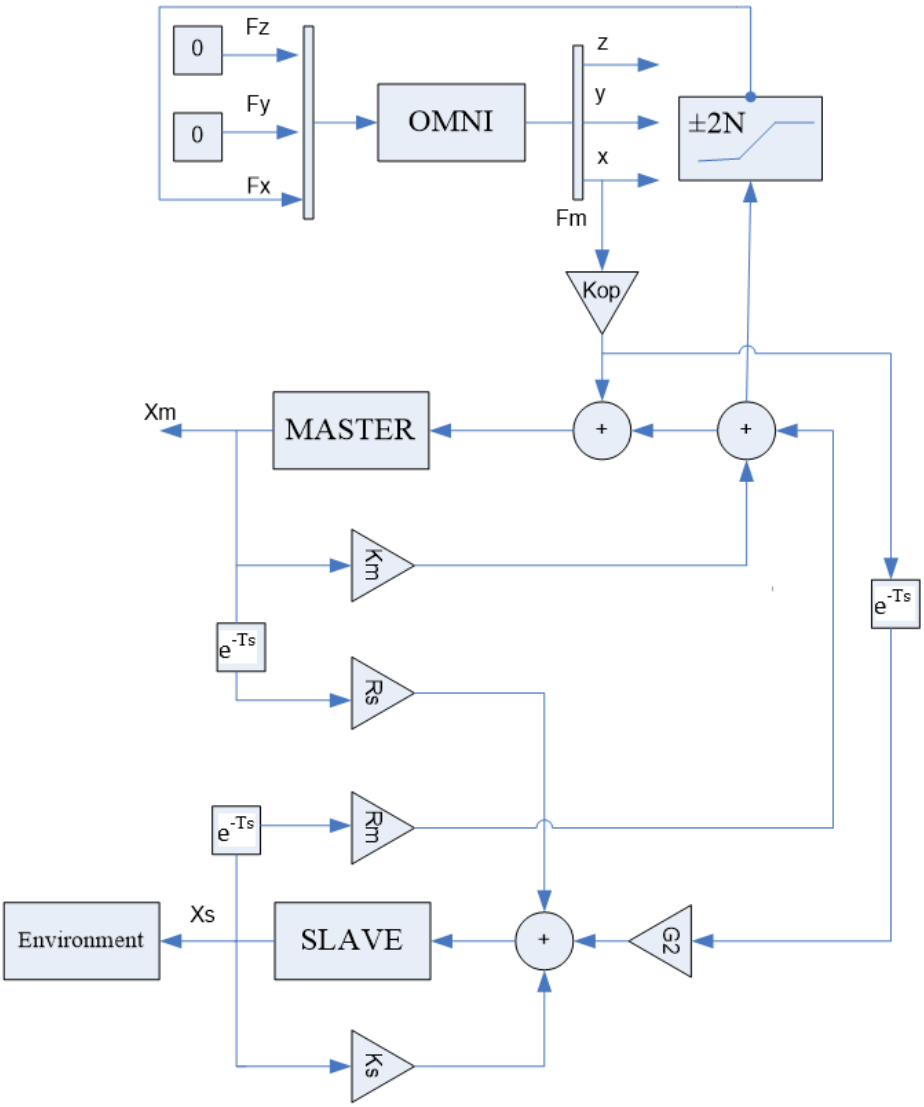

Figure 3.8: Experimental framework: More detailed view (observer part is not shown for simplicity

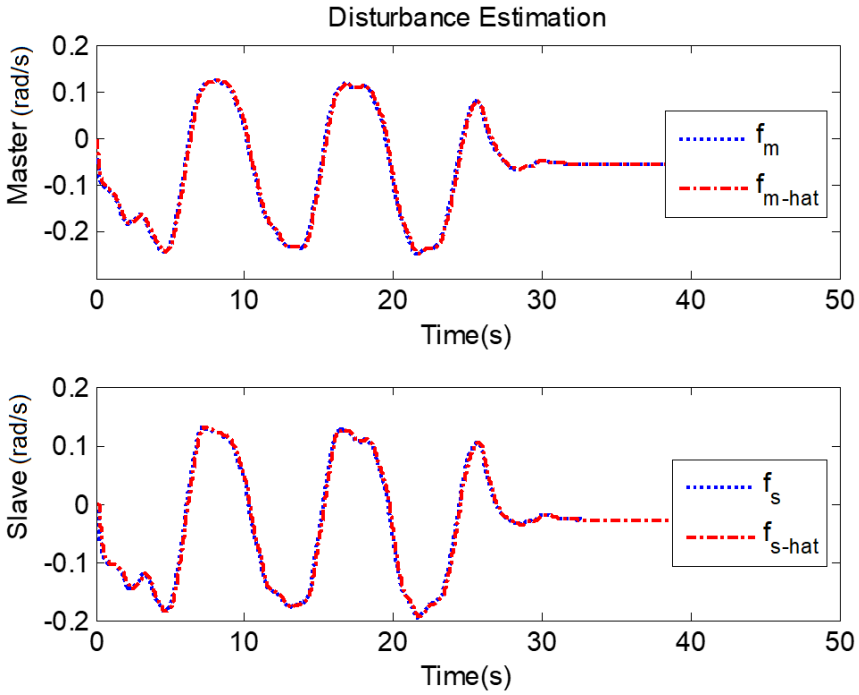

Figure 3.9: Experimental results: disturbance estimation

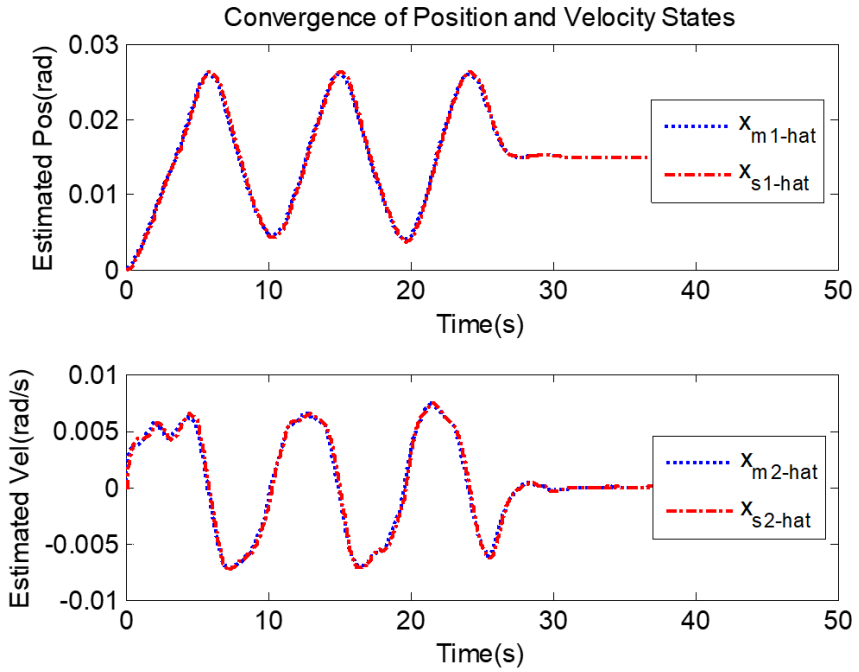

Figure 3.10: Experimental results: estimated position and velocity states

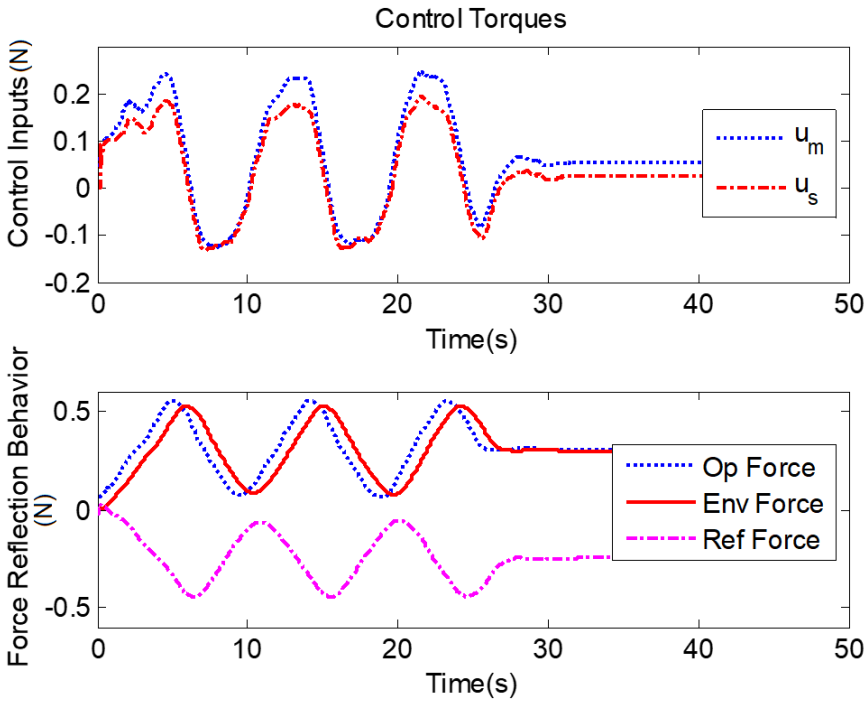

Figure 3.11: Experimental results: control input torques and force reflection behavior

Controller	Simulation in MATLAB/Simulink	Semi Real-time QUARC/Simulink
System	1-DoF (Master/Slave)	1-DoF (Master/Slave)
Operator Force (N)	0.5 (constant)	Time-varying force using Omni Bundle
Environment Stiffness k_e (Nm/rad)	20	20
Environment Damping b_e (Nm/rad)	0.1	0.1
Feedback gain K_f	1	1
Scaling factor K_{op}	0	5
Time delay (Sec)	0.2	0.2

Table 3.1: Proposed controller parameters for simulation and semi-real time experiment

3.5 Conclusion

This chapter introduced an enhancement in the state convergence architecture for bilateral teleoperation systems through the use of disturbance observers. The proposed scheme suggests treating uncertainties in the master and slave systems as disturbances and employing extended state observers to estimate them. State convergence control

laws are then updated with these estimates. Closed loop stability of the teleoperation system is finally established by following the method of state convergence. To validate the proposal, simulations and semi-real-time experiments are also performed in MATLAB/Simulink environment by considering a single-degree-of-freedom nonlinear time-delayed teleoperation system. Future work involves designing and integrating the operator and environment estimation laws in the proposed framework with the consideration of time-varying delays in the communication channel.

Chapter 4

Disturbance Observer Supported Fuzzy-Model-Based Bilateral Control Architecture

This chapter presents a disturbance observer-supported Takagi-Sugeno (TS) fuzzy model-based control scheme for uncertain systems. The baseline controller is a guaranteed performance fuzzy-model-based parallel distributed controller (PDC) constructed using the nominal system's parameters. The model approximation error and parametric uncertainties are treated as a lumped disturbance and a nonlinear disturbance observer (NDOB) is introduced to counter the lumped disturbance. The applicability of the proposed scheme is demonstrated in the bilateral control of a nonlinear teleoperation system in MATLAB/Simulink/QUARC environment through simulations as well as semi-real-time experiments.

4.1 TS Fuzzy Modeling

Consider an affine n^{th} order single input single output (SISO) nonlinear system as:

$$\begin{aligned} \dot{x}_1 &= x_2 \\ \dot{x}_2 &= x_3 \\ &\vdots \\ \dot{x}_n &= f_n(x) + g_n(x)\,u + \Delta f(x) + \Delta g(x)\,u \end{aligned} \tag{4.1}$$

where $f_n(x)$ and $g_n(x)$ are nonlinear functions with nominal system parameters while $\Delta f(x) = f(x) - f_n(x)$, $\Delta g(x) = g(x) - g_n(x)$ represent the respective uncertainties.

An 'r' rule TS fuzzy model of nonlinear system in Eq (4.1) can be constructed as:

$$\begin{aligned} \dot{x}_1 &= x_2 \\ \dot{x}_2 &= x_3 \\ &\vdots \\ \dot{x}_n &= \textstyle\sum_{i=1}^{r} h_i(z) \sum_{j=1}^{n} -a_{ij}x_j + b_{i1}u + \delta \end{aligned} \tag{4.2}$$

where $h_i(z)$ is normalized firing strength of i^{th} fuzzy rule i.e. $h_i(z) = \mu_i(z) / \sum_{i=1}^{r} \mu_i$ and $\mu_i(z)$ is determined as minimum of the degrees of memberships of $z_j(x)$ $(j = 1, 2, ..., l)$ in fuzzy set A_{ij} for the i^{th} rule i.e. $\mu_i(z) = A_{i1}(z_1) \times A_{i2}(z_2) \times \ldots \times A_{il}(z_l)$. Note that $z_j(x)\,(j = 1, 2, ..., l)$ is a scheduling variable. In Eq (4.2), δ contains the modeling error and uncertainties as:

$$\delta = \left((f_n(x) + g_n(x)\,u) - \left(\sum_{i=1}^{r} h_i(x) \sum_{j=1}^{n} -a_{ij}x_j + b_{i1}u \right) \right) + (\Delta f(x) + \Delta g(x)\,u) \tag{4.3}$$

In Eq (4.3), the first term on the right-hand side is the model approximation error while the second term includes parametric uncertainties.

4.2 Integrated NDOB TS Fuzzy Controller

We integrate an NDOB with a baseline TS fuzzy PDC controller of [86]. This PDC controller provides the desired closed-loop performance by introducing time-invariant coefficients. However, parametric uncertainties are not considered in the design procedure. To address this limitation, we propose to integrate an NDOB that can estimate the lumped disturbances and ensures robust closed-loop performance. NDOB-based fuzzy PDC controller is proposed as:

$$u = -\sum_{i=1}^{r} h_i(z) \sum_{j=1}^{n} \frac{d_{ij}}{b_{i1}} x_j - \hat{\delta} \tag{4.4}$$

$$\begin{cases} \hat{\delta} = \xi - \lambda x_n \\ \dot{\xi} = \lambda \left(\hat{\delta} - \sum_{i=1}^{r} h_i(z) \sum_{j=1}^{n} a_{ij}x_j + b_{i1}u \right) \end{cases} \tag{4.5}$$

In Eq (4.4), the denominator part of the control law, b_{i1} is a known nominal plant parameter while the numerator part, d_{ij} is to be designed against a desired closed-loop performance. In Eq (4.5), λ is a negative constant whose magnitude can be selected to be sufficiently large. By substituting Eq (4.4) in Eq (4.2), we obtain the closed loop system as:

$$\begin{aligned} \dot{x}_1 &= x_2 \\ \dot{x}_2 &= x_3 \\ &\vdots \\ \dot{x}_n &= -\sum_{i=1}^{r} h_i(z) \sum_{j=1}^{n} (d_{ij} + a_{ij})\, x_j + \delta_e \end{aligned} \tag{4.6}$$

In Eq (4.6), δ_e is the disturbance estimation error:

$$\delta_e = \delta - \hat{\delta} \tag{4.7}$$

Let $c_j, j = 1, 2, ..., n$ be the coefficients that do not depend upon the time-varying membership functions, i.e.:

$$c_j = d_{ij} + a_{ij}, j = 1, 2, ..., n \tag{4.8}$$

By substituting Eq (4.8) in Eq (4.6), we obtain the differential equation representation of the closed-loop system as:

$$x^{(n)} + c_n x^{(n-1)} + ... + c_2 \dot{x} + c_1 x = \delta_e \tag{4.9}$$

Now the coefficients $c_j, j = 1, 2, ..., n$ can be chosen according to the desired dynamic response, and the fuzzy implemental gains can then be determined using Eq (4.8). Eq (4.9) implies that regulation error is governed by the estimation error of NDOB. Thus, bound on the estimation error translates to the performance of the fuzzy PDC regulator. Estimation error dynamics can be written as:

$$\dot{\delta}_e = \lambda \delta_e + \dot{\delta} \tag{4.10}$$

Provided that disturbance and its derivative are bounded as $\|\delta\| \leq \phi_1$, $\left\|\dot{\delta}\right\| \leq \phi_2$, we can find a bound on the disturbance estimation error as in [186]:

$$\delta_e = e^{\lambda t}\delta_{e0} + \int_0^t e^{\lambda(t-\tau)}\dot{\delta}(\tau) \tag{4.11}$$

$$\begin{aligned} &\leq \varepsilon\phi_1 e^{\lambda t} + \varepsilon\phi_2 \int_0^t e^{\lambda(t-s)} ds \\ &= \varepsilon\phi_1 e^{\lambda t} + \frac{\varepsilon\phi_2}{\lambda}\left(e^{\lambda t} - 1\right) \end{aligned} \tag{4.12}$$

4.3 Application to Bilateral Teleoperation

Bilateral teleoperation is a key framework to allow human interaction with a remote environment by providing the force feedback present in the remote environment. Over the decades, many algorithms have been proposed to improve the time delay present in the communication channel, uncertainties related to the environment, and modeling errors, and improve decision support mechanisms [113], [14].

Consider a single-degree-of-freedom teleoperation system as:

$$\begin{aligned} J_m\ddot{\theta}_m + B_m\dot{\theta}_m + m_m g l_m \sin\theta_m &= u_m \\ J_s\ddot{\theta}_s + B_s\dot{\theta}_s + m_s g l_s \sin\theta_s &= u_s \end{aligned} \tag{4.13}$$

Let the state variables be $x_1 = \theta, x_2 = \dot{\theta}$. By selecting the scheduling variable as $z = \sin(x_1/x_1)$ and using the nominal system parameters, a two-rule TS fuzzy model of a system described by Eq (4.13) is constructed as:

$$\begin{aligned} \dot{x}_{m1} &= x_{m2} \\ \dot{x}_{m2} &= -\sum_{i=1}^{2} h_{mi}(z_m) \tfrac{m_{mn} g l_{mn}}{J_{mn}} z_{mi} x_{m1} - \tfrac{B_{mn}}{J_{mn}} x_{m2} + \tfrac{1}{J_{mn}} u_m + \delta_m \end{aligned} \tag{4.14}$$

$$\begin{aligned} \dot{x}_{s1} &= x_{s2} \\ \dot{x}_{s2} &= -\sum_{i=1}^{2} h_{si}(z_s) \tfrac{m_{sn} g l_{sn}}{J_{sn}} z_{si} x_{s1} - \tfrac{B_{sn}}{J_{sn}} x_{s2} + \tfrac{1}{J_{sn}} u_s + \delta_s \end{aligned} \tag{4.15}$$

The degrees of memberships in Eq (4.14) and Eq (4.15) are computed as:

$$\begin{aligned} \mu_1(z) &= \begin{cases} 1 & , x_1 = 0 \\ \frac{z - z_{\min}}{z_{\max} - z_{\min}} & , x_1 \neq 0 \end{cases} \\ \mu_2(z) &= 1 - \mu_1(z) \end{aligned} \tag{4.16}$$

where minimum value of the scheduling variable ($z_{\min} = 0.827$) corresponds to the link operation around $x_1 = \pi/3$ while maximum value ($z_{\max} = 1$) corresponds to the operation around $x_1 = 0$. The definition and numerical values of different master and slave systems' parameters in Eq (4.13) - Eq (4.15) are provided in Table 4.1.

To establish bilateral communication between the master and slave systems, the method of state convergence is used and proposed NDOB fuzzy PDC regulators are deployed on both sides, as shown in Figure 4.1. Observer-based control laws for the master and slave sides are defined as:

$$u_m = J_{mn} \sum_{i=1}^{2} h_i(z_m) \sum_{j=1}^{2} d_{mij} x_{mj} + \sum_{j=1}^{2} r_{mj} x_{sj}(t - T) + F_m - J_{mn}\hat{\delta}_m \tag{4.17}$$

$$\begin{cases} \hat{\delta}_m = \xi_m - \lambda_m x_{m2} \\ \dot{\xi}_m = \lambda_m \left(\hat{\delta}_m - \sum_{i=1}^{2} h_{mi} \frac{m_{mn} g l_{mn}}{J_{mn}} z_{mi} x_{m1} - \frac{B_{mn}}{J_{mn}} x_{m2} + \frac{1}{J_{mn}} u_m \right) \end{cases} \tag{4.18}$$

Table 4.1: Numerical values for fuzzy controller parameters

No	Definition of Master/Slave Parameters	Actual Value	Nominal Value
1	Mass of master link (kg)	$m_m = 2.2$	$m_{mn} = 2.0$
2	Length of master link (m)	$l_m = 0.35$	$l_{mn} = 0.5$
3	Inertial of master link (kg-m^2)	$J_m = 0.0898$	$J_{mn} = 0.16$
4	Viscous friction coefficient of master link (Nms/rad)	$B_m = 5.2$	$B_{mn} = 5.0$
5	Mass of slave link (kg)	$m_s = 7.8$	$m_{sn} = 80.$
6	Length of slave link (m)	$l_s = 0.75$	$l_{sn} = 1.0$
7	Inertial of slave link (kg-m^2)	$J_s = 1.4625$	$J_{sn} = 2.6$
8	Viscous friction coefficient of slave link (Nms/rad)	$B_s = 10.5$	$B_{sn} = 10.0$
9	Acceleration due to gravity (m/s^2)	$g = 9.8$	$g = 9.8$

$$u_n = J_{sn} \sum_{i=1}^{2} h_i(z_n) \sum_{j=1}^{2} d_{sij} x_{nj} + \sum_{j=1}^{n} r_{sj} x_{mj}(t-T) + g_2 F_m(t-T) - J_{sn} \dot{\hat{\delta}}_s \tag{4.19}$$

$$\begin{cases} \hat{\delta}_s = \xi_s - \lambda_s x_{s2} \\ \dot{\xi}_s = \lambda_s \left(\hat{\delta}_s - \sum_{i=1}^{2} h_{si} \frac{m_{smgll_m}}{J_m} z_{ni} x_{s1} - \frac{B_{mi}}{J_{n+1}} x_{n2} + \frac{1}{J_{mm}} u_s \right) \end{cases} \tag{4.20}$$

The definition of various parameters in these control laws is included in Table 4.2. With the help of the above control laws, closed-loop master and slave systems are computed, and time-invariant coefficients are introduced, as described above:

$$c_{mj} = d_{mij} - a_{mij}, c_{sj} = d_{sij} - a_{sij} \tag{4.21}$$

where $a_{i1} = m_n g l_n z_i / J_n$ and $a_{i2} = B_n / J_n$. The resulting closed-loop master and slave systems are now in a suitable form for the method of state convergence to be applicable. Interested readers are referred to [160], [161] for details on this bilateral

scheme. To determine the control gains of the scheme including the NDOB-integrated fuzzy PDC regulators, the following design conditions need to be solved:

$$g_2 \left(J_{mn} + Tr_{m2}\right) - \left(J_{sn} + Tr_{s2}\right) = 0 \tag{4.22}$$

$$\left(J_{mn} + Tr_{m2}\right)\left(r_{s1} + c_{s1}J_{sn}\right) - \left(J_{sn} + Tr_{s2}\right)\left(r_{m1} + c_{m1}J_{mn}\right) = 0 \tag{4.23}$$

$$\begin{aligned} &\left(J_{mn} + Tr_{m2}\right)\left(r_{s2} + c_{s2}J_{sn}\right) - \left(J_{sn} + Tr_{s2}\right)\left(r_{m2} + c_{m2}J_{mn}\right) \\ &-T\left(J_{mn} + Tr_{m2}\right)r_{s1} + T\left(J_{sn} + Tr_{s2}\right)r_{m1} = 0 \end{aligned} \tag{4.24}$$

$$J_{mn}\left(r_{s1} + J_{sn}c_{s1} - Tr_{s2}c_{m1}\right) + p_1\left(J_{mn}J_{sn} - T^2 r_{m2}r_{s2}\right) = 0 \tag{4.25}$$

$$\begin{aligned} &J_{mn}r_{s2} - Tr_{s2}r_{m2} + J_{mn}J_{sn}c_{s2} - TJ_{mn}r_{s2}c_{m2} - TJ_{mn}r_{s1} + T^2 r_{s2}r_{m1} \\ &+p_2\left(J_{mn}J_{sn} - T^2 r_{m2}r_{s2}\right) = 0 \end{aligned} \tag{4.26}$$

$$\left(J_{mn} + Tr_{m2}\right)r_{s1} - J_{mn}\left(J_{sn} + Tr_{s2}\right)c_{m1} - q_1\left(J_{mn}J_{sn} - T^2 r_{m2}r_{s2}\right) = 0 \tag{4.27}$$

$$\left(J_{mn} + Tr_{m2}\right)\left(r_{s2} - Tr_{s1}\right) - J_{mn}\left(J_{sn} + Tr_{s2}\right)c_{m2} - q_2\left(J_{mn}J_{sn} - T^2 r_{m2}r_{s2}\right) = 0 \tag{4.28}$$

Table 4.2: Parameters of fuzzy state convergence scheme

No	Parameters	Description
1	F_m	Operators force
2	G_2	Force feed-forward gain
3	$R_m = \begin{bmatrix} r_{m1} & r_{m2} \end{bmatrix}$ $r_{m1} = k_f k_e, r_{m2} = k_f b_e$	Force feedback gain vector
4	$C_m = \begin{bmatrix} c_{m1} & c_{m2} \end{bmatrix}$	Stabilizing gain for the master
5	$C_s = \begin{bmatrix} c_{s1} & c_{s2} \end{bmatrix}$	Stabilizing gain for the slave
6	$D_{m1} = \begin{bmatrix} d_{m11} & d_{m12} \end{bmatrix}$ $D_{m2} = \begin{bmatrix} d_{m21} & d_{m22} \end{bmatrix}$	Fuzzy implemental gains for master
7	$D_{s1} = \begin{bmatrix} d_{s11} & d_{s12} \end{bmatrix}$ $D_{s2} = \begin{bmatrix} d_{s21} & d_{s22} \end{bmatrix}$	Fuzzy implemental gains for slave
8	$R_s = \begin{bmatrix} r_{s1} & r_{s2} \end{bmatrix}$	Effect of master's motion in slave
9	T	Time delay of communication channel

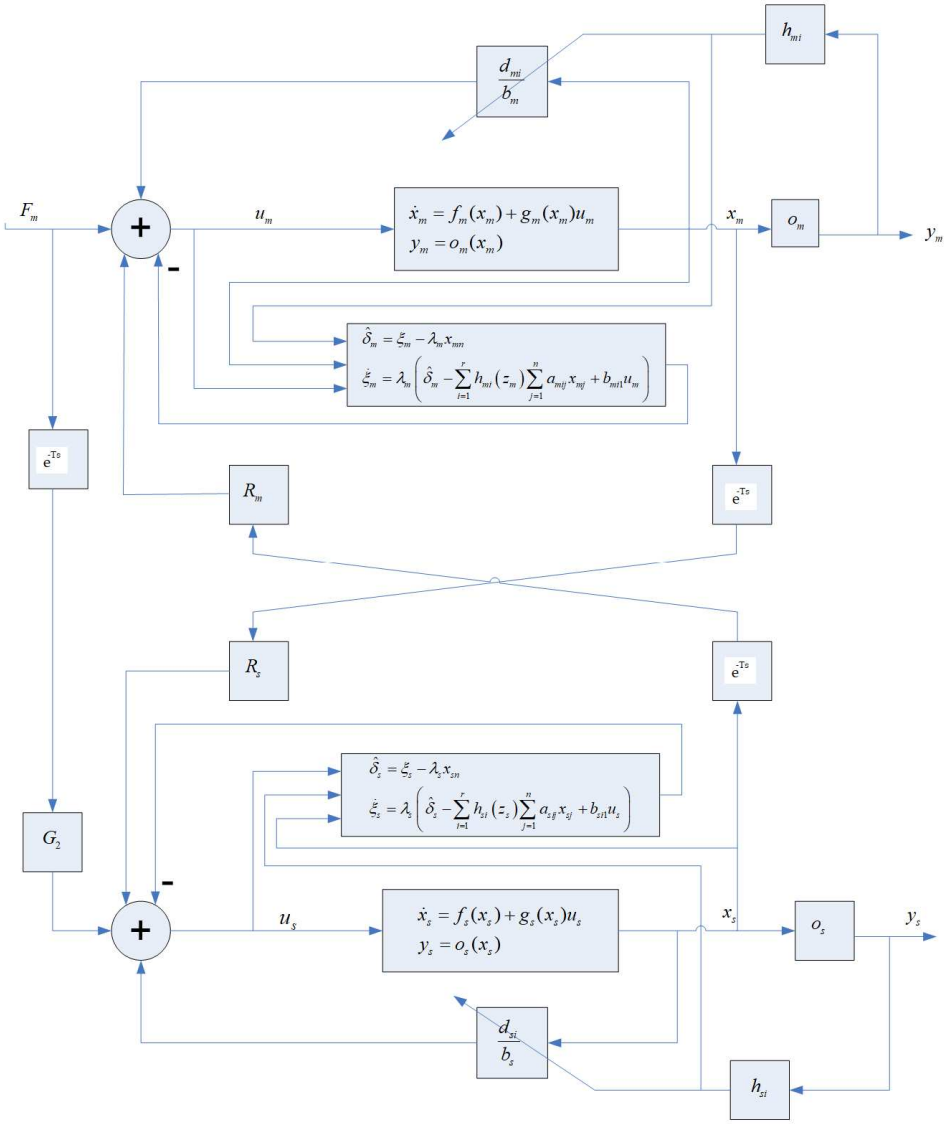

Figure 4.1: NDOB based fuzzy-model-based state convergence controller for bilateral teleoperation system

4.4 Simulation Results

By assuming the stiffness of the environment as $k_e = 5Nm/rad$ with $k_f = 0.1$ and selecting the desired response of the slave as well as error systems as $s^2+20s+100 = 0$ ($p_1 = q_1 = p_2 = q_2 = -10$), we obtain following control gains as a solution of Eq (4.22) and Eq (4.28).

$$\begin{aligned} c_{m1} &= -103.00, c_{m2} = -19.70 \\ c_{s1} &= -97.0, c_{s2} = -20.30 \\ r_{s1} &= -8, r_{s2} = 0, g_2 = 16 \end{aligned} \tag{4.29}$$

Control gains for fuzzy PDC regulators are derived using Eq (4.21) along with nominal parameters as:

$$\begin{aligned} d_{m11} &= -44.14, d_{m12} = 10.30 \\ d_{m21} &= -54.32, d_{m22} = 10.30 \\ d_{s11} &= -67.57, d_{s12} = -16.55 \\ d_{s21} &= -72.66, d_{s22} = -16.55 \end{aligned} \tag{4.30}$$

We now simulate fuzzy PDC-driven bilateral teleoperation by applying a constant operator's force of 1N. First, an uncertain teleoperation system is run without utilizing NDOB, and the system response is plotted in Figure 4.2. It can be seen that position error exists between the master and slave systems due to the discrepancy in actual and nominal parameters. Also, differences can be seen in the desired and actual slave responses.

Now, NDOB ($\lambda_m = \lambda_s = -50$) is switched on and simulation results are depicted in Figure 4.3 - Figure 4.6. It can be seen that NDOB based fuzzy PDC regulator recovers the performance as the slave tracks the master with zero steady-state error and exhibits the desired behavior. Disturbances on the master and slave sides are well estimated and compensated by NDOB as displayed in Figure 4.5 and Figure 4.6. Results in Figure 4.2 and Figure 4.3 - Figure 4.6 also serve the purpose of comparison of proposed disturbance observer-based fuzzy PDC technique with fuzzy PDC. Comparison with other fuzzy PDC techniques involving disturbance observer is not provided as they do not offer desired dynamic performance and thus state convergence controller with desired slave response cannot be constructed to establish bilateral communication.

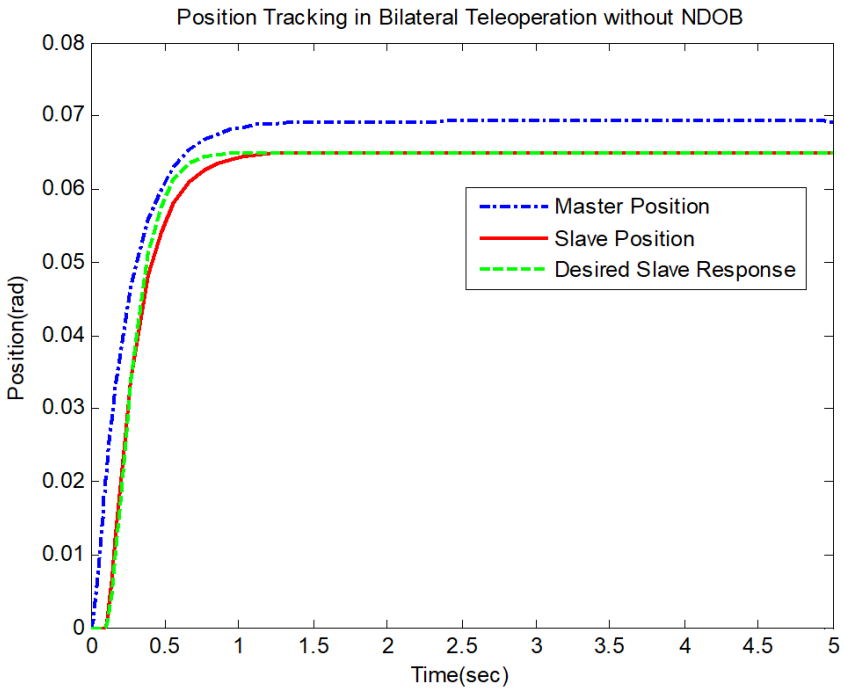

Figure 4.2: Fuzzy model-based state convergence convergence controller under parameter variations without NDOB [31]

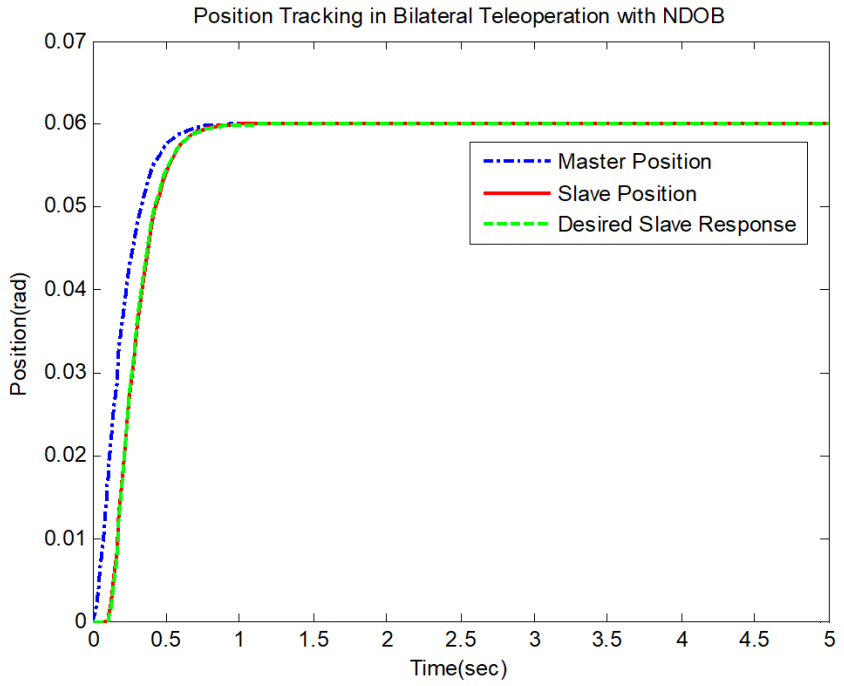

Figure 4.3: NDOB-integrated fuzzy model-based control: position tracking

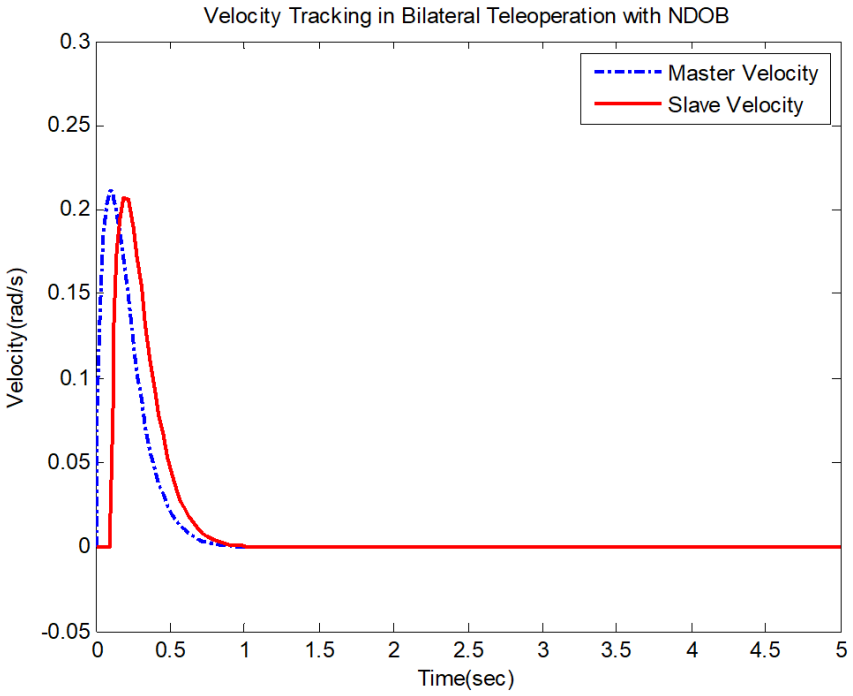

Figure 4.4: NDOB-integrated fuzzy model-based control: velocity tracking

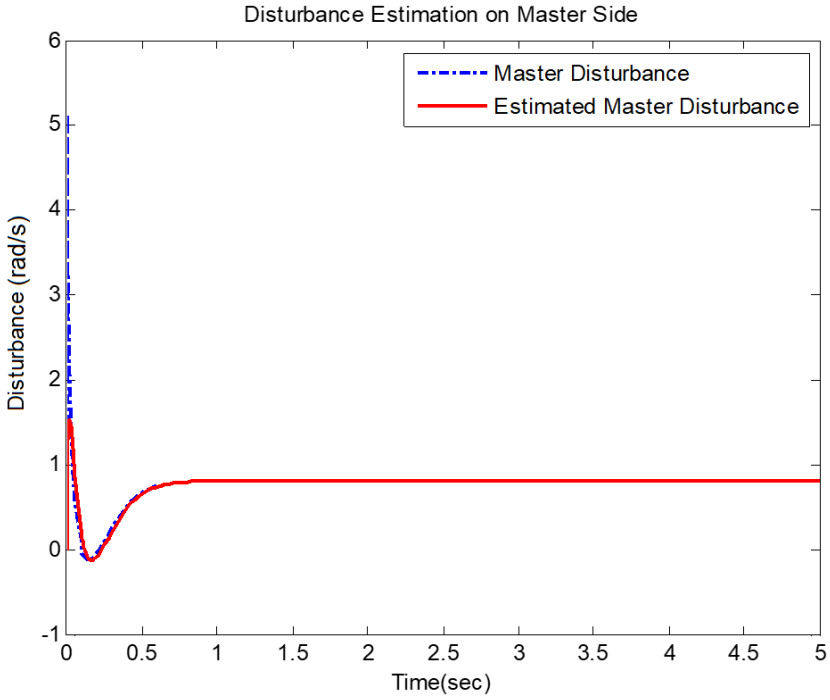

Figure 4.5: NDOB-integrated fuzzy model-based control: disturbance estimation on master side

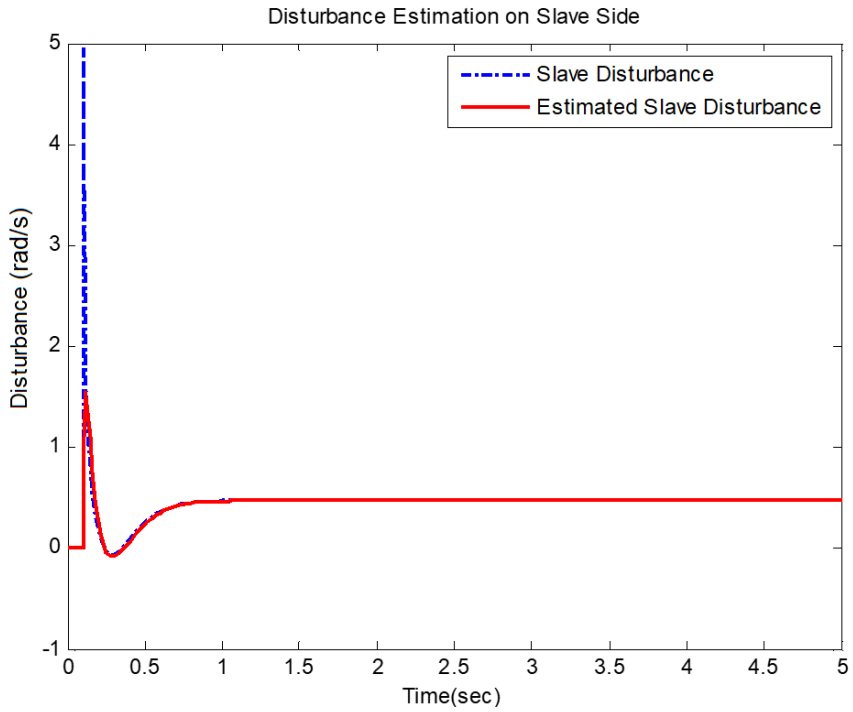

Figure 4.6: NDOB-integrated fuzzy model-based control: disturbance estimation on slave side

4.5 Experimental Results

Finally, we perform semi-real-time experiments using QUARC/Simulink environment using a haptic device and a virtual slave system. The experimental setup is shown in Fig 4.7. The experiment is initiated by the human operator who drives the haptic device. The resulting motion and force commands are transmitted over a time-delayed communication channel to the slave system, which interacts with the environment and provides force feedback to the master side. The reflected force is provided to the operator through a haptic device. NDOB-based fuzzy PDC controllers are implemented on both the master and slave sides with the control gains of Eq (4.29) and Eq (4.30). The recorded position tracking, velocity tracking, disturbance estimation, and force reflection results are shown in Figure 4.8 - Figure 4.12. The proposed scheme provides excellent position tracking and disturbance estimation performance and possesses force reflection ability. The proposed controller parameters are summarized in Table 4.3.

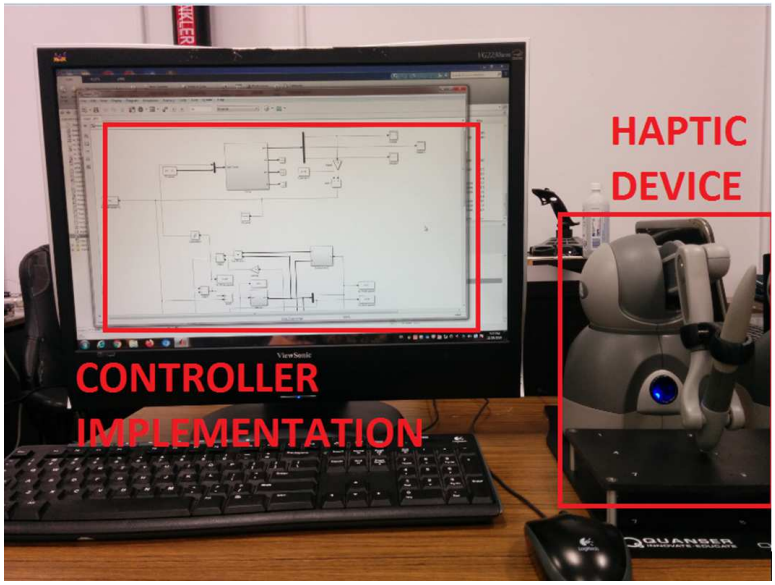

Figure 4.7: Experimental setup to implement NDOB TS fuzzy controller

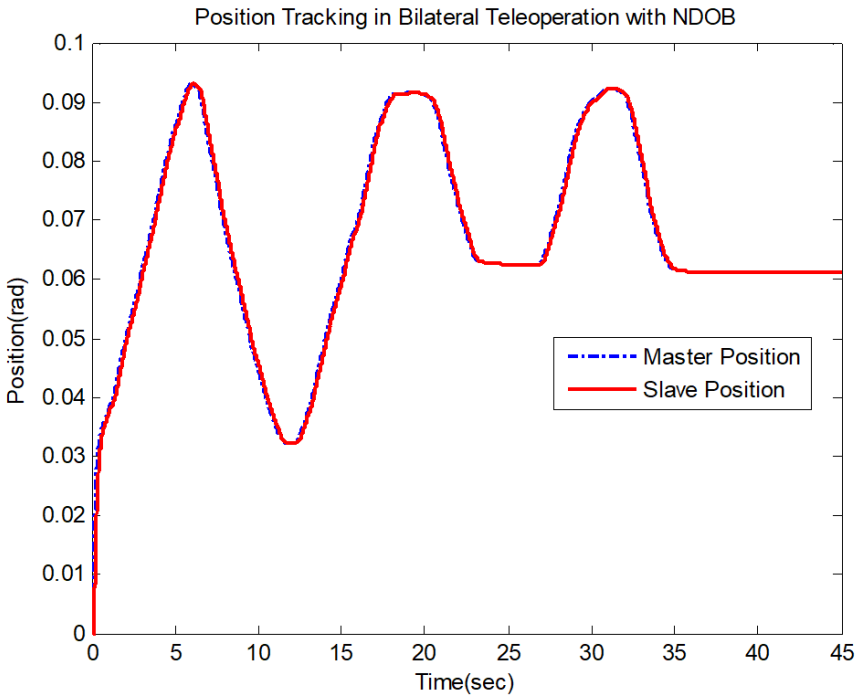

Figure 4.8: NDOB-integrated fuzzy model-based control: position tracking

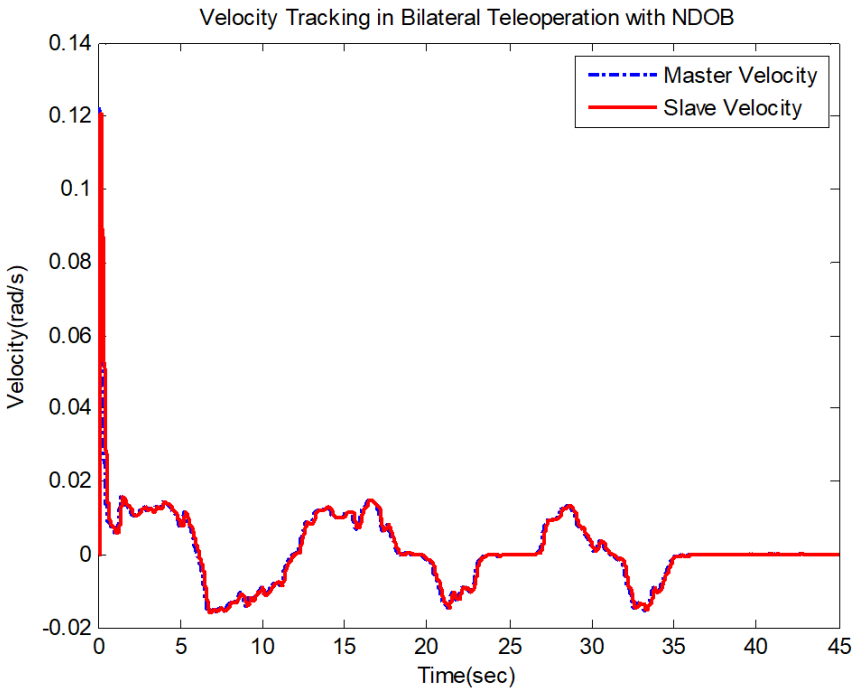

Figure 4.9: NDOB-integrated fuzzy model-based control: velocity tracking

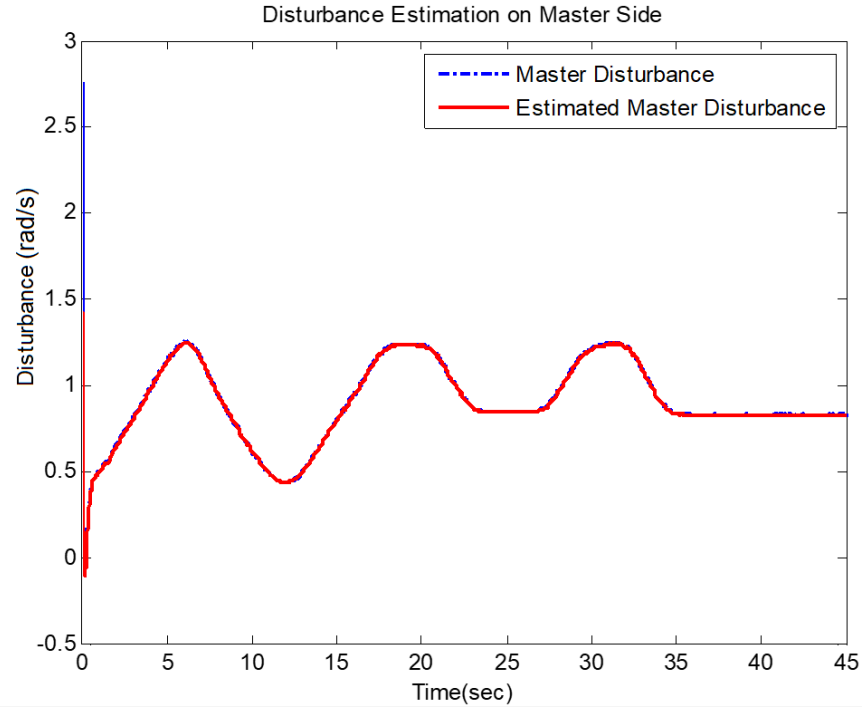

Figure 4.10: NDOB-integrated fuzzy model-based control: disturbance estimation on master side

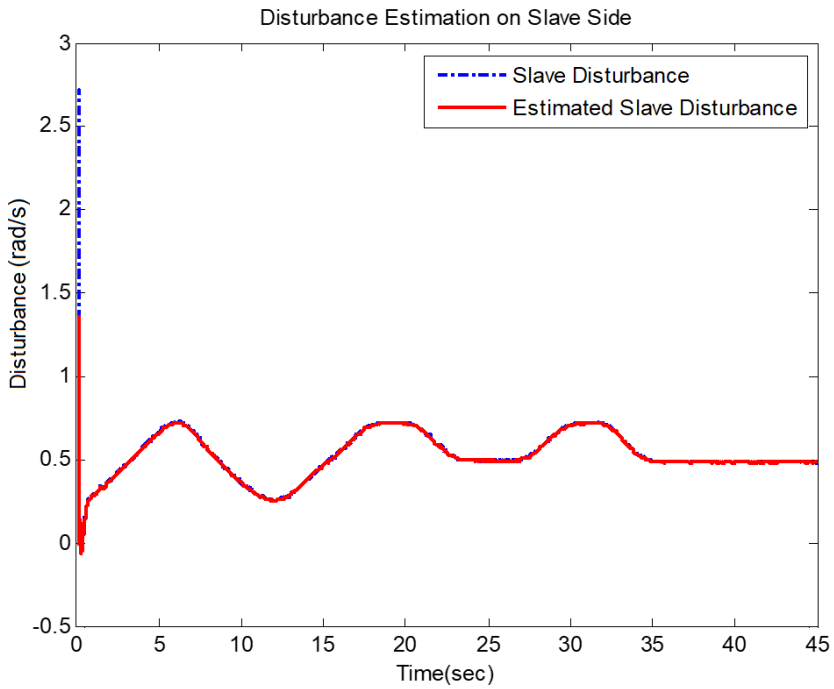

Figure 4.11: NDOB-integrated fuzzy model-based control: disturbance estimation on slave side

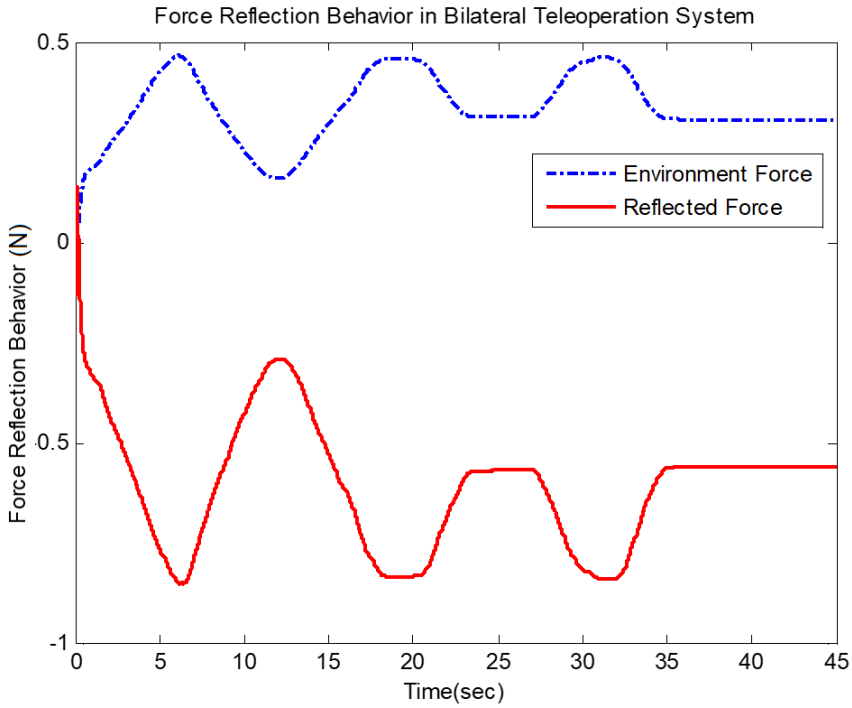

Figure 4.12: NDOB-integrated fuzzy model-based control: force reflection behavior

Controller	Simulation in MATLAB/Simulink	Semi Real-time QUARC/Simulink
System	1-DoF (Master/Slave)	1-DoF (Master/Slave)
Operator Force (N)	1 (constant)	Time-varying force using Omni Bundle
Environment Stiffness k_e (Nm/rad)	5	5
Environment Damping b_e (Nm/rad)	0.1	0.1
Feedback gain K_f	0.1	0.1
Scaling factor K_{op}	0	5
Time delay (Sec)	0.2	0.2

Table 4.3: Proposed controller parameters for simulation and semi-real time experiment

4.6 Conclusion

This chapter presents the design of a disturbance observer-based fuzzy PDC controller for the regulation task in uncertain nonlinear systems. A numerator-denominator type PDC controller can offer desired dynamic performance. However, its performance deteriorates in the presence of parametric uncertainties. To recover its performance, a nonlinear disturbance observer is designed, which considers the parametric uncertainties and modelling errors. The proposed NDOB-based fuzzy PDC controller is applied to a bilateral teleoperation system where a slave manipulator is required to track the master manipulator while exhibiting a desired behaviour. Simulations and experimental results confirm the validity and effectiveness of the proposed robust regulation scheme. The proposed regulator will be used to control more complex systems.

Chapter 5

Disturbance Observer Based Extended State Convergence Architecture for Multilateral Teleoperation Systems

In the existing extended state convergence architecture [159], k-master systems can control the motion of l-slave systems to perform a certain task in a remote environment. However, the dependency of this control framework on systems' parameters leads to degraded control performance in the presence of significant parameter variations. In this study, we have integrated extended state observers in extended state convergence architecture [159] to counter the effect of uncertainties, which has resulted in a more practical architecture for multilateral teleoperation systems. In order to validate the proposed enhanced architecture, simulations are performed in MATLAB/Simulink environment by considering a symmetric (2x2) as well as asymmetric (2x1) teleoperation system. A comparative assessment with the existing state convergence architecture proves the superiority of the proposed architecture. In addition, hardware experimentation is carried out on Quanser QUBE-servo systems by setting up an asymmetric (1x2) teleoperation system in the QUARC environment.

To the best of the authors' knowledge, robustness improvement of extended state convergence architecture has not been reported in the literature. This chapter is structured as follows: Section 5.1 describes the proposed architecture, and the associated design procedure is presented in Section 5.2. Simulation and experimental results are presented in Sections 5.3 and 5.4, followed by conclusions.

5.1 Proposed Architecture

In extended state convergence architecture, $n\,(k+l) + (n+1)\,kl$ design conditions are required to be solved to determine the same number of control gains. In the proposed version, an extra $(n+1)\,kl$ design conditions are required to be solved to determine disturbance observers' gains. Although computational cost is increased in the proposed architecture, however, its ability to deal with parameter variations is greatly improved. The proposed architecture is shown in Figure 5.1. We include various notations describing the architecture in Table 5.1.

Table 5.1: Notations describing observer-based extended state convergence architecture

Notation	Description	Notation	Description
F_{hk}	Force exerted by k^{th} operator on k^{th} master system	G_{slk}	Effect of k^{th} operator's force in l^{th} slave system
K_{mke}	Stabilizing extended gain for k^{th} master system	K_{sle}	Stabilizing extended gain for l^{th} slave system
R_{mkl}	Effect of motion of l^{th} slave system in k^{th} master system	R_{slk}	Effect of motion of k^{th} master system in l^{th} slave system
L_{mke}	Extended state observer's gain for k^{th} master system	L_{ske}	Extended state observer's gain for l^{th} slave system

5.2 Design Procedure

The design methodology is a two-stage procedure in which an augmented system containing closed loop master and error systems is formed at the first step. Then the augmented system is stabilized by placing the poles in the left half plane with error systems set as autonomous systems. Let master and slave systems ($z = m, s$) be modeled on state space given in Eq (5.1). In Eq (5.1), system and input matrices contain nominal plant values, whereas parametric uncertainties are included as disturbance terms. We form extended master and slave systems by considering disturbance terms as additional states given in Eq (5.2):

$$\begin{aligned} \dot{x}_{zi} &= A_{zi}x_{zi} + B_{zi}u_{zi} + d_{zi} \\ y_{zi} &= C_{zi}x_{zi} \end{aligned} \tag{5.1}$$

$$\begin{aligned} \dot{x}_{zie} &= A_{zie}x_{zie} + B_{zie}u_{zi} \\ y_{zi} &= C_{zie}x_{zie} \end{aligned} \tag{5.2}$$

To estimate master and slave systems' states, including disturbances, extended state observers are designed as follows:

$$\begin{aligned} \dot{\hat{x}}_{zie} &= A_{zie}\hat{x}_{zie} + B_{zie}u_{zi} + L_{zie}\left(y_{zi} - \hat{y}_{zi}\right) \\ \hat{y}_{zi} &= C_{zie}\hat{x}_{zie} \end{aligned} \tag{5.3}$$

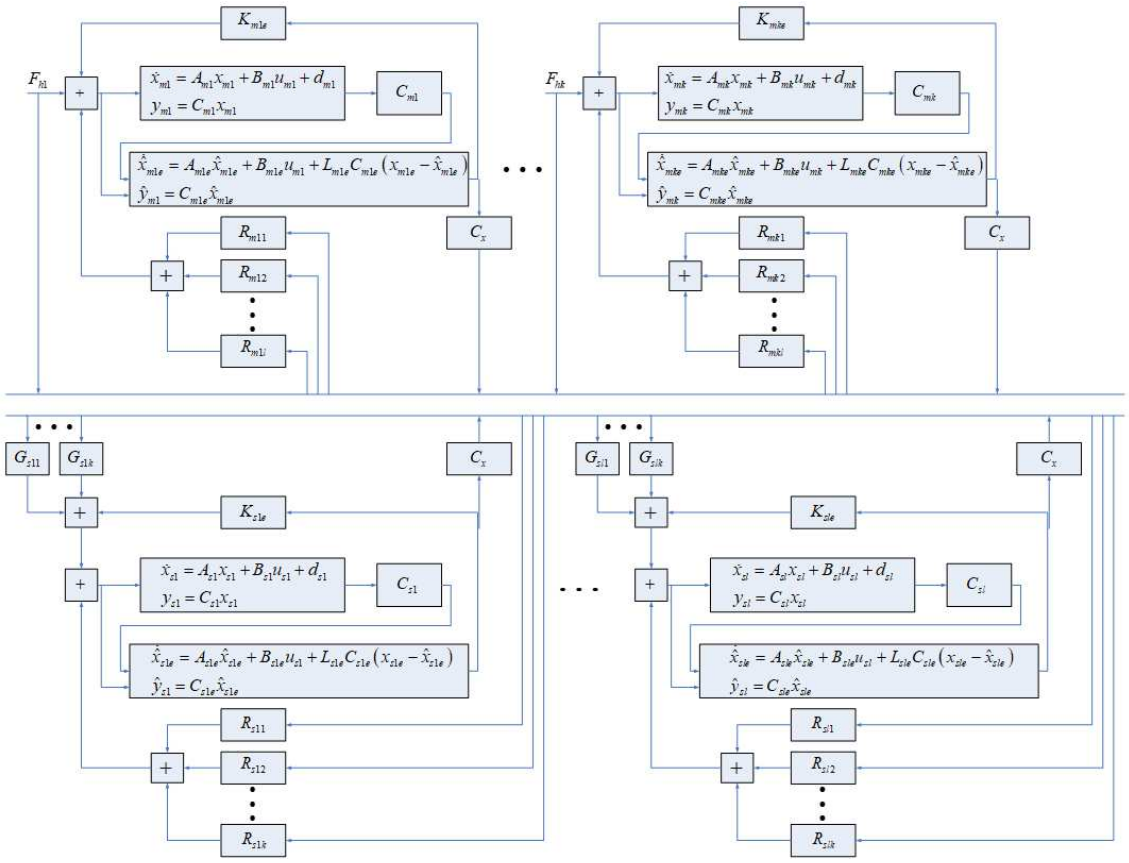

Figure 5.1: Proposed disturbance observer-based architecture for multilateral teleoperation systems

The control inputs for the k^{th} master and l^{th} slave systems are introduced as:

$$u_{mk} = K_{mke}\hat{x}_{mke} + \sum_{i=1}^{l} R_{mki}\hat{x}_{si}\left(t - T_{mki}\right) + F_{hk} \tag{5.4}$$

$$u_{sl} = K_{sle}\hat{x}_{sle} + \sum_{i=1}^{k} R_{sli}\hat{x}_{mi}\left(t - T_{sli}\right) + \sum_{i=1}^{k} G_{sli}F_{hi}\left(t - T_{sli}\right) \tag{5.5}$$

In Eq (5.4) and Eq (5.5), last element of stabilizing gain, K_{zie} compensates for the parameter variations. By plugging Eq (5.4) and Eq (5.5) in Eq (5.1), closed loop master and slave systems are obtained as:

$$\dot{x}_{mk} = \left(A_{mk} + B_{mk}K_{mk}\right)x_{mk} + \sum_{i=1}^{l} B_{mk}R_{mki}x_{si}\left(t - T_{mki}\right) + B_{mk}F_{hk} + e_{dmk} \tag{5.6}$$

$$\dot{x}_{sl} = (A_{sl} + B_{sl}K_{sl})\, x_{sl} + \sum_{i=1}^{k} B_{sl}R_{sli}x_{mi}\,(t - T_{sli}) + \sum_{i=1}^{k} B_{sl}G_{sli}F_{hi}\,(t - T_{sli}) + e_{dsl} \tag{5.7}$$

In Eq (5.6) and Eq (5.7), e_{dzi} contains estimation error terms. Using Taylor expansion on time-delayed signals in Eq (5.6), Eq (5.7) and discarding higher order terms, we get:

$$\begin{bmatrix} \dot{x}_{m1} \\ \vdots \\ \dot{x}_{mk} \\ \dot{x}_{s1} \\ \vdots \\ \dot{x}_{sl} \end{bmatrix} = \begin{bmatrix} A_{m1}+B_{m1}K_{m1} & \dots & 0 & B_{m1}R_{m11} & \dots & B_{m1}R_{m1l} \\ & \ddots & & & \vdots & \\ 0 & \dots & A_{mk}+B_{mk}K_{mk} & B_{mk}R_{mk1} & \dots & B_{mk}R_{mkl} \\ B_{s1}R_{s11} & \dots & B_{s1}R_{s1k} & A_{s1}+B_{s1}K_{s1} & \dots & 0 \\ & \vdots & & & \ddots & \\ B_{sl}R_{sl1} & \dots & B_{sl}R_{slk} & 0 & \dots & A_{sl}+B_{sl}K_{sl} \end{bmatrix}$$
$$\begin{bmatrix} x_{m1} \\ \vdots \\ x_{mk} \\ x_{s1} \\ \vdots \\ x_{sl} \end{bmatrix} - \begin{bmatrix} 0 & \dots & 0 & B_{m1}T_{m11}R_{m11} & \cdots & B_{m1}T_{m1l}R_{m1l} \\ & \vdots & & & \vdots & \\ 0 & \dots & 0 & B_{mk}T_{mk1}R_{mk1} & \dots & B_{mk}T_{mkl}R_{mkl} \\ B_{s1}T_{s11}R_{s11} & \dots & B_{s1}T_{s1k}R_{s1k} & 0 & \dots & 0 \\ & \vdots & & & \vdots & \\ B_{sl}T_{sl1}R_{sl1} & \dots & B_{sl}T_{slk}R_{slk} & 0 & \dots & 0 \end{bmatrix}$$
$$\begin{bmatrix} \dot{x}_{m1} \\ \vdots \\ \dot{x}_{mk} \\ \dot{x}_{s1} \\ \vdots \\ \dot{x}_{sl} \end{bmatrix} + \begin{bmatrix} B_{m1} & \dots & 0 \\ & \ddots & \\ 0 & \dots & B_{mk} \\ B_{s1}G_{s11} & \dots & B_{s1}G_{s1k} \\ & \vdots & \\ B_{sl}G_{sl1} & \dots & B_{sl}G_{slk} \end{bmatrix} \begin{bmatrix} F_{h1} \\ \vdots \\ F_{hk} \end{bmatrix} + \begin{bmatrix} e_{dm1} \\ \vdots \\ e_{dmk} \\ e_{ds1} \\ \vdots \\ e_{dsl} \end{bmatrix} \tag{5.8}$$

Let us define the following matrices:

$$\begin{aligned} &x_m = \begin{bmatrix} x_{m1} & \dots & x_{mk} \end{bmatrix}^T, x_s = \begin{bmatrix} x_{s1} & \dots & x_{sl} \end{bmatrix}^T, A_m = \operatorname{diag}(A_{m1} \dots A_{mk}) \\ &A_k = \operatorname{diag}(A_{s1}, \dots . A_{sl}), B_m = \operatorname{diag}(B_{m1} \dots, B_{mk}), B_s = \operatorname{diag}(B_{s1}, \dots, B_{sk}) \\ &K_m = \operatorname{diag}(K_{m1}, \dots, K_{mk}), K_s = \operatorname{diag}(K_{s1}, \dots, K_{sl}) \end{aligned} \tag{5.9}$$

$$
\begin{aligned}
R_m &= \begin{bmatrix} R_{m11} & \dots & R_{m1l} \\ & \vdots & \\ R_{mk1} & \dots & R_{mkl} \end{bmatrix}, R_s = \begin{bmatrix} R_{n11} & \dots & R_{s1k} \\ & \vdots & \\ R_{sl1} & \dots & R_{slk} \end{bmatrix}, T_m = \begin{bmatrix} T_{m11} & \dots & T_{m1l} \\ & \vdots & \\ T_{mk1} & \dots & T_{mkl} \end{bmatrix} \\
T_s &= \begin{bmatrix} T_{s11} & \dots & T_{s1k} \\ & \vdots & \\ T_{sl1} & \dots & T_{slk} \end{bmatrix}, F_h = \begin{bmatrix} F_{h1} & \dots & F_{hk} \end{bmatrix}^T, G_s = \begin{bmatrix} G_{s11} & \dots & G_{s1k} \\ & \vdots & \\ G_{sl1} & \dots & G_{slk} \end{bmatrix} \\
e_{dm} &= \begin{bmatrix} e_{dm1} & \dots & e_{dmk} \end{bmatrix}^T, e_{ds} = \begin{bmatrix} e_{ds1} & \dots & e_{dsl} \end{bmatrix}^T
\end{aligned} \tag{5.10}
$$

With the help of Eq (5.9) and Eq (5.10) we can write Eq (5.8) in compact form as:

$$
\begin{bmatrix} I_{nk} & T_m \circ (B_m R_m) \\ T_s \circ (B_s R_s) & I_{nl} \end{bmatrix} \begin{bmatrix} \dot{x}_m \\ \dot{x}_s \end{bmatrix} = \begin{bmatrix} A_m + B_m K_m & B_m R_m \\ B_s R_s & A_s + B_s K_s \end{bmatrix} \begin{bmatrix} x_m \\ x_s \end{bmatrix} + \begin{bmatrix} B_m \\ B_s G_s \end{bmatrix} F_m + \begin{bmatrix} e_{dn} \\ e_{dv} \end{bmatrix} \tag{5.11}
$$

In Eq (5.11), operator 'o' denotes Hadamard product. By defining, $D_m = T_m \circ (B_m R_m)$, $D_s = T_s \circ (B_s R_s)$,we can further simplify Eq (5.11) as:

$$
\begin{bmatrix} \dot{x}_m \\ \dot{x}_s \end{bmatrix} = \begin{bmatrix} A_{11} & A_{12} \\ A_{21} & A_{22} \end{bmatrix} \begin{bmatrix} x_m \\ x_s \end{bmatrix} + \begin{bmatrix} B_1 \\ B_2 \end{bmatrix} F_h \tag{5.12}
$$

$$
\begin{aligned}
A_{11} &= (I_{nk} - D_m D_s)^{-1} K_m - D_m (I_{nl} - D_s D_m)^{-1} B_s R_s \\
A_{12} &= (I_{nk} - D_m D_s)^{-1} B_m R_m - D_m (I_{nl} - D_s D_m)^{-1} K_s \\
A_{21} &= -D_s (I_{nk} - D_m D_s)^{-1} K_m - (I_{nl} - D_s D_m)^{-1} B_s R_s \\
A_{22} &= -D_s (I_{nk} - D_m D_s)^{-1} B_m R_m - (I_{nl} - D_s D_m)^{-1} K_s \\
B_1 &= (I_{nk} - D_m D_s)^{-1} B_m - D_m (I_{nl} - D_s D_m)^{-1} B_s G_s \\
B_2 &= -D_s (I_{nk} - D_m D_s)^{-1} B_m - (I_{nl} - D_s D_m)^{-1} B_s G_s
\end{aligned} \tag{5.13}
$$

We now transform the augmented system Eq (5.12) into a new augmented system

with tracking errors defined on the slave systems. To this end, following linear transformation is introduced:

$$\begin{bmatrix} x_m \\ x_e \end{bmatrix} = \begin{bmatrix} I_{nk} & 0 \\ -\mathrm{A} & I_{nl} \end{bmatrix} \begin{bmatrix} x_m \\ x_s \end{bmatrix} \tag{5.14}$$

In Eq (5.14), matrix Acontains authority factors exercised by master systems to influence slave systems and is given as:

$$\mathrm{A} = \begin{bmatrix} \alpha_{11} I_n & \alpha_{12} I_n & \dots & \alpha_{1k} I_n \\ \alpha_{21} I_n & \alpha_{22} I_n & \dots & \alpha_{2k} I_n \\ & & \vdots & \\ \alpha_{l1} I_n & \alpha_{l2} I_n & \dots & \alpha_{lk} I_n \end{bmatrix} \tag{5.15}$$

The time derivative of Eq (5.14) along with Eq (5.12) yields transformed augmented system as:

$$\begin{bmatrix} \dot{x}_m \\ \dot{x}_e \end{bmatrix} = \begin{bmatrix} \tilde{A}_{11} & \tilde{A}_{12} \\ \tilde{A}_{21} & \tilde{A}_{22} \end{bmatrix} \begin{bmatrix} x_m \\ x_e \end{bmatrix} + \begin{bmatrix} \tilde{B}_1 \\ \tilde{B}_2 \end{bmatrix} F_m \tag{5.16}$$

$$\begin{aligned} &\tilde{A}_{11} = A_{11} + A_{12}\mathrm{A}, \tilde{A}_{12} = A_{12}, \tilde{A}_{21} = (A_{21} - \mathrm{A}A_{11}) + (A_{22} - \mathrm{A}A_{12})\,\mathrm{A} \\ &\tilde{A}_{22} = A_{22} - \mathrm{A}A_{12}, \tilde{B}_1 = B_1, \tilde{B}_2 = B_2 - \mathrm{A}B_1 \end{aligned} \tag{5.17}$$

According to the method of state convergence, the error should evolve as an autonomous system, and stability of the augmented system is ensured by placing poles of closed-loop master and error systems on the left half plane. This gives rise to the following design conditions whose solution returns control gains of the extended state convergence architecture:

$$\tilde{A}_{21} = 0, \tilde{B}_2 = 0, \left|sI_{nk} - \tilde{A}_{11}\right| \times \left|sI_{nl} - \tilde{A}_{22}\right| = |sI_{nk} - P| \times |sI_{nl} - Q| \tag{5.18}$$

In Eq (5.18), matrices P and Q contain poles locations. Observer gains are found independently of the controller gains and no augmented system is formed to determine

these gains.

5.3 Simulation Results

In order to validate the proposed architecture, simulations are performed in MATLAB/Simulink environment by considering symmetric and asymmetric configurations of teleoperation systems. The following master and slave systems are considered where $x^1_{zi}$and x^2_{zi} are position and velocity signals:

$$\begin{aligned} m_i : \begin{cases} \dot{x}^1_{mi} = x^2_{mi} \\ \dot{x}^2_{mi} = -\beta_{mi} \sin\left(x^1_{mi}\right) - 7.1429 x^2_{mi} + 0.2656 u_{mi} \end{cases} \\ s_i : \begin{cases} \dot{x}^1_{si} = x^2_{si} \\ \dot{x}^2_{si} = -\beta_{si} \sin\left(x^1_{si}\right) - 6.25 x^2_{si} + 0.2729 u_{si} \end{cases} \end{aligned} \tag{5.19}$$

First, consider a symmetrical 2x2 teleoperation system. To compute the controller and observer gains for this configuration, following nominal models are assumed:

$$\begin{aligned} A_{m1} &= \begin{bmatrix} 0 & 1 \\ 0 & -7.0 \end{bmatrix}, A_{m2} = \begin{bmatrix} 0 & 1 \\ 0 & -5.0 \end{bmatrix}, A_{s1} = \begin{bmatrix} 0 & 1 \\ 0 & -4.0 \end{bmatrix}, A_{s2} = \begin{bmatrix} 0 & 1 \\ 0 & -6.0 \end{bmatrix} \\ B_{m1} &= \begin{bmatrix} 0 \\ 0.2 \end{bmatrix}, B_{m2} = \begin{bmatrix} 0 \\ 0.1 \end{bmatrix}, B_{s1} = \begin{bmatrix} 0 \\ 0.4 \end{bmatrix}, B_{s2} = \begin{bmatrix} 0 \\ 0.3 \end{bmatrix} \end{aligned} \tag{5.20}$$

Further, slaves are interacting with environments having stiffness as $k_{ei} = 10 Nms/rad$ and force feedback gains are assumed to be 0.1 which yields, $R_{mkl} = \begin{bmatrix} 0.1 & 0 \end{bmatrix}$. Time delays are ignored during the computation but will be considered during the simulations. Characteristic polynomial for the closed loop master system is selected as $s^4 + 28s^3 + 292s^2 + 1344s + 2304 = 0$ while for error systems, it is selected as $s^4 + 31s^3 + 354s^2 + 1764s + 3240 = 0$. Design conditions in Eq (5.18) are solved using MATLAB symbolic toolbox with nominal models Eq (5.20) and authority factors, $\alpha_{11} = 0.6, \alpha_{12} = 0.4, \alpha_{21} = 0.7, \alpha_{22} = 0.3$, which yields the following control gains:

$$
\begin{aligned}
&G_{s11} = 0.3, G_{s12} = 0.1, G_{s21} = 0.4667, G_{s22} = 0.1 \\
&K_{m1} = \begin{bmatrix} -321.5036 & -45.0226 \end{bmatrix}, K_{m2} = \begin{bmatrix} -360.4739 & -69.9548 \end{bmatrix} \\
&K_{s1} = \begin{bmatrix} -224.6373 & -37.5033 \end{bmatrix}, K_{s2} = \begin{bmatrix} -119.4145 & -19.9956 \end{bmatrix} \\
&R_{s11} = \begin{bmatrix} 38.8513 & 4.4952 \end{bmatrix}, R_{s12} = \begin{bmatrix} 54.0875 & 7.0058 \end{bmatrix} \\
&R_{s21} = \begin{bmatrix} -65.7082 & -9.3470 \end{bmatrix}, R_{s22} = \begin{bmatrix} 0.1736 & 0.0032 \end{bmatrix}
\end{aligned} \tag{5.21}
$$

Observer gains are determined by placing the poles of the extended master and slave systems at $(s+30)^3$. This, in combination with Eq (5.20), yields the following observer gains:

$$
\begin{aligned}
&L_{m1e} = \begin{bmatrix} 83 & 2119 & 27000 \end{bmatrix}^T, L_{m2e} = \begin{bmatrix} 85 & 2275 & 27000 \end{bmatrix}^T \\
&L_{s1e} = \begin{bmatrix} 86 & 2356 & 27000 \end{bmatrix}^T, L_{s2e} = \begin{bmatrix} 84 & 2196 & 27000 \end{bmatrix}^T
\end{aligned} \tag{5.22}
$$

Simulations are now performed by considering constant operator forces of 1N and communication time delays as {0.1s, 0.2s}. Results of the proposed as well as existing architecture are recorded for various levels of disturbances and displayed in Figure 5.2 and Figure 5.5. It can be observed that existing architecture, which does not have disturbance observers, offers good tracking performance in the presence of parameter mismatches of Eq (5.19) and Eq (5.20) with $\beta_{zi} = 0.1$ as shown in Figure 5.2 and Figure 5.3. However, as the magnitude of β_{zi} is increased, the reference tracking performance of the existing extended convergence architecture is affected while the proposed disturbance observer-based version of the said architecture maintains good performance as demonstrated in Figure 5.4 and Figure 5.5. Note that, in these simulations, reference for the slaves are set as $x^1_{s1,ref} = \alpha_{11}x^1_{m1} + \alpha_{12}x^1_{m2}$ and $x^1_{s2,ref} = \alpha_{21}x^1_{m1} + \alpha_{22}x^1_{m2}$.

Now, we consider an asymmetrical 2x1 teleoperation system Eq (5.19) with the following nominal plant models:

$$A_{m1} = \begin{bmatrix} 0 & 1 \\ 0 & -9.2858 \end{bmatrix}, A_{m2} = \begin{bmatrix} 0 & 1 \\ 0 & -8.5715 \end{bmatrix}, A_{s1} = \begin{bmatrix} 0 & 1 \\ 0 & -5.0 \end{bmatrix}$$
$$B_{m1} = \begin{bmatrix} 0 \\ 0.3187 \end{bmatrix}, B_{m2} = \begin{bmatrix} 0 \\ 0.3187 \end{bmatrix}, B_{s1} = \begin{bmatrix} 0 \\ 0.2183 \end{bmatrix} \tag{5.23}$$

Let the stiffness of the slave's environment be $k_e = 20Nms/rad$ and let the force feedback gain be 0.1. This gives rise to $R_{m11} = R_{m12} = \begin{bmatrix} 2.0 & 0 \end{bmatrix}$. Let desired polynomials for the master and error systems be $p(s) : s^4+13s^3+58.25s^2+110s+75 = 0$ and $q(s) : s^2 + 15s + 54 = 0$. Communication time delays are assumed to be 1ms during the design phase while authority factors are taken to be $\alpha_{11} = 0.6, \alpha_{12} = 0.4$.

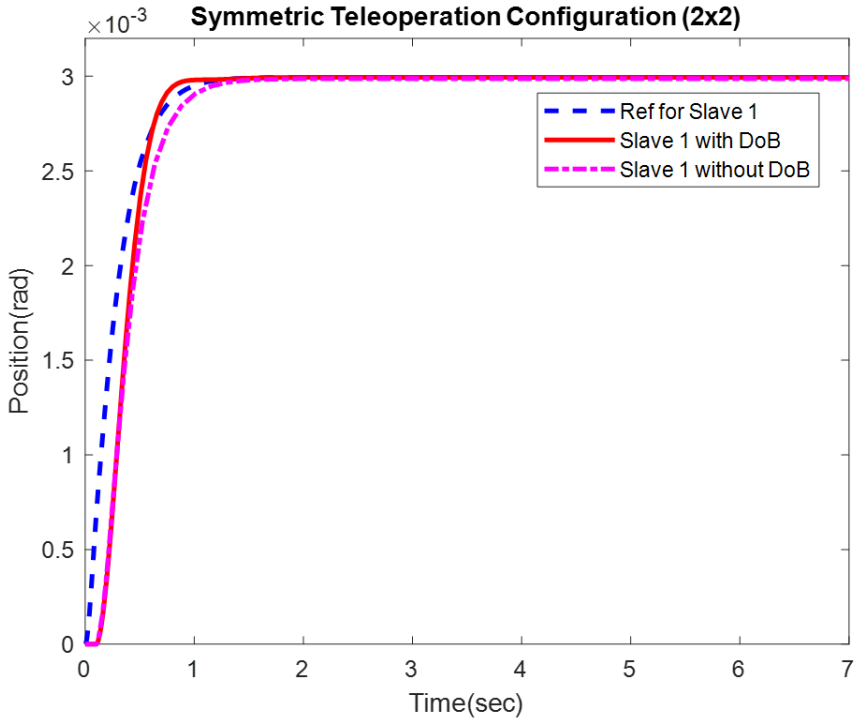

Figure 5.2: Symmetric teleoperation system: (a) slave systems tracking performance with low level of disturbance

Disturbance observer gains are computed based on nominal models in Eq (5.23) and a desired polynomial of $o(s) : (s + 30)^3 = 0$:

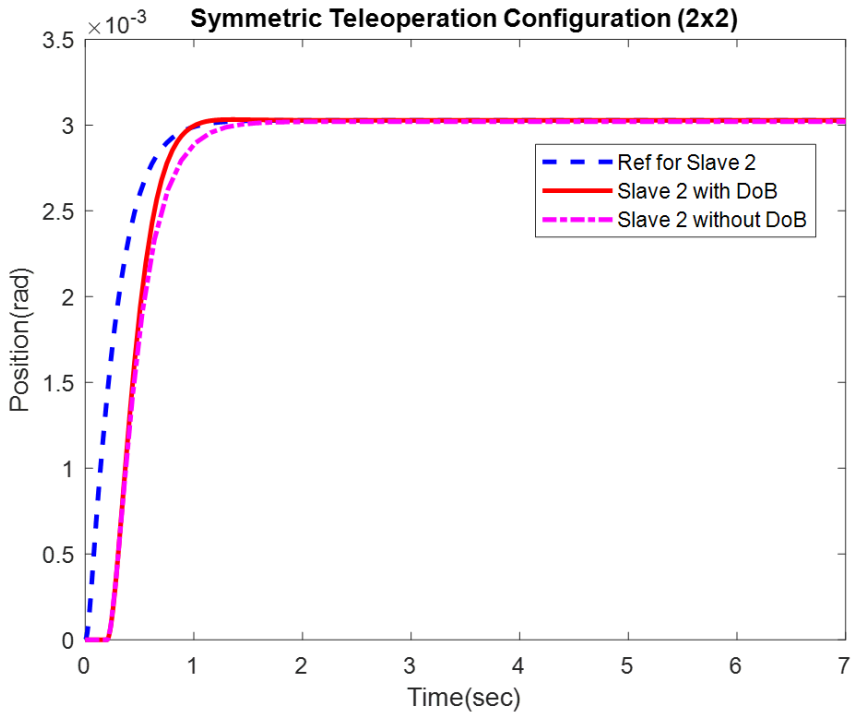

Figure 5.3: Symmetric teleoperation system: (b) slave systems tracking performance with low level of disturbance

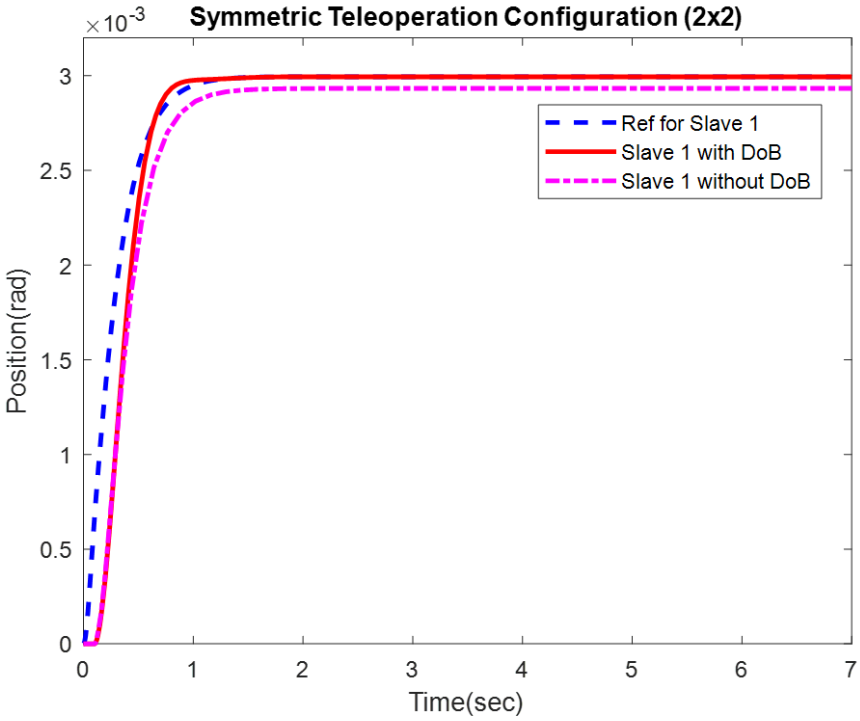

Figure 5.4: Symmetric teleoperation system: (c) slave systems tracking performance with increased disturbance activity

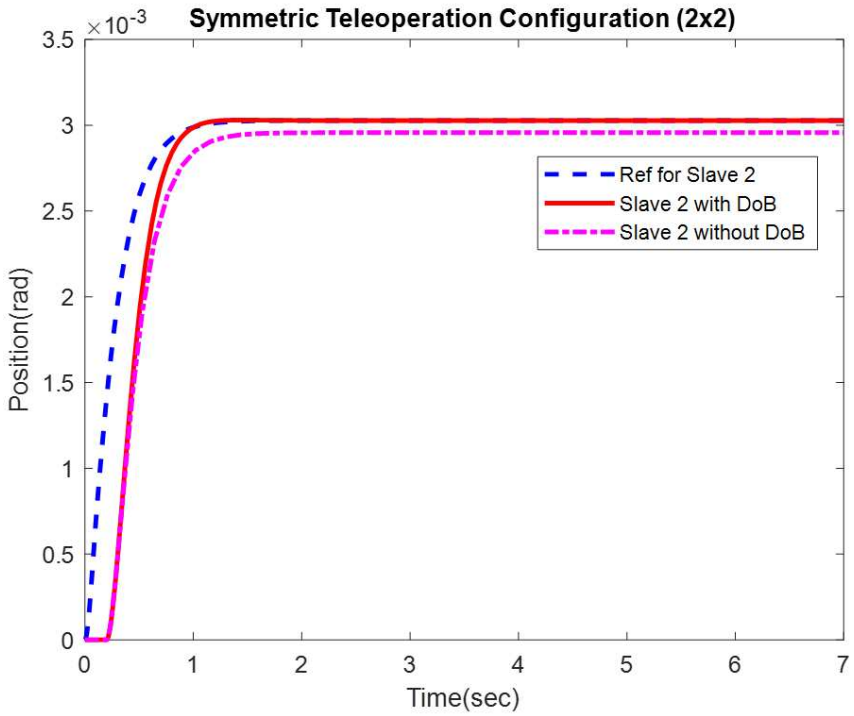

Figure 5.5: Symmetric teleoperation system: (d) slave systems tracking performance with increased disturbance activity

$$
\begin{aligned}
L_{m1e} &= \begin{bmatrix} 80.71 & 1950.5 & 27000 \end{bmatrix}^T \\
L_{m2e} &= \begin{bmatrix} 81.43 & 2002 & 27000 \end{bmatrix}^T \\
L_{s1e} &= \begin{bmatrix} 85 & 2275 & 27000 \end{bmatrix}^T
\end{aligned} \tag{5.24}
$$

Simulation results with operator's forces of 0.2N, time delays of {0.1s, 0.2s} and varying levels of disturbances are included in Figure 5.6 - Figure 5.9. It can be seen that the proposed architecture can establish communication between master and slave systems with good position tracking and force reflection abilities.

We also evaluate the tracking performance when time-varying delays exist in the communication channel. To this end, the asymmetric teleoperation system in Eq (5.23)- Eq (5.24) is simulated in the presence of time-varying delays and time-varying operators' forces, and results are depicted in Figure 5.10 and Fig 5.11. It can be seen that the proposed scheme can establish communication between master and slave systems with varying communication delays.

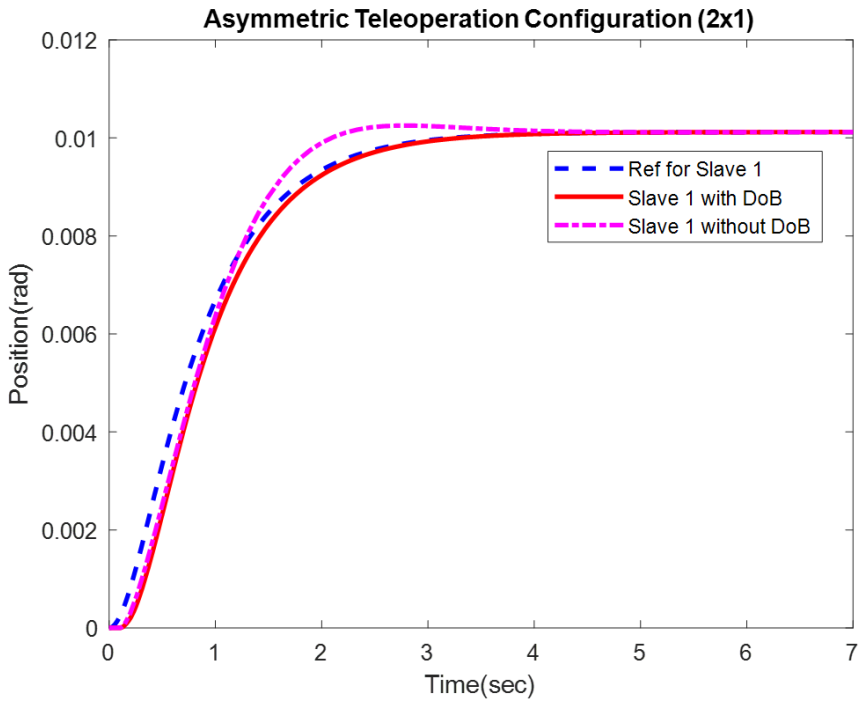

Figure 5.6: Asymmetric teleoperation system (a) slave position tracking performance with parameter mismatches ($\beta_{zi} = 0$)

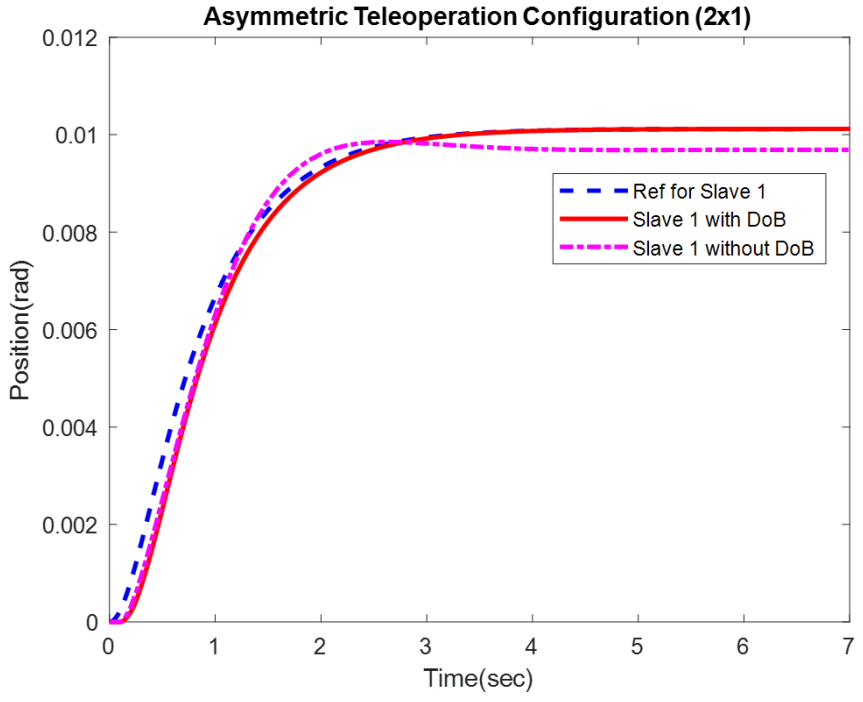

Figure 5.7: (b) Slave tracking performance with additional disturbance ($\beta_{zi} = 0.2$)

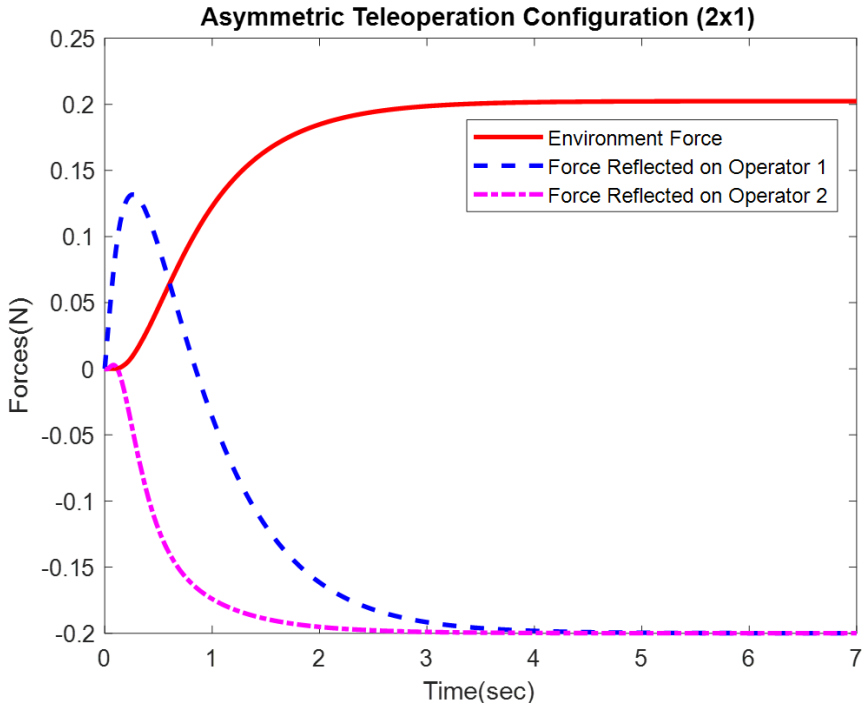

Figure 5.8: Asymmetric teleoperation system: force reflection ability of proposed scheme

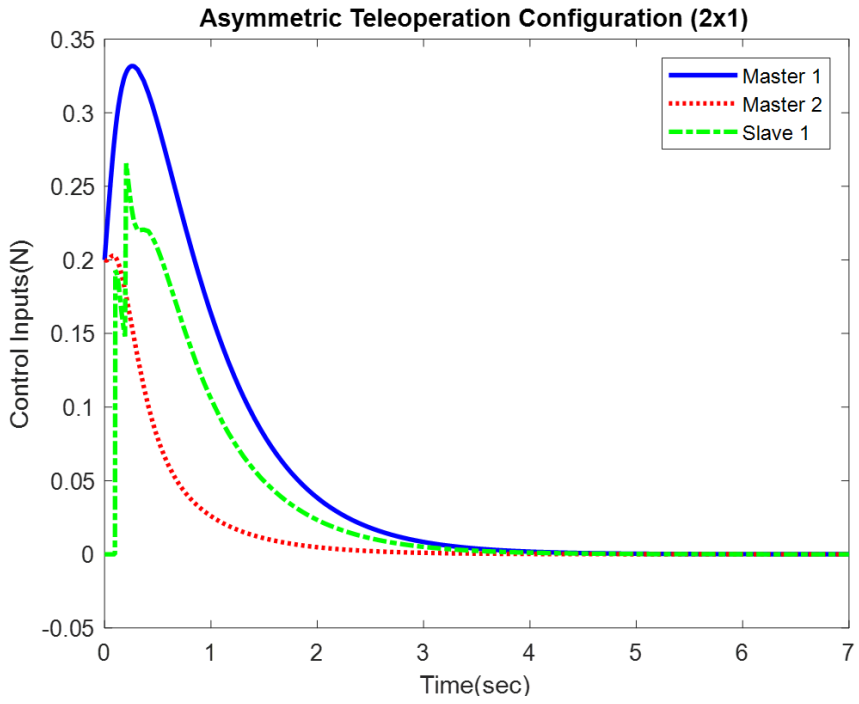

Figure 5.9: Asymmetric teleoperation system: control inputs

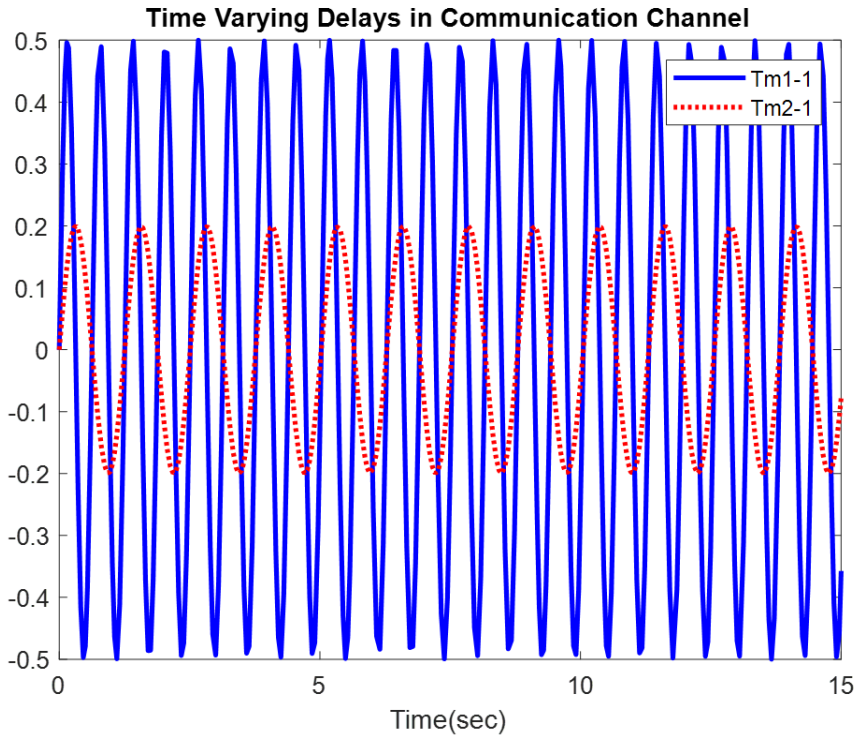

Figure 5.10: Asymmetric teleoperation system with time-varying delays (a) time-varying delays of the communication channel

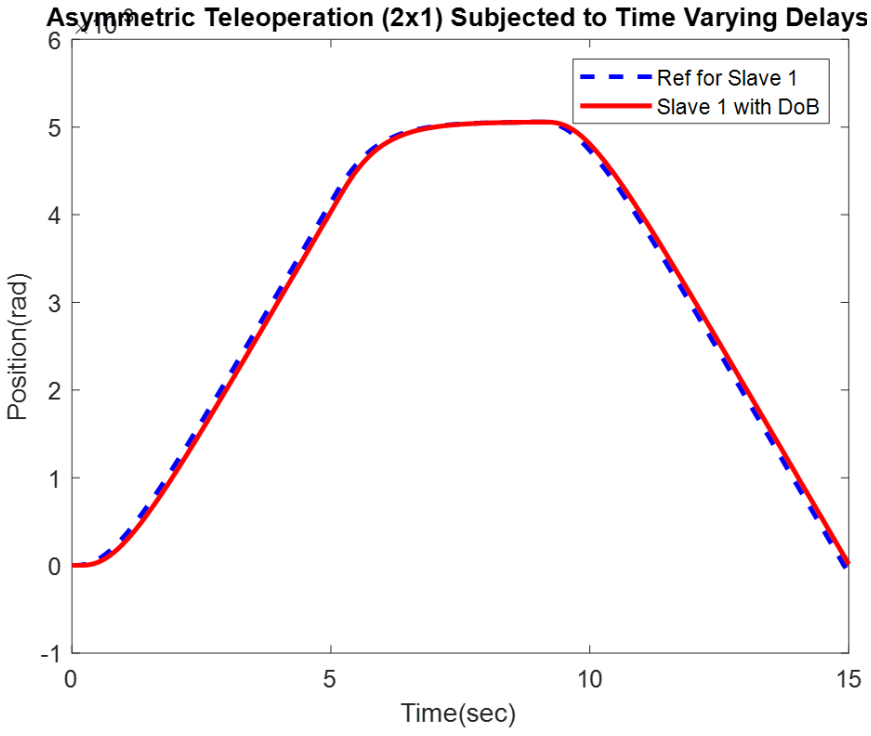

Figure 5.11: Slave position tracking performance with variable time delays

5.4 Experimental Results

Finally, experimental results are obtained using Qube-Servos manufactured by Quanser. Here, the asymmetric configuration is set up by using two real Qube-Servos while the master is a virtual device. The following nominal models are used for the controller and observer design:

$$\begin{aligned} A_{m1} &= \begin{bmatrix} 0 & 1 \\ 0 & -8.6710 \end{bmatrix}, A_{s1} = A_{s2} = \begin{bmatrix} 0 & 1 \\ 0 & -6.67 \end{bmatrix} \\ B_{m1} &= \begin{bmatrix} 0 \\ 179.208 \end{bmatrix}, B_{s1} = B_{s2} = \begin{bmatrix} 0 \\ 149.34 \end{bmatrix} \end{aligned} \tag{5.25}$$

By assuming a soft environment with a stiffness of 1Nms/rad, force feedback gain of 0.1, unity authority factor, no communication delays, $p(s) : (s+5)^2 = 0$ as desired polynomial for master, $q(s) : (s+10)^4 = 0$ as desired polynomial for error systems and $o(s) : (s+30)^3 = 0$ as desired polynomial for observers, we obtain following controller and observer gains:

$$\begin{aligned} G_{s11} &= G_{s21} = 1.2 \\ K_{m1} &= \begin{bmatrix} -0.3395 & -0.0074 \end{bmatrix} \\ K_{s1} &= \begin{bmatrix} -1.0705 & -0.1293 \end{bmatrix} \\ K_{s2} &= \begin{bmatrix} -0.2687 & -0.0492 \end{bmatrix} \\ R_{s11} &= \begin{bmatrix} 0.9031 & 0.1070 \end{bmatrix} \\ R_{s21} &= \begin{bmatrix} 0.1013 & 0.0269 \end{bmatrix} \\ L_{m1e} &= \begin{bmatrix} 81.329 & 1994.8 & 27000 \end{bmatrix}^T \\ L_{s1e} &= L_{s2e} = \begin{bmatrix} 83.33 & 2144.2 & 27000 \end{bmatrix}^T \end{aligned} \tag{5.26}$$

To evaluate the performance of the proposed architecture, a time-varying operator force profile is generated using ramp signals and time-delayed communication (T_{m11}=T_{s11}=0.1s, T_{m12}=T_{s21}=0.2s) is set up using UDP server and client blocks among three separate QUARC files. Only position signals and force signals are transmitted on the communication channel, while velocity signals are obtained through derivative filtering of time-delayed position signals with a cut-off frequency of 30rad/s.

Results of experimentation are recorded using QUARC blocks and displayed in Figure 5.12 - Figure 5.14. It can be seen that slaves are tracking the motion of the master system in the presence of uncertainties which validates the proposed enhanced architecture. The proposed controller parameters are summarized in Table 5.2.

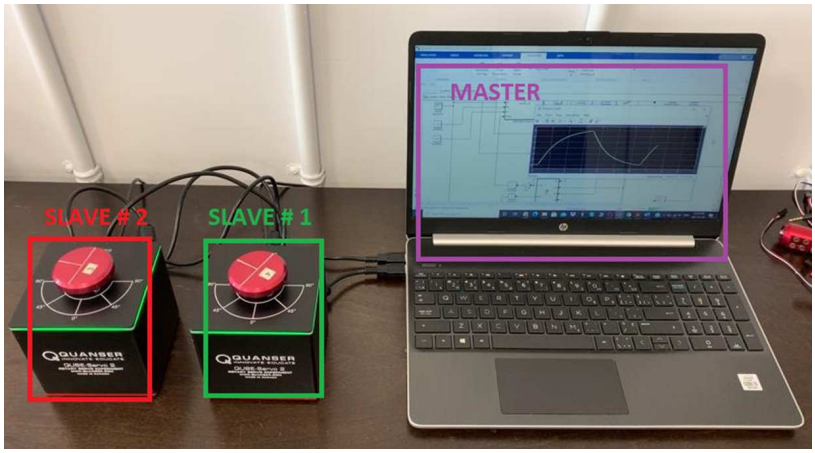

Figure 5.12: Experimental setup to test asymmetric teleoperation system (ATS)

Controller	Simulation in MATLAB/ Simulink	Simulation in MATLAB/ Simulink	Semi Real-time QUARC/Simulink
System	2x2 symmetrical system (2-Master/2-Slave)	2x1 asymmetrical system (2-Master/1-Slave)	1x2 asymmetrical system (1-Master/2-Slave)
Operator Force (N)	0.2 (constant)	0.2 (constant)	Time-varying force using Omni Bundle
Environment Stiffness k_e (Nm/rad)	10	20	1
Environment Damping b_e (Nm/rad)	0.1	0.1	0.1
Feedback gain K_f	0.1	0.1	0.1
Scaling factor K_{op}	0	0	5
Time delay (Sec)	$0.1, 0.2$	$0.1, 0.2$	0

Table 5.2: Proposed controller parameters for simulation and semi-real time experiment

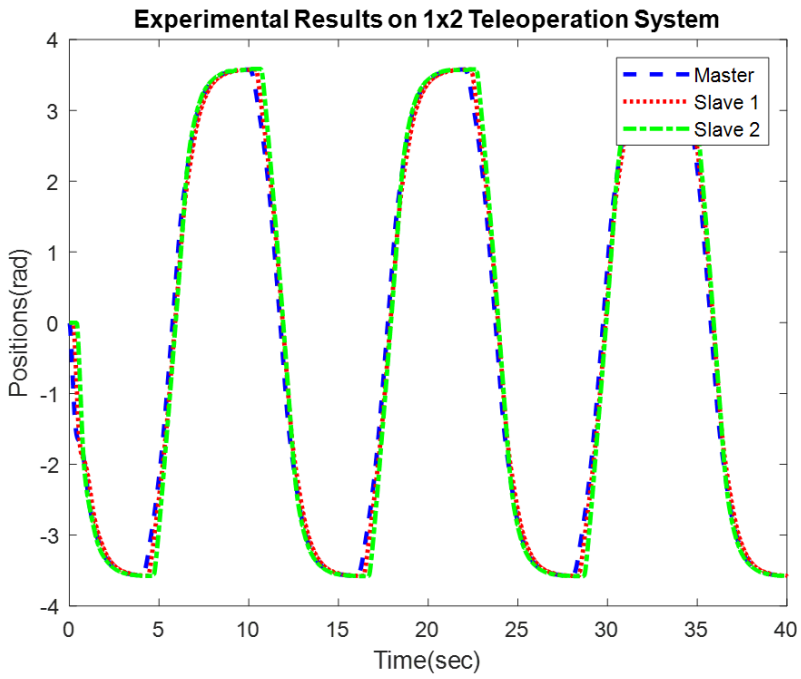

Figure 5.13: Experimental results on ATS: Position states

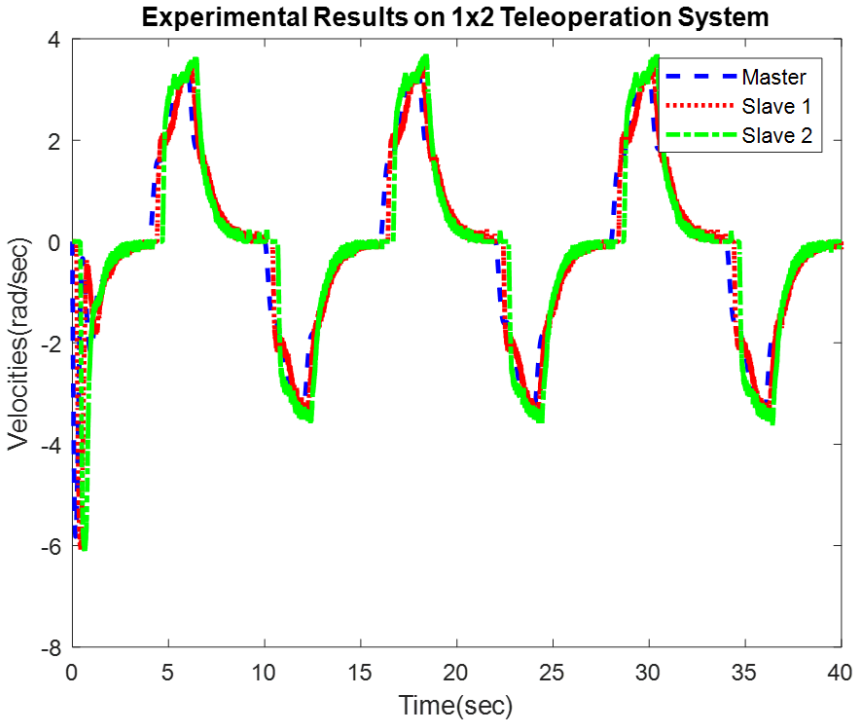

Figure 5.14: Experimental results on ATS: velocity states

5.5 Conclusion

This chapter presented the design of a disturbance observer-based extended state convergence architecture for multilateral teleoperation systems. A systematic procedure is presented to determine the controller and observer gains for synchronizing k-master and l-slave systems. The proposed architecture has been validated through MATLAB simulations on teleoperation systems' symmetric and asymmetric configurations. Finally, experimental results are also presented using Quanser's Qube-Servos platforms. Comparison with the existing extended state convergence architecture proves the superiority of the proposed architecture in dealing with uncertainties. In the future, the proposed architecture will be tested on multi-degrees-of-freedom systems.

Chapter 6

A Composite State Convergence Architecture for Bilateral Teleoperation System

The original version of the state convergence controller is applicable to bilateral teleoperation systems modeled on state space where both the master and slave devices are considered to be n^{th} order systems [73], [72], [71]. In practice, this controller is designed for each joint of the master and slave devices, where the joint's motion is modeled as a second-order system. To this end, consider a single joint model of the master and slave systems as shown in Eq (6.1), Eq (6.2):

$$\begin{aligned} \dot{x}_{m1} &= x_{m2} \\ \dot{x}_{m2} &= a_{m1}x_{m1} + a_{m2}x_{m2} + b_m u_m \end{aligned} \tag{6.1}$$

$$\begin{aligned} \dot{x}_{s1} &= x_{s2} \\ \dot{x}_{s2} &= a_{s1}x_{s1} + a_{s2}x_{s2} + b_s u_s \end{aligned} \tag{6.2}$$

Where $(x_{m1}, x_{m2})$and (x_{s1}, x_{s2}) are the states of the master and slave systems respectively while (a_{m1}, a_{m2}, b_m) and (a_{s1}, a_{s2}, b_s) are the systems' parameters of master and slave devices, respectively. To establish the motion synchronization of master and slave systems, the state convergence scheme considers all the possible interactions between these systems.

Lowering the complexity of state convergence architecture is proposed here by reducing the number of communication channels which subsequently reduces the number of control gains. In addition, it is demonstrated that the method of state convergence can still be applied to compute the gains of the proposed reduced complexity state convergence architecture. It is also shown that the attractive feature of assigning the desired dynamic response is preserved in the proposed scheme. It is further shown that motion scaling can also be achieved in the proposed scheme, a feature that is not offered by its standard counterpart.

The proposed scheme is verified through simulations and semi-real-time experiments in MATLAB/Simulink/QUARC environment by considering a single degree of freedom teleoperation system. The proposed scheme is also compared with an equal complexity error force compensated bilateral control scheme where control parameters of both the schemes are found through a Genetic algorithm by minimizing the integral time absolute error (ITAE) criterion.

This chapter is structured as follows: The proposed composite state convergence scheme is presented in Section 6.1. Simulation and experimental results are included in sections 6.2 and 6.3. Finally, conclusions are drawn in the end.

6.1 Proposed Composite State Convergence Scheme

The essence of the proposed composite state convergence scheme is to reduce the number of design variables while achieving the objective of motion synchronization of master and slave systems in a desired dynamic way by following the state convergence algorithm. The proposed way of reducing the design variables helps transmit fewer variables across the communication channel and paves the way for motion scaling of the slave system. This feature is desired for a class of teleoperation systems. The block diagram of the proposed composite state convergence scheme is shown in Figure 6.1, and various scalar parameters forming the scheme are defined below:

F_m: This represents the force applied by the human operator onto the master system.

G_2: This unknown scalar represents the influence of the operator's force in slave system and will be found as a part of the design procedure.

s_m: This is the composite variable for the master system and is defined as: $s_m = x_{m2} + \lambda_m x_{m1}$where $\lambda_m$is a positive constant.

s_s: This is the composite variable for the slave system and is defined as: $s_s = x_{s2} + \lambda_s x_{s1}$where $\lambda_s$is a positive constant.

k_m: This unknown parameter represents the feedback gain of the master composite system.

k_s: This unknown parameters represents the feedback gain of the slave composite system.

r_m: This known scalar variable feeds the motion of the slave system back to the master system and is computed as: $r_m = k_f k_e$where $k_e$is the stiffness of the environment

while$k_f$is the force feedback gain.

r_s: This unknown parameter feeds the motion of the master system back to the slave system and will be determined as a part of the design procedure.

T: This known parameter represents the small constant time delay of the communication channel.

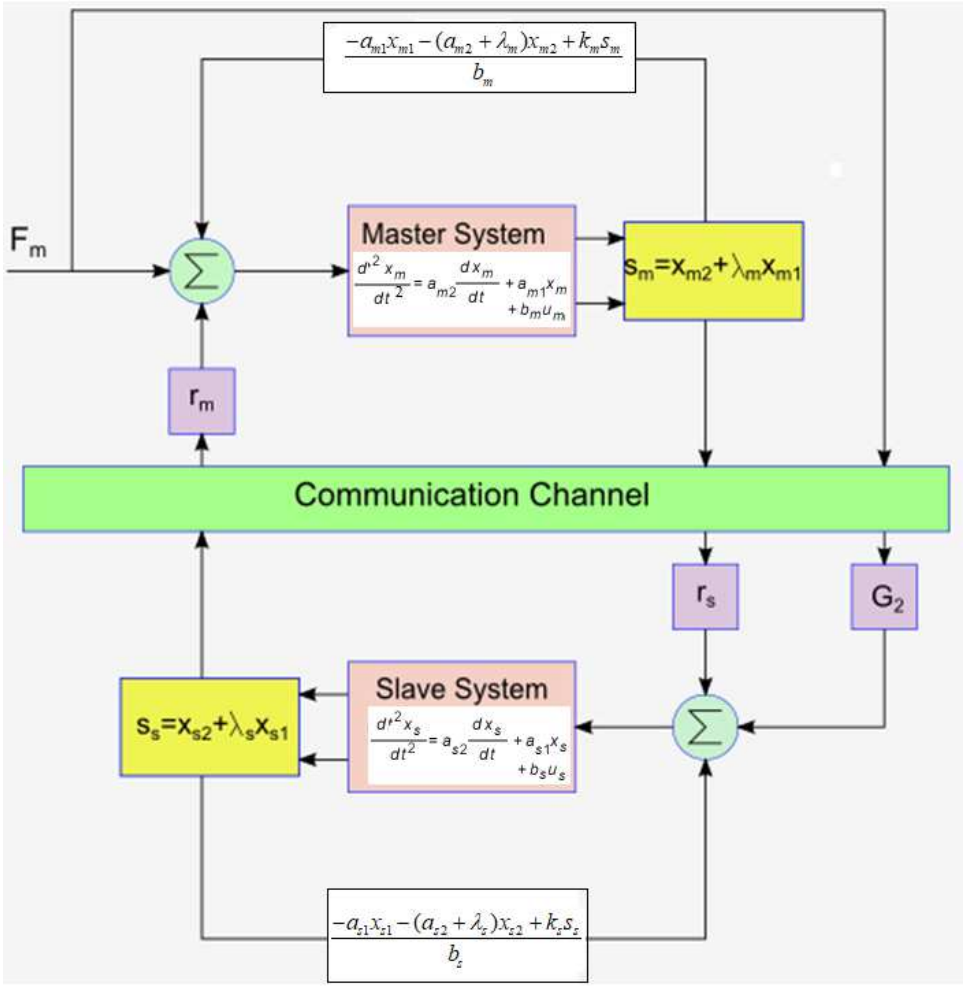

Figure 6.1: Proposed composite state convergence architecture for 1DoF teleoperation systems

Note that, in the proposed composite state convergence scheme, composite variables $(s_m, s_s)$are transmitted across the communication channel instead of full master and slave states, which is the case in standard state convergence methodology. These composite variables are indeed scalars, and consequently, the motion-feedback variables $(r_m, r_s)$are also scalars. Thus, only unknowns in the proposed scheme are

G_2, k_m, k_s, r_s. To determine these parameters, a design procedure is presented in this section to ensure that the states of master and slave systems converge in the absence and presence of small time delays and the desired dynamic behavior of the teleoperation system is also achieved. To this end, we present two theorems here.

Theorem 6.1. *In the absence of time delays, the slave system in Eq (6.2) will follow the master system in Eq (6.1) if control gains of the composite state convergence architecture are found as a solution of the following equations:*

$$b_m - b_s g_2 = 0 \tag{6.3}$$

$$k_m - b_s r_s + b_m r_m - k_s = 0 \tag{6.4}$$

$$k_m + b_m r_m = -p \tag{6.5}$$

$$b_m r_m - k_s = q \tag{6.6}$$

Proof. Recall the definitions of composite variables for the master (s_m) and slave (s_s) systems:

$$s_m = x_{m2} + \lambda_m x_{m1} \tag{6.7}$$

$$s_s = x_{s2} + \lambda_s x_{s1} \tag{6.8}$$

By taking the time derivative of master composite variable in Eq (6.7) and using Eq (6.1), we have:

$$\dot{s}_m = a_{m1} x_{m1} + (a_{m2} + \lambda_m)\, x_{m2} + b_m u_m \tag{6.9}$$

The time derivative of slave composite variable in Eq (6.8) in conjunction with Eq (6.2) yields:

$$\dot{s}_s = a_{s1} x_{s1} + (a_{s2} + \lambda_s)\, x_{s2} + b_s u_s \tag{6.10}$$

Let us introduce the control inputs for master and slave systems as:

$$u_m = \frac{1}{b_m}\left(-a_{m1} x_{m1} - (a_{m2} + \lambda_m)\, x_{m2} + k_m s_m\right) + r_m s_s + F_m \tag{6.11}$$

$$u_s = \frac{1}{b_s}\left(-a_{s1} x_{s1} - (a_{s2} + \lambda_s)\, x_{s2} + k_s s_s\right) + r_s s_m + G_2 F_m \tag{6.12}$$

By plugging Eq (6.11) in Eq (6.9), we obtain the closed loop composite master system

as:

$$\dot{s}_m = k_m s_m + b_m r_m s_s + b_m F_m \tag{6.13}$$

Similarly, by substituting Eq (6.12) in Eq (6.10), we obtain the closed loop composite slave system as:

$$\dot{s}_s = k_s s_s + b_s r_s s_m + b_s G_2 F_m \tag{6.14}$$

Let us form an augmented system using composite master in Eq (6.13) and composite slave in Eq (6.14) systems as:

$$\begin{pmatrix} \dot{s}_m \\ \dot{s}_s \end{pmatrix} = \begin{pmatrix} k_m & b_m r_m \\ b_s r_s & k_s \end{pmatrix} \begin{pmatrix} s_m \\ s_s \end{pmatrix} + \begin{pmatrix} b_m \\ b_s G_2 \end{pmatrix} F_m \tag{6.15}$$

Now, we convert the composite master-slave augmented system of Eq (6.15) into a composite master-error augmented system. For this purpose, we define the following linear transformation:

$$\begin{pmatrix} s_m \\ s_e \end{pmatrix} = \begin{pmatrix} 1 & 0 \\ 1 & -1 \end{pmatrix} \begin{pmatrix} s_m \\ s_s \end{pmatrix} \tag{6.16}$$

where s_e is the composite error between composite master and composite slave systems. By taking the time derivative of Eq (6.16) and using Eq (6.15) and Eq (6.16), we obtain the composite master-error augmented system as:

$$\begin{pmatrix} \dot{s}_m \\ \dot{s}_e \end{pmatrix} = \begin{pmatrix} k_m + b_m r_m & -b_m r_m \\ k_m - b_s r_s - k_s + b_m r_m & k_s - b_m r_m \end{pmatrix} \begin{pmatrix} s_m \\ s_e \end{pmatrix} + \begin{pmatrix} b_m \\ b_m - b_s G_2 \end{pmatrix} F_m \tag{6.17}$$

Now, to ensure that the composite error evolves as an autonomous system, following conditions must hold:

$$b_m - b_s G_2 = 0 \tag{6.18}$$

$$k_m - b_s r_s - k_s + b_m r_m = 0 \tag{6.19}$$

After the conditions Eq (6.18) and (6.19) are met, we assign the desired dynamic behavior to composite master-error augmented system of Eq (6.17). The desired

dynamic behavior for Eq (6.17) is specified by selecting the pole for composite master ($s = -p$) and composite error ($s = -q$) systems. Thus, we have obtained the following polynomial:

$$(s - (k_m + b_m r_m))\,(s - (k_s - b_m r_m)) = (s + p)\,(s + q) \tag{6.20}$$

Eq (6.20) leads to the following design conditions:

$$k_m + b_m r_m = -p \tag{6.21}$$

$$k_s - b_m r_m = -q \tag{6.22}$$

Thus, we have four design equations i.e. Eq (6.18), Eq (6.19), Eq (6.21) and Eq (6.22) which are the same as Eq (6.3) - Eq (6.6). The solution of these equations will yield the unknown control gains G_2, k_m, k_s, r_s. Now, we analyze the convergence of master and slave states under these control gains. Since composite error has been made a stable system with dynamics $\dot{s}_e + q s_e = 0$ so 's_e' will vanish in a finite time as determined by the position of the pole 'q'. This implies that during steady state, we have $s_m = s_s$ and $\dot{s}_m = \dot{s}_s = 0$ (under the assumption of constant force). By plugging the master control law Eq (6.11) in Eq (6.1) and using Eq (6.13), we obtain the closed loop master system as $\dot{x}_{m2} + \lambda_m x_{m2} = \dot{s}_m = 0$ which shows that x_{m2} will converge to zero in a finite time. Similarly, by substituting the slave control law Eq (6.12) in Eq (6.2) and using Eq (6.14), we obtain the closed loop slave system as $\dot{x}_{s2} + \lambda_s x_{s2} = \dot{s}_s = 0$ which implies that x_{s2} will also approach zero in a finite time. Now, $s_m = s_s$ implies $(x_{m2} - x_{s2}) + (\lambda_m x_{m1} - \lambda_s x_{s1}) = 0$ which further implies that $\lambda_m x_{m1} - \lambda_s x_{s1} = 0$ as states x_{m2}, x_{s2} have been shown to be zero at steady state. Thus, by selecting the constants λ_m, λ_s to be unity, the convergence of states is ensured, and the slave system will now follow the motion of the master system. This completes the proof.

□

Remark 6.1. *The standard state convergence scheme does not consider motion scaling of the slave system, which is desired in some teleoperation applications. To add this extra feature, an alpha-modified version of the state convergence controller is proposed in [2]. However, the same number of design equations are required to be solved*

as that of the standard scheme. The proposed composite controller provides a lower complexity solution as fewer design equations are involved. In principle, motion scaling can be achieved by adjusting the constants λ_m *and* λ_s*. This follows from the steady state analysis of the proposed composite state convergence controller, which yields the following expression:*

$$x_{s1} = \frac{\lambda_m}{\lambda_s} x_{m1} \tag{6.23}$$

Remark 6.2. *In a standard state convergence scheme, desired dynamic behavior is directly assigned to the master or slave system. However, in the proposed composite state convergence scheme, desired dynamic response is indirectly assigned to the master or slave system. As can be seen from Eq (6.20), desired poles are assigned to the composite system which implies that the composite master system, and not the actual master system, shall possess the desired behavior* $(s + p = 0)$ *along with composite error system* $(s + q = 0)$*. To analyze the behavior of actual master system, we compute its closed loop dynamics using Eq (6.1), Eq (6.7), Eq (6.11), Eq (6.16), and Eq (6.21) as:*

$$\ddot{x}_{m1} + (\lambda_m + p)\,\dot{x}_{m1} + p\lambda_m x_{m1} = -b_m r_m s_e + b_m F_m \tag{6.24}$$

Since composite error evolves as an autonomous system, the motion of the master system is governed by the following polynomial:

$$s^2 + (\lambda_m + p)\,s + p\lambda_m = 0 \tag{6.25}$$

It is evident from Eq (6.25) that the desired dynamic behavior of the master system can also be guaranteed by choosing appropriate values of 'p' and 'λ_m*'. A similar analysis for the slave system reveals that it also possesses the dynamic behavior determined by the values of 'p' and '*λ_s*' as* $s^2 + (\lambda_s + p)\,s + p\lambda_s = 0$*.*

Remark 6.3. *To counter the effect of environmental force, the control input for the slave system in Eq (6.12) is modified as:*

$$u_s = \frac{1}{b_s}\left((-a_{s1} + b_s k_e)\,x_{s1} - (a_{s2} + \lambda_s)\,x_{s2} + k_s s_s\right) + r_s s_m + G_2 F_m \tag{6.26}$$

Note that the above modification in slave control law will not affect the design procedure.

Remark 6.4. *The force reflection behaviour of the proposed composite state convergence controller is imperative to be analyzed. Given that environmental force is described by* $F_e = k_e x_{s1}$ *and with the knowledge of Eq* (6.5) *and steady state values of the composite-master and slave variables i.e.* $s_m = \lambda_m x_{m1} = {}^{b_m F_m}/_{p}, s_s = \lambda_s x_{s1}$, *we can write steady-state control input of the master system as:*

$$u_m = -\frac{1}{p}\left(\frac{a_{m1}}{\lambda_m} + b_m r_m\right) F_m + k_f \lambda_s F_e \tag{6.27}$$

It is evident from Eq (6.27) *that human operator will feel the true environmental force in a steady state if force feedback gain,* k_f *is set as the inverse of motion-scaling constant,* λ_s *and desired pole of the composite master system is chosen as* $p = \frac{a_{m1}}{\lambda_m} + b_m r_m$. *In this way, the operator's perception of the remote environment will be improved.*

Remark 6.5. *Although the development of a composite state convergence controller has been shown here purposefully for a second-order system, the procedure can be readily extended to higher-order systems. For instance, consider a third-order master system in phase variable form* $\dot{x}_{m1} = x_{m2}$, $\dot{x}_{m2} = x_{m3}$, $\dot{x}_{m3} = a_{m1}x_{m1} + a_{m2}x_{m2} + a_{m3}x_{m3} + b_m u_m$. *The composite variable for this system can be defined as* $s_m = x_{m3} + \lambda_{m2}x_{m2} + \lambda_{m1}x_{m1}$ *which gives rise to the composite master system as* $\dot{s}_m = a_{m1}x_{m1} + (a_{m2} + \lambda_{m1})\, x_{m2} + (a_{m3} + \lambda_{m2})\, x_{m3} + b_m u_m$. *Appropriate master control input can now be selected to transform this composite master system to Eq* (6.13) *and thus, the rest of the procedure remains the same.*

Theorem 6.2. *In the presence of constant time delay, slave system Eq* (6.1) *will follow the master system Eq* (6.2) *if control gains of the composite state convergence scheme are found as a solution of the following design conditions:*

$$b_m - (T b_m r_m b_s + b_s)\, g_2 + T b_s r_s b_m = 0 \tag{6.28}$$

$$k_m\,(1 + T b_s r_s) - k_s\,(1 + T b_m r_m) - b_s r_s + b_m r_m = 0 \tag{6.29}$$

$$k_m - T b_m r_m k_s - T\,(1 + pT)\, b_m r_m b_s r_s + p + b_m r_m = 0 \tag{6.30}$$

$$(1 + T b_m r_m)\, k_s - T\,(1 + qT)\, b_m r_m b_s r_s + q - b_m r_m = 0 \tag{6.31}$$

Proof. Let us define the control inputs for the master Eq (6.1) and slave Eq (6.2) systems in time-delayed composite state convergence scheme as:

$$u_m = \frac{1}{b_m}\left(-a_{m1}x_{m1} - \left(a_{m2} + \lambda_m\right)x_{m2} + k_m s_m\right) + r_m s_s\left(t - T\right) + F_m \tag{6.32}$$

$$u_s = \frac{1}{b_s}\left(-a_{s1}x_{s1} - \left(a_{s2} + \lambda_s\right)x_{x2} + k_s s_s\right) + r_s s_m\left(t - T\right) + G_2 F_m\left(t - T\right) \tag{6.33}$$

By plugging Eq (6.32) in Eq (6.9), we obtain the closed loop composite master system as:

$$\dot{s}_m = k_m s_m + b_m r_m s_s\left(t - T\right) + b_m F_m \tag{6.34}$$

Also, by substituting Eq (6.33) in Eq (6.9), we obtain the closed loop composite slave system as:

$$\dot{s}_s = k_s s_s + b_s r_s s_m\left(t - T\right) + b_s G_2 F_m\left(t - T\right) \tag{6.35}$$

Under the assumption of small time delay and constant operator's force, we approximate the time-delayed variables in Eq (6.34) and Eq (6.35) using Taylor series as:

$$\begin{aligned} s_s\left(t - T\right) &\approx s_s - T\dot{s}_s \\ s_m\left(t - T\right) &\approx s_m - T\dot{s}_m \\ F_m\left(t - T\right) &\approx F_m \end{aligned} \tag{6.36}$$

By plugging Eq (6.36) in Eq (6.34), Eq (6.35) and forming the augmented composite master-slave system, we have:

$$\begin{aligned} \begin{pmatrix} \dot{s}_m \\ \dot{s}_s \end{pmatrix} = {} & \frac{1}{\left(1 - T^2 b_m r_m b_s r_s\right)} \begin{pmatrix} k_m - T b_m r_m b_s r_s & b_m r_m - T b_m r_m k_s \\ b_s r_s - T b_s r_s k_m & k_s - T b_s r_s b_m r_m \end{pmatrix} \begin{pmatrix} s_m \\ s_s \end{pmatrix} \\ & + \frac{1}{\left(1 - T^2 b_m r_m b_s r_s\right)} \begin{pmatrix} b_m - T b_m r_m b_s G_2 \\ b_s G_2 - T b_s r_s b_m \end{pmatrix} F_m \end{aligned} \tag{6.37}$$

Now, we convert the above augmented system of Eq (6.37) into a composite master-error augmented system using the transformation in Eq (6.16) as:

$$\begin{pmatrix} \dot{s}_m \\ \dot{s}_e \end{pmatrix} = \frac{1}{(1-T^2 b_m r_m b_s r_s)} \begin{pmatrix} a_{11} & a_{12} \\ a_{21} & a_{22} \end{pmatrix} \begin{pmatrix} s_m \\ s_e \end{pmatrix} + \frac{1}{(1-T^2 b_m r_m b_s r_s)} \begin{pmatrix} b_{11} \\ b_{21} \end{pmatrix} F_m \quad (6.38)$$

where,

$$\begin{aligned}
a_{11} &= (k_m - T b_m r_m b_s r_s) + (b_m r_m - T b_m r_m k_s) \\
a_{12} &= -b_m r_m + T b_m r_m k_s \\
a_{21} &= (k_m - T b_m r_m b_s r_s) - (b_s r_s - T b_s r_s k_m) + (b_m r_m - T b_m r_m k_s) - (k_s - T b_s r_s b_m r_m) \\
a_{22} &= -(b_m r_m - T b_m r_m k_s) + (k_s - T b_s r_s b_m r_m) \\
b_{11} &= b_m - T b_m r_m b_s G_2 \\
b_{21} &= (b_m - T b_m r_m b_s G_2) - (b_s G_2 - T b_s r_s b_m)
\end{aligned} \quad (6.39)$$

If the composite error system in Eq (6.38) is to evolve autonomously, the following conditions must be satisfied:

$$(b_m - T b_m r_m b_s G_2) - (b_s G_2 - T b_s r_s b_m) = 0 \quad (6.40)$$

$$\begin{aligned}
&(k_m - T b_m r_m b_s r_s) - (b_s r_s - T b_s r_s k_m) + \\
&(b_m r_m - T b_m r_m k_s) - (k_s - T b_s r_s b_m r_m) = 0
\end{aligned} \quad (6.41)$$

We now impose the desired dynamic behavior on the composite master-error system which is specified by the polynomial $(s+p)(s+q) = 0$ where left-hand plane poles 'p' and 'q' fix the behavior of composite master and composite error systems respectively. This pole assignment procedure results in the following conditions:

$$(k_m - T b_m r_m b_s r_s) + (b_m r_m - T b_m r_m k_s) = -p\left(1 - T^2 b_m r_m b_s r_s\right) \quad (6.42)$$

$$-(b_m r_m - T b_m r_m k_s) + (k_s - T b_s r_s b_m r_m) = -q\left(1 - T^2 b_m r_m b_s r_s\right) \quad (6.43)$$

The design conditions Eq (6.40) - Eq (6.43) are the same as Eq (6.28) - Eq (6.31) which can be solved to find the control gains (G_2, k_m, k_s, r_s) of the composite state

convergence scheme. These control gains are displayed in Appendix A. An analysis similar to that of Theorem 6.1 reveals that the slave system indeed follows the master system in the presence of constant time delays. This completes the proof □

Remark 6.6. *Similar to Remark 6.2 of Theorem 6.1, we compute the dynamic behavior of the master and slave systems under small constant time delay as* $s^2 + (\lambda_m + \psi_m)\, s + \lambda_m \psi_m = 0$, $s^2 + (\lambda_s + \psi_s)\, s + \lambda_s \psi_s = 0$. *In addition, the force reflection behavior of the proposed controller under time delay is also investigated following the lines of Remark 6.4 of Theorem 6.1. It is found that for full force reflection at steady state, condition* $\left(-\frac{a_{m1}}{b_m} + k_m\right) \frac{\beta_m}{\psi_m} = -2$ *must be satisfied. Note that* ψ_m, ψ_s, *and* β_m *can be found from the closed loop analysis of the teleoperation system.*

6.2 Simulation Results

For the purpose of simulations, parameters of master and slave systems are adopted from [71]:

$$\begin{aligned} a_{m1} &= 0, a_{m2} = -7.1429, b_m = 0.2656 \\ a_{s1} &= 0, a_{s2} = -6.25, b_s = 0.2729 \end{aligned} \tag{6.44}$$

It is assumed that the slave system interacts with a soft environment having $k_e = 10 Nm/rad$. Let motion scaling constants be unity, i.e., $\lambda_m = \lambda_s = 1$, so force feedback gain is unity as well. Thus, r_m is the same as k_e. First, we study the performance of the proposed controller when no time delay exists in the communication channel. To this end, control gains of the composite state convergence controller are found as a solution of the design conditions Eq (6.3) - Eq (6.6) where desired pole locations are selected as $p = 2$, and $q = 6$:

$$\begin{aligned} G_2 &= 0.9733 \\ k_m &= -4.6560 \\ k_s &= -3.3440 \\ r_s &= 4.9249 \end{aligned} \tag{6.45}$$

By assuming zero initial conditions for master and slave systems, we simulate the proposed bilateral tele-controller under the control of Eq (6.45), and the results are shown in Figure 6.2 and Figure 6.3.

It can be seen from Figure 6.2 that composite master and slave variables are indistinguishable and exhibit the desired dynamic response $(s + 2 = 0)$ as well. It is also

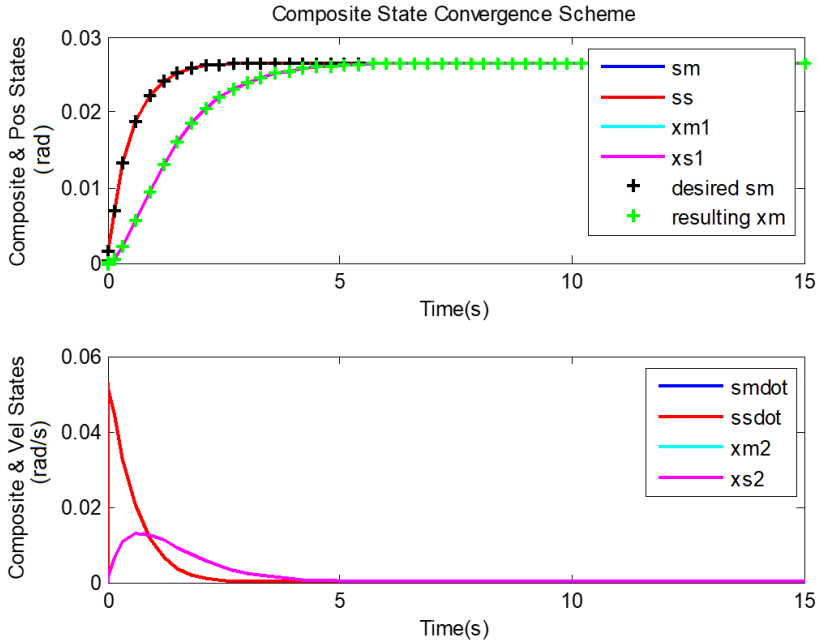

Figure 6.2: Convergence of states with delay-free composite state convergence controller

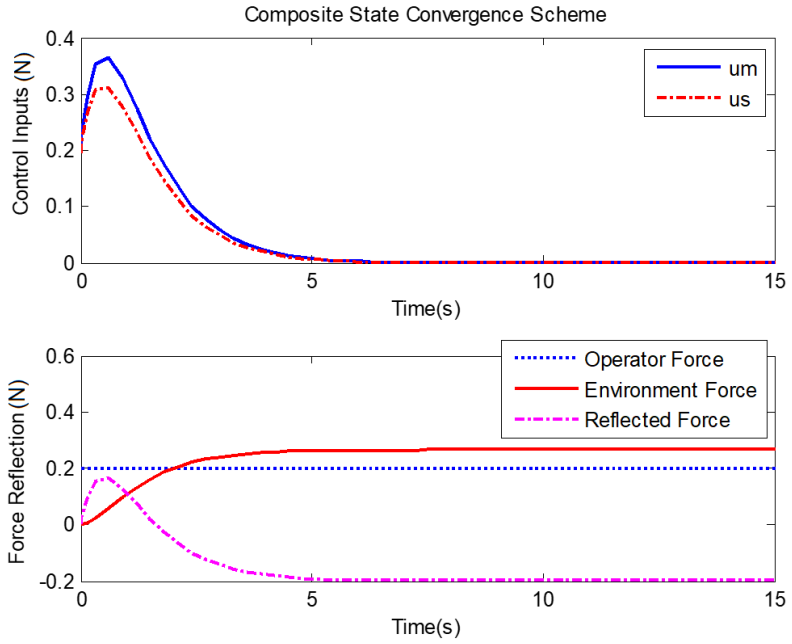

Figure 6.3: Control inputs and force reflection behavior of composite state convergence controller with no communication delay

evident that the slave system follows the master system as their position and velocity states remain synchronized. Further, as pointed out in Remark 6.2, the master system should possess the dynamic behavior of Eq (6.25), which, in the present case, is $s^2 + 3s + 2 = 0$ and has been plotted in Figure 6.2. The analysis reveals that the master system indeed displays this behavior, and so does the slave system. The control inputs for the master and slave system are shown in Figure 6.3 along with the force reflection behavior of the proposed controller. It can be seen that the proposed controller indeed establishes a kinesthetic link between the operator and the environment. However, the environmental force is not fully reflected to the operator even though the product $\lambda_s k_f$ is unity. This is because of the fact that pole 'p' has not been selected to exactly cancel the term in the parenthesis of Eq (6.27). When exact cancellation occurs, i.e., the pole is placed at $p = 2.6560$, operators and environmental forces match at steady state, as shown in Figure 6.4. Note that control gains are recomputed as the pole location is changed.

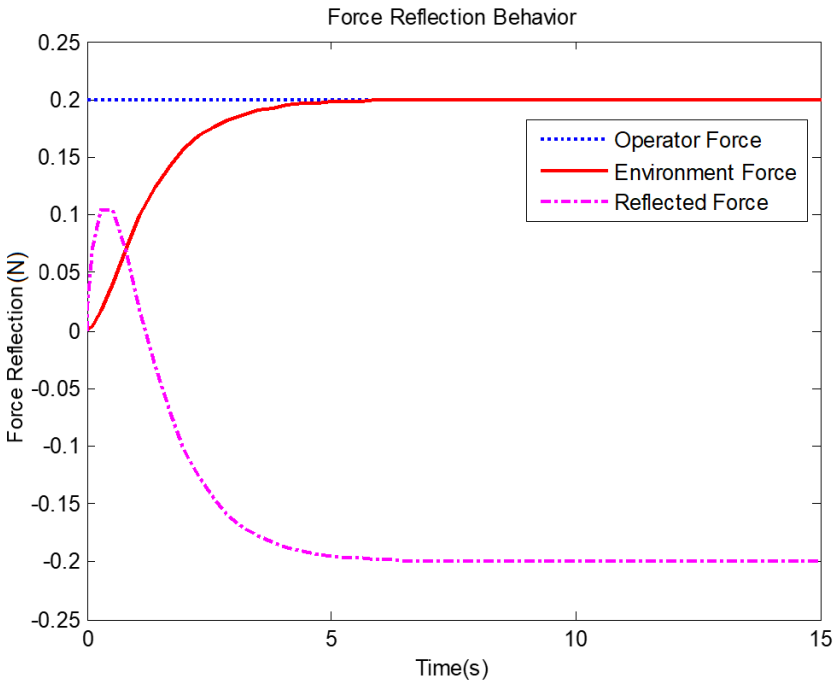

Figure 6.4: Improved force reflection behavior of composite state convergence controller

We now investigate the motion scaling property of the proposed controller. Suppose that we want the slave system to acquire and maintain a final position that is half of the master's final position. To achieve this, we change the slave's motion scaling constant to $\lambda_s = 2$, which, according to Remark 6.4, also scales the force feedback

gain to $k_f = {}^1/_{\lambda_s} = 0.5$ and therefore $r_m = k_f k_e = 5$. By solving the design conditions Eq (6.3) - Eq (6.6) using the parameters in Eq (6.44) and $p = 2.6560, q = 6, \lambda_m = 1$, we find the control gains as:

$$\begin{aligned} G_2 &= 0.9733 \\ k_m &= -2.6560 \\ k_s &= -4.6720 \\ r_s &= 12.2536 \end{aligned} \tag{6.46}$$

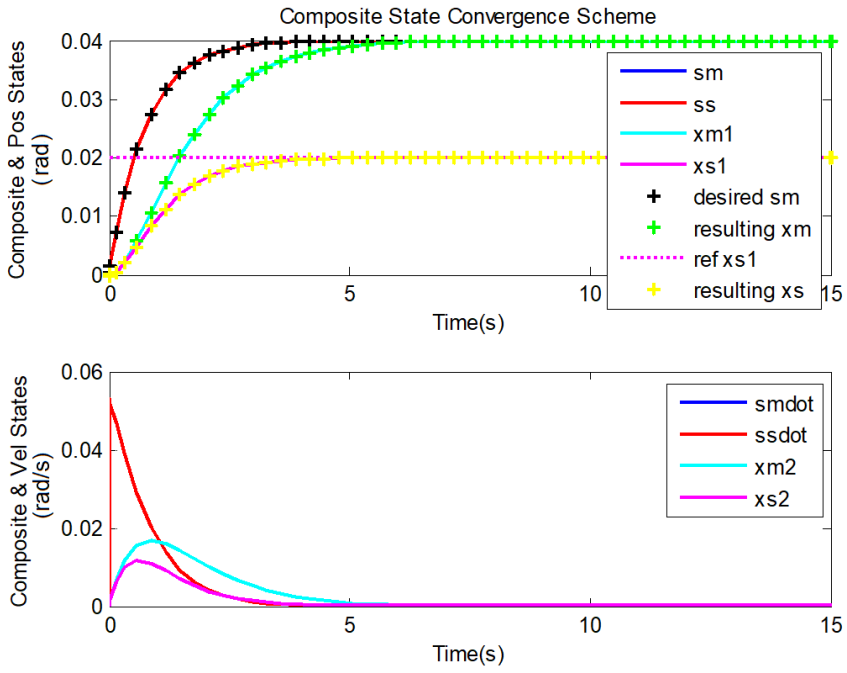

Figure 6.5: Motion scaling property of composite state convergence controller with no communication time delay

Now we consider the case when constant time delay exists in the communication channel. We assume that the slave system is interacting with a much stiffer environment ($k_e = 50Nm/rad$)than the previous case, and the communication channel offers a time delay of $T = 0.5s$. By setting the motion scaling constants and force feedback gain as unity and selecting the pole locations as $p = 1.7, q = 4.0$, we solve the design conditions Eq (6.28) - Eq (6.31) for the teleoperation system in Eq (6.44) and obtain the following control gains:

$$\begin{aligned} G_2 &= 0.0857 \\ k_m &= -26.2680 \\ k_s &= -0.4903 \\ r_s &= -2.3961 \end{aligned} \tag{6.47}$$

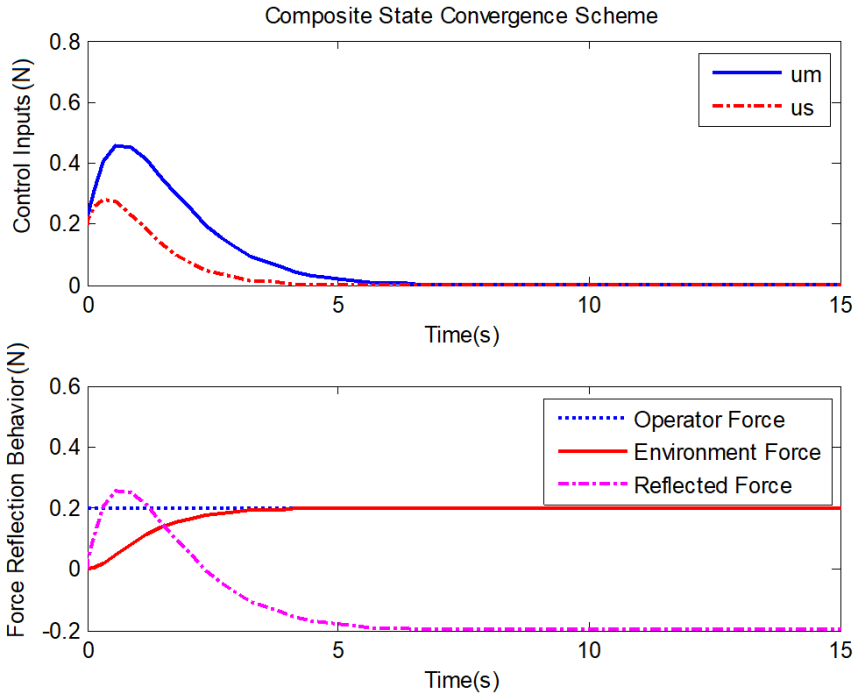

Figure 6.6: Control inputs and force reflection behavior of composite state convergence controller with scaled slave motion of Fig 6.5

The teleoperation system is now simulated under the control gains of Eq (6.47), and results are shown in Figure 6.7 and Figure 6.8. It can be seen that the slave system is able to follow the master system in the presence of time delay, and a good amount of environmental force is also reflected to the operator. As pointed out earlier, force error at steady state can be eliminated by properly choosing the location of pole 'p'. We also evaluate the motion scaling performance of the proposed composite controller. To this end, let the reference for the slave system be set as $x_{s1ref} = 0.25x_{m1}$. Thus, the motion scaling constant of the slave system and force feedback gain must be selected as $\lambda_s = 4$,$k_f = \lambda_s^{-1}$. To ensure proper force feedback, we roughly select the pole 'p' as $p = 1.3$ while keeping all other system parameters the same. The solution of design conditions Eq (6.28) - Eq (6.31) yield the control gains as:

$$\begin{aligned} G_2 &= 0.3116 \\ k_m &= -6.7780 \\ k_s &= -0.8108 \\ r_s &= -1.0865 \end{aligned} \tag{6.48}$$

We now simulate the teleoperation system under the control of Eq (6.48), and results

are shown in Figure 6.9 and Figure 6.10. It can be seen that the slave system has achieved the set point, and the force reflection behavior of the controller is also promising.

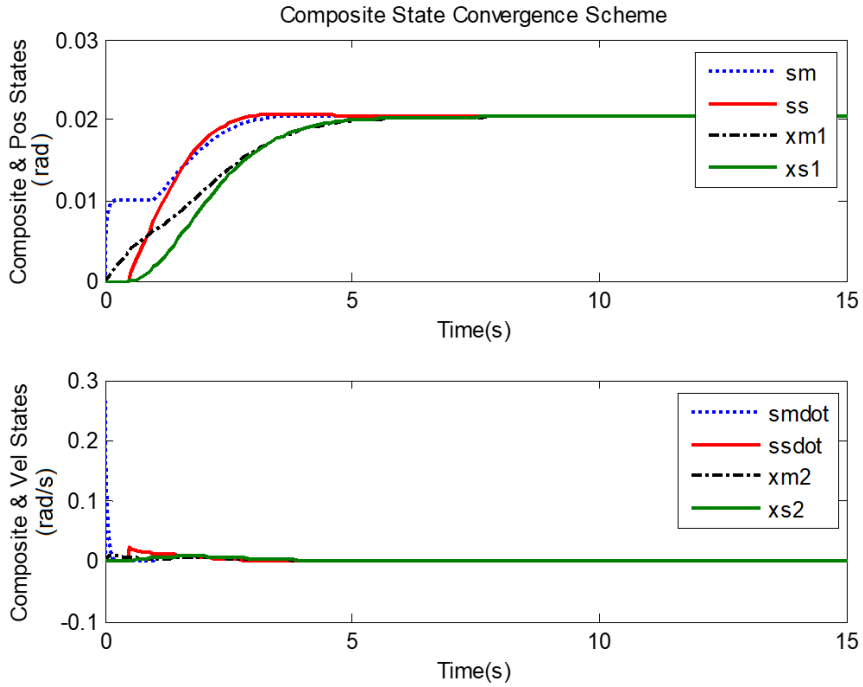

Figure 6.7: Convergence of states with CSC controller under time-delayed communication

Comparative Study

In order to show the superiority of the proposed scheme, a comparative study is performed in MATLAB/Simulink environment. Note that the proposed scheme forms three-channel control architecture owing to the transmission of the operator's force as well as composite master and slave variables across the communication channel. Therefore, three-channel architecture, namely error force compensated scheme [53], is selected for the purpose of comparison. In this scheme, velocities of the master and slave systems as well as an environmental force, are transmitted across the communication channel, and the control laws are defined as:

$$\begin{aligned} u_m &= (1 + C_6)\, F_h - C_m V_m - C_2 F_e - C_4 V_s \\ u_s &= -(1 + C_5)\, F_e - C_s V_s + C_1 V_m \end{aligned} \tag{6.49}$$

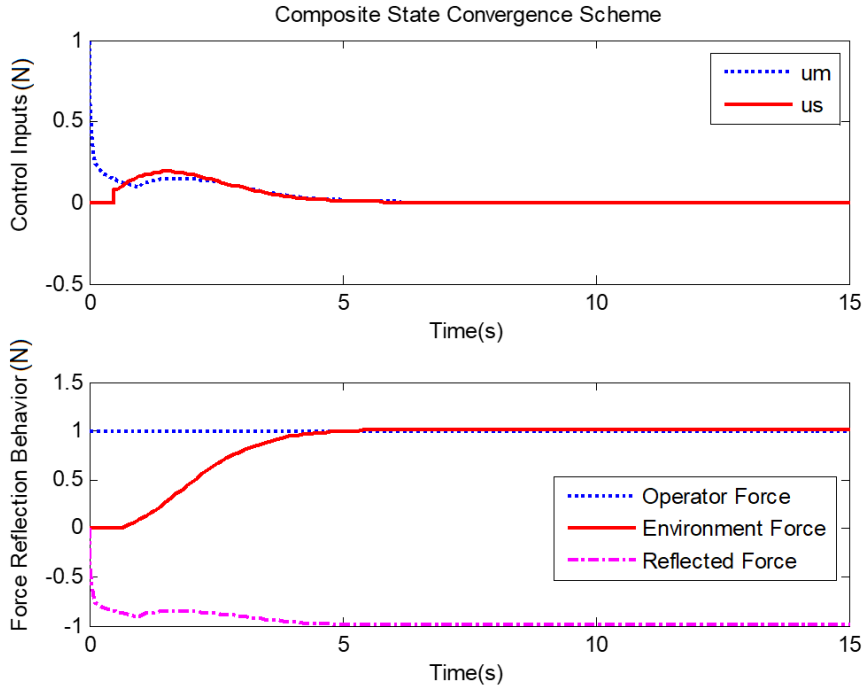

Figure 6.8: Control inputs and force reflection behavior of CSC controller under communication delay

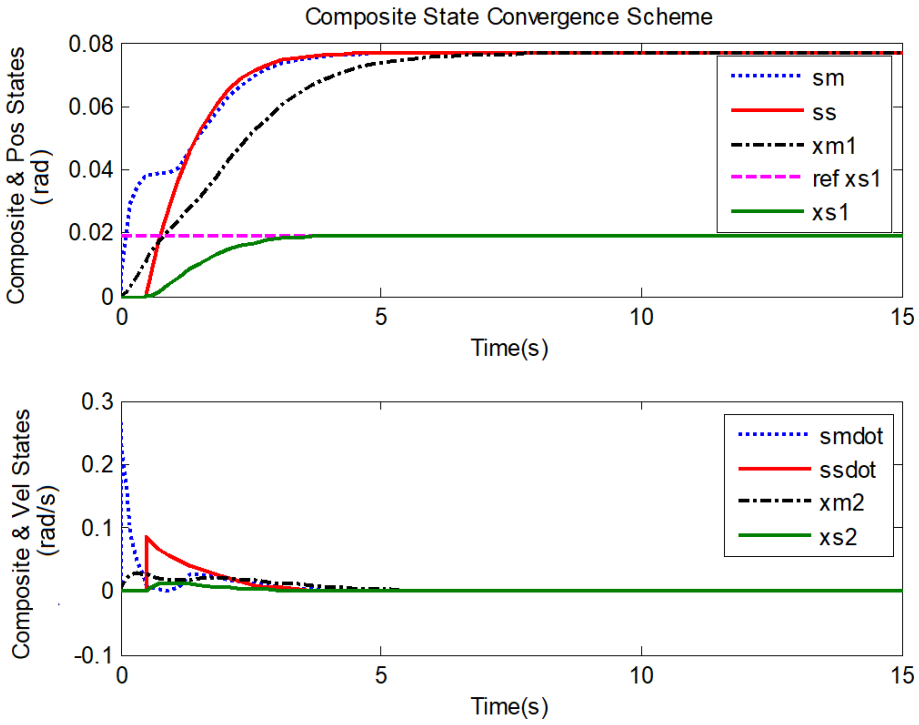

Figure 6.9: Motion scaling results of CSC controller under communication time delay

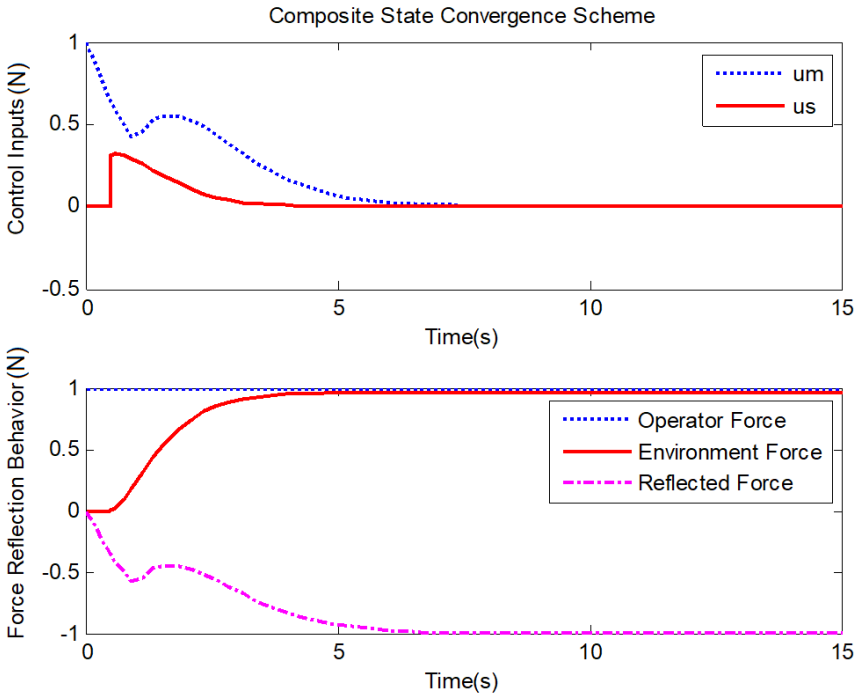

Figure 6.10: Control inputs and force reflection behavior of CSC controller with scaled slave motion of Figure 6.9

where the compensators C_x are proposed [38] as:

$$\begin{aligned} C_m &= \left(2\xi_m\omega_m + \tfrac{\omega_m^2}{s}\right) J_m, C_s = \left(2\xi_s\omega_s + \tfrac{\omega_s^2}{s}\right) J_s \\ C_1 &= \left(2\xi_s\omega_s + \tfrac{\omega_s^2}{s} + s\right) J_s, C_4 = -\left(2\xi_m\omega_m + \tfrac{\omega_m^2}{s} + s\right) J_m \\ C_5 &= -1, C_2 = 1 + C_6 \neq 0 \end{aligned} \tag{6.50}$$

where $\xi_m, \xi_s, \omega_m, \omega_s, C_2, C_6$ are the parameters to be determined. It is important to mention that the proposed composite state convergence scheme offers a systematic procedure to determine associated control gains, while no such design procedure exists for the error force compensation scheme. Thus, for a fair comparison, the design parameters of both schemes are found through a genetic algorithm by employing the ITAE criterion as:

$$f_{obj} = \int_0^t t\left(|e_m| + |e_f|\right) dt \tag{6.51}$$

where $e_m = x_m - x_s$ is the position error while $e_f = F_m - F_e$ is the force error. We now revisit the teleoperation system of Eq (6.44) with a time delay of 100ms and an environment stiffness of 50Nm/rad. By executing the genetic algorithm with

default parameters and a population size of 50 chromosomes, design parameters of the two schemes are found through minimization of objective function Eq (6.51) as $\xi_m = 0.3855, \xi_s = 0.983, \omega_m = 0.0348, \omega_s = 3.0386$, $C_6 = 0, C_2 = 1$, $G_2 = 0.5377, k_m = -10.9353, k_s = -7.4588$, $r_s = 0.4489, r_m = -8.8197$.

With these optimized control gains, simulations are run under a constant operator's force of 1N, and the resulting position as well as force errors are recorded which are depicted in Figure 6.11. Analysis of Figure 6.11 reveals that the composite state convergence scheme offers better transient performance as compared to the error force compensated scheme.

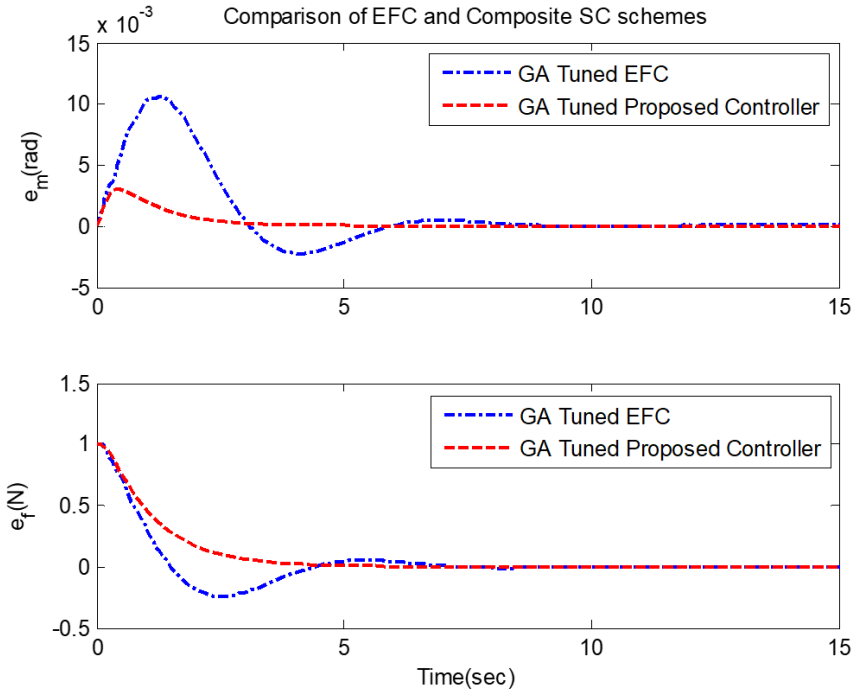

Figure 6.11: Comparison of error force compensated and proposed composite state convergence schemes

6.3 Experimental Results

To further validate the proposed composite state convergence controller, semi-real-time experiments are performed using the geomagic haptic device in QUARC/Simulink environment. Since a mathematical model of the haptic device is not available, we use a haptic device to generate the operator force for the virtual master-slave tele-operation system. Along with this, reflected environmental force, as generated by the controller, is also displayed to the haptic device so that the person driving the haptic device can feel the environment. This implementation framework is depicted

in Figure 6.12. As the operator moves the device along x-axis between the positions 2 and 8 on the cardboard, force is generated proportional to the position information as $F_m = k_{op}x_{op}$ where $k_{op} = 5$ and $x_{op} \in [0.1, 0.2]$. This force is applied to the virtual master system and the reflected environmental force is provided to the haptic device in addition to the virtual master system. In this way, the loop is closed around the operator as reflected force is felt by the operator. We use this setup to perform experiments in the absence and presence of time delays. In both cases, the stiffness of the environment is considered as $k_e = 10Nm/rad$ while motion and force scaling constants are assumed to be unity. Pole 'p' is placed at the position $p = 2.6560$ in case of no communication delay while it is placed at the position $p = 1.15$ in case of time delay, which is assumed to be $T = 0.5s$. The location of pole 'q' remains the same in both cases at $q = 6$. Using the teleoperation system's parameters in Eq (6.44), control gains in the absence of time delay are obtained as:

$$\begin{aligned} G_2 &= 0.9733 \\ k_m &= -5.3120 \\ k_s &= -3.3440 \\ r_s &= 2.5211 \end{aligned} \tag{6.52}$$

Also, the control gains in the presence of time delay are obtained as:

$$\begin{aligned} G_2 &= 0.4336 \\ k_m &= -5.3332 \\ k_s &= -1.2670 \\ r_s &= 0.2721 \end{aligned} \tag{6.53}$$

We first evaluate the performance of the proposed controller in the absence of time delays. By considering the initial position of the master as 0.05rad, the teleoperation system is run in QUARC/Simulink environment under the control of Eq (6.52) where the operator exerts a time-varying force on the master system using the haptic device. Note that the composite state convergence controller is designed under the assumption of constant applied force but here we are evaluating its performance under variable operator's force, which is the case in practice. During the operation, various system trajectories, as well as forces, are recorded, which are shown in Figure 6.13, Figure 6.14, Figure 6.15.

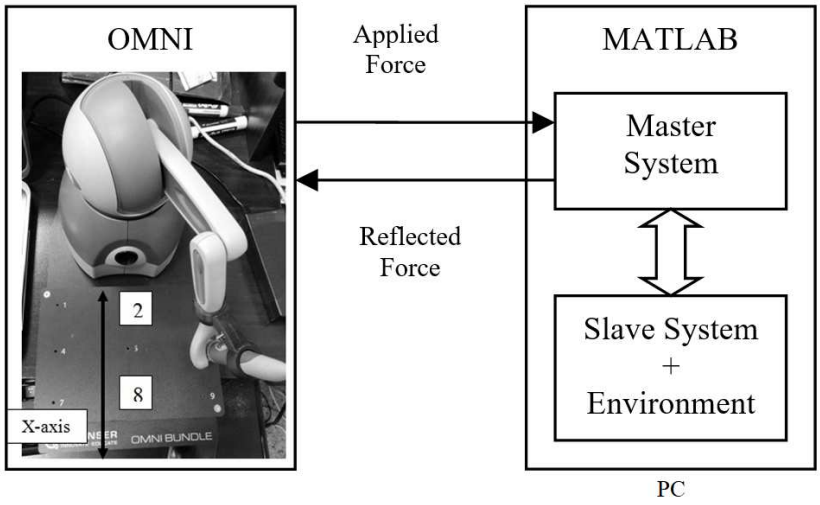

Figure 6.12: Experimental framework to implement CSC controller

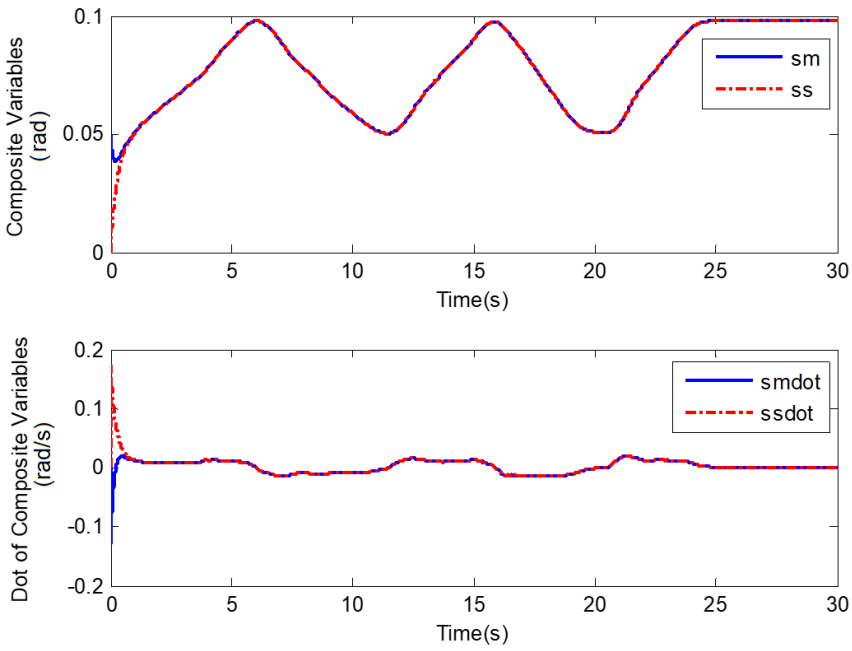

Figure 6.13: CSC controller with no delay: composite variables

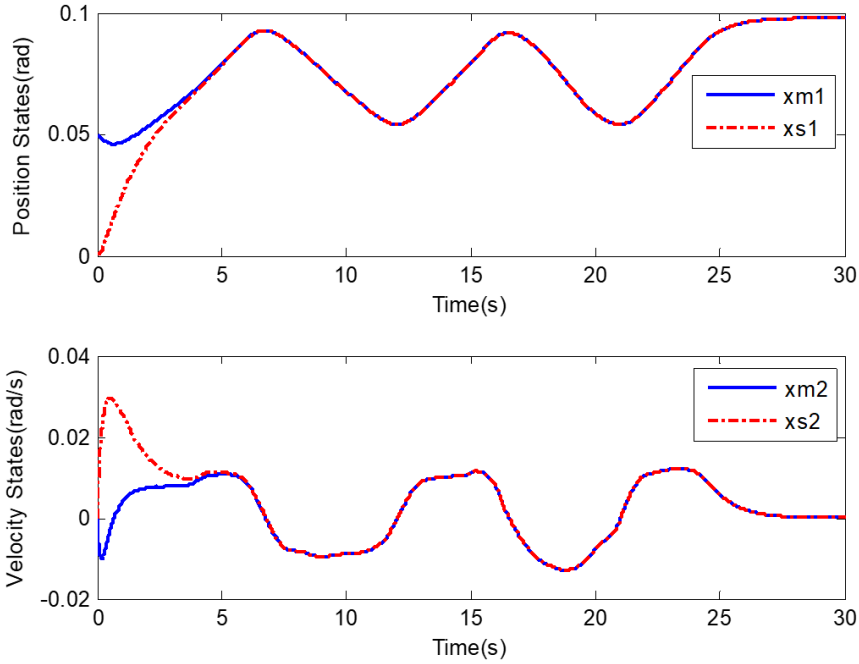

Figure 6.14: CSC controller with no delay: position and velocity variables

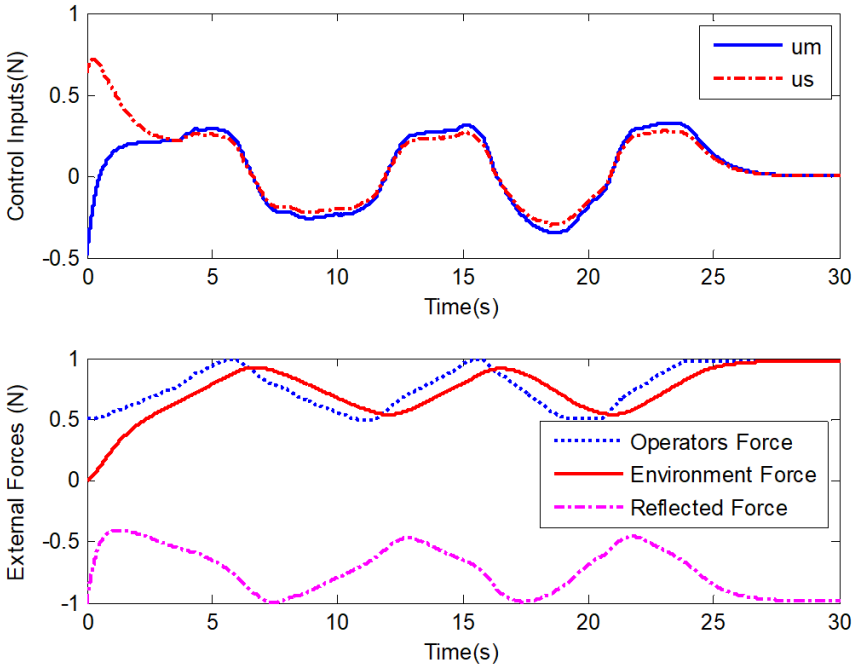

Figure 6.15: CSC controller with no delay: external forces

It can be seen that composite states, as well as the original states, are converged after an initial transient, and thus the slave is following the master while the reaction force is also being displayed to the operator.

We now run the teleoperation system in the presence of time delays. In this case, control gains of Eq (6.53) are used, and the operator exerts a time-varying force through the haptic device. The resulting system states and forces are displayed in Figure 6.16, Figure 6.17, Figure 6.18.

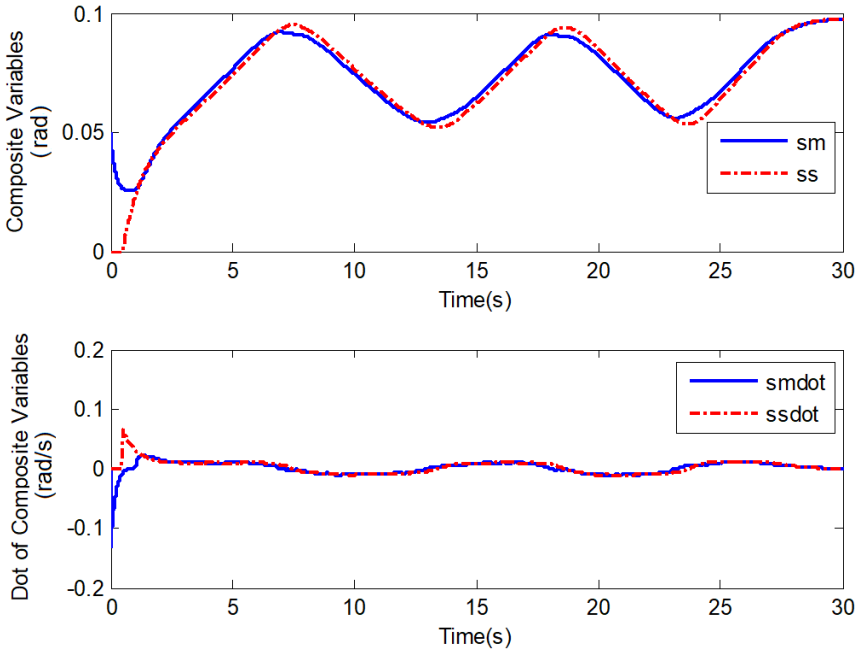

Figure 6.16: CSC controller with time delay: composite variables

It can be seen that the slave system follows the master system, but error exists between their states. The error is caused by the fact that the operator's force is not constant, and the delayed force received by the slave is, therefore, different from the transmitted force. Any abrupt change in the applied force, along with long-time delays, is likely to result in increased position error, a case discussed in [71]. Thus, the state convergence scheme and the proposed one are viable in the presence of small time delays, although control gains of the scheme can be found for larger time delays. The proposed controller parameters are summarized in Table 6.1.

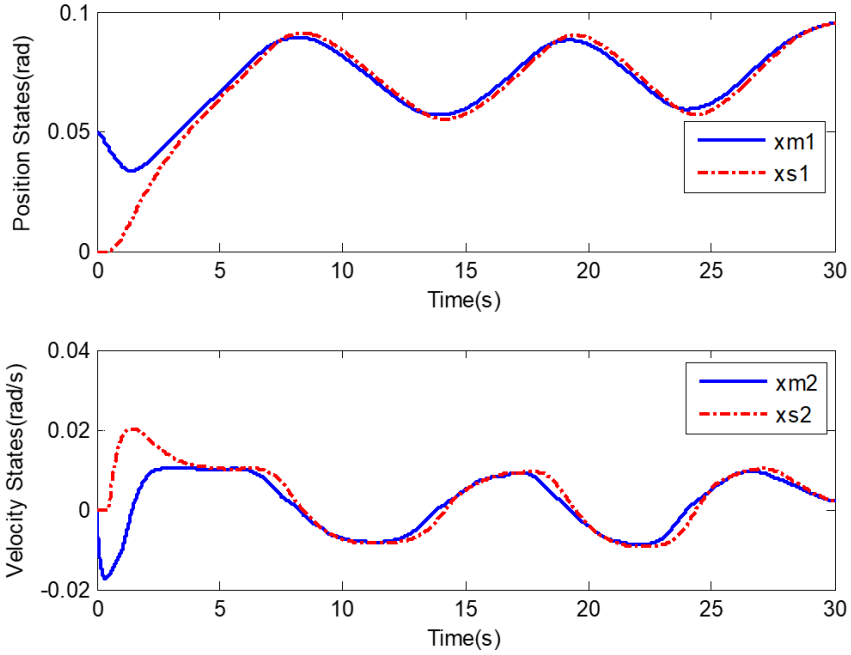

Figure 6.17: CSC controller with time delay: position and velocity variables

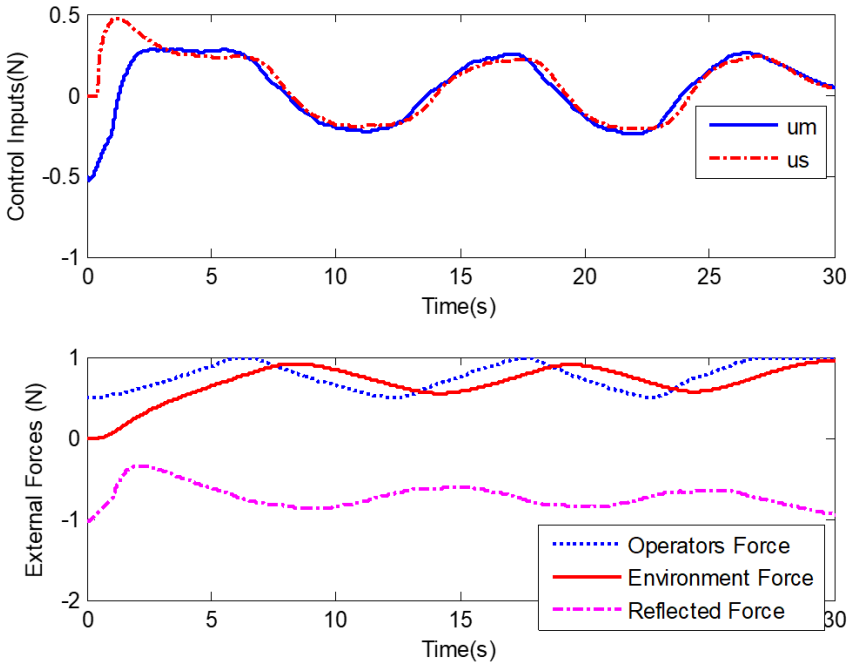

Figure 6.18: CSC controller with time delay: external forces

Controller	Simulation in MATLAB/Simulink	Semi Real-time QUARC/Simulink
System	1-DoF (Master/Slave)	1-DoF (Master/Slave)
Operator Force (N)	1 (constant)	Time-varying force using Omni Bundle
Environment Stiffness k_e (Nm/rad)	10	10
Environment Damping b_e (Nm/rad)	0.1	0.1
Force Feedback gain K_f	unity	unity
Motion Scaling factor λ_m/λ_s	1	1
Time delay (Sec)	0.5	0.5

Table 6.1: Proposed controller parameters for simulation and semi-real time experiment

6.4 Conclusion

This chapter discussed a composite version of the state convergence controller for bilaterally controlling a teleoperation system. The composite scheme allows transmitting fewer variables across communication channels while still ensuring the convergence of master and slave states in a desired dynamic way. Control gains of the scheme are found by constructing an augmented system using composite variables and applying the method of state convergence to this augmented system. The proposed scheme has been validated through MATLAB/Simulink environment simulations by considering a single-degree-of-freedom teleoperation system. Moreover, the proposal is compared with the error force compensated scheme and offers better transient performance than the latter. Semi-real-time experiments using a geomagic haptic device are finally performed in QURAC/Simulink environment to establish the success of the proposed scheme.

Chapter 7

A Composite State Convergence Architecture for a Nonlinear Telerobotic System

This chapter is an extension of our earlier work on the channel simplification of state convergence controller where we have only considered linear telerobotic system [104]. The design of a reduced complex state convergence controller, termed as composite state convergence controller, is proposed for a single-degree-of-freedom nonlinear telerobotic system. To this end, we first utilize feedback linearization theory to transform the nonlinear telerobotic system into a controllable linear system. In the second stage, composite states are constructed for the transformed master and slave systems. These composite master and slave states, along with the operator's force, are then transmitted across the communication channel instead of full states. In this way, the complexity of the communication structure is reduced. An augmented system comprising composite master and slave states is finally constructed, and the method of state convergence is applied to compute the control gains of the proposed scheme. It has shown that the position and velocity states of the master and slave systems still converge in the absence and presence of time delays, even though the design is based on the reduced-order composite system. In order to validate the proposed scheme, simulations are performed in MATLAB/Simulink environment where both the delay-free and delayed communication is considered. Semi-real-time experiments using the haptic device are also conducted.

7.1 Problem Definition

Consider a single degree-of-freedom nonlinear teleoperation system as:

$$\begin{cases} Master : J_m\ddot{\theta}_m + b_m\dot{\theta}_m + m_m g l_m \sin\theta_m = u'_m + F_m = u_m \\ Slave : J_s\ddot{\theta}_s + b_s\dot{\theta}_s + m_s g l_s \sin\theta_s = u'_s - F_e = u_s \end{cases} \tag{7.1}$$

where $m_x, l_x, b_x, J_x, \theta_x, \dot{\theta}_x, \ddot{\theta}_x, g, u_x$ are the mass, length, friction coefficient, inertia, angular position, angular velocity, angular acceleration, acceleration due to gravity and torque inputs for the master $(x = m)$/slave $(x = s)$ systems, respectively. Also,

F_m and F_e are the operator's and environment forces, respectively. By defining the angular position and angular velocity as state variables i.e. $x_{1x} = \theta_x, x_{2x} = \dot{\theta}_x, y_x = x_{1x}$, nonlinear dynamics of Eq (7.1) can be written as:

$$\begin{aligned} Master: & \begin{cases} \dot{x}_{1m} = x_{2m} \\ \dot{x}_{2m} = -\frac{m_m g l_m}{J_m} \sin x_{1m} - \frac{b_m}{J_m} x_{2m} + \frac{1}{J_m} u_m \\ y_m = x_{1m} \end{cases} \\ Slave: & \begin{cases} \dot{x}_{1s} = x_{2s} \\ \dot{x}_{2s} = -\frac{m_s g l_s}{J_s} \sin x_{1s} - \frac{b_s}{J_s} x_{2s} + \frac{1}{J_s} u_s \\ y_s = x_{1s} \end{cases} \end{aligned} \tag{7.2}$$

The objective of the present study is to design control inputs for the master and slave system such that the slave is able to follow the master system and the environment force is also reflected to the operator as the slave interacts with the environment. Mathematically,

$$\begin{aligned} \lim_{t\to\infty} x_{1m} - \alpha x_{1s} = 0 \\ \lim_{t\to\infty} F_m + \beta F_e = 0 \end{aligned} \tag{7.3}$$

where α, β are scaling constants for the position and force responses, respectively. To achieve the objective in Eq (7.3), we present a feedback-linearization-supported composite state convergence controller in the next section.

7.2 Proposed Controller

The proposed tele-controllers for the position and force tracking task in Eq (7.3) are developed using feedback linearization and composite state convergence theories. To start with, we recall the fundamentals of exact linearization.

Theorem 7.1. *For a nonlinear system $\dot{x} = f(x) + g(x)u, y = h(x)$ having a relative degree n where $x \in \mathbb{R}^n$, there exists a transformation $\phi(x)$ such that the resulting system $\dot{z} = Az + Bv$ is linear and controllable in new coordinates. The coordinate transform, nonlinear input, and the resulting linear system are given as [70]:*

$$z = \phi(x) = \begin{bmatrix} z_1 \\ z_2 \\ \vdots \\ z_n \end{bmatrix} = \begin{bmatrix} \phi_1(x) \\ \phi_2(x) \\ \vdots \\ \phi_n(x) \end{bmatrix} = \begin{bmatrix} h(x) \\ L_f h(x) \\ \vdots \\ L_f^{n-1} h(x) \end{bmatrix} \tag{7.4}$$

$$u = \frac{1}{L_g L_f^{n-1} h(x)} \left(-L_f^n h(x) + v \right) \tag{7.5}$$

$$\dot{z} = \begin{bmatrix} \dot{z}_1 \\ \dot{z}_2 \\ \vdots \\ \dot{z}_n \end{bmatrix} = \begin{bmatrix} 0 & 1 & 0 & \dots & 0 \\ 0 & 0 & 1 & \dots & 0 \\ & & \vdots & & \\ 0 & 0 & 0 & \dots & 1 \\ 0 & 0 & 0 & \dots & 0 \end{bmatrix} \begin{bmatrix} z_1 \\ z_2 \\ \vdots \\ z_n \end{bmatrix} + \begin{bmatrix} 0 \\ 0 \\ \vdots \\ 1 \end{bmatrix} v \tag{7.6}$$

where $L_f h(x)$ is lie-derivative of $h(x)$ in the direction of $f(x)$ and is determined as $L_f h(x) = \sum_{i=1}^{n} \frac{\partial h}{\partial x_i} f_i(x)$.

The application of Theorem 7.1 on the nonlinear master and slave models in Eq (7.2) yields the following linearized tele-robotic system:

$$\begin{aligned} Master: & \begin{cases} \phi_m = \begin{bmatrix} x_{1m} & x_{2m} \end{bmatrix}^T \\ \dot{z}_{1m} = z_{2m} \\ \dot{z}_{2m} = v_m \\ u_m = b_m x_{2m} + m_m g l_m \sin x_{1m} + J_m v_m \\ y_m = x_{1m} = z_{1m} \end{cases} \\ Slave: & \begin{cases} \phi_s = \begin{bmatrix} x_{1s} & x_{2s} \end{bmatrix}^T \\ \dot{z}_{1s} = z_{2s} \\ \dot{z}_{2s} = v_s \\ u_s = b_s x_{2s} + m_s g l_s \sin x_{1s} + J_s v_s \\ y_s = x_{1s} = z_{1s} \end{cases} \end{aligned} \tag{7.7}$$

After the master and slave systems are exactly linearized through Eq (7.7), communication between them is established using the composite state convergence methodology proposed by the authors. The overall control scheme is shown in Figure 7.1. We now show the convergence of master and slave systems' states as well as the force reflection ability of the proposed scheme.

Theorem 7.2. *The slave system is able to follow the master system in the absence of communication time delay if gains of the composite state convergence controller are found as a solution of the following design conditions:*

$$G_2 - 1 = 0 \tag{7.8}$$

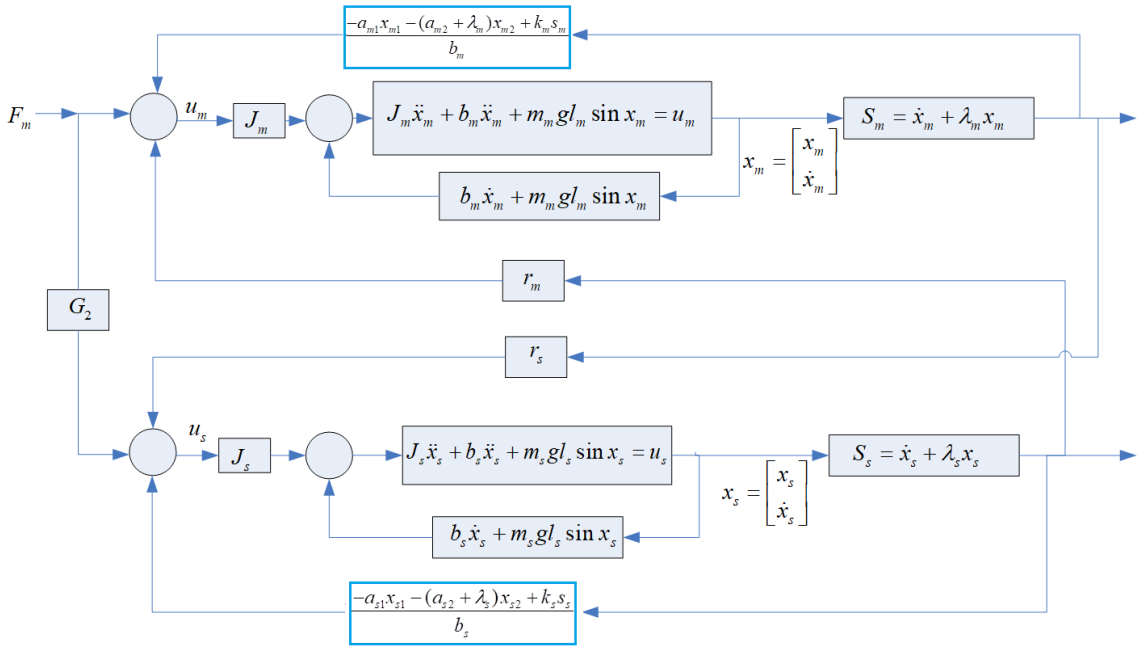

Figure 7.1: Proposed Scheme using feedback-linearization and CSC theory

$$k_s + r_s - k_m - r_m = 0 \tag{7.9}$$

$$k_s + r_s = -p \tag{7.10}$$

$$k_m - r_s = -q \tag{7.11}$$

Proof. Let us define the composite states for the master (s_m) and slave (s_s) systems as:

$$\begin{aligned} s_m &= x_{2m} + \lambda_m x_{m1} \\ s_s &= x_{2s} + \lambda_s x_{1s} \end{aligned} \tag{7.12}$$

The time derivative of Eq (7.12) along with Eq (7.7) yields the composite dynamical system as:

$$\begin{aligned} \dot{s}_m &= v_m + \lambda_m x_{m2} \\ \dot{s}_s &= v_s + \lambda_s x_{s2} \end{aligned} \tag{7.13}$$

Let us define the control inputs for the feedback-linearized telerobotic system as:

$$\begin{aligned} v_m &= -\lambda_m x_{m2} + k_m s_m + r_m s_s + F_m \\ v_s &= -\lambda_s x_{s2} + k_s s_s + r_s s_m + G_2 F_m \end{aligned} \tag{7.14}$$

By plugging Eq (7.14) in Eq (7.13), we get:

$$\begin{aligned} \dot{s}_m &= k_m s_m + r_m s_s + F_m \\ \dot{s}_s &= k_s s_s + r_s s_m + G_2 F_m \end{aligned} \tag{7.15}$$

Let $s_e = s_s - s_m$ be the composite error. The composite error dynamics can be written using Eq (7.15) as:

$$\dot{s}_e = (k_s + r_s - k_m - r_m)\, s_s + (k_m - r_s)\, s_e + (G_2 - 1)\, F_m \tag{7.16}$$

We now form an augmented system comprising composite slave and error systems as:

$$\begin{bmatrix} \dot{s}_s \\ \dot{s}_e \end{bmatrix} = \begin{bmatrix} k_s + r_s & -r_s \\ k_s + r_s - k_m - r_m & k_m - r_s \end{bmatrix} \begin{bmatrix} s_s \\ s_e \end{bmatrix} + \begin{bmatrix} G_2 \\ G_2 - 1 \end{bmatrix} F_m \tag{7.17}$$

We now allow the composite error to evolve as an autonomous system which yields the design conditions Eq (7.8) and Eq (7.9). The characteristic equation of the remaining augmented system is finally compared with the desired polynomial $(s+p)(s+q) = 0$ which yields the design condition Eq (7.10) and Eq (7.11). Now, it is left to show that states of the slave system converge to the states of the master system with the control gains in Eq (7.8) - Eq (7.11). These control gains yield the closed loop master as well as slave system as $\ddot{x}_{1z} + (\lambda_z + p)\, \dot{x}_{1z} + \lambda_z p = F_m$ which implies that slave position can be made to track the master position with the scaling factor as $\alpha = {}^{\lambda_m}/_{\lambda_s}$ which also implies the zero convergence of the velocity states. This completes the proof.

□

Theorem 7.3. *The motion of the slave system will be synchronized with the master system in the presence of communication time delay (T) if control gains of the composite nonlinear controller are found as a solution of the following design conditions:*

$$G_2\,(1 + T r_m) - T r_s = 1 \tag{7.18}$$

$$k_s + (1 - T k_m)\, r_s - k_m + (T k_s - 1)\, r_m = 0 \tag{7.19}$$

$$k_s - T r_s r_m + r_s - T r_s k_m = -p \tag{7.20}$$

$$r_s - T r_s k_m - r_m + T r_m k_s = -q \tag{7.21}$$

Proof. Consider the tele-robotic system of Fig. 7.1 with time delay, T in the communication paths. Let the virtual inputs for the master and slave systems be introduced as:

$$v_m = -\lambda_m x_{m2} + k_m s_m + r_m s_s\left(t-T\right) + F_m \tag{7.22}$$

$$v_s = -\lambda_s x_{s2} + k_s s_s + r_s s_m\left(t-T\right) + G_2 F_m\left(t-T\right) \tag{7.23}$$

The delayed dynamical composite master and slave systems can be derived as:

$$\begin{aligned} \dot{s}_m &= k_m s_m + r_m s_s\left(t-T\right) + F_m \\ \dot{s}_s &= k_s s_s + r_s s_m\left(t-T\right) + G_2 F_m\left(t-T\right) \end{aligned} \tag{7.24}$$

Let us now use the first-order Taylor series expansion on the time-delayed signals with the assumption of constant operator force i.e.

$$\begin{aligned} s_x\left(t-T\right) &\approx s_x - T\dot{s}_x, x = m, s \\ F_m\left(t-T\right) &\approx F_m - T\dot{F}_m = F_m \end{aligned} \tag{7.25}$$

Based on the above Taylor expansion and using the definition of composite error, the closed loop delayed composite master and slave systems can be written as:

$$\begin{aligned} \dot{s}_m = &\frac{1}{\left(1-T^2 r_s r_m\right)}\left(\left(k_m - T r_s r_m + r_m - T r_m k_s\right) s_s - \left(r_m - T r_m k_s\right) s_e\right. \\ &\left. + \left(1 - T r_m G_2\right) F_m\right) \end{aligned} \tag{7.26}$$

$$\begin{aligned} \dot{s}_s = &\frac{1}{\left(1-T^2 r_s r_m\right)}\left(\left(k_s - T r_s r_m + r_s - T r_s k_m\right) s_s - \left(r_s - T r_s k_m\right) s_e\right. \\ &\left. + \left(G_2 - T r_s\right) F_m\right) \end{aligned} \tag{7.27}$$

We now write the composite slave-error augmented system:

$$\begin{bmatrix} \dot{s}_s \\ \dot{s}_e \end{bmatrix} = \frac{1}{\left(1-T^2 r_s r_m\right)}\left(\begin{bmatrix} a_{11} & a_{12} \\ \left(\ a_{21}\ \right) & \left(\ a_{22}\ \right) \end{bmatrix}\begin{bmatrix} s_s \\ s_e \end{bmatrix} + \begin{bmatrix} b_{11} \\ \left(\ b_{21}\ \right) \end{bmatrix} F_m\right) \tag{7.28}$$

where,

$a_{11} = k_s - Tr_s r_m + r_s - Tr_s k_m, a_{12} = -r_s + Tr_s k_m,$
$a_{21} = k_s + r_s - Tr_s k_m - k_m - r_m + Tr_m k_s, a_{22} = r_s - Tr_s k_m - r_m + Tr_m k_s,$
$b_{11} = G_2 - Tr_s, b_{21} = G_2 - Tr_s - 1 + Tr_m G_2$

The composite error system is now allowed to evolve as an autonomous system which leads to the design conditions Eq (7.18) - Eq (7.19). The rest of the augmented system is then assigned the desired dynamics formed from the poles $s = -p, s = -q$. This assignment leads to the design conditions in Eq (7.20) - Eq (7.21). An analysis similar to Theorem 7.2 reveals that the slave system indeed follows the master system. The proof is now completed. □

7.3 Simulation Results

The proposed composite nonlinear state convergence controller is simulated in MATLAB/Simulink environment to evaluate its effectiveness in motion synchronization of master and slave systems. For the purpose of simulations, parameters of the telerobotic system are adopted from [69]:

$$\begin{aligned} &Master : m_m = 1, l_m = 0.2, b_m = 10, J_m = 0.33 m_m l_m^2 \\ &Slave : m_s = 10, l_s = 1, b_s = 15, J_s = 0.33 m_s l_s^2 \\ &Environment : k_e = 10, k_f = 1 \end{aligned} \tag{7.29}$$

We first perform simulations when no time delay exists in the communication channel. To this end, let the desired poles be placed at $s+p = s+2, s+q = s+20$ and let the motion scaling constants be selected as unity. The design conditions in Theorem 7.1 are then solved, and the following control gains are obtained:

$$G_2 = 1, k_m = -12, k_s = -10, r_s = 8 \tag{7.30}$$

By assuming zero initial conditions for both the master and slave systems, the telerobotic system is simulated under a constant operator's force of 0.2N and the control gains of Eq (7.30). The result is depicted in Figure 7.2 and Figure 7.3. It can be seen that the composite states converge, and this leads to the convergence of master and slave systems' states. The motion scaling property of the proposed controller is also evaluated in simulations. It is desired that the slave's motion converges to 50% of the motion of the master system, which leads to the selection of the slave's scaling constant as $\lambda_s = 2$. The simulations are now run with the control gains of Eq (7.30), and the result is shown in Figure 7.4. It can be seen that the slave's position response

is indeed 0.5 times the position profile of the master system.

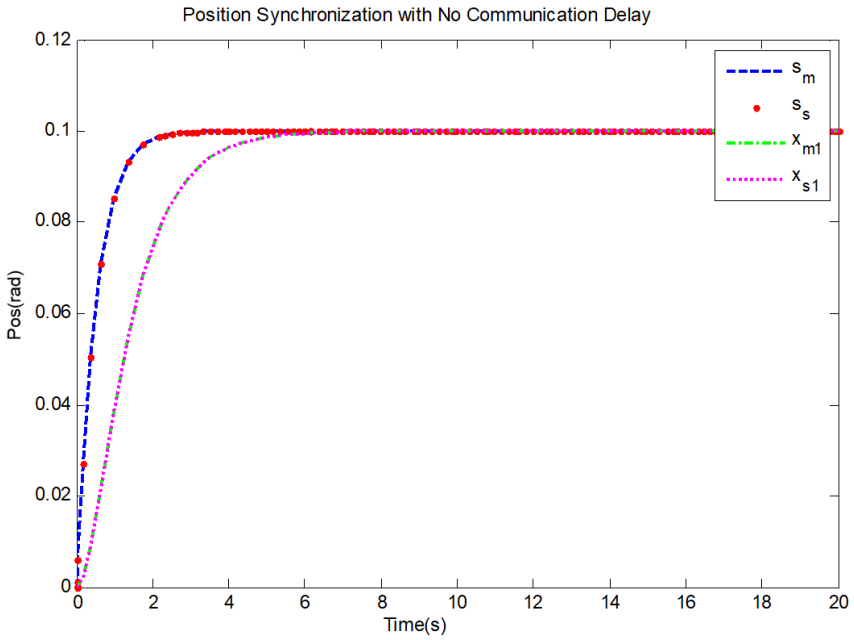

Figure 7.2: Position synchronization with no communication time delay

We now test the proposed controller when a time delay exists in the communication channel. Let the time delay be 0.2s in each direction. With the parameters of the telerobotic system in Eq (7.29) and using the same desired dynamics as in the delay-free case, control gains are found based on the design conditions of Theorem 7.3 as:

$$G_2 = 0.3521, k_m = -16, k_s = -2.3944, r_s = 0.2817 \tag{7.31}$$

By selecting $x_m(0) = x_s(0) = 0, \lambda_m = \lambda_s = 1$ and with a constant operator's force of 0.2N, we run the time-delayed telerobotic system under the control gains of Eq (7.31) and the results are shown in Figure 7.5 and Figure 7.6. The analysis reveals that the composite slave system follows the composite master system, which leads to the convergence of the position and velocity states of the master and slave systems. The motion scaling ability of the time-delayed telerobotic system is also investigated. To this end, the reference for the slave system is set as $0.25x_{m1}$, which implies $\lambda_s = 4$. The simulation result, as obtained under the control gains of Eq (7.31), is shown in Figure 7.7. It can be seen that the motion of the slave system has been achieved as desired.

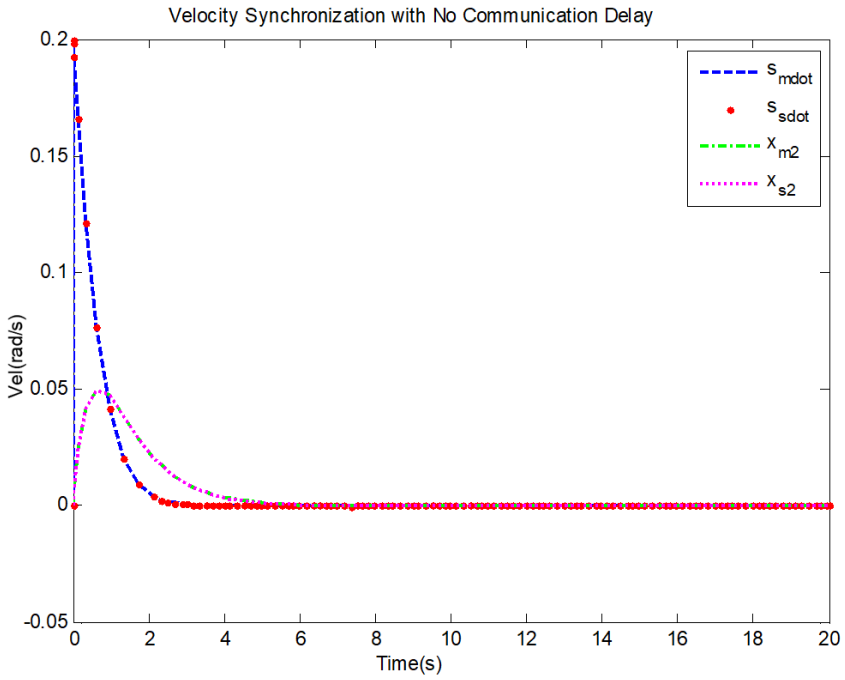

Figure 7.3: Velocity synchronization with no communication time delay

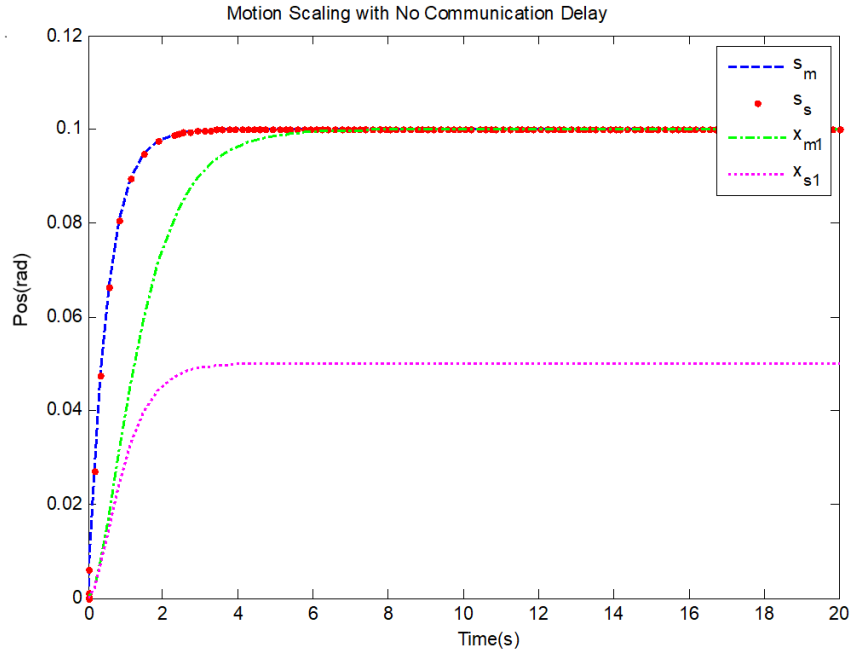

Figure 7.4: Motion scaling with no communication time delay

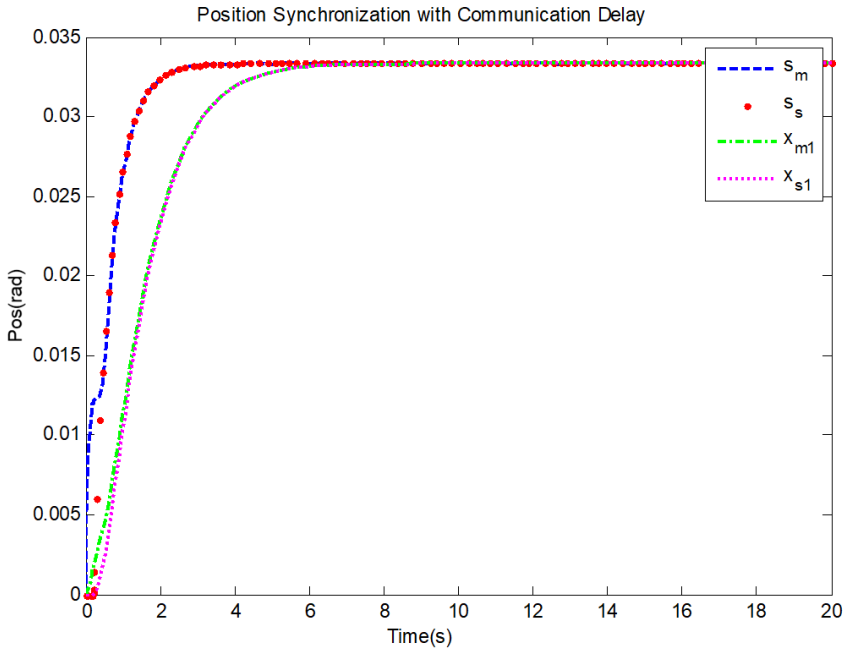

Figure 7.5: Position synchronization with communication time delay

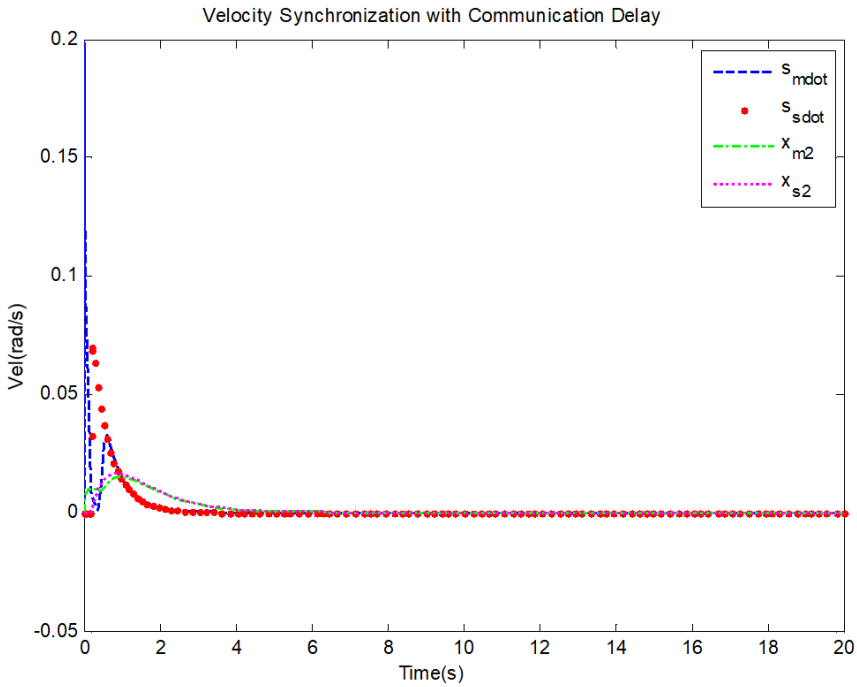

Figure 7.6: Velocity synchronization with communication time delay

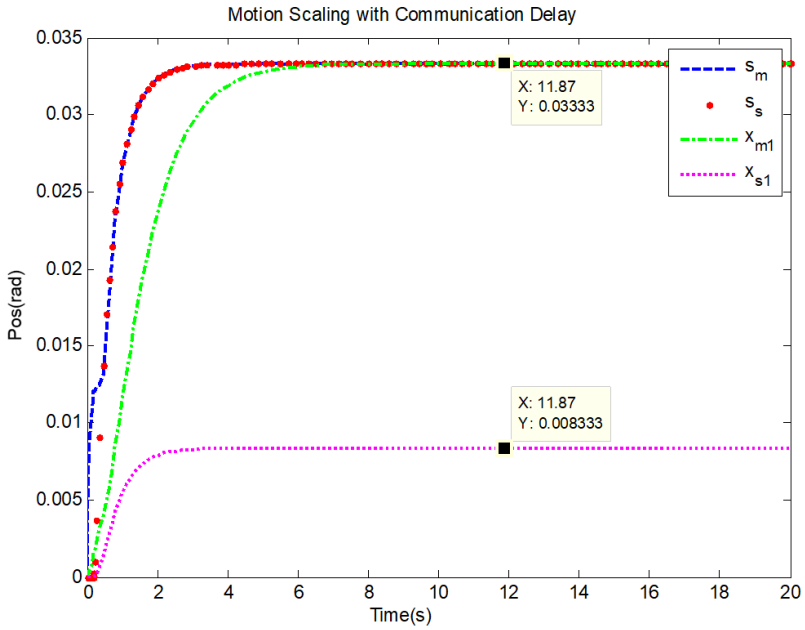

Figure 7.7: Motion scaling with communication time delay

7.4 Experimental Results

We now include some semi-real-time results of the proposed nonlinear controller, which are obtained using the haptic device in the QUARC/Simulink environment. A time-varying operator's force is generated by operating the haptic device along a single axis, and trajectories of the resulting master and slave systems are recorded in a time-delayed environment under the control of Eq (7.31). The results are shown in Figure 7.8 and Figure 7.9 and controller parameters are summarized in Table 7.1.

Controller	Simulation in MATLAB/Simulink	Semi Real-time QUARC/Simulink
System	1-DoF (Master/Slave)	1-DoF (Master/Slave)
Operator Force (N)	0.2 (constant)	Time-varying force using Omni Bundle
Environment Stiffness k_e (Nm/rad)	10	10
Environment Damping b_e (Nm/rad)	0.1	0.1
Force Feedback gain K_f	unity	unity
Scaling constant λ_m/λ_s	1	1
Time delay (Sec)	0.2	0.2

Table 7.1: Proposed controller parameters for simulation and semi-real time experiment

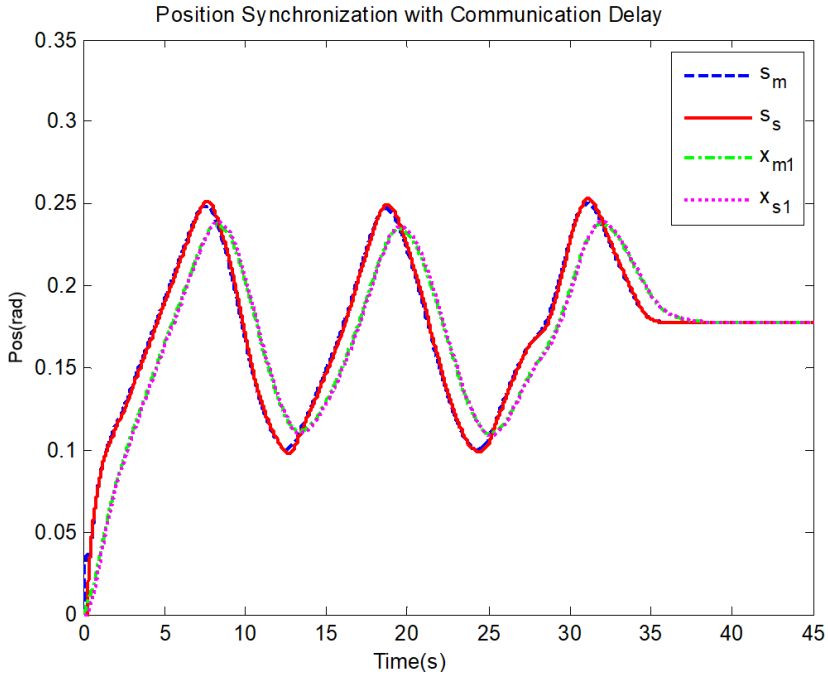

Figure 7.8: Position synchronization with communication time delay under time-varying applied force

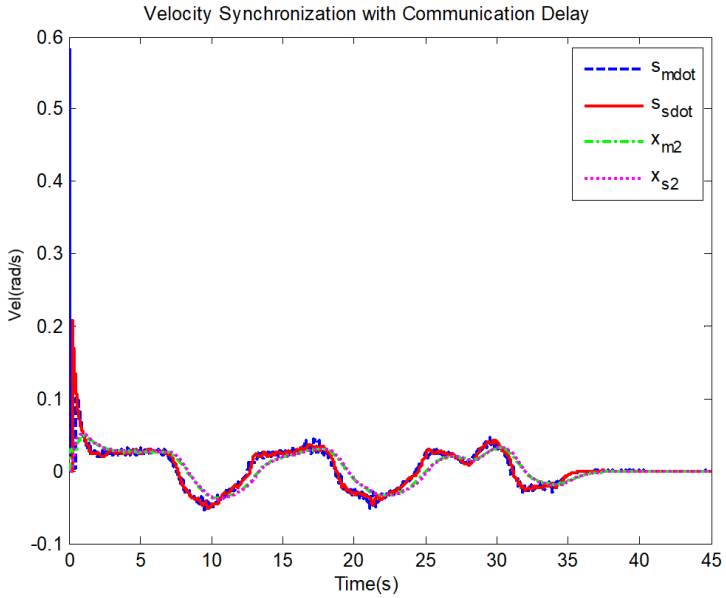

Figure 7.9: Velocity synchronization with communication time delay under time-varying applied force

7.5 Conclusion

This chapter presented the design of a composite state convergence controller for a one-degree-of-freedom nonlinear telerobotic system. To deal with the nonlinearity in the master and slave systems, a feedback linearization algorithm is used. The exactly linearized master and slave systems are then used to form the lower complexity composite systems. Through the use of a similarity transformation, a composite slave-error augmented system is constructed. After the composite error is made to evolve as an autonomous, desired behavior is assigned to the telerobotic system. This results in four design conditions which are solved to determine the four unknown control gains. Simulations, as well as semi-real-time experiments, are finally performed in MATLAB/Simulink environment, which shows good performance of the telerobotic system in the absence and presence of communication time delays.

Chapter 8

A Composite State Convergence Architecture for Multi-Degrees-of-Freedom System

This chapter is devoted to exploring the applicability of the composite state convergence scheme for multi-degrees-of-freedom bilateral teleoperation systems. The composite state convergence scheme presents an elegant design procedure for computing the control gains by allowing the composite error to evolve as an autonomous system and imposing the desired dynamical behavior to the augmented composite master-error system [104]. Here, the composite variables corresponding to the joints of the master and slave manipulators as well as the operator's force, are transmitted across the communication channel. A similar design procedure has been followed to compute the gains for a multi-degrees-of-freedom teleoperation system and have shown that the closed-loop system is Lyapunov-stable. The control laws for the master and slave systems are defined according to the composite state convergence scheme with the addition of cancellation terms containing the nonlinear dynamics of master and slave manipulators. It is shown that the convergence of composite variables of respective master and slave joints guarantees the convergence of respective joint positions of the master and slave systems under the composite state convergence control laws. To validate the proposed extension, simulations are performed in MATLAB/Simulink environment on two-link manipulators with time delay in the communication channel.

8.1 Composite State Convergence Scheme

Consider a bilateral teleoperation system that is comprised of second-degree-of-freedom robotic manipulators as:

$$\begin{aligned} M_m(q_m)\,\ddot{q}_m + C_m(q_m,\dot{q}_m)\,\dot{q}_m + G_m(q_m) &= u_m + F_m \\ M_s(q_s)\,\ddot{q}_s + C_s(q_s,\dot{q}_s)\,\dot{q}_s + G_s(q_s) &= u_s - F_e \end{aligned} \tag{8.1}$$

where inertia, coriolis/centrifugal, and gravity matrices are given as:

$$M_z = \begin{pmatrix} m_{2z}l_z^2 + (m_{1z} + m_{2z})\, l_z^2 + 2m_{2z}l_z^2 \cos(q_{2z}) & m_{2z}l_z^2 + m_{2z}l_z^2 \cos(q_{2z}) \\ m_{2z}l_z^2 + m_{2z}l_z^2 \cos(q_{2z}) & m_{2z}l_z^2 \end{pmatrix} \quad (8.2)$$

$$C_z = \begin{pmatrix} -\dot{q}_{2z}m_{2z}l_z^2 \sin(q_{2z}) & -(\dot{q}_{1z} + \dot{q}_{2z})\, m_{2z}l_z^2 \sin(q_{2z}) \\ -\dot{q}_{1z}m_{2z}l_z^2 \sin(q_{2z}) & 0 \end{pmatrix} \quad (8.3)$$

$$G_z = \begin{pmatrix} gm_{2z}l_z \sin(q_{1z} + q_{2z}) + g(m_{1z} + m_{2z})\, l_z \sin(q_{1z}) \\ gm_{2z}l_z \sin(q_{1z} + q_{2z}) \end{pmatrix} \quad (8.4)$$

where subscript 'z' represents either master or slave manipulators, m_{1z} is the mass of link 1, m_{2z} is the mass of link 2, l_z is length of both links, $q_z = (q_{1z}, q_{2z})^T$ are the joint angles, $\dot{q}_z = (\dot{q}_{1z}, \dot{q}_{2z})^T$ are the joint velocities, and $\ddot{q}_z = (\ddot{q}_{1z}, \ddot{q}_{2z})^T$ are the joint accelerations.

To establish the bilateral communication between master and slave manipulators as per the composite state convergence scheme, composite variables are transmitted across the communication channel along with the operator's force from the master side. Thus, a total of 6 variables are transmitted over the channel, i.e., $S_m = (s_{m1}, s_{m2})^T, S_s = (s_{s1}, s_{s2})^T$ and $F_m = (F_{m1}, F_{m2})^T$. The composite variables for the master and slave are defined as:

$$S_m = \dot{q}_m + \Lambda_m q_m \quad (8.5)$$

$$S_s = \dot{q}_s + \Lambda_s q_s \quad (8.6)$$

where $\Lambda_m = diag(\lambda_{m1}, \lambda_{m2}), \Lambda_s = diag(\lambda_{s1}, \lambda_{s2})$ are the auxiliary constants. The time derivative of composite variables in conjunction with manipulator dynamics yields the following composite master and slave systems:

$$\dot{S}_m = M_m^{-1}(-C_m\dot{q}_m - G_m + u_m + F_m) + \Lambda_m\dot{q}_m \quad (8.7)$$

$$\dot{S}_s = M_s^{-1}(-C_s\dot{q}_s - G_s + u_s - F_e) + \Lambda_s\dot{q}_s \quad (8.8)$$

The control inputs for the master and slave systems are introduced:

$$u_m = C_m\dot{q}_m + G_m + (M_mB_m - I)\, F_m + M_m(-\Lambda_m\dot{q}_m + K_mS_m + B_mR_mS_s) \quad (8.9)$$

$$u_s = C_s\dot{q}_s + G_s + F_e + M_s\left(-\Lambda_s\dot{q}_s + K_sS_s + B_sR_sS_m + B_sG_2F_m\right) \tag{8.10}$$

where $K_m = diag\left(k_{m1}, k_{m2}\right)$ and $K_s = diag\left(k_{s1}, k_{s2}\right)$ are the stabilizing gains for the master and slave manipulators respectively. The force feedback gain matrix is $R_m = diag\left(r_{m1}, r_{m2}\right)$ while force feed-forward gain matrix is $G_2 = diag\left(G_{21}, G_{22}\right)$. The motion-affecting gain matrix from the slave to master is $R_s = diag\left(r_{s1}, r_{s2}\right)$. Here, we need to determine K_m, K_s, R_s, and G_2 gain matrices to synchronize the master and slave manipulators while calculation of $R_m$is based on the environment information, $R_m = K_fK_e$.

By plugging Eq (8.9) in Eq (8.7) and Eq (8.10) in Eq (8.8), we obtain the following closed-loop composite master and slave systems as:

$$\dot{S}_m = K_mS_m + B_mR_mS_s + B_mF_m \tag{8.11}$$

$$\dot{S}_s = K_sS_s + B_sR_sS_m + B_sG_2F_m \tag{8.12}$$

Now, let us define the composite error as:

$$S_e = S_m - S_s \tag{8.13}$$

By re-writing Eq (8.11) in terms of the composite error, we have:

$$\dot{S}_m = \left(K_m + B_mR_m\right)S_m - B_mR_mS_e + B_mF_m \tag{8.14}$$

Let $S_{m,ss}$ denote the steady state values of the composite master states. As will be shown later, the composite error can be driven to zero by the appropriate selection of control gains. Thus, the steady-state value of the composite master state can be computed as:

$$S_{m,ss} = -\left(K_m + B_mR_m\right)^{-1}B_mF_m \tag{8.15}$$

Let $\tilde{S}_m$ be the deviation of the composite master state from its steady state value:

$$\tilde{S}_m = S_m - S_{m,ss} \tag{8.16}$$

The time derivative of the perturbed composite master system Eq (8.16) along with

Eq (8.14) and Eq (8.15) yields:

$$\dot{\tilde{S}}_m = (K_m + B_m R_m)\,\tilde{S}_m - B_m R_m S_e \tag{8.17}$$

The time derivative of Eq (8.13) along with Eq (8.12), Eq (8.14) - Eq (8.17) yields:

$$\begin{aligned}\dot{S}_e = {} & (K_m + B_m R_m - K_s - B_s R_s)\,\tilde{S}_m + (K_s - B_m R_m)\,S_e - \\ & (K_m + B_m R_m - K_s - B_s R_s)\,(K_m + B_m R_m)^{-1}\,B_m F_m + \\ & (B_m - B_s G_2)\,F_m\end{aligned} \tag{8.18}$$

Next, we show that the composite master and slave systems can be synchronized by selecting appropriate stabilizing gains, force feed-forward, and motion-affecting gains.

Theorem 8.1. *The convergence of the composite error Eq (8.18) and perturbed composite master systems Eq (8.17) to zero is guaranteed after the gains of the composite state convergence scheme are selected as:*

$$\begin{aligned}K_m &= -P - B_m R_m \\ K_s &= -Q + B_m R_m \\ R_s &= B_s^{-1}\,(-P + Q - B_m R_m) \\ G_2 &= B_s^{-1} B_m\end{aligned} \tag{8.19}$$

Proof. Consider the Lyapunov function as:

$$V\left(\tilde{S}_m, S_e\right) = \frac{1}{2}\tilde{S}_m^T \tilde{S}_m + \frac{1}{2} S_e^T S_e$$

The time derivative of Lyapunov function yields:

$$\dot{V} = \tilde{S}_m^T \dot{\tilde{S}}_m + S_e^T \dot{S}_e$$

By plugging the closed loop composite systems of Eq (8.17) and Eq (8.18) in $\dot{V}$, we obtain

$$\begin{aligned}\dot{V} = {} & \tilde{S}_m^T \left((K_m + B_m R_m)\,\tilde{S}_m - B_m R_m S_e\right) + \\ & S_e^T \left((K_m + B_m R_m - K_s - B_s R_s)\,\tilde{S}_m + (K_s - B_m R_m)\,S_e\right) - \\ & S_e^T \left((K_m + B_m R_m - K_s - B_s R_s)\,(K_m + B_m R_m)^{-1}\,B_m F_m\right) + \\ & S_e^T\,(B_m - B_s G_2)\,F_m\end{aligned}$$

By substituting the control gains of Eq (8.19) and using the matrix inequality, $XY + Y^TX^T \leq \delta XX^T + \delta^{-1}Y^TY$ we have:

$$\dot{V} = -\tilde{S}_m^T P \tilde{S}_m - \tilde{S}_m^T B_m R_m S_e - S_e^T Q S_e$$

Since $\dot{V} < 0$, the errors $\left(\tilde{S}_m, S_e\right)$ are bounded and $\left(\tilde{S}_m, S_e\right) \to 0$ as $t \to \infty$. This implies that the composite slave system does converge to the composite master system i.e., $S_m \to S_{m,ss}$ and $S_s \to S_m$. This completes the proof. □

Theorem 8.2. *The joint positions of the slave system converge to the joint positions of the master system iff the convergence of the respective composite systems is ensured.*

Proof. By plugging the control inputs Eq (8.9), Eq (8.10) in Eq (8.1), we have:

$$\ddot{q}_m + \Lambda_m \dot{q}_m = \dot{S}_m, \ddot{q}_s + \Lambda_s \dot{q}_s = \dot{S}_s \tag{8.20}$$

Theorem 8.1 states that $S_m = S_s = S_{m,ss}$ are in a steady state with the assumption of constant operator's force. Thus, joint velocities converge to zero since $\dot{S}_m, \dot{S}_s \to 0$. Recall that $S_m = \dot{q}_m + \Lambda_m q_m$, $S_s = \dot{q}_s + \Lambda_s q_s$ and $\dot{q}_m, \dot{q}_s \to 0$, so $q_s = \Lambda_s^{-1}\Lambda_m q_m$. If the auxiliary matrices are the same, then $q_s = q_m$ in steady state. The proof is now completed. □

Remark 8.1. *The closed loop analysis also shows that the proposed composite state convergence scheme can yield a desired dynamic response. This can be verified for the master system by plugging the control gains in Eq(8.19) in* $\ddot{q}_m + \Lambda_m \dot{q}_m = (K_m + B_m R_m) S_m + B_m F_m$ *with the assumption that composite error system is driven to the origin. Thus, we have:* $\ddot{q}_m + \Lambda_m \dot{q}_m + P\Lambda_m q_m = B_m F_m$.

Let us now consider that time delay exists in the communication channel with the assumption of constant operator force. The control inputs in this case are modified as:

$$u_m = C_m \dot{q}_m + G_m + (M_m B_m - I) F_m + M_m \left(-\Lambda_m \dot{q}_m + K_m S_m + B_m R_m S_s (t - T)\right) \tag{8.21}$$

$$u_s = C_s \dot{q}_s + G_s + F_e + M_s \left(-\Lambda_s \dot{q}_s + K_s S_s + B_s R_s S_m (t - T) + B_s G_2 F_m\right) \tag{8.22}$$

By using Eq (8.21), Eq (8.22) with Eq (8.7), (8.8), the augmented closed loop composite master and error system in the absence of operator's forces can be written

as:

$$\begin{aligned} &\dot{\mathrm{Z}} = A\mathrm{Z} + A_d\mathrm{Z}\left(t-T\right), \mathrm{Z} = \begin{pmatrix} S_m & S_e \end{pmatrix}^T \\ &A = \begin{pmatrix} K_m & 0 \\ 0 & K_s \end{pmatrix}, A_d = \begin{pmatrix} B_m R_m & -B_m R_m \\ B_m R_m - B_s R_s & -B_m R_m \end{pmatrix} \end{aligned} \tag{8.23}$$

The stability of the time delayed system Eq (8.23) can now be guaranteed by using the delay-independent methodology.

Theorem 8.3. *The stability of the composite state convergence scheme is established with time delay in the communication channel if there exist two symmetric positive definite matrices L_1, L_2 such that the following LMIs are satisfied [33]:*

$$\begin{aligned} &L_1 > 0, L_2 > 0 \\ &\begin{pmatrix} A^T L_1 + L_1 A + L_2 & L_1 A_d \\ A_d^T L_1 & -L_2 \end{pmatrix} < 0 \end{aligned} \tag{8.24}$$

Proof. Consider the following Krasovskii-Lyapunov function:

$$V\left(x_t\right) = \mathrm{Z}^T\left(t\right) L_1 Z\left(t\right) + \int_{t-T}^{t} \mathrm{Z}^T\left(\tau\right) L_2 Z\left(\tau\right) d\tau$$

The time derivative of V along the trajectories of Eq (8.23) and imposing $\dot{V} < 0$ yields the LMIs in Eq (8.24). The detailed proof can be found in [33]. □

Remark 8.2. *The stability of the composite time-delayed system refers to the stability of the master and slave manipulators of the teleoperation system. We use the control gains of Eq (8.19) in Eq (8.23) and then use the LMIs in Eq (8.24) to find the matrices L_1 and L_2. In case of success, the control gains Eq (8.19) can also be used in case of time delay in the communication channel.*

8.2 Simulation Results

In order to validate the theoretical findings, simulations are conducted in MATLAB/Simulink environment on a time-delayed teleoperation system. The parameters for the master and slave manipulators are chosen as $m_{1z} = m_{1z} = 2kg$ and $l_z = 1m$. The control gains for the composite state convergence scheme are found to be $K_m = diag\left(-2.2, -2.2\right)$, $K_s = diag\left(-5.8, -5.8\right)$, $R_s = diag\left(3.8, 3.8\right)$ and $G_2 = diag\left(0.2, 0.2\right)$. Simulations are run by considering a time delay of $0.5s$ in the communication channel, and recorded results are displayed in Figure 8.1, Figure 8.2, Figure 8.3.

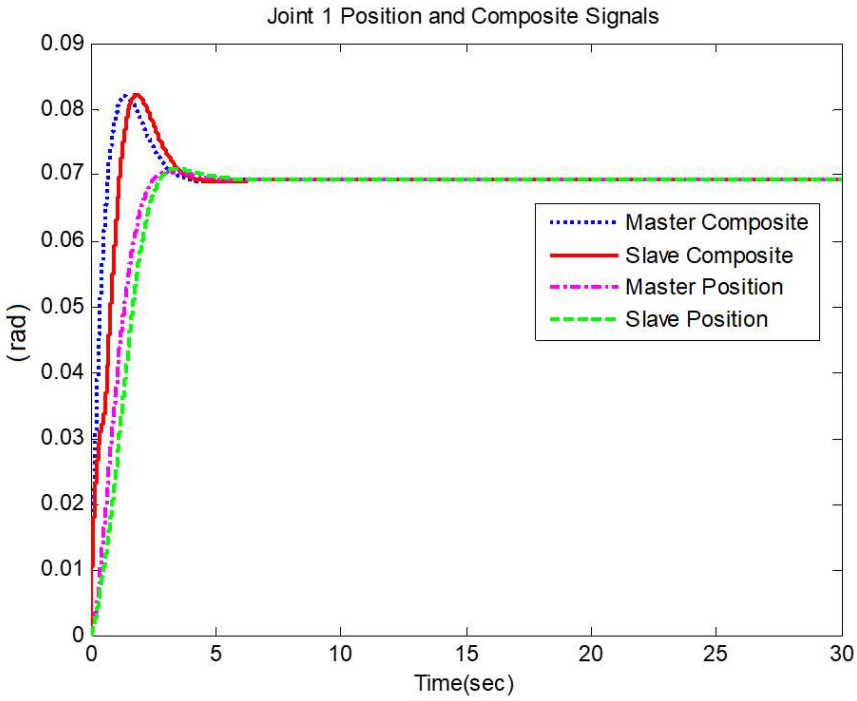

Figure 8.1: Composite and position signals for joint 1 of master and slave manipulators

Figure 8.1 shows that composite variables for joint #1 of the master and slave manipulators converge in the steady state with a constant operator's force of $1N$. A similar trend can be located in Figure 8.2 for joint #2 of master and slave manipulators. The convergence of velocity states can be seen in Figure 8.3.

The stability of the composite state convergence controller is confirmed through LMI conditions Eq (8.24), which yield the following positive definite matrices as shown in Eq (8.25) and Eq (8.26):

$$L_1 = \begin{bmatrix} 10.8258 & 0 & 0.1672 & 0 \\ 0 & 10.8258 & 0 & 0.1672 \\ 0.1672 & 0 & 3.1263 & 0 \\ 0 & 0.1672 & 0 & 3.1263 \end{bmatrix} \tag{8.25}$$

$$L_2 = \begin{bmatrix} 23.2592 & 0 & 0.4458 & 0 \\ 0 & 23.2592 & 0 & 0.4458 \\ 0.4458 & 0 & 19.4699 & 0 \\ 0 & 0.4458 & 0 & 19.4699 \end{bmatrix} \tag{8.26}$$

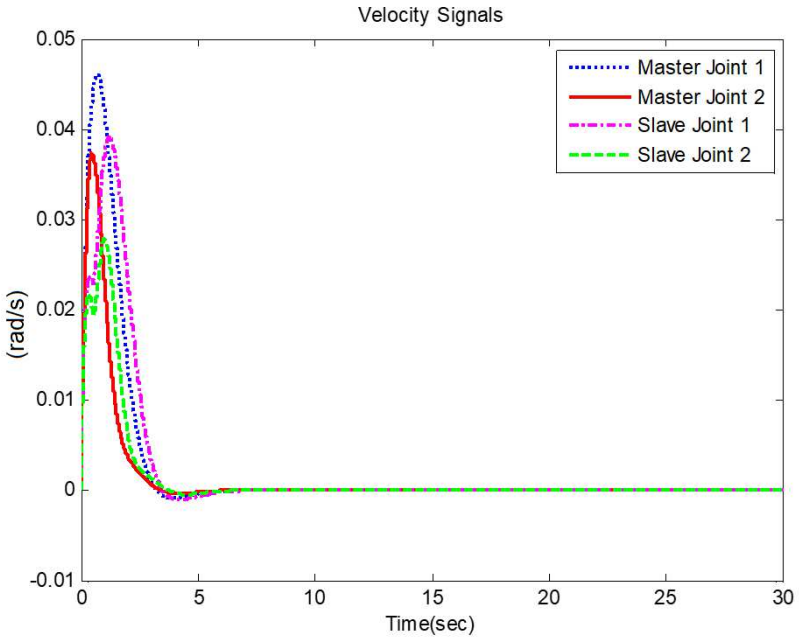

Figure 8.2: Composite and position signals for joint 2 of master and slave manipulators

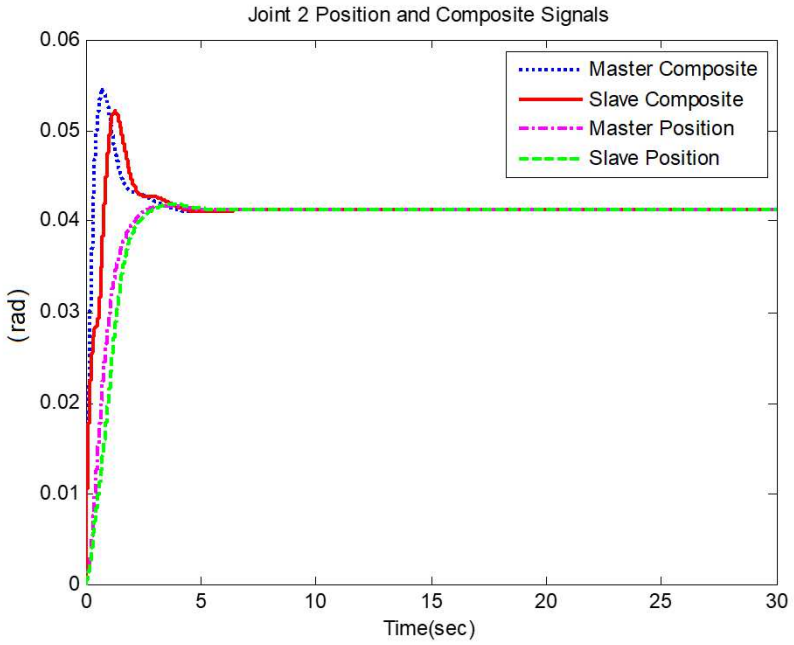

Figure 8.3: Velocity signals for joint no.1 and 2 of master and slave manipulator

8.3 Conclusion

This chapter presents the extension of the composite state convergence scheme for teleoperation systems to multi-degrees-of-freedom manipulators. The structure of control laws for the master and slave systems is in line with the composite state convergence scheme. The convergence of composite variables of the master and slave manipulators leads to the convergence of respective joint positions under the proposed framework. MATLAB simulations are performed to validate the proposal.

Chapter 9

Disturbance Observer Supported Three-Channel Composite State Convergence Architecture

Based on composite variables, three-channel state convergence is a novel architecture for the bilateral control of teleoperation systems modeled on state space. Although simple to design and easy to implement, this bilateral control algorithm relies on model parameters. To lower this dependence, this chapter proposes a disturbance observer-supported three-channel state convergence architecture. At first, extended state observers are used to estimate the position and velocity states of the master and slave systems along with their lumped uncertainties. These position and velocity estimates are then fused to form composite variables, which are transmitted along with the operator's force. With the knowledge of composite variables and the estimates of uncertainties, bilateral control laws are developed for the master and slave systems by following the method of state convergence. To validate the proposal, simulations, as well as semi-real-time experiments, are performed in MATLAB/Simulink environment by considering a single-degree-of-freedom time-delayed teleoperation system.

9.1 Review of Composite State Convergence Architecture

Like state convergence architecture, its composite version also establishes a joint-to-joint bilateral motion between the master and slave robots during the contact phase of the teleoperation system. Each joint is modeled as a second-order system on state space:

$$\begin{aligned} \dot{x}_z &= A_z x_z + B_z u_z \\ y_z &= C_z x_z \end{aligned} \tag{9.1}$$

where subscript 'z' is to be replaced with 'm' and 's' for the master and slave systems, respectively, while various matrix entries in Eq (9.1) are given as:

$$A_z = \begin{bmatrix} 0 & 1 \\ a_{z1} & a_{z2} \end{bmatrix}, B_z = \begin{bmatrix} 0 \\ b_z \end{bmatrix} C_z = \begin{bmatrix} 1 & 0 \end{bmatrix} \tag{9.2}$$

The communication framework provided by the state convergence architecture is shown in Fig 9.1, and various parameters defining the architecture are listed below:

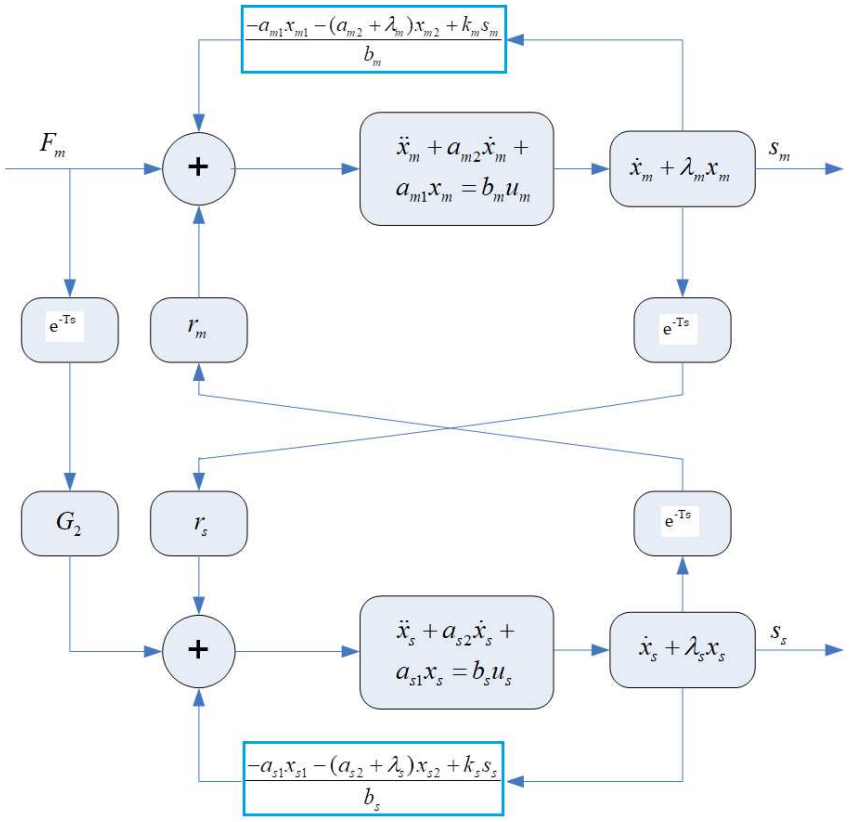

Figure 9.1: Composite state convergence scheme [104]

k_m is the stabilizing gain for the composite master system, k_s is the stabilizing gain for the composite slave system, which also takes into account the interaction of the slave with the environment where the environment is modeled by a stiffness (k_e) element, $r_m = k_f k_e$ transfers the scaled effect of the slave's motion to the master system as the slave interacts with the environment where scaling is achieved through a force feedback gain (k_f), r_s models the effect of master's motion into the slave system, T is the time delay offered by the communication channel, F_m is the force applied by the operator onto the master system which is assumed to be constant and G_2 transfers the effect of this force into the slave system. Of these parameters, k_m, k_s, r_s and G_2 are unknown scalars and determined by a design procedure provided by the composite state convergence scheme.

9.2 Proposed Disturbance Observer Based Composite State Convergence Architecture

The proposed composite state convergence architecture establishes bilateral communication between the master and slave systems by transmitting three variables, namely the operator's force, the observed composite-master state, and the observed composite-slave state. At the same time, nonlinear dynamical models of the master and slave systems are considered as opposed to linear dynamic models in the case of standard composite state convergence architecture. The lumped nonlinearities are estimated through extended state observers which also provide estimates of the position and velocity states. Fig 9.2 displays the proposed architecture, and various parameters defining the architecture are listed below:

1. $s_m = \hat{x}_{m2} + \lambda_m \hat{x}_{m1}$ is the composite-master state constructed from the observed master's position ($\hat{x}_{m1}$) and velocity ($\hat{x}_{m2}$) states where λ_m serves the purpose of scaling the master's position.

2. $s_s = \hat{x}_{s2} + \lambda_s \hat{x}_{s1}$ is the composite-slave state constructed from the observed slave's position ($\hat{x}_{s1}$) and velocity ($\hat{x}_{s2}$) states where λ_s serves the purpose of scaling the slave's position.

3. Other parameters $k_m, k_s, r_m, r_s, G_2, F_m, T$ are the same as in standard composite state convergence architecture.

4. The design of control gains k_m, k_s, r_s, G_2 along with disturbance observer gains is discussed in the sequel.

To this end, we first consider a more general form of the master and slave systems as:

$$\begin{aligned} \dot{x}_{z1} &= x_{z2} \\ \dot{x}_{z2} &= d_z(t) + b_z u_z \end{aligned} \tag{9.3}$$

where $d_z = f_z(x_z)$ encapsulates the nonlinearities of the master and slave systems. By considering $d_z(t)$ as an extra state, system in Eq (9.3) can be equivalently written as:

$$\begin{aligned} \dot{x}_z &= A_z x_z + B_z u_z + E_z h_z \\ y_z &= C_z x_z \end{aligned} \tag{9.4}$$

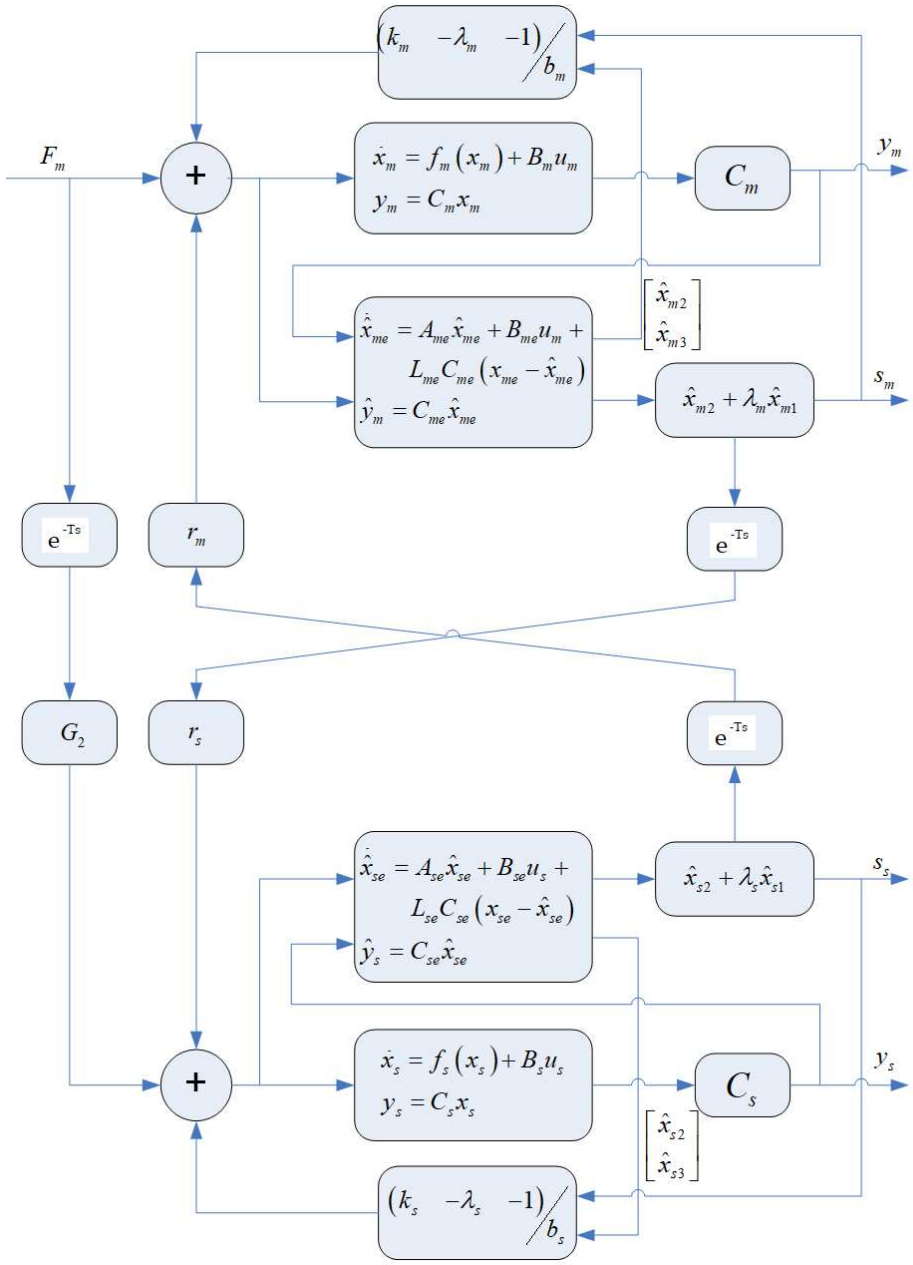

Figure 9.2: Proposed composite state convergence architecture

where $h_z(t) = \dot{d}_z(t)$ and various matrix entries are given as:

$$A_z = \begin{bmatrix} 0 & 1 & 0 \\ 0 & 0 & 1 \\ 0 & 0 & 0 \end{bmatrix}, B_z = \begin{bmatrix} 0 \\ 0 \\ b_z \end{bmatrix}, E_z = \begin{bmatrix} 0 \\ 0 \\ 1 \end{bmatrix} C_z = \begin{bmatrix} 1 & 0 & 0 \end{bmatrix} \tag{9.5}$$

To estimate the disturbance terms as well as the systems' states of Eq (9.3), we introduce extended state observers based on Eq (9.4) as:

$$\begin{aligned} \dot{\hat{x}}_z &= A_z \hat{x}_z + B_z u_z + L_z C_z \left(x_z - \hat{x}_z\right) \\ \hat{y}_z &= C_z \hat{x}_z \end{aligned} \tag{9.6}$$

In Eq (9.6), $L_z = \begin{bmatrix} l_{z1} & l_{z2} & l_{z3} \end{bmatrix}^T$ are observer gains while other matrix entries are given in Eq (9.5). Let us define the observer error $e_{zo} = \begin{bmatrix} e_{zo1} & e_{zo2} & e_{zo3} \end{bmatrix}^T$ as:

$$e_{zo} = x_z - \hat{x}_z \tag{9.7}$$

Observer error dynamics can be found using Eq (9.4), Eq (9.6), and Eq (9.7) as:

$$\dot{e}_{zo} = \left(A_z - L_z C_z\right) e_{zo} + E_z h_z \tag{9.8}$$

Control laws for the master and slave systems in three-channel state convergence architecture are proposed as:

$$u_m = \frac{1}{b_m}\left(-\hat{d}_m - \lambda_m \hat{x}_{m2} + k_m s_m\right) + r_m s_s \left(t - T\right) + F_m \tag{9.9}$$

$$u_s = \frac{1}{b_s}\left(-\hat{d}_s - \lambda_s \hat{x}_{s2} + k_s s_s\right) + r_s s_m \left(t - T\right) + G_2 F_m \left(t - T\right) \tag{9.10}$$

Here, we will construct the augmented system using composite-master and composite–slave states instead of full position and velocity states of master and slave robots. To this end, derivative of the composite-master state along with Eq (9.9) yields:

$$\dot{s}_m = k_m s_m + b_m r_m s_s \left(t - T\right) + b_m F_m + \left(l_{m2} + \lambda_m l_{m1}\right) e_{mo1} \tag{9.11}$$

Similarly, by taking the time derivative of composite-slave state and using Eq (9.10), we get:

$$\dot{s}_s = k_s s_s + b_s r_s s_m \left(t - T\right) + b_s G_2 F_m \left(t - T\right) + \left(l_{s2} + \lambda_s l_{s1}\right) e_{so1} \tag{9.12}$$

By applying first order Taylor approximation on time-delayed signals in Eq (9.11), Eq (9.12) with constant operator's force assumption and simplifying the resulting expressions, we have:

$$\dot{s}_s = A_{11}s_s + A_{12}s_m + A_{13}e_{so} + A_{14}e_{mo} + B_1F_m \tag{9.13}$$

$$\dot{s}_m = A_{21}s_s + A_{22}s_m + A_{23}e_{so} + A_{24}e_{mo} + B_2F_m \tag{9.14}$$

where

$$\begin{aligned}
&A_{11} = D\left(k_s - Tb_sr_sb_mr_m\right), A_{12} = D\left(b_sr_s - Tb_sr_sk_m\right)\\
&A_{13} = D\begin{pmatrix} l_{s2} + \lambda_s l_{s1} & 0 & 0 \end{pmatrix}, A_{14} = D\begin{pmatrix} -Tb_sr_s\left(l_{m2} + \lambda_m l_{m1}\right) & 0 & 0 \end{pmatrix}\\
&A_{21} = D\left(b_mr_m - Tb_mr_mk_s\right), A_{22} = D\left(k_m - Tb_mr_mb_sr_s\right)\\
&A_{23} = -D\begin{pmatrix} Tb_mr_m\left(l_{s2} + \lambda_s l_{s1}\right) & 0 & 0 \end{pmatrix}, A_{24} = D\begin{pmatrix} l_{m2} + \lambda_m l_{m1} & 0 & 0 \end{pmatrix}\\
&B_1 = D\left(b_sG_2 - Tb_sr_sb_m\right), B_2 = D\left(b_m - Tb_mr_mb_sG_2\right), D = \left(1 - T^2b_mr_mb_sr_s\right)^{-1}
\end{aligned} \tag{9.15}$$

Now, we form an augmented system using Eq (9.13), Eq (9.14) and Eq (9.8) as:

$$\begin{bmatrix} \dot{s}_s \\ \dot{s}_m \\ \dot{e}_{so} \\ \dot{e}_{mo} \end{bmatrix} = \begin{bmatrix} A_{11} & A_{12} & A_{13} & A_{14} \\ A_{21} & A_{22} & A_{23} & A_{24} \\ 0 & 0 & A_{33} & 0 \\ 0 & 0 & 0 & A_{44} \end{bmatrix} \begin{bmatrix} s_s \\ s_m \\ e_{so} \\ e_{mo} \end{bmatrix} + \begin{bmatrix} B_1 \\ B_2 \\ 0 \\ 0 \end{bmatrix} F_m + \begin{bmatrix} 0 & 0 \\ 0 & 0 \\ E_s & 0 \\ 0 & E_m \end{bmatrix} \begin{bmatrix} h_s \\ h_m \end{bmatrix} \tag{9.16}$$

Let us introduce a linear transformation to replace the composite-master system in Eq (9.16) with the composite-error system, $s_e = s_s - s_m$:

$$\begin{bmatrix} s_s \\ s_e \\ e_{so} \\ e_{mo} \end{bmatrix} = \begin{bmatrix} I & 0 & 0 & 0 \\ I & -I & 0 & 0 \\ 0 & 0 & I & 0 \\ 0 & 0 & 0 & I \end{bmatrix} \begin{bmatrix} s_s \\ s_m \\ e_{so} \\ e_{mo} \end{bmatrix} \tag{9.17}$$

The time-derivative of Eq (9.17) along with Eq (9.16), Eq (9.17) yields the transformed augmented system as:

$$\begin{bmatrix} \dot{s}_s \\ \dot{s}_e \\ \dot{e}_{so} \\ \dot{e}_{mo} \end{bmatrix} = \begin{bmatrix} \widetilde{A}_{11} & \widetilde{A}_{12} & \widetilde{A}_{13} & \widetilde{A}_{14} \\ \widetilde{A}_{21} & \widetilde{A}_{22} & \widetilde{A}_{23} & \widetilde{A}_{24} \\ 0 & 0 & \widetilde{A}_{34} & 0 \\ 0 & 0 & 0 & \widetilde{A}_{44} \end{bmatrix} \begin{bmatrix} s_s \\ s_e \\ e_{so} \\ e_{mo} \end{bmatrix} + \begin{bmatrix} \widetilde{B}_1 \\ \widetilde{B}_2 \\ 0 \\ 0 \end{bmatrix} F_m + \begin{bmatrix} 0 & 0 \\ 0 & 0 \\ \widetilde{E}_{31} & 0 \\ 0 & \widetilde{E}_{42} \end{bmatrix} \begin{bmatrix} h_s \\ h_m \end{bmatrix} \tag{9.18}$$

where

$\widetilde{A}_{11} = A_{11} + A_{12}$, $\widetilde{A}_{12} = -A_{12}$, $\widetilde{A}_{13} = A_{13}$, $\widetilde{A}_{14} = A_{14}$, $\widetilde{A}_{21} = A_{11} - A_{21} + A_{12} - A_{22}$, $\widetilde{A}_{22} = -A_{12} + A_{22}$, $\widetilde{A}_{23} = A_{13} - A_{23}$, $\widetilde{A}_{24} = A_{14} - A_{24}$, $\widetilde{A}_{33} = A_{33}$, $\widetilde{A}_{44} = A_{44}$, $\widetilde{B}_1 = B_1$, $\widetilde{B}_2 = B_1 - B_2$, $\widetilde{E}_{31} = E_s$, $\widetilde{E}_{42} = E_m$.

Based on the assumption that disturbance observers have much faster dynamics than the composite-error system, following conditions must hold for composite-error to evolve as an autonomous system:

$$\widetilde{A}_{21} = 0, \widetilde{B}_2 = 0 \tag{9.19}$$

The characteristic polynomial of the augmented system in Eq (9.18) can now be compared to the desired polynomial to yield the following conditions:

$$\begin{vmatrix} sI - \widetilde{A}_{11} \end{vmatrix} = s + p \\ \begin{vmatrix} sI - \widetilde{A}_{22} \end{vmatrix} = s + q \tag{9.20}$$

$$\begin{vmatrix} sI - \widetilde{A}_{34} \end{vmatrix} = s^3 + r_2 s^2 + r_1 s + r_0 \\ \begin{vmatrix} sI - \widetilde{A}_{44} \end{vmatrix} = s^3 + w_2 s^2 + w_1 s + w_0 \tag{9.21}$$

Design conditions in Eq (9.20) fix the dynamics of composite-slave and composite-error systems while disturbance observers for master and slave systems are designed according to Eq (9.21). The solution of design conditions Eq (9.19) - Eq (9.21) yields the control gains k_m, k_s, r_s, G_2 and observer gains $l_{m1}, l_{m2}, l_{m3}, l_{s1}, l_{s2}, l_{s3}$. Thus, the composite slave system will follow the composite-master system under the control laws Eq (9.9) and Eq (9.10). However, the convergence of position and velocity states of the master and slave systems needs to be investigated. To this end, first note that

$s_e = 0 \Rightarrow s_m = s_s$ and $\dot{s}_m = \dot{s}_s = 0$ under constant operator's force assumption. This leads to $\hat{x}_{m2} + \lambda_m \hat{x}_{m1} = \hat{x}_{s2} + \lambda_s \hat{x}_{s1}$. Thus, convergence of $\hat{x}_{m2}$ and $\hat{x}_{s2}$ to zero has to be ensured. By plugging control laws from Eq (9.9) and Eq (9.10) in Eq (9.3) and using Eq (9.7), Eq (9.11), Eq (9.12), we have:

$$\begin{aligned} \dot{x}_{m2} + \lambda_m x_{m2} &= \dot{s}_m + \xi_m e_{mo} \\ \dot{x}_{s2} + \lambda_s x_{s2} &= \dot{s}_s + \xi_s e_{so} \end{aligned} \tag{9.22}$$

where $\xi_m = \begin{pmatrix} -l_{m2} - \lambda_m l_{m1} & \lambda_m & 1 \end{pmatrix}$ and $\xi_s = \begin{pmatrix} -l_{s2} - \lambda_s l_{s1} & \lambda_s & 1 \end{pmatrix}$ Since observers have fast dynamics as compared to the composite states and under the assumption of slowly varying disturbances, we arrive at $\dot{x}_{m2} + \lambda_m x_{m2} = 0$ and $\dot{x}_{s2} + \lambda_s x_{s2} = 0$. Thus, velocity states x_{m2} and x_{s2} will converge to zero along with their estimates and we have: $\lambda_m \hat{x}_{m1} = \lambda_s \hat{x}_{s1}$ and $\lambda_m x_{m1} = \lambda_s x_{s1}$ which implies that slave system will follow the master system. These results further suggest that the motion of the slave system can also be scaled by adjusting the constant λ_s.

Let us now investigate the closed-loop dynamic behavior of the master system in the proposed three-channel state convergence architecture. By plugging the control law from Eq (9.9) in Eq (9.3) and ignoring the effects of composite error plus observer error dynamics, we have the following simplified closed loop master system driven by the operator's force:

$$\ddot{x}_{m1} + \left(\lambda_m + p\overline{1 + T b_m r_m}\right) \dot{x}_{m1} + \lambda_m p \left(1 + T b_m r_m\right) x_{m1} = b_m F_m \tag{9.23}$$

This result suggests that master system response can indeed be adjusted by varying constant λ_m and pole location p. The selection of pole p also controls the force-reflection behaviour of the proposed state convergence architecture. By choosing the pole location to be $p = {}^{b_m r_m}/_{(1 + T b_m r_m)}$ and $k_f = {}^{1}/_{\lambda_s}$, full force reflection can be guaranteed at steady state. However, this requires the time delay and environment stiffness to be exactly known. This result can be verified from the steady state analysis of master control law in Eq (9.9) which yields

$$u_{m,kn} = -\frac{b_m r_m}{p\left(1 + T b_m r_m\right)} F_m + k_f \lambda_n F_k. \tag{9.24}$$

9.3 Simulation Results

In order to validate the proposed disturbance observer based three-channel state convergence architecture, simulations are performed in MATLAB/Simulink environment by considering master and slave systems with single degree-of-freedom motion. Let the nonlinearities in these systems be

$$f_z = -a_{z1}x_{z1}\sin(x_{z1}) - a_{z2}x_{z2} \tag{9.25}$$

By assuming the parameters as

$$\begin{aligned} &a_{m2} = 7.1429, a_{s2} = 6.25 \\ &b_m = 0.2656, b_s = 0.2729 \\ &k_e = 50, \lambda_m = 1, \lambda_s = 1 \\ &k_f = 1, T = 0.1s, q = 10, p = 5 \\ &r_0 = w_0 = 27000, r_1 = w_1 = 2700, r_2 = w_2 = 90 \end{aligned} \tag{9.26}$$

Now solve the design conditions in Eq (9.19) - Eq (9.21) and obtain the controller and observer gains as:

$$\begin{aligned} &G_2 = 0.3084 \\ &k_m = -26.5496 \\ &k_s = -1.5829 \\ &r_s = -9.6092 \\ &L_{me} = L_{se} = \begin{bmatrix} 90 & 2700 & 27000 \end{bmatrix}^T \end{aligned} \tag{9.27}$$

The nonlinear time-delayed teleoperation system is now simulated under the control of Eq (9.27) with an operator's force of 0.5N and results are shown in Figure 9.3 and Figure 9.4. It can be seen that motion synchronization of the master and slave systems is achieved. Further, full environmental force is also reflected to the operator at a steady state.

9.4 Experimental Results

To further validate the proposed architecture, semi-real-time experiments are performed using geomagic haptic device. The device is driven by the operator along x-axis to generate the time varying-force, $F_m(t) = k_{op}(x_{op}(t) - x_0)$ with $k_{op} = 10$

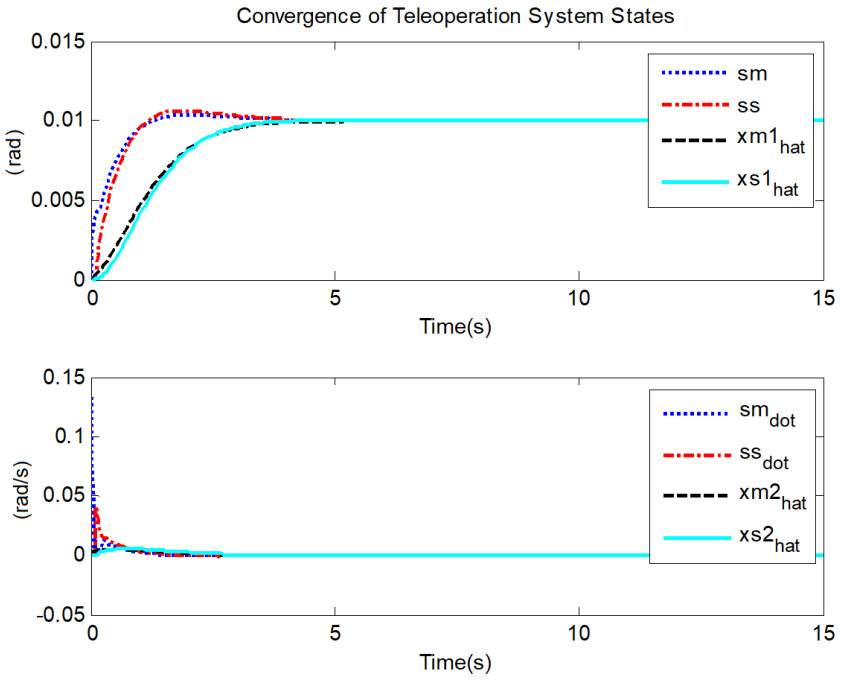

Figure 9.3: Simulation results: convergence of teleoperation system's states

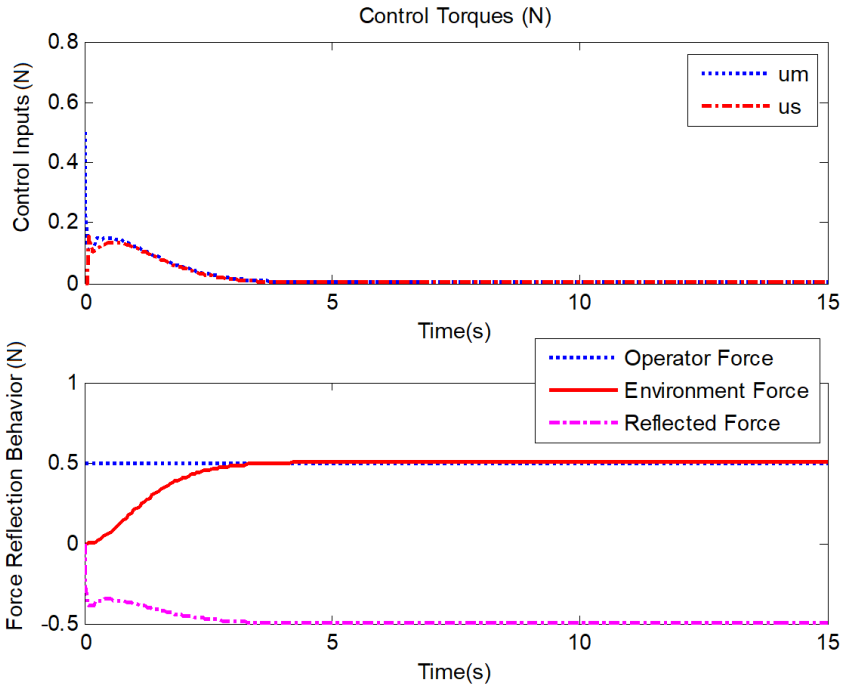

Figure 9.4: Simulation results: control torques

and $x_{op} \in [0.1, 0.2]\, m$. This force is provided as an input to the master-slave teleoperation system running in QUARC/Simulink environment. At the same time, reflected force as generated by the controller is also fed back to the haptic device. Thus, the loop is closed around the operator as he/she will feel the virtual environment during teleoperation. The experimental results are shown in Figure 9.5, Figure 9.6, Figure 9.7. It is evident that disturbances are well-estimated by the observers and the systems remain synchronized with proper force reflection to the operator.

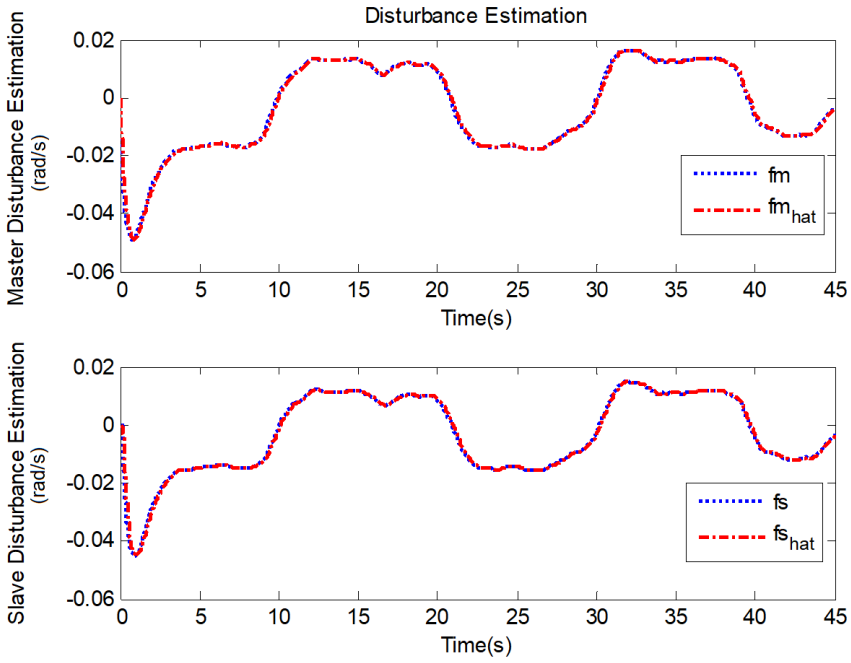

Figure 9.5: Semi-real time results: disturbance estimation

Finally, a comparison of the proposed tele-control algorithm with a proportional-derivative (PD) controller is drawn to show superiority of the former scheme. Here, PD controller employs delayed position signals mentioned in Eq (9.28):

$$(e_m = y_s\,(t-T) - y_m, e_s = y_m\,(t-T) - y_s) \tag{9.28}$$

With environment force compensation (EFC-PD) in the slave side in (9.29):

$$u_m = k_{pm}e_m + k_{dm}\dot{e}_m, u_s = k_{ps}e_s + k_{ds}\dot{e}_s + \tau_e \tag{9.29}$$

For a fair comparison, gains of EFC-PD controller are optimized through Genetic

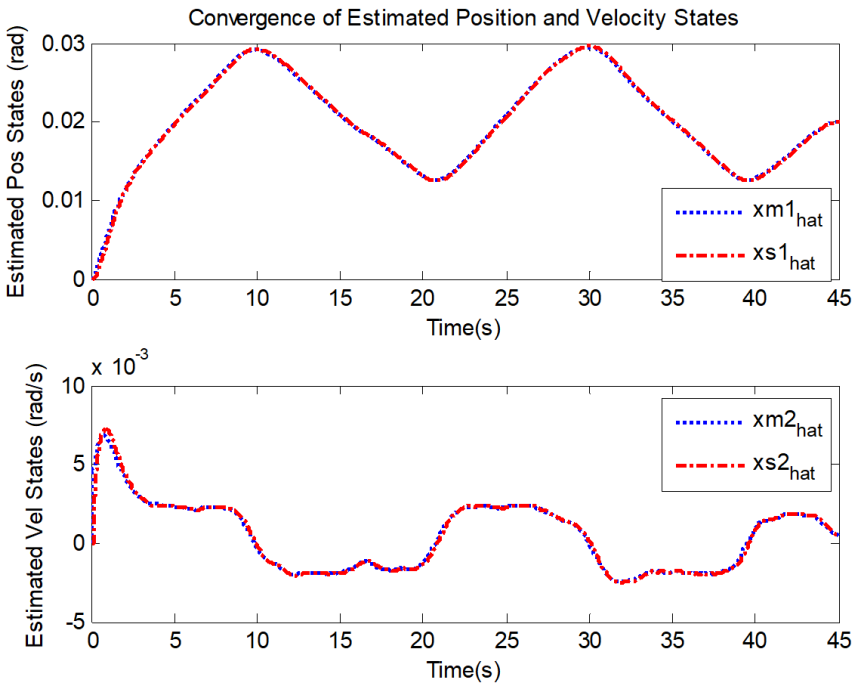

Figure 9.6: Semi-real time results: convergence of teleoperation system's states

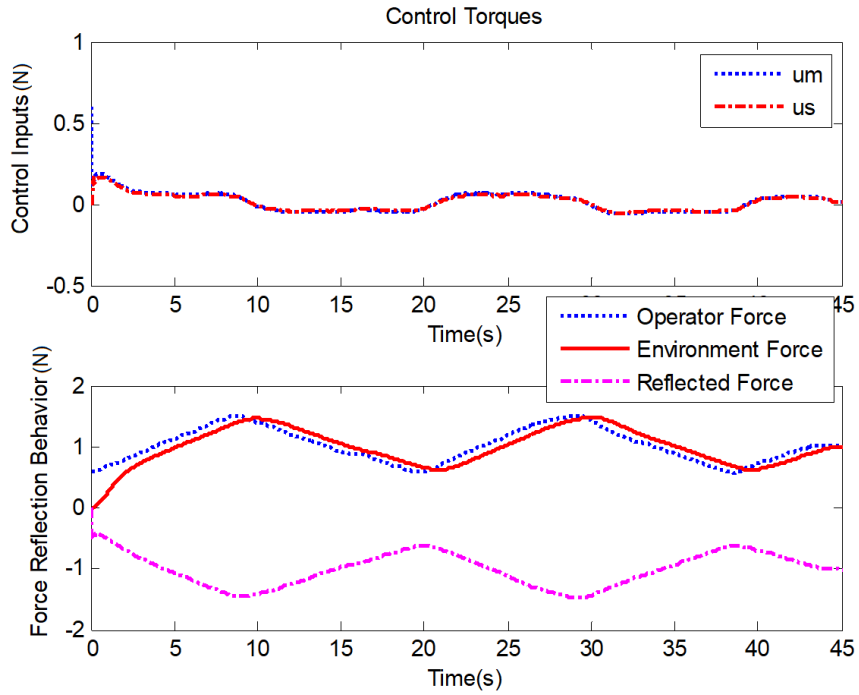

Figure 9.7: Semi-real time results: Control torques

algorithm by minimizing an integral-time-absolute-error (ITAE) criterion defined in Eq (9.31).

$$f_{obj} = \int t\left(|y_m - y_s| + |f_m - f_e|\right) dt \tag{9.30}$$

Here, Genetic algorithm is run with a population size of 50 and control gains are found to be in Eq (9.31)

$$\begin{aligned} k_{pm} &= 15.8996 \\ k_{dm} &= 2.3574 \\ k_{ps} &= 0.0005 \\ k_{ds} &= 7.1134 \end{aligned} \tag{9.31}$$

With the teleoperation system parameters reported earlier, MATLAB simulations are performed under a time-varying operator's force and the results are depicted in Figure 9.8 and Figure 9.9.

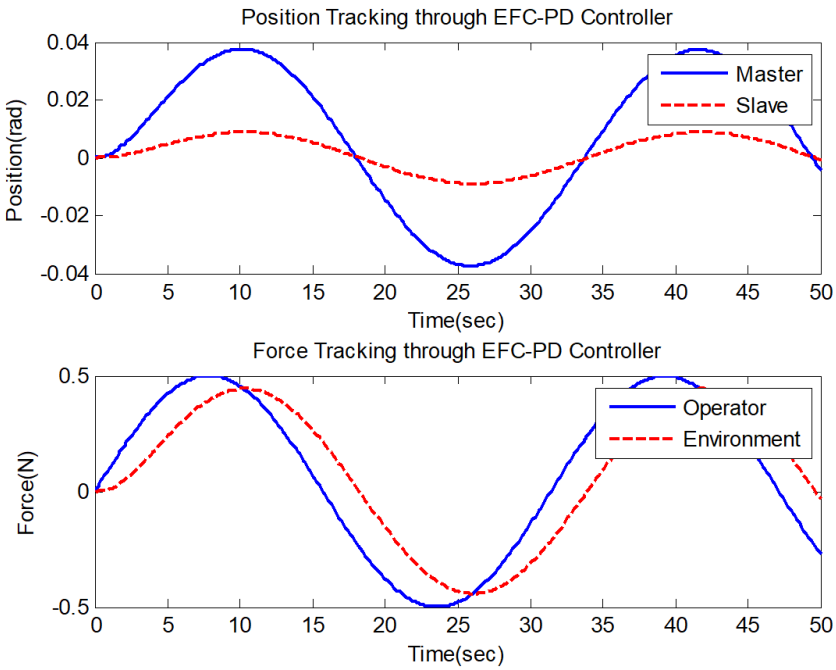

Figure 9.8: Comparative assessment: EFC-PD controller

It can be seen that the proposed controller offers better position and force tracking performance than the EFC-PD controller. The proposed controller parameters are summarized in Table 9.1.

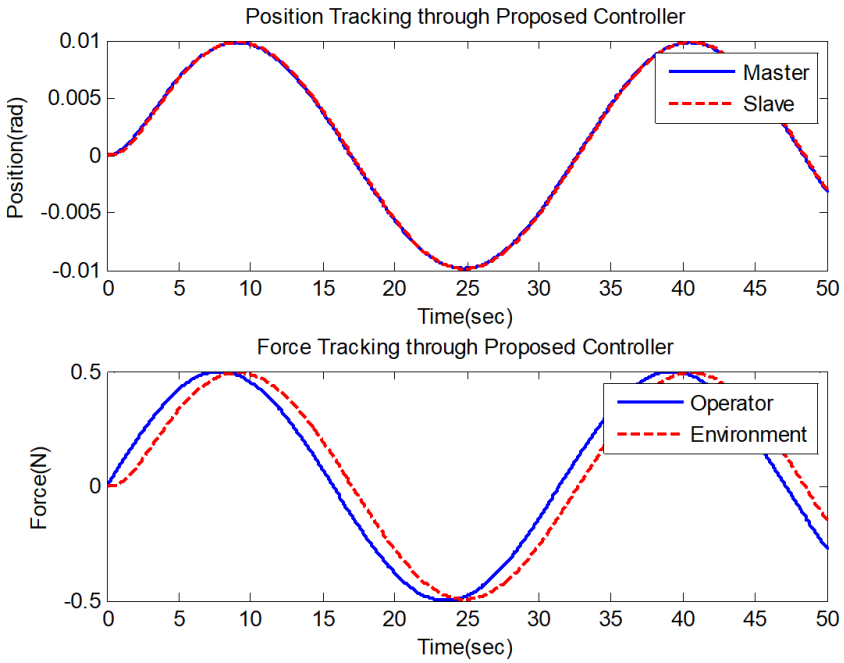

Figure 9.9: Comparative assessment: proposed controller

Controller	Simulation in MATLAB/Simulink	Semi Real-time QUARC/Simulink
System	1-DoF (Master/Slave)	1-DoF (Master/Slave)
Operator Force (N)	0.5 (constant)	Time-varying force using Omni Bundle
Environment Stiffness k_e (Nm/rad)	50	10
Environment Damping b_e (Nm/rad)	0.1	0.1
Force Feedback gain K_f	unity	unity
Scaling constant λ_m/λ_s	1	1
Time delay (Sec)	0.1	0.1

Table 9.1: Proposed controller parameters for simulation and semi-real time experiment

9.5 Conclusion

This chapter presented the design of disturbance observer-based three-channel state convergence architecture for bilateral teleoperation systems. It is shown that state convergence between the master and slave systems can still be achieved by transmitting composite variables instead of full states, which helps in reducing the number of channels. Further, state convergence architecture is made capable of dealing with

non-linearities by integrating extended state observers into it. Simulations and semi-real-time experiments show the effectiveness of the proposed architecture.

Chapter 10

A Multi-Master-Single-Slave Composite State Convergence Architecture

The aim of the chapter is to explore the possibility of extending the transparent bilateral state convergence architecture to accommodate the case of a multi-master-single-slave (MM/SS) teleoperation system. In addition, the channel complexity is kept at a minimum when multiple systems are communicating. To achieve the former objective, multiple masters-slave interconnections are considered with a new set of control gains while the later objective is achieved by adopting composite variables from authors' earlier work [104], [160]. In this proposed architecture, composite variables are transmitted across the communication channel instead of full systems' states. In addition, control gains are defined to consider masters-slave interactions. Through the method of state convergence, design conditions are derived to determine the control gains by allowing the tracking error to evolve as an autonomous system. To validate the findings, a single-degree-of-freedom tri-master-single-slave system time-delayed system is simulated in MATLAB/QUARC/Simulink environment. It is found that the proposed architecture can establish communication between multiple systems to achieve position and force tracking.

This chapter is organized as follows: Section 10.1 describes the architecture of the proposed multilateral system. Section 10.2 presents the design methodology, while simulation results are included in Section 10.3 followed by conclusions and references.

10.1 Proposed MM/SS Architecture

The proposed MMSS architecture is shown in Figure 10.1. Interactions between masters and slaves are modeled by different control gains, which will be determined by using the method of state convergence. Different parameters associated with the proposed architecture are defined below:

F_m^k: It represents the force exerted by the kth operator

g_{s1}^k: It represents the influence of the kth operator's force on the slave system

s_m^k: It represents the composite variable of k^{th} master system and is formed by fusing the velocity and position signals of the respective master system

s_s^1: It represents the composite variable of the slave system and is formed by fusing the velocity and position signals of the slave system

r_{s1}^k: It models the effect of the motion of k^{th} master system onto the slave system

r_{mk}^1: It models the effect of the motion of slave system onto k^{th} master system. It also carries environment information to the masters

g_{mk}^1: It scales the environmental force as it is reflected to the k^{th} master system

T_{mk}^1: It represents communication time delay from the slave to the k^{th} master system

T_{s1}^k: It represents communication time delay from the k^{th} master system to the slave system

k_s^1: It represents the stabilizing gain for the slave system

Of these, $2k+1$ parameters, k_s^1, g_{s1}^k, r_{s1}^k are designed through state convergence methodology as detailed in next section.

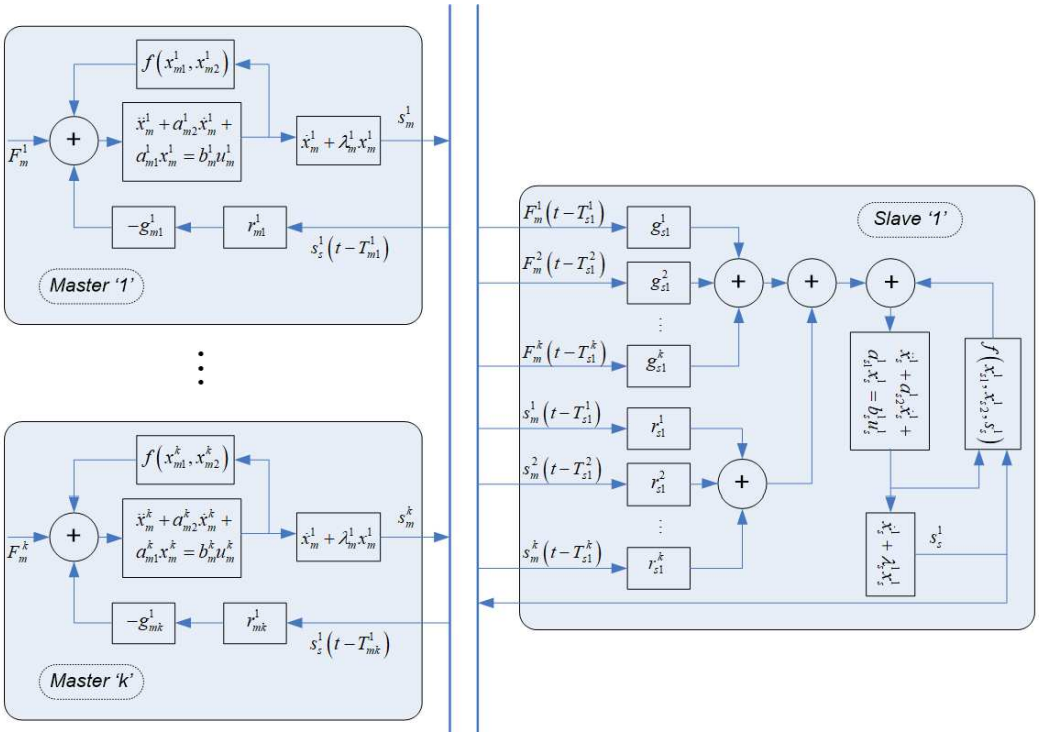

Figure 10.1: Proposed multi-master single slave architecture

10.2 Design Procedure for MM/SS Teleoperation System

Consider a single degree of freedom MM/SS teleoperation system:

$$\begin{aligned}
\dot{x}^1_{m1} &= x^1_{m2} \\
\dot{x}^1_{m2} &= a^1_{m1}x^1_{m1} + a^1_{m2}x^1_{m2} + b^1_m u^1_m \\
&\vdots \\
\dot{x}^k_{m1} &= x^k_{m2} \\
\dot{x}^k_{m2} &= a^k_{m1}x^k_{m1} + a^k_{m2}x^k_{m2} + b^k_m u^k_m \\
\dot{x}^1_{s1} &= x^1_{s2} \\
\dot{x}^1_{s2} &= a^1_{s1}x^1_{s1} + a^1_{s2}x^1_{s2} + b^1_s u^1_s
\end{aligned} \tag{10.1}$$

Let composite variables for the participant systems be defined as:

$$\begin{aligned}
s^1_m &= x^1_{m2} + \lambda_{m1}x^1_{m1} \\
&\vdots \\
s^k_m &= x^k_{m2} + \lambda_{mk}x^k_{m1} \\
s^1_s &= x^1_{s2} + \lambda_{s1}x^1_{s1}
\end{aligned} \tag{10.2}$$

We now introduce control inputs for the participant systems as:

$$\begin{aligned}
&u^1_m = \tfrac{1}{b^1_m}\left(-a^1_{m1}x^1_{m1} - \overline{a^1_{m2} + \lambda_{m1}}x^1_{m2}\right) - g^1_{m1}r^1_{m1}s^1_s\left(t - T^1_{m1}\right) + F^1_m \\
&\vdots \\
&u^k_m = \tfrac{1}{b^k_m}\left(-a^k_{m1}x^k_{m1} - \overline{a^k_{m2} + \lambda_{mk}}x^k_{m2}\right) - g^1_{mk}r^1_{mk}s^1_s\left(t - T^1_{mk}\right) + F^k_m \\
&u^1_s = \tfrac{1}{b^1_s}\left(-a^1_{s1}x^1_{s1} - \overline{a^1_{s2} + \lambda_{s1}}x^1_{s2} + k^1_s s^1_s\right) + \textstyle\sum_{j=1}^k r^j_{s1}s^j_m\left(t - T^j_{s1}\right) \\
&+ \textstyle\sum_{j=1}^k g^j_{s1}F^j_m\left(t - T^j_{s1}\right)
\end{aligned} \tag{10.3}$$

The time-derivative of the composite variables Eq (10.2) along with control inputs Eq (10.3) yields the following closed loop composite systems:

$$\begin{aligned}
\dot{s}^1_m &= -b^1_m g^1_{m1}r^1_{m1}s^1_s\left(t - T^1_{m1}\right) + b^1_m F^1_m \\
&\vdots \\
\dot{s}^k_m &= -b^k_m g^1_{mk}r^1_{mk}s^1_s\left(t - T^1_{mk}\right) + b^k_m F^k_m \\
\dot{s}^1_s &= k^1_s s^1_s + \textstyle\sum_{j=1}^k b^1_s r^j_{s1}s^j_m\left(t - T^j_{s1}\right) + \sum_{j=1}^k b^1_s g^j_{s1}F^j_m\left(t - T^j_{s1}\right)
\end{aligned} \tag{10.4}$$

By linearizing Eq (10.4) and employing constant operators' force assumption, we obtain:

$$\begin{aligned}
\dot{s}_m^1 &= -b_m^1 g_{m1}^1 r_{m1}^1 s_s^1 + b_m^1 g_{m1}^1 r_{m1}^1 T_{m1}^1 \dot{s}_s^1 + b_m^1 F_m^1 \\
&\vdots \\
\dot{s}_m^k &= -b_m^k g_{mk}^1 r_{mk}^1 s_s^1 + b_m^k g_{mk}^1 r_{mk}^1 T_{mk}^1 \dot{s}_s^1 + b_m^k F_m^k \\
\dot{s}_s^1 &= k_s^1 s_s^1 + \sum_{j=1}^{k} b_s^1 r_{s1}^j s_m^j - \sum_{j=1}^{k} b_s^1 r_{s1}^j T_{s1}^j \dot{s}_m^j + \sum_{j=1}^{k} b_s^1 g_{s1}^j F_m^j
\end{aligned} \tag{10.5}$$

Further processing of Eq (10.5) yields the following:

$$\begin{aligned}
&\dot{s}_m^1 = -b_m^1 g_{m1}^1 r_{m1}^1 s_s^1 + b_m^1 g_{m1}^1 r_{m1}^1 T_{m1}^1 \dot{s}_s^1 + b_m^1 F_m^1 \\
&\vdots \\
&\dot{s}_m^k = -b_m^k g_{mk}^1 r_{mk}^1 s_s^1 + b_m^k g_{mk}^1 r_{mk}^1 T_{mk}^1 \dot{s}_s^1 + b_m^k F_m^* \\
&\dot{s}_s^1 = \frac{1}{\left(1 + \sum_{j-1}^{k} b_s^1 r_{s1}^j T_{s1}^j b_m^j s_m^1 r_{mj}^1 T_{mj}^1\right)} \left(\left(k_s^1 + \sum_{j=1}^{k} b_s^1 r_{s1}^j T_{s1}^j b_m^j g_{mj}^1 r_{mj}^1 \right) s_s^1 + \right. \\
&\left. \sum_{j=1}^{k} b_s^1 r_{s1}^j s_m^j + \sum_{j=1}^{k} \left(b_s^1 g_{s1}^j - b_s^1 r_{s1}^j T_{s1}^j b_m^j \right) F_m^j \right.
\end{aligned} \tag{10.6}$$

Let us define a composite error as:

$$s_e = s_s^1 - \sum_{j=1}^{k} \alpha_{1j} s_m^j \tag{10.7}$$

The time derivative of Eq (10.7) along with Eq (10.6) yields composite error dynamics as:

$$\dot{s}_e = \left(k_s^1 + \left(b_s^1 r_{s1}^j T_{s1}^j + \alpha_{1j}\right) b_m^j g_{mj}^1 r_{mj}^1\right) s_s^1 + \sum_{j=1}^{k} b_s^1 r_{s1}^j s_m^j - \sum_{j=1}^{k} \left(b_s^1 r_{s1}^j T_{s1}^j + \alpha_{1j}\right) \left(b_m^j g_{mj}^1 r_{mj}^1 T_{mj}^1\right) \dot{s}_s^1 + \sum_{j=1}^{k} \left(b_s^1 g_{s1}^j - \left(b_s^1 r_{s1}^j T_{s1}^j + \alpha_{1j}\right) b_m^j\right) F_m^j \tag{10.8}$$

Further processing of Eq (10.8) yields:

$$\begin{aligned}\dot{s}_e = & \begin{pmatrix} k_s^1 + \left(b_s^1 r_{s1}^j T_{s1}^j + \alpha_{1j}\right) b_m^j g_{mj}^1 r_{mj}^1 \\ -\frac{\sum_{j=1}^{k}\left(b_s^1 r_{s1}^j T_{s1}^j + \alpha_{1j}\right)\left(b_m^j g_{mj}^1 r_{mj}^1 T_{mj}^1\right)}{\left(1+\sum_{j=1}^{k} b_s^1 r_{s1}^j T_{s1}^j b_m^j g_{mj}^1 r_{mj}^1 T_{mj}^1\right)} \left(k_s^1 + \sum_{j=1}^{k} b_s^1 r_{s1}^j T_{s1}^j b_m^j g_{mj}^1 r_{mj}^1\right) \end{pmatrix} s_s^1 \\ & + \sum_{j=1}^{k} b_s^1 r_{s1}^j \left(1 - \frac{\sum_{j=1}^{k} \left(b_s^1 r_{s1}^j T_{s1}^j + \alpha_{1j}\right) \left(b_m^j g_{mj}^1 r_{mj}^1 T_{mj}^1\right)}{\left(1 + \sum_{j=1}^{k} b_s^1 r_{s1}^j T_{s1}^j b_m^j g_{mj}^1 r_{mj}^1 T_{mj}^1\right)}\right) s_m^j \\ & + \sum_{j=1}^{k} \begin{pmatrix} \left(b_s^1 g_{s1}^j - \left(b_s^1 r_{s1}^j T_{s1}^j + \alpha_{1j}\right) b_m^j\right) \\ -\frac{\sum_{j=1}^{k}\left(b_s^1 r_{s1}^j T_{s1}^j + \alpha_{1j}\right)\left(b_m^j g_{mj}^1 r_{mj}^1 T_{mj}^1\right)}{\left(1+\sum_{j=1}^{k} b_s^1 r_{s1}^j T_{s1}^j b_m^j g_{mj}^1 r_{mj}^1 T_{mj}^1\right)} \sum_{j=1}^{k} \left(b_s^1 g_{s1}^j - b_s^1 r_{s1}^j T_{s1}^j b_m^j\right) \end{pmatrix} F_m^j \end{aligned} \tag{10.9}$$

Let us introduce the following assignments:

$$k_s^1 + \left(b_s^1 r_{s1}^j T_{s1}^j + \alpha_{1j}\right) b_m^j g_{mj}^1 r_{mj}^1 - \frac{\sum_{j=1}^{k} \left(b_s^1 r_{s1}^j T_{s1}^j + \alpha_{1j}\right) \left(b_m^j g_{mj}^1 r_{mj}^1 T_{mj}^1\right)}{\left(1 + \sum_{j=1}^{k} b_s^1 r_{s1}^j T_{s1}^j b_m^j g_{mj}^1 r_{mj}^1 T_{mj}^1\right)} \left(k_s^1 + \sum_{j=1}^{k} b_s^1 r_{s1}^j T_{s1}^j b_m^j g_{mj}^1 r_{mj}^1\right) = -q \tag{10.10}$$

$$b_s^1 r_{s1}^j \left(1 - \frac{\sum_{j=1}^{k} \left(b_s^1 r_{s1}^j T_{s1}^j + \alpha_{1j}\right) \left(b_m^j g_{mj}^1 r_{mj}^1 T_{mj}^1\right)}{\left(1 + \sum_{j=1}^{k} b_s^1 r_{s1}^j T_{s1}^j b_m^j g_{mj}^1 r_{mj}^1 T_{mj}^1\right)}\right) = \alpha_{1j} q \tag{10.11}$$

$$\frac{\sum_{j=1}^{k}\left(b_s^1 r_{s1}^j T_{s1}^j + \alpha_{1j}\right)\left(b_m^j g_{mj}^1 r_{mj}^1 T_{mj}^1\right)}{\left(1+\sum_{j=1}^{k} b_s^1 r_{s1}^j T_{s1}^j b_m^j g_{mj}^1 T_{mj}^1 T_{mj}^1\right)} \sum_{j=1}^{k}\left(b_s^1 g_{s1}^j - b_s^1 r_{s1}^j T_{s1}^j b_m^j\right) \\ = b_s^1 g_{s1}^j - \left(b_s^1 T_{s1}^j T_{s1}^j + \alpha_{1j}\right) b_m^j \tag{10.12}$$

The above assignments allow the composite error to evolve as an autonomous system. Thus, convergence of composite error is ensured i.e. $s_s^1 - \sum_{j=1}^{k} \alpha_{1j} s_m^j \to 0$. Since, $\dot{x}_{s2}^1 + \lambda_{s1} x_{s2}^1 = \dot{s}_s^1 \to 0$, we have $x_{s1}^1 = \sum_{j=1}^{k} \alpha_{1j} x_{m1}^j$ in steady state. In this way, position coordination is achieved. A similar analysis shows that force reflected to all the masters converges to the environmental force when applied forces are the same.

10.3 Simulation Results

To validate the proposed framework, 3MSS is adopted and tested in MATLAB Simulink environment. The following system parameters are assumed:

$$\begin{aligned} &a_{m1}^k = 0, a_{m2}^k = -7.1429, b_m^k = 0.2656, g_{mk}^1 = 1 \\ &a_{s1}^1 = 0, a_{s2}^1 = -6.25, b_m^k = 0.2729 \\ &k_e^1 = 10, \alpha_{11} = 0.1, \alpha_{12} = 0.5, \alpha_{13} = 0.4 \\ &T_{m1}^1 = T_{s1}^1 = 0.1, T_{m2}^1 = T_{s1}^2 = 0.15, T_{m3}^1 = T_{s1}^3 = 0.2 \end{aligned} \tag{10.13}$$

The control gains are obtained as a solution of design conditions Eq (10.10) - Eq (10.12):

$$\begin{aligned} &g_{s1}^1 = 0.7824, g_{s1}^2 = 4.5637, g_{s1}^3 = 4.1726 \\ &k_s^1 = -52.7717 \\ &r_{s1}^1 = 9.8187, r_{s1}^2 = 49.0936, r_{s1}^3 = 39.2749 \end{aligned} \tag{10.14}$$

Now, under constant operators' forces of F_m^k=0.25N, we simulate 3MSS system and the results are shown in Figure 10.2, Figure 10.3, Figure 10.4, Figure 10.6.

Slave is following the weighted motion of the master system while environment force is also reflected to the operators. It is also evident that transient phase of force reflection behavior is not appropriate while steady state phase truly reflects the environment to the operators.

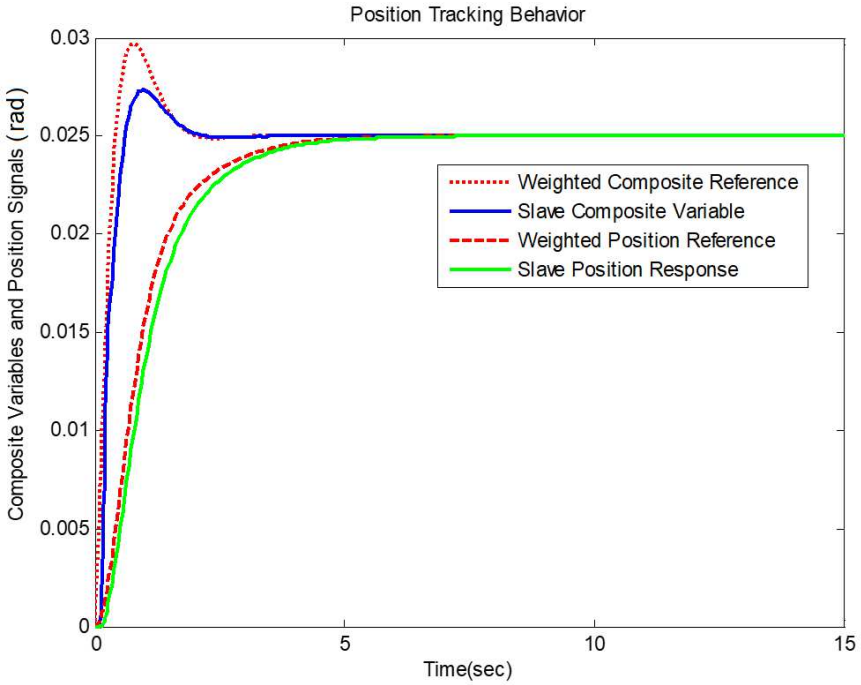

Figure 10.2: Simulation results of 3MSS teleoperation system (a) position response

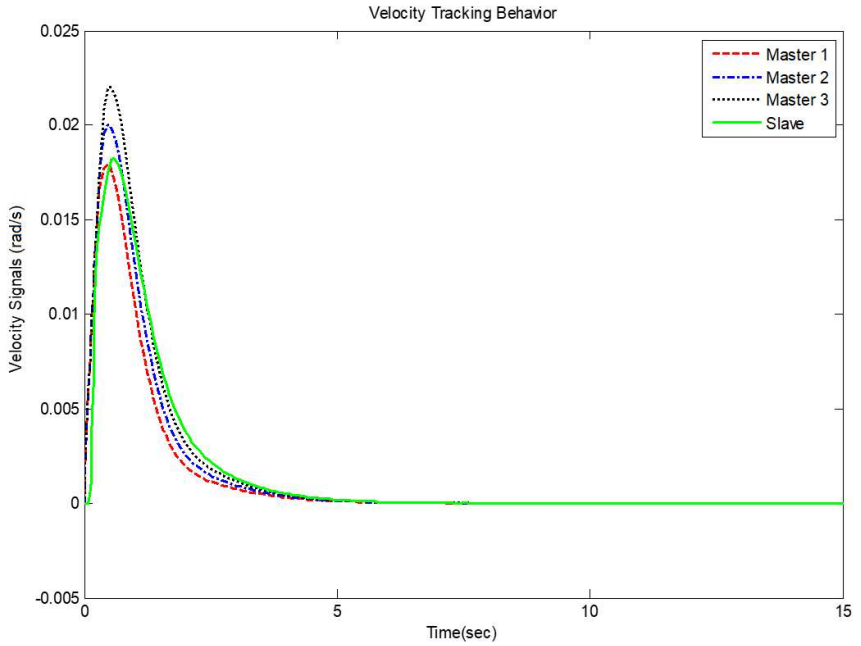

Figure 10.3: Simulation results of 3MSS teleoperation system: (b) velocity signals

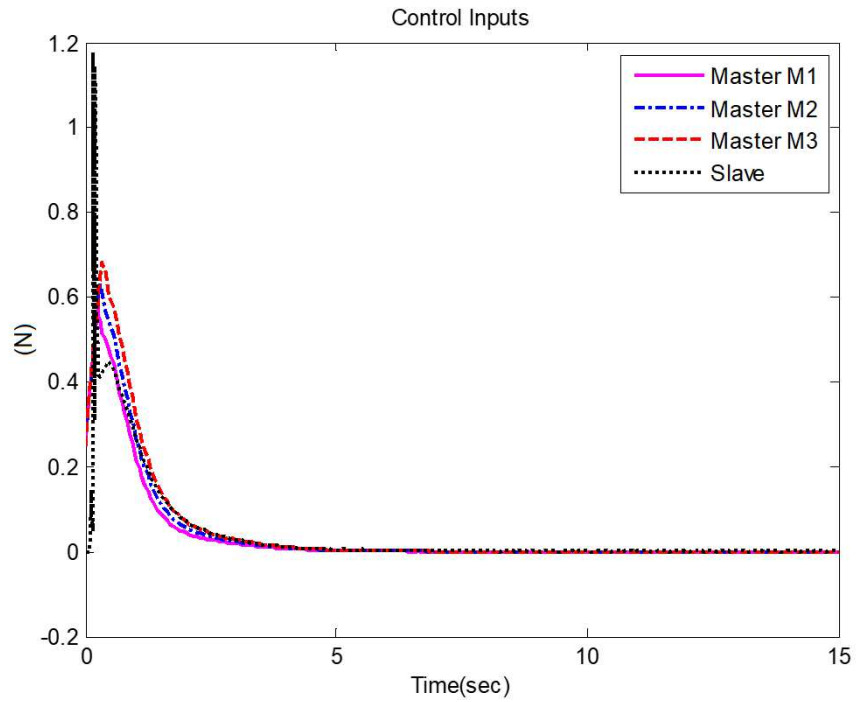

Figure 10.4: Simulation results of 3MSS teleoperation system: (c) control inputs

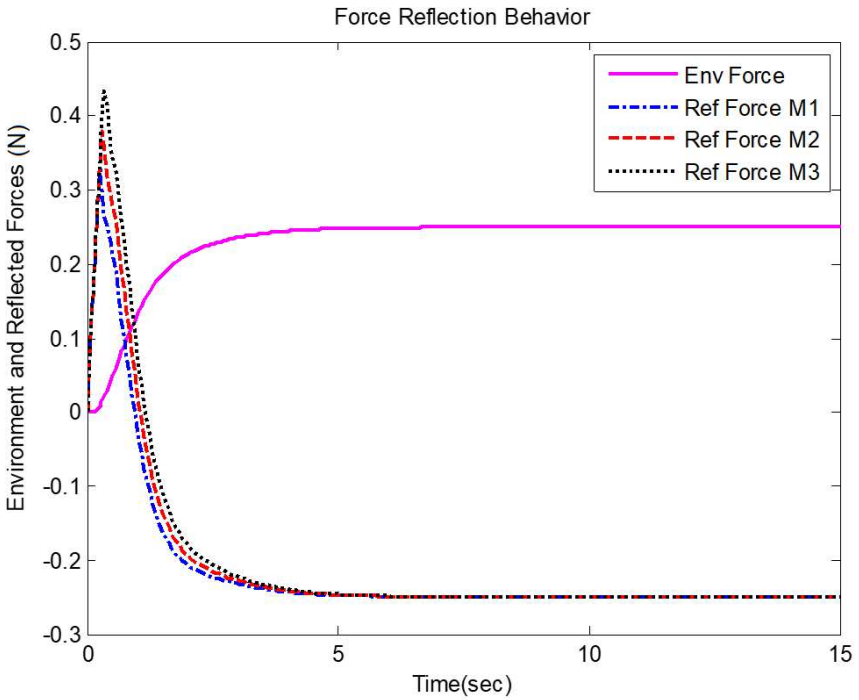

Figure 10.5: Simulation results of 3MSS teleoperation system: (d) force reflection

10.4 Experimental Results

We have also performed semi-real-time experiments in MATLAB/QUARC /Simulink environment, where one haptic device is used to drive three master systems. During the operation, the force from the virtual slave environment is transmitted to the haptic device via the time-delayed communication channel. The recorded experimental results are displayed in Figure 10.7, Figure 10.8, Figure 10.9.

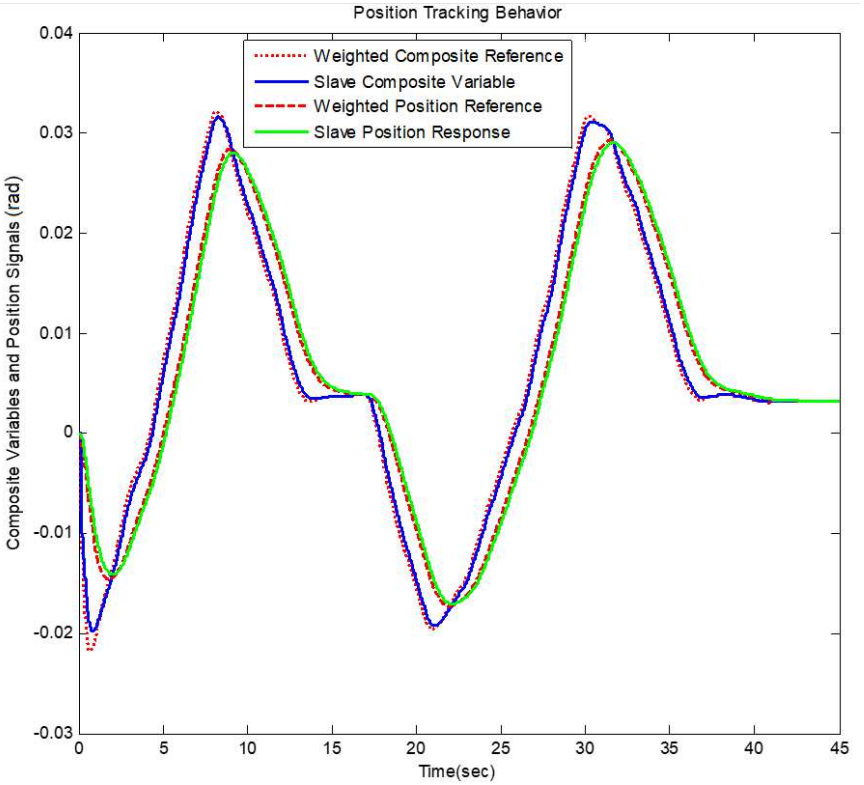

Figure 10.6: Experimental results of 3MSS teleoperation system (a) position response

It is evident that the slave is synchronized to the combined motion of the master systems while environment force is also being reflected in the masters. The results obtained from both the simulations and experiment validate the proposed extended architecture.

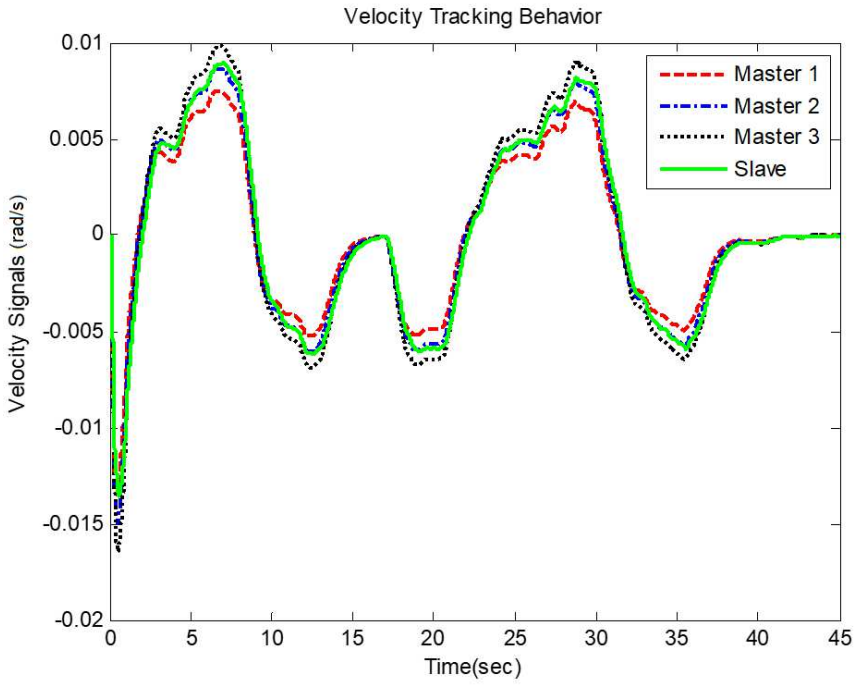

Figure 10.7: Experimental results of 3MSS teleoperation system (b) velocity signals

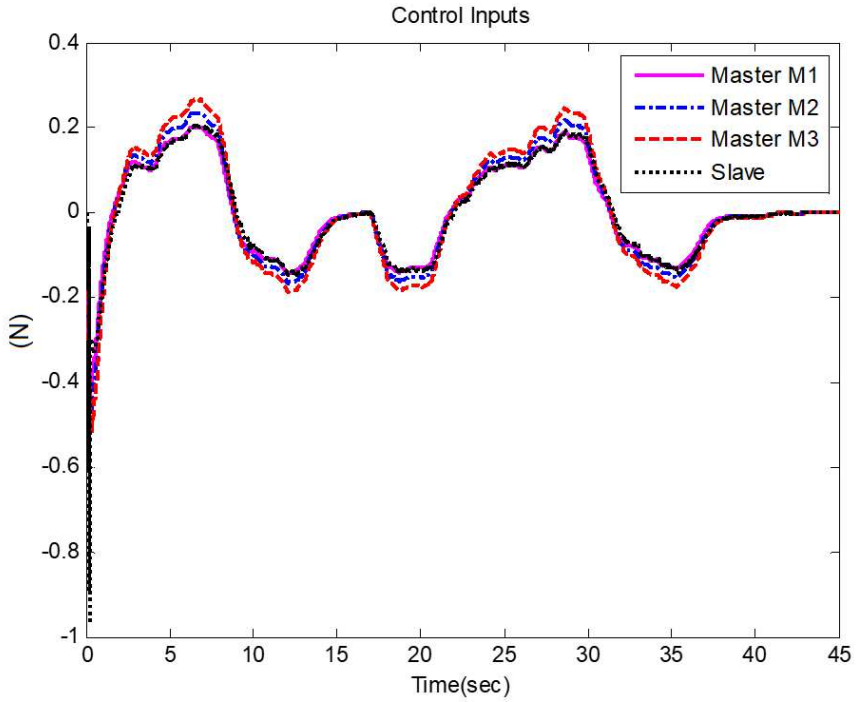

Figure 10.8: Experimental results of 3MSS teleoperation system (c) control inputs

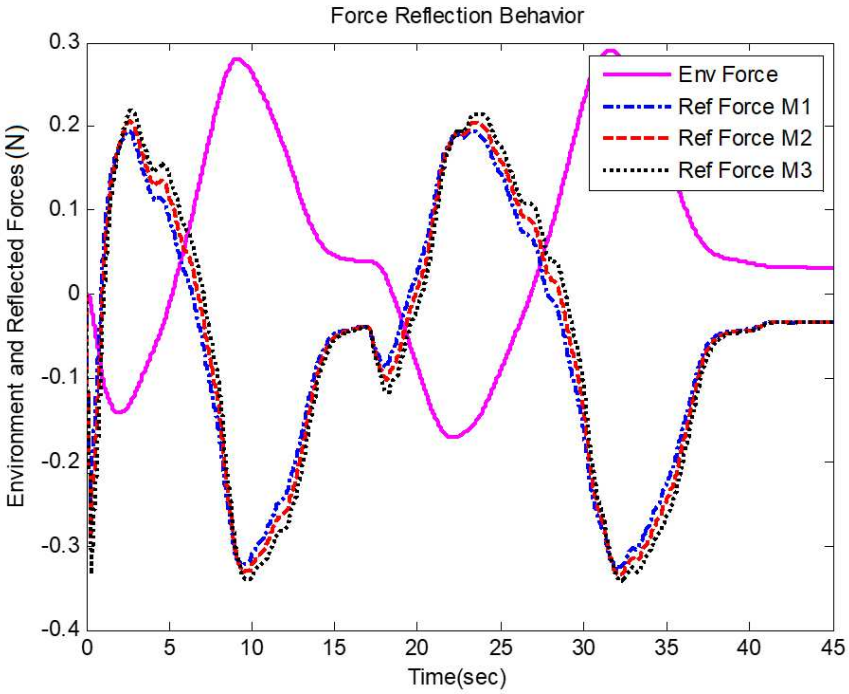

Figure 10.9: Experimental results of 3MSS teleoperation system (d) force reflection

10.5 Conclusion

In this chapter, the design of a multilateral teleoperation system is presented by considering the case of multiple masters and single slave systems. The proposed architecture is an extended version of transparent state convergence architecture which is developed earlier for bilateral control. The extension is realized by considering additional interactions and control gains. At the same time, the concept of a bilateral composite state convergence scheme is employed to reduce the control gains and simplify the communication channel. Method of state convergence is finally utilized to derive the design conditions, and control gains are determined as a solution of coupled equations. MATLAB simulations show that the proposed architecture possesses position and force tracking ability. Future works involve robustifying the proposed architecture against parameter variations.

Chapter 11

A Generalized Composite State Convergence Architecture for Multilateral Teleoperation Systems

A composite state convergence scheme is a reduced-complexity version of the state convergence controller for the teleoperation system. It employs a smaller number of control gains and communication channels to synchronize the motion of a single master-slave system in a desired dynamic way. The chapter aims to generalize the composite state convergence scheme so that l-slave systems can follow the weighted motion of k-master systems. To achieve this, at first, composite variables of all master and slave systems are transmitted across the communication channel along with operators' forces, and a set of $k+l+2kl$ control gains are defined. In the second stage, the design procedure of the existing composite state convergence scheme is extended for multiple systems, and control gains are determined through the solution of coupled equations. Finally, to validate the findings, simulations and semi-real-time experiments are performed in MATLAB/Simulink/QUARC environment by considering different configurations of teleoperation systems. This chapter reported a generalization of the composite state convergence scheme, which enables l-slave systems to track k-master systems. In addition, the number of communication channels are reduced as compared to the extended state convergence architecture [159]. In addition, the number of control gains are also reduced as compared to the extended state convergence architecture. It is shown that synchronization of l- composite-slave systems to k-composite- master systems guarantee the synchronization of original l-slave systems to the original k-master systems under the proposed systematic design procedure. In addition, the stability of the proposed scheme is verified through Lyapunov analysis. The proposed scheme is validated through simulations and semi-real-time experiments in MATLAB, Simulink, and QUARC environments.

Remark 11.1. *Although the composite state convergence scheme offers lower complexity (three communication channels and four design variables) as compared to its standard counterpart (2n+1 communication channel and 3n+1 design variables), a*

generalization is desired in order for the scheme to accommodate any number of master and slave systems involved in the joint task. This has motivated us to investigate the possibility of extending composite state convergence scheme for multiple systems.

The rest of the chapter is organized as follows: The proposed generalization is presented in Section 11.1, while MATLAB simulations and experimental results are included in Section 11.2 and 11.3, respectively. Conclusions are given in Section 11.4 and stability analysis is provided in Appendix B.

11.1 Proposed Scheme for Multilateral Teleoperation Systems

The proposed extension enables composite state convergence scheme to synchronize l-slave systems to the reference motions generated by k-master systems. The objective is to allow j^{th} slave system to track combined motions of k-master systems as:

$$x_s^j - \sum_{i=1}^{k} \alpha_{sj}^i x_m^i \to 0, t \to \infty \tag{11.1}$$

where x denotes the states while α_{sj}^i are defined as authority factors for the master systems affecting j^{th} slave system such that $\sum_{i=1}^{k} \alpha_{sj}^i = 1$.

Communication Structure

To achieve this objective, communication is first established by transmitting composite variables from all the master systems $(s_m^j, j = 1, 2, ..., k)$ to all the slave systems as well as from all the slave systems $(s_m^j, j = 1, 2, ..., k)$ to all the master systems over the communication channel, which offers constant time-delays to the incoming signals. Here, T_{mi}^j is the time delay from the j^{th} slave system to the i^{th} master system while T_{si}^j is the time delay from the j^{th} master system to the i^{th} slave system. Thus, j^{th} slave system will receive delayed copies of composite variables of all k-master systems $\left(s_{mjd}^i = s_m^i\left(t - T_{sj}^i\right), i = 1, 2, ..., k\right)$ while j^{th} master system will receive delayed copies of composite variables of all l-slave systems $\left(s_{sjd}^i = s_s^i\left(t - T_{mj}^i\right), i = 1, 2, ..., l\right)$. In addition, all the operators' forces $(F_m^j, j = 1, 2, ..., k)$ are also transmitted to the slave systems over the communication channel. Thus, j^{th} slave system will receive delayed copies of all k-operators forces $\left(F_{mjd}^i, i = 1, 2, ..., k\right)$.

After transmitting the composite variables and force signals over the channel, control gains are introduced in line with the composite state convergence scheme. First, j^{th} slave system is stabilized with $k_s^j, j = 1, 2, ..., l$. Since j^{th} slave system also receives

delayed composite variables from all the master systems, gains $r^i_{sj}, i = 1, 2, ..., k$ are introduced to scale the incoming composite variables from the master systems. In addition, operators' forces are also scaled at j^{th} slave system with $G^i_{sj}, i = 1, 2, ..., k$. We proceed in the same manner and introduce control gains for the master systems. First, j^{th} master system is stabilized with $k^j_m, j = 1, 2, ..., k$. Since, j^{th} master system also receives delayed composite variables from all the slave systems, gains $r^i_{mj}, i = 1, 2, ..., l$ are introduced to scale the incoming composite variables. These r^i_{mj} gains are pre-computed as $r^i_{mj} = k^i_{fj} k^i_e$ where k^i_{fj} is the force-feedback gain from the i^{th} slave to the j^{th} master system while k^i_e is the environment stiffness associated with the i^{th} slave system. All other control gains will be determined through the proposed design procedure, which is an extended version of the composite state convergence methodology. The proposed scheme is depicted in Figure 11.1.

11.2 Design Procedure

Let us consider single-degrees-of-freedom master and slave systems as $(z = m, s)$:

$$\begin{aligned} \dot{x}^i_{z1} &= x^i_{z2} \\ \dot{x}^i_{z2} &= a^i_{z1} x^i_{z1} + a^i_{z2} x^i_{z2} + b^i_z u^i_z \end{aligned} \tag{11.2}$$

The composite variables for the master and slave systems are defined as:

$$s^i_z = x^i_{z2} + \lambda^i_z x^i_{z1} \tag{11.3}$$

The control inputs for the master systems are proposed as in Eq (11.4):

$$\begin{aligned} u^1_m &= \tfrac{1}{b^1_m} \left(-a^1_{m1} x^1_{m1} - \left(a^1_{m2} + \lambda^1_m \right) x^1_{m2} + k^1_m s^1_m \right) + \textstyle\sum_{j=1}^{l} r^j_{m1} s^j_{s1d} + F^1_m \\ &\vdots \\ u^k_m &= \tfrac{1}{b^k_m} \left(-a^k_{m1} x^k_{m1} - \left(a^k_{m2} + \lambda^k_m \right) x^k_{m2} + k^k_m s^k_m \right) + \textstyle\sum_{j=1}^{l} r^j_{mk} s^j_{skd} + F^k_m \end{aligned} \tag{11.4}$$

The control inputs for the slave systems are proposed as in Eq (11.5):

$$\begin{aligned} u^1_s &= \tfrac{1}{b^1_s} \left(-a^1_{s1} x^1_{s1} - \left(a^1_{s2} + \lambda^1_s \right) x^1_{s2} + k^1_s s^1_s \right) + \textstyle\sum_{j=1}^{k} r^j_{s1} s^j_{m1d} + \sum_{j=1}^{k} G^j_{s1} F^j_{m1d} \\ &\vdots \\ u^l_s &= \tfrac{1}{b^l_s} \left(-a^l_{s1} x^l_{s1} - \left(a^l_{s2} + \lambda^l_s \right) x^l_{s2} + k^l_s s^l_s \right) + \textstyle\sum_{j=1}^{k} r^j_{sl} s^j_{mld} + \sum_{j=1}^{k} G^j_{sl} F^j_{mld} \end{aligned} \tag{11.5}$$

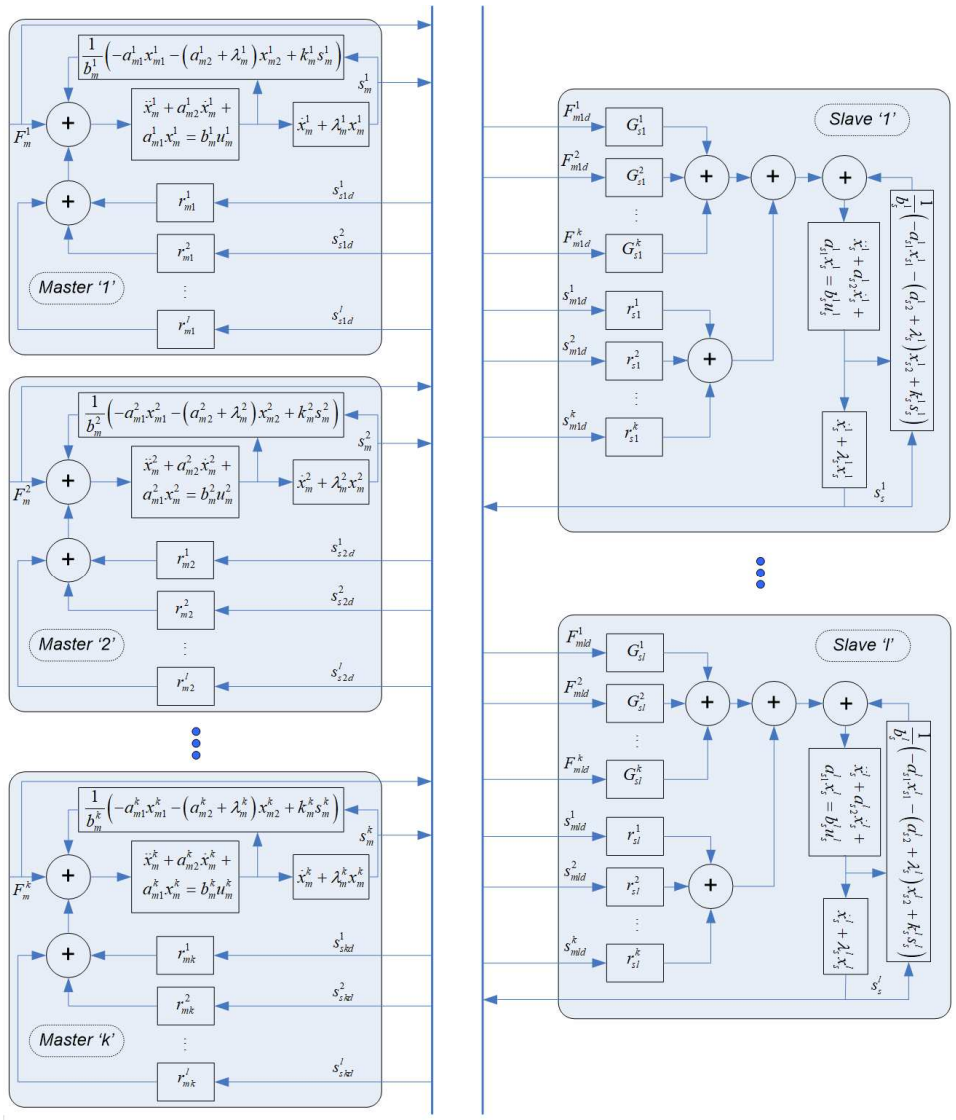

Figure 11.1: Proposed generalized state convergence scheme for multiple systems

Using the master control input, the closed-loop composite-master systems can be written as:

$$\begin{aligned} \dot{s}_m^1 &= k_m^1 s_m^1 + b_m^1 \textstyle\sum_{j=1}^{l} r_{m1}^j s_s^j \left(t - T_{m1}^j\right) + b_m^1 F_m^1 \\ &\vdots \\ \dot{s}_m^k &= k_m^k s_m^k + b_m^k \textstyle\sum_{j=1}^{l} r_{mk}^j s_s^j \left(t - T_{mk}^j\right) + b_m^k F_m^k \end{aligned} \tag{11.6}$$

Using the slave control inputs, the closed loop slave composite systems can be given as:

$$\begin{aligned} \dot{s}_s^1 &= k_s^1 s_s^1 + b_s^1 \textstyle\sum_{j=1}^{k} r_{s1}^j s_m^j \left(t - T_{s1}^j\right) + b_s^1 \sum_{j=1}^{k} G_{s1}^j F_m^j \left(t - T_{s1}^j\right) \\ &\vdots \\ \dot{s}_s^l &= k_s^l s_s^l + b_s^l \textstyle\sum_{j=1}^{k} r_{sl}^j s_m^j \left(t - T_{sl}^j\right) + b_s^1 \sum_{j=1}^{k} G_{sl}^j F_m^j \left(t - T_{sl}^j\right) \end{aligned} \tag{11.7}$$

Now, we approximate the time-delay entities using first order Taylor expansion as:

$$\begin{aligned} s_m^j\left(t-T_{sl}^j\right) &\approx s_m^j(t)-T_{sl}^j\dot{s}_m^j(t) \\ s_s^j\left(t-T_{mk}^j\right) &\approx s_s^j(t)-T_{mk}^j\dot{s}_s^j(t) \\ F_m^j\left(t-T_{sl}^j\right) &\approx F_m^j-T_{sl}^j\dot{F}_m^j=F_m^j \end{aligned} \tag{11.8}$$

The closed loop composite-systems under the above approximations can be written as:

$$\begin{aligned} \begin{bmatrix} \dot{s}_m^1 \\ \vdots \\ \dot{s}_m^k \\ \dot{s}_s^1 \\ \vdots \\ \dot{s}_s^l \end{bmatrix} &= \begin{bmatrix} k_m^1 & \dots & 0 & b_m^1 r_{m1}^1 & \dots & b_m^1 r_{m1}^l \\ & \ddots & & & \vdots & \\ 0 & \dots & k_m^k & b_m^k r_{mk}^1 & \dots & b_m^k r_{mk}^l \\ b_s^1 r_{s1}^1 & \dots & b_s^1 r_{s1}^k & k_s^1 & \dots & 0 \\ & \vdots & & & \ddots & \\ b_s^l r_{sl}^1 & \dots & b_s^l r_{sl}^k & 0 & \dots & k_s^l \end{bmatrix} \begin{bmatrix} s_m^1 \\ \vdots \\ s_m^k \\ s_s^1 \\ \vdots \\ s_s^l \end{bmatrix} - \\ &\begin{bmatrix} 0 & \dots & 0 & b_m^1 T_{m1}^1 r_{m1}^1 & \cdots & b_m^1 T_{m1}^l r_{m1}^l \\ & \vdots & & & \vdots & \\ 0 & \dots & 0 & b_m^k T_{mk}^1 r_{mk}^1 & \dots & b_m^k T_{mk}^l r_{mk}^l \\ b_s^1 T_{s1}^1 r_{s1}^1 & \dots & b_s^1 T_{s1}^k r_{s1}^k & 0 & \dots & 0 \\ & \vdots & & & \vdots & \\ b_s^l T_{sl}^1 r_{sl}^1 & \dots & b_s^l T_{sl}^k r_{sl}^k & 0 & \dots & 0 \end{bmatrix} \begin{bmatrix} \dot{s}_m^1 \\ \vdots \\ \dot{s}_m^k \\ \dot{s}_s^1 \\ \vdots \\ \dot{s}_s^l \end{bmatrix} + \\ &\begin{bmatrix} b_m^1 & \dots & 0 \\ & \ddots & \\ 0 & \dots & b_m^k \\ b_s^1 G_{s1}^1 & \dots & b_s^1 G_{s1}^k \\ & \vdots & \\ b_s^l G_{sl}^1 & \dots & b_s^l G_{sl}^k \end{bmatrix} \begin{bmatrix} F_m^1 \\ \vdots \\ F_m^k \end{bmatrix} \end{aligned} \tag{11.9}$$

To write above expression in a compact form, we introduce the following notations:

$$\begin{aligned} &s_m = \begin{bmatrix} s_m^1 & \dots & s_m^k \end{bmatrix}^T, s_s = \begin{bmatrix} s_s^1 & \dots & s_s^l \end{bmatrix}^T \\ &B_m = \operatorname{diag}\left(b_m^1,\dots,b_m^k\right), B_s = \operatorname{diag}\left(b_s^1,\dots,b_s^l\right) \\ &K_m = \operatorname{diag}\left(k_m^1,\dots,k_m^k\right), K_s = \operatorname{diag}\left(k_s^1,\dots,k_s^l\right) \end{aligned} \tag{11.10}$$

$$R_m = \begin{bmatrix} r_{m1}^1 & \dots & r_{m1}^l \\ & \vdots & \\ r_{mk}^1 & \dots & r_{mk}^l \end{bmatrix}, R_s = \begin{bmatrix} r_{s1}^1 & \dots & r_{s1}^k \\ & \vdots & \\ r_{sl}^1 & \dots & r_{sl}^k \end{bmatrix} T_m = \begin{bmatrix} T_{m1}^1 & \dots & T_{m1}^l \\ & \vdots & \\ T_{mk}^1 & \dots & T_{mk}^l \end{bmatrix},$$
$$T_s = \begin{bmatrix} T_{s1}^1 & \dots & T_{s1}^k \\ & \vdots & \\ T_{sl}^1 & \dots & T_{sl}^k \end{bmatrix} F_m = \begin{bmatrix} F_m^1 & \dots & F_m^k \end{bmatrix}^T, G_s = \begin{bmatrix} G_{s1}^1 & \dots & G_{s1}^k \\ & \vdots & \\ G_{sl}^1 & \dots & G_{sl}^k \end{bmatrix} \tag{11.11}$$

The closed loop composite system in Eq (11.9) can now be written as:

$$\begin{bmatrix} I_k & T_m \circ (B_m R_m) \\ T_s \circ (B_s R_s) & I_l \end{bmatrix} \begin{bmatrix} \dot{s}_m \\ \dot{s}_s \end{bmatrix} = \begin{bmatrix} K_m & B_m R_m \\ B_s R_s & K_s \end{bmatrix} \begin{bmatrix} s_m \\ s_s \end{bmatrix} + \begin{bmatrix} B_m \\ B_s G_s \end{bmatrix} F_m \tag{11.12}$$

where '$\circ$' denotes the Hadamard product. By letting $D_m = T_m \circ (B_m R_m), D_s = T_s \circ (B_s R_s)$ in above equation and using matrix inversion lemma, we obtain:

$$\begin{bmatrix} \dot{s}_m \\ \dot{s}_s \end{bmatrix} = \begin{bmatrix} A_{11} & A_{12} \\ A_{21} & A_{22} \end{bmatrix} \begin{bmatrix} s_m \\ s_s \end{bmatrix} + \begin{bmatrix} B_1 \\ B_2 \end{bmatrix} F_m \tag{11.13}$$

where:

$$\begin{aligned} A_{11} &= (I_k - D_m D_s)^{-1} K_m - D_m (I_l - D_s D_m)^{-1} B_s R_s \\ A_{12} &= (I_k - D_m D_s)^{-1} B_m R_m - D_m (I_l - D_s D_m)^{-1} K_s \\ A_{21} &= -D_s (I_k - D_m D_s)^{-1} K_m - (I_l - D_s D_m)^{-1} B_s R_s \\ A_{22} &= -D_s (I_k - D_m D_s)^{-1} B_m R_m - (I_l - D_s D_m)^{-1} K_s \\ B_1 &= (I_k - D_m D_s)^{-1} B_m - D_m (I_l - D_s D_m)^{-1} B_s G_s \\ B_2 &= -D_s (I_k - D_m D_s)^{-1} B_m - (I_l - D_s D_m)^{-1} B_s G_s \end{aligned}$$

Now, we define the following linear transformation:

$$\begin{bmatrix} s_m \\ s_e \end{bmatrix} = \begin{bmatrix} I_k & 0_{kl} \\ -\mathrm{A} & I_l \end{bmatrix} \begin{bmatrix} s_m \\ s_s \end{bmatrix} \tag{11.14}$$

where matrix A governs the set-points for the slave systems:

$$\mathrm{A} = \begin{bmatrix} \alpha_{s1}^1 & \dots & \alpha_{s1}^k \\ & \vdots & \\ \alpha_{sl}^1 & \dots & \alpha_{sl}^k \end{bmatrix} \tag{11.15}$$

In addition, $s_e = \begin{bmatrix} s_e^1 & \dots & s_e^l \end{bmatrix}^T$ is the composite-error system with l-entries described as $s_e^i = s_s^i - \sum_{j=1}^{k} \alpha_{si}^j s_m^j$. The time-derivative of the transformed composite master-error system in conjunction with the earlier composite master-slave system yields:

$$\begin{bmatrix} \dot{s}_m \\ \dot{s}_e \end{bmatrix} = \begin{bmatrix} \tilde{A}_{11} & \tilde{A}_{12} \\ \tilde{A}_{21} & \tilde{A}_{22} \end{bmatrix} \begin{bmatrix} s_m \\ s_e \end{bmatrix} + \begin{bmatrix} \tilde{B}_1 \\ \tilde{B}_2 \end{bmatrix} F_m \tag{11.16}$$

where:

$$\begin{aligned} \tilde{A}_{11} &= A_{11} + A_{12}\mathrm{A} \\ \tilde{A}_{12} &= A_{12} \\ \tilde{A}_{21} &= (A_{21} - \mathrm{A}A_{11}) + (A_{22} - \mathrm{A}A_{12})\,\mathrm{A} \\ \tilde{A}_{22} &= A_{22} - \mathrm{A}A_{12} \\ \tilde{B}_1 &= B_1 \\ \tilde{B}_2 &= B_2 - \mathrm{A}B_1 \end{aligned} \tag{11.17}$$

As per the guidelines provided by the composite state convergence method, we allow the composite error to evolve as an autonomous system. This leads to the following $2kl$ design conditions:

$$\tilde{A}_{21} = 0, \tilde{B}_2 = 0 \tag{11.18}$$

The remaining $k + l$ design conditions are obtained by assigning the desired dynamic behavior to the composite master-error system with Eq (11.19) enforced:

$$\left| sI_k - \tilde{A}_{11} \right| \times \left| sI_l - \tilde{A}_{22} \right| = |sI_k - P| \times |sI_l - Q| \tag{11.19}$$

where P and Q are diagonal matrices with the desired poles for the composite-master and composite-error systems, respectively i.e. $P = diag\,(p_1, ..., p_k)\,, Q = diag\,(q_1, ..., q_l)$.

Now, it is left to show that the slave systems indeed follow the weighted reference motions of the master systems with the proposed algorithm. To this end, observe that the composite-error system has a closed loop dynamic of $\dot{s}_e + Qs_e = 0$ which implies that $s_s - \mathrm{A}s_m = 0$ in steady state. Thus, composite-slave systems will attain the weighted reference composite-master states. Since poles of the composite master systems have also been placed on the left half plane, the composite master states will reach to some final value as determined by the constant operators' forces. This

implies that composite slave states will converge, which ascertains the stability of composite master and slave systems ($\dot{s}_m = \dot{s}_s = 0$). Based on these results, we can investigate the stability and convergence of the original master and slave systems. Let λ_m, λ_s be diagonal matrices and $x_{m1} = \left(x_{m1}^1, ..., x_{m1}^k\right)^T, x_{m2} = \left(x_{m2}^1, ..., x_{m2}^k\right)^T$,$x_{s1} = \left(x_{s1}^1, ..., x_{s1}^l\right)^T, x_{s2} = \left(x_{s2}^1, ..., x_{s2}^l\right)^T$. In steady state, we have $\dot{s}_z = \dot{x}_{z2} + \lambda_z x_{z2} = 0\,(z = m, s)$ which implies that x_{z2} will go to zero. This finding combined with earlier result $s_s - \mathrm{A}s_m = 0$ yields $x_{s1} = {\lambda_s}^{-1}\mathrm{A}\lambda_m x_{m1}$. By selecting the same diagonal entries in λ_m, λ_s, reference tracking of slave systems is achieved.

Remark 11.2. *The proposed algorithm requires fewer equations,$k + l + 2kl$, to be solved for synchronizing l-slaves to the references set by k-masters as compared to the extended state convergence architecture [38] which requires the solution of $n \times (k + l) + (n + 1) \times kl$ design conditions for achieving the same task.*

11.3 Simulations Results

The proposed algorithm is validated in MATLAB Simulink environment by considering two types of teleoperation systems. In the first case, same numbers of master and salve systems are considered while different numbers of master and slave systems are considered in the second instance. It will be shown that slave systems are able to follow the weighted motion of the master systems and synchronization is, therefore, achieved.

First, a square teleoperation system is set up in simulations where two masters are communicating with two slaves in the proposed framework. The parameters of the master systems are assumed to be $a_{m1}^i = 0, a_{m2}^i = -7.1429, b_m^i = 0.2656$ while slave systems are identified as $a_{s1}^i = 0, a_{s2}^i = -6.25, b_s^i = 0.2729$. The time delays in the communication channel are assumed as $T_{mi}^i = 0.1s, T_{si}^i = 0.3s, T_{mi}^j\big|_{i \neq j} = T_{si}^j\big|_{i \neq j} = 0.2s$. It is further assumed that the slaves are interacting with soft environments having stiffness $k_e^i = 20Nm/rad$ and all force feedback gains are considered as $k_{fi}^j = 0.1$. The alpha factors are selected as $\alpha_{s1}^1 = 0.7, \alpha_{s1}^2 = 0.3, \alpha_{s2}^1 = 0.6, \alpha_{s2}^2 = 0.4$ while poles are placed at $p_1 = -2, p_2 = -10, q_1 = -4, q_2 = -10$. The design conditions are solved using MATLAB symbolic toolbox by discarding the time delays and the following gains are obtained:

$$\begin{aligned} &G_{s1}^1 = 0.6813, G_{s1}^2 = 0.2920, G_{s2}^1 = 0.5840, G_{s2}^2 = 0.3893 \\ &k_m^1 = -10.6583, k_m^2 = -2.4041, k_s^1 = -3.5162, k_s^2 = -9.4214 \\ &r_{s1}^1 = -15.7894, r_{s1}^2 = 2.5851, r_{s2}^1 = -0.1891, r_{s2}^2 = 11.6481 \end{aligned} \tag{11.20}$$

Note that although time delays are ignored in the above calculations, these are being considered during simulations. This will establish the robustness of the proposed scheme to time delays of the communication channel. Now, we run the simulations with the control gains in Eq (11.20), and the synchronization results are shown in Figure 11.2 and Figure 11.3. It can be observed that both the slaves are following the weighted motion of the master systems. Here weighted composite references, $s^1_{s,ref} = \alpha^1_{s1} s^1_m + \alpha^2_{s1} s^2_m$and $s^2_{s,ref} = \alpha^1_{s2} s^1_m + \alpha^2_{s2} s^2_m$ are defined for the first and second slaves, respectively while corresponding position references for the slaves are obtained through the proposed algorithm and are being tracked effectively.

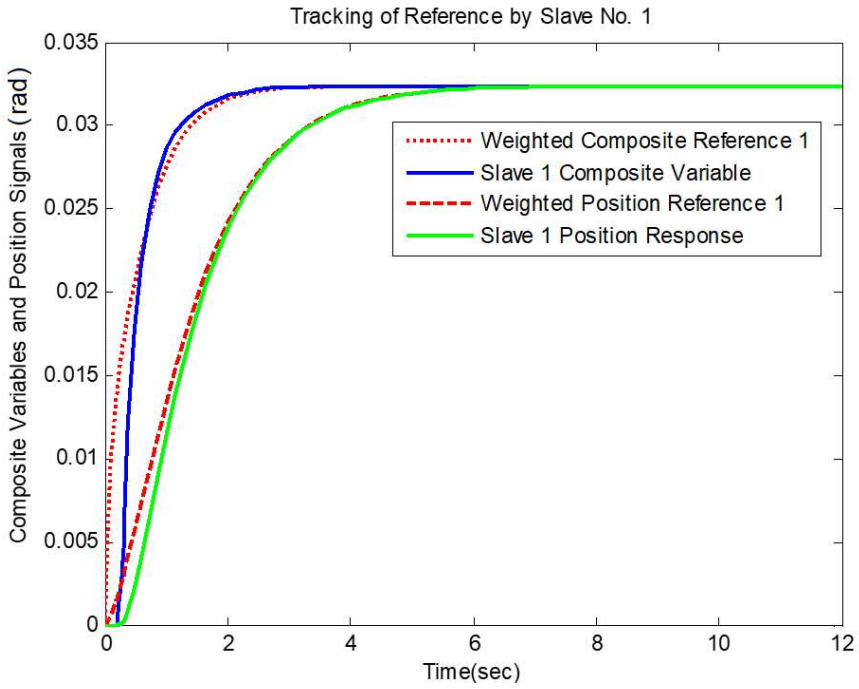

Figure 11.2: Reference tracking by first slave in 2x2 teleoperation system

We now consider a teleoperation system where three slaves are being operated by a single master. The parameters for the master and slave systems are the same as used in previous example. The poles are placed at $p_1 = -1.6, q_1 = -4, q_2 = -6, q_3 = -10$. Also, stiffness of the environments are assumed as $k^1_e = 10Nm/rad, k^2_e = 20Nm/rad, k^3_e = 30Nm/rad$. The design conditions are solved with unity alpha factors and ignoring time delay information and the following control gains are obtained:

$$\begin{aligned} &G^1_{s1} = G^1_{s2} = G^1_{s3} = 0.9733 \\ &k^1_m = -3.1936, k^1_s = -5.7444, k^2_s = -3.5943, k^3_s = -9.0677 \\ &r^1_{s1} = 15.1863, r^1_{s2} = 7.3080, r^1_{s3} = 27.3642 \end{aligned} \tag{11.21}$$

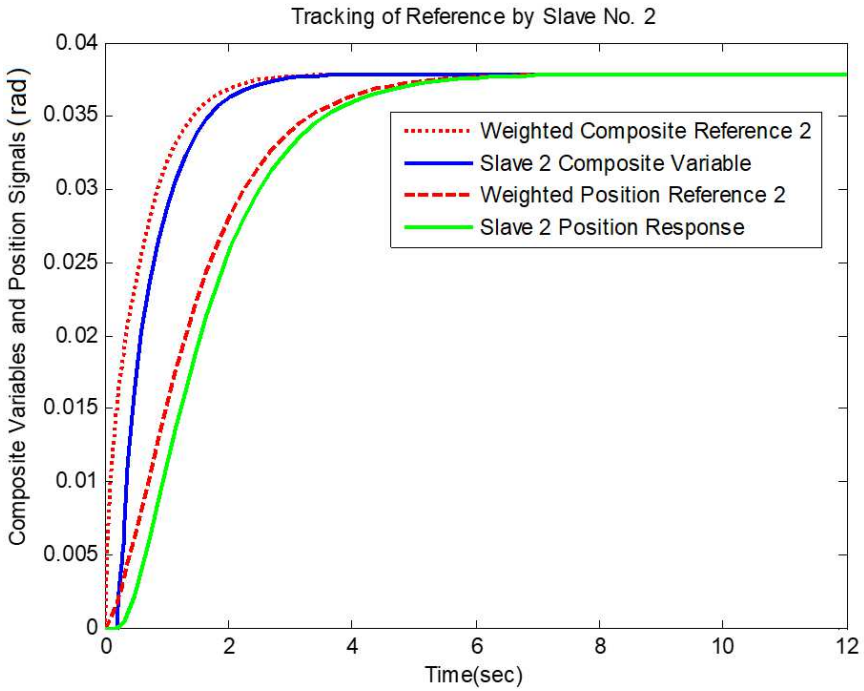

Figure 11.3: Reference tracking by second slave in 2x2 teleoperation system

The teleoperation system is now setup in MATLAB/Simulink environment with the time delays in the communication channel being $T^1_{m1} = T^1_{s1} = 0.1s, T^2_{m1} = T^1_{s2} = 0.15s, T^3_{m1} = T^1_{s3} = 0.2s$. By running the simulations under the control of Eq (**??**), we obtain the results as shown in Figure 11.4. It can be observed that slave systems are following the master system. The force-reflecting behavior of the 1x3 teleoperation system is also shown in Figure 11.6. It can be seen that weighted force from slaves, $0.1 \times \sum_{i=1}^{3} F_e^i$ is reflected to the master in a steady state.

The above results show that the proposed scheme can indeed accommodate arbitrary number of master and slave systems. A comparison of the proposed scheme with [38] is shown in Table 11.1. It can be seen that the proposed scheme requires fewer control gains and communication channels as compared to the extended state convergence architecture while offering similar performance.

11.4 Experimental Results

The proposed scheme is also validated through semi-real-time experiments. Owing to the availability of a single OMNI device, a 1x3 teleoperation system is set up, as shown in Figure 11.6. Only the block connections are shown, as the detailed setup follows Figure 11.1. The motion of the haptic device is constrained to the x-axis, and

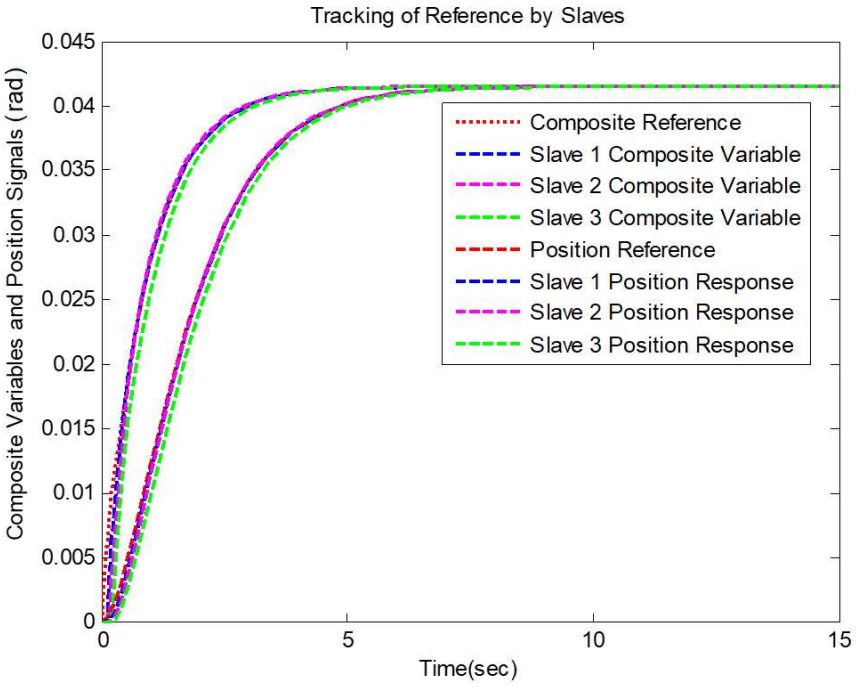

Figure 11.4: Reference tracking by three slaves in 1x3 teleoperation system

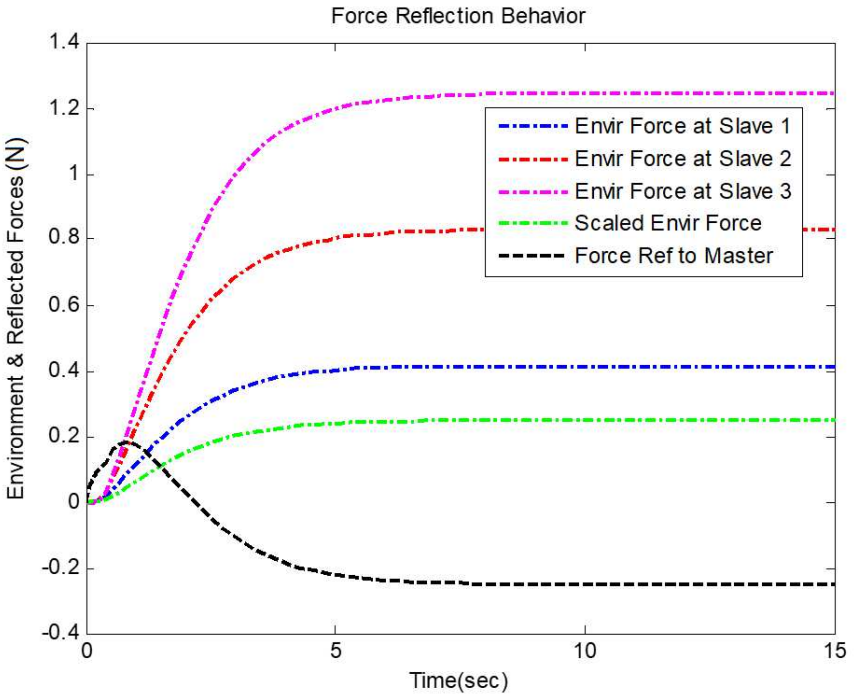

Figure 11.5: Force reflection behaviour of 1x3 teleoperation system

Table 11.1: Comparison with [38]

Sr. No	System Config.	Number of Control Gains (n=2)		Number of Communication Channels	
		[38]	Proposed	[38]	Proposed
01	2x2	20	12	20	12
02	1x3	17	10	15	9

an operator's force is generated to drive the master system as given in Eq 11.2. The master communicates with slaves on time-delayed channels. The reflected force from the slaves is provided to the haptic device, and thus the force feedback loop is closed around the operator.

To initiate the experiment, the operator applies a time-varying force onto the master by moving the haptic device in the reachable x-direction. The resulting motion of all the slaves is recorded along with the reflected force as sensed by the operator. These data are displayed in Figure 11.7, Figure 11.8. It can be seen that slave systems are tracking the reference motion of the master system while a weighted force is sensed by the operator as well.

11.5 Conclusion

This chapter presents a generalization of the composite state convergence schemes with respect to the number of master and slave systems. First, possible interactions between the master and slave systems are considered, and the closed-loop composite-master and composite-error systems are computed. Second, the composite-error systems are made autonomous, and the desired responses are assigned to both the composite-master and composite–error systems, giving rise to a total of $k + l + 2kl$ design conditions. MATLAB simulations show that the proposed scheme can successfully synchronize $l - slave$ systems with the references set by $k - master$ systems. In the future, the robustness of the scheme to parametric uncertainties will be analyzed by considering multi-degrees-of-freedom teleoperation systems.

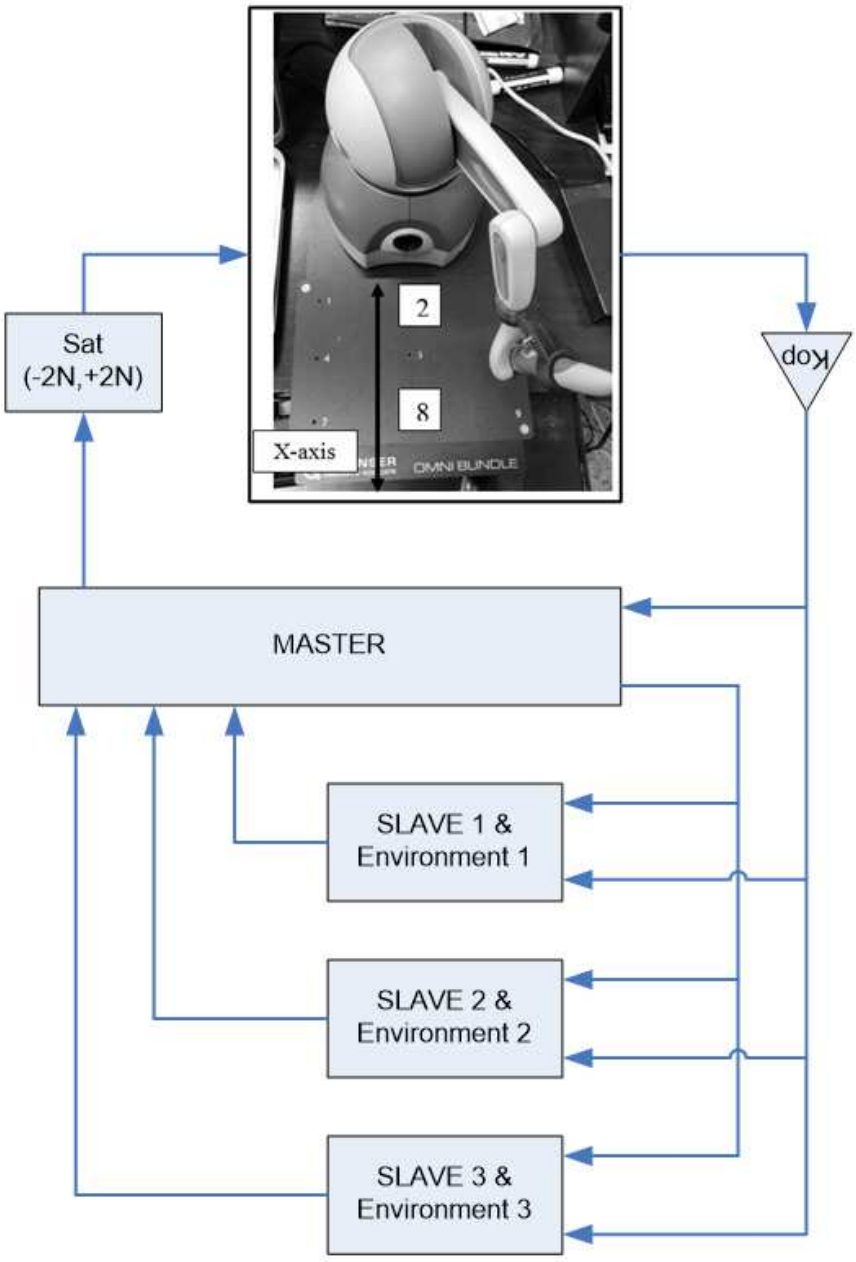

Figure 11.6: Semi real-time experimental setup for 1x3 system

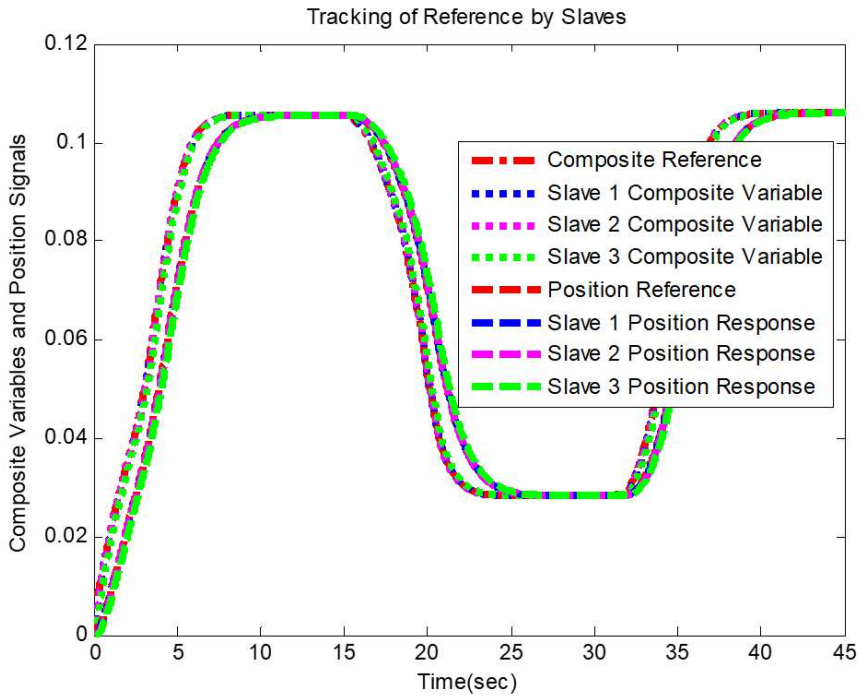

Figure 11.7: Reference tracking by slaves in 1x3 teleoperation system

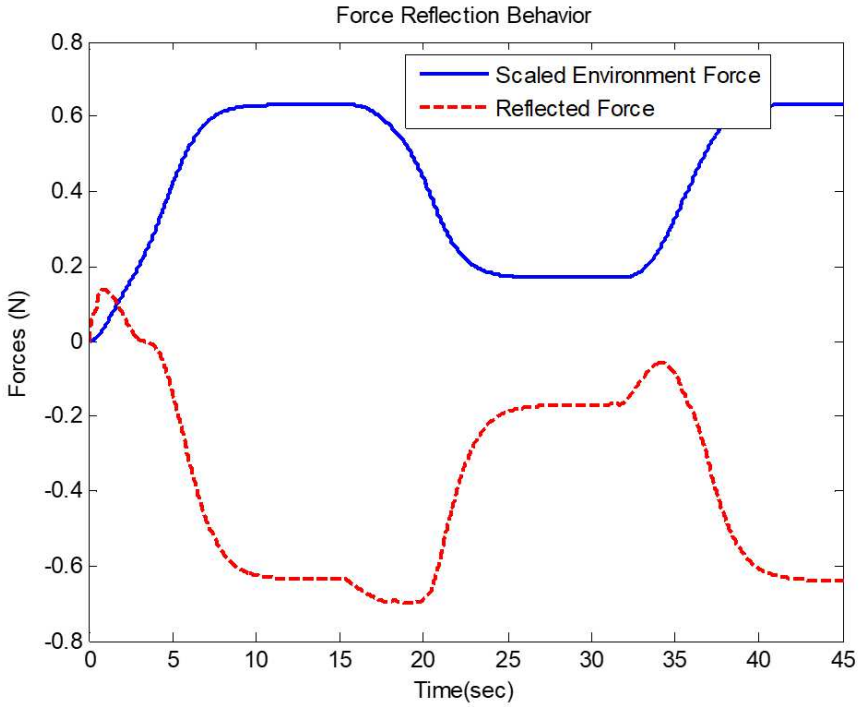

Figure 11.8: Force reflection behaviour of 1x3 teleoperation system

Chapter 12

An Improved Composite State Convergence Architecture with Disturbance Compensation for Multilateral Teleoperation Systems

Composite state convergence is a novel scheme for bilaterally controlling a telerobotic system. The scheme offers an elegant design procedure and employs only three communication channels to establish synchronization between a single master and a single-slave robotic system. This chapter expands the capability of the composite state convergence scheme to accommodate any number of master and slave systems. It proposes a disturbance observer-based composite state convergence architecture where $k-master$ systems can cooperatively control $l-slave$ systems in the presence of uncertainties. A systematic method is presented to compute the control gains, while observer gains are determined in a standard way. MATLAB simulations are performed on symmetric and asymmetric arrangements of single-degree-of-freedom teleoperation systems to validate the proposed architecture. Finally, experimental results are obtained using Quanser's Qube-Servo systems in QUARC/Simulink environment.

12.1 Improved CSC Scheme for Multilateral Teleoperation Systems

The proposed scheme offers an improvement over the existing composite state convergence scheme in that the lumped uncertainties can be estimated and compensated to improve the tracking performance. In addition, measurement of velocity signals is not required as disturbance observers also estimate these signals. The proposed enhancement transmits composite variables constructed from the estimated position and velocity signals. However, measurement of operators' and environmental forces is still required for the implementation of the controller. The block diagram of the proposed scheme is shown in Figure 12.1. Let us consider a single-degree-of-freedom master and slave system as:

$$\left.\begin{aligned}\dot{x}^i_{m1} &= x^i_{m2}\\ \dot{x}^i_{m2} &= a^i_{m1}x^i_{m1} + a^i_{m2}x^i_{m2} + b^i_m u^i_m + f^i_m\end{aligned}\right\}, i = 1, 2, ..., k \tag{12.1}$$

$$\left.\begin{aligned}\dot{x}^i_{s1} &= x^i_{s2}\\ \dot{x}^i_{s2} &= a^i_{s1}x^i_{s1} + a^i_{s2}x^i_{s2} + b^i_s u^i_s + f^i_s\end{aligned}\right\}, i = 1, 2, ..., l \tag{12.2}$$

where, subscript 'z' is used to denote either master ($z = m$) or slave ($z = s$) systems, and superscript 'i' is used to number the master ($i = 1, 2, \ldots, k$) and slave ($i = 1, 2, \ldots, l$) systems. The term f^i_z contains lumped uncertainty i.e.

$$f^i_z = \left(a^i_{z1o} - a^i_{z1}\right) x^i_{z1} + \left(a^i_{z2o} - a^i_{z2}\right) x^i_{z2} + \left(b^i_{zo} - b^i_z\right) u^i_z$$

$$\left.\begin{aligned}u^i_m &= \tfrac{1}{b^i_m}\left(\begin{array}{l}-a^i_{m1}\hat{x}^i_{m1} - (a^i_{m2} + \lambda^i_m)\\ \hat{x}^i_{m2} + k^i_m s^i_m - \hat{f}^i_m\end{array}\right) + \textstyle\sum_{j=1}^{l} r^j_{mk} s^j_{sid} + F^i_m\\ \dot{\hat{x}}^i_{m1} &= \hat{x}^i_{m2} + l^i_{m1}\left(x^i_{m1} - \hat{x}^i_{m1}\right)\\ \dot{\hat{x}}^i_{m2} &= a^i_{m1}\hat{x}^i_{m1} + a^i_{m2}\hat{x}^i_{m2} + b^i_m u^i_m + l^i_{m2}\left(x^i_{m1} - \hat{x}^i_{m1}\right) + \hat{f}^i_m\\ \dot{\hat{f}}^i_m &= l^i_{m3}\left(x^i_{m1} - \hat{x}^i_{m1}\right)\end{aligned}\right\} \tag{12.3}$$
$$, i = 1, 2, ..., k$$

The objective of the proposed controller is to make the slave systems follow the combined motion of the master systems in the presence of uncertainties. Precisely, the position of l^{th} slave system will converge to the weighted position of k-master systems in the presence of uncertainties following the introduction of control inputs and disturbance observers in Eq (12.3) and Eq (12.4), and the application of the method of state convergence.

$$\left.\begin{aligned}u^i_s &= \tfrac{1}{b^i_s}\left(-a^i_{s1}\hat{x}^i_{s1} - \left(a^i_{s2} + \lambda^i_s\right)\hat{x}^i_{s2} + k^i_s s^i_s - \hat{f}^i_s\right)\\ &+ \textstyle\sum_{j=1}^{k} r^j_{sl} s^j_{mid} + \sum_{j=1}^{k} G^j_{sl} F^j_{mid}\\ \dot{\hat{x}}^i_{s1} &= \hat{x}^i_{s2} + l^i_{s1}\left(x^i_{s1} - \hat{x}^i_{s1}\right)\\ \dot{\hat{x}}^i_{s2} &= a^i_{s1}\hat{x}^i_{s1} + a^i_{s2}\hat{x}^i_{s2} + b^i_s u^i_s + l^i_{s2}\left(x^i_{s1} - \hat{x}^i_{s1}\right) + \hat{f}^i_s\\ \dot{\hat{f}}^i_s &= l^i_{s3}\left(x^i_{s1} - \hat{x}^i_{s1}\right)\end{aligned}\right\} \tag{12.4}$$
$$, i = 1, 2, ..., l$$

Let us now perform a closed-loop analysis to verify the claims. Let us first introduce

the composite variables for the master systems as:

$$s_m^i = x_{m2}^i + \lambda_m^i x_{m1}^i, i = 1, 2, ..., k \tag{12.5}$$

Taking the time derivative of Eq (12.5) and introducing the control inputs yields the following closed-loop composite master systems:

$$\dot{s}_m^i = k_m^i s_m^i + b_m^i \sum_{j=1}^{l} r_{mi}^j s_{sid}^j + b_m^i F_m^i + \xi_m^i e_m^i, i = 1, 2, ..., k \tag{12.6}$$

where

$$e_m^i = \begin{bmatrix} e_{m1}^i & e_{m2}^i & e_{m3}^i \end{bmatrix}^T = \begin{bmatrix} x_{m1}^i - \hat{x}_{m1}^i & x_{m2}^i - \hat{x}_{m2}^i & x_{m3}^i - \hat{x}_{m3}^i \end{bmatrix}^T$$

$i = 1, 2, ..., k$ constitute observation errors for the master systems with $\xi_m^i = \begin{bmatrix} a_{m1}^i & a_{m2}^i + \lambda_m^i & 1 \end{bmatrix}$. The observer error dynamics of master systems can be written as:

$$\left.\begin{aligned} \dot{e}_{m1}^i &= -l_{m1}^i e_{m1}^i + e_{m2}^i \\ \dot{e}_{m2}^i &= (a_{m1}^i - l_{m2}^i) e_{m1}^i + a_{m2}^i e_{m2}^i + e_{m3}^i \\ e_{m3}^i &= -l_{m3}^i e_{m1}^i + \dot{f}_m^i \end{aligned}\right\}, i = 1, 2, ..., k \tag{12.7}$$

Linearizing the time delayed terms in Eq (12.6), we obtain:

$$\begin{aligned} &\dot{s}_m^i = k_m^i s_m^i + b_m^i \textstyle\sum_{j=1}^{l} r_{mi}^j s_s^j - b_m^i \sum_{j=1}^{l} r_{mi}^j T_{mi}^j \dot{s}_s^j + b_m^i F_m^i + \xi_m^i e_m^i \\ &i = 1, 2, ..., k \end{aligned} \tag{12.8}$$

By stacking composite master systems in Eq (12.8), we obtain Eq (C.1). This can be conveniently written as:

$$\dot{s}_m = k_m s_m + b_{rm} s_s - b_{rmT} \dot{s}_s + b_m F_m + \xi_m e_m \tag{12.9}$$

Combining the closed loop composite master system in Eq (12.9) with observer error dynamics in Eq (12.7), we obtain:

$$\begin{bmatrix} \dot{s}_m \\ \dot{e}_m \end{bmatrix} = \begin{bmatrix} k_m & \xi_m \\ 0 & o_m \end{bmatrix} \begin{bmatrix} s_m \\ e_m \end{bmatrix} + \begin{bmatrix} b_{rm} & -b_{rmT} \\ 0 & 0 \end{bmatrix} \begin{bmatrix} s_s \\ \dot{s}_s \end{bmatrix} + \begin{bmatrix} b_m \\ 0 \end{bmatrix} F_m + \begin{bmatrix} 0 \\ h_m \end{bmatrix} \dot{f}_m \tag{12.10}$$

It can be seen that observer design can be carried out separately from controller design. It is assumed that lumped disturbance is slowly varying and therefore convergence of observation error to origin is ensured by comparing the characteristic equation with the desired polynomial which yields the observer gains.

$$p_m(s) : s^3 + (l^i_{m1} - a^i_{m2})\, s^2 + (l^i_{m2} - a^i_{m1} - a^i_{m2} l^i_{m1})\, s + l^i_{m3} = 0, i = 1, 2, ..., k \tag{12.11}$$

Now, we define composite variables for the slave systems as:

$$s^i_s = x^i_{s2} + \lambda^i_s x^i_{s1}, i = 1, 2, ..., l \tag{12.12}$$

Time-derivative of Eq (12.12) along with control inputs yields closed loop composite slave systems as:

$$\dot{s}^i_s = k^i_s s^i_s + b^i_s \sum_{j=1}^{k} r^j_{si} s^j_{mid} + b^i_s \sum_{j=1}^{k} G^j_{si} F^j_{mid} + \xi^i_s e^i_s, i = 1, 2, ..., l \tag{12.13}$$

where $e^i_s = \begin{bmatrix} x^i_{s1} - \hat{x}^i_{s1} & x^i_{s2} \hat{x}^i_{s2} & x^i_{s3} - \hat{x}^i_{s3} \end{bmatrix}^T, i = 1, 2, ..., l$ constitute observation errors for the slave systems with $\xi^i_s = \begin{bmatrix} a^i_{s1} & a^i_{s2} + \lambda^i_s & 1 \end{bmatrix}$. The observer error dynamics of slave systems can be written as:

$$\begin{aligned} \dot{e}^i_{s1} &= -l^i_{s1} e^i_{s1} + e^i_{s2} \\ \dot{e}^i_{s2} &= \left(a^i_{s1} - l^i_{s2}\right) e^i_{s1} + a^i_{s2} e^i_{s2} + e^i_{s3} \\ e^i_{s3} &= -l^i_{s3} e^i_{s1} + \dot{f}^i_s \end{aligned} \tag{12.14}$$

where $i = 1, 2, ..., l$

The linearization of time-delay entities in Eq (12.13) leads to:

$$\begin{aligned}&\dot{s}_s^i = k_s^i s_s^i + b_s^i \sum_{j=1}^{k} r_{si}^j s_m^j - b_s^i \sum_{j=1}^{k} r_{si}^j T_{si}^j s_m^j + b_s^i \sum_{j=1}^{k} G_{si}^j F_{mi}^j + \xi_s^i e_s^i \\ &i = 1, 2, ..., l\end{aligned} \tag{12.15}$$

By stacking the composite slave systems in Eq (12.15), we obtain Eq (C.2). This can be written in compact form as:

$$\dot{s}_s = k_s s_s + b_{rs} s_m - b_{rsT} \dot{s}_m + b_{sG} F_m + \xi_s e_s \tag{12.16}$$

By augmenting closed loop slave composite systems in Eq (12.16) with observer error dynamics, we obtain:

$$\begin{bmatrix} \dot{s}_s \\ \dot{e}_s \end{bmatrix} = \begin{bmatrix} k_s & \xi_s \\ 0 & o_s \end{bmatrix} \begin{bmatrix} s_s \\ e_s \end{bmatrix} + \begin{bmatrix} b_{rs} & -b_{rsT} \\ 0 & 0 \end{bmatrix} \begin{bmatrix} s_m \\ \dot{s}_m \end{bmatrix} + \begin{bmatrix} b_{sG} \\ 0 \end{bmatrix} F_m + \begin{bmatrix} 0 \\ h_s \end{bmatrix} \dot{f}_s \tag{12.17}$$

The above system implies that observers for slave systems can be designed separately from controllers. To determine the observer gains for slave systems, the characteristic equation is compared with the desired polynomial. The convergence of observation error follows from the assumption of slowly varying lumped uncertainties.

$$p_s(s) : s^3 + (l_{s1}^i - a_{s2}^i) s^2 + (l_{s2}^i - a_{s1}^i - a_{s2}^i l_{s1}^i) s + l_{s3}^i = 0, i = 1, 2, ..., l \tag{12.18}$$

Now that observer design is performed separately for the master and slave systems, we can manipulate composite master and slave system without considering observation error terms for the purpose of designing control gains. To this end, we plug Eq (12.16) in Eq (12.9) and rearrange to obtain closed loop composite master systems as:

$$\dot{s}_m = (I - b_{rmT} b_{rsT})^{-1} \begin{bmatrix} (k_m - b_{rmT} b_{rs}) s_m \\ + (b_{rm} - b_{rmT} k_s) s_s \\ + (b_m - b_{rmT} b_{sG}) F_m \end{bmatrix} \tag{12.19}$$

We now plug Eq (12.9) in Eq (12.16) and do some algebraic manipulations to get:

$$\dot{s}_s = (I - b_{rmT} b_{rsT})^{-1} \begin{bmatrix} (k_s - b_{rsT} b_{rm}) s_s \\ + (b_{rs} - b_{rsT} k_m) s_m \\ + (b_{sG} - b_{rsT} b_m) F_m \end{bmatrix} \tag{12.20}$$

Let α contain the authority factors for the slave systems. Now, we introduce composite state convergence error as:

$$s_e = s_s - \alpha s_m \tag{12.21}$$

By taking time-derivative of composite state convergence error and using Eq (12.21), we obtain:

$$\begin{aligned}\dot{s}_e = &\begin{pmatrix} (I - b_{rmT}b_{rsT})^{-1}(k_s - b_{rsT}b_{rm}) \\ -\alpha (I - b_{rmT}b_{rsT})^{-1}(b_{rm} - b_{rmT}k_n) \end{pmatrix} s_e + \\ &\begin{pmatrix} (I - b_{rmI}b_{rsT})^{-1}(k_s - b_{rsT}b_{rm})\,\alpha \\ -\alpha (I - b_{rmT}b_{rsT})^{-1}(b_{rm} - b_{rmT}k_s)\,\alpha + \\ (I - b_{rmT}b_{rsT})^{-1}(b_{rs} - b_{rsT}k_m) \\ -\alpha (I - b_{rmT}b_{rsT})^{-1}(k_m - b_{rmT}b_{rs}) \end{pmatrix} s_m + \\ &\begin{pmatrix} (I - b_{rmT}b_{rsT})^{-1}(b_{sG} - b_{rsT}b_{mm}) \\ -\alpha (I - b_{rmT}b_{rsT})^{-1}(b_m - b_{rmT}b_{sG}) \end{pmatrix} F_m \end{aligned} \tag{12.22}$$

We now let the composite state convergence error to behave as an autonomous system. This leads to the following conditions:

$$\begin{aligned}&(I - b_{rmT}b_{rsT})^{-1}(k_s - b_{rsT}b_{rm})\,\alpha - \alpha (I - b_{rmT}b_{rsT})^{-1}(b_{rm} - b_{rmT}k_s)\,\alpha \\ &+ (I - b_{rmT}b_{rsT})^{-1}(b_{rs} - b_{rsT}k_m) - \alpha (I - b_{rmT}b_{rsT})^{-1}(k_m - b_{rmT}b_{rs}) = 0 \end{aligned} \tag{12.23}$$

$$(I - b_{rmT}b_{rsT})^{-1}(b_{sG} - b_{rsT}b_m) - \alpha (I - b_{rmT}b_{rsT})^{-1}(b_m - b_{rmT}b_{sG}) = 0 \tag{12.24}$$

We now write augmented system comprising of composite master and composite error systems as:

$$\begin{bmatrix} \dot{s}_m \\ \dot{s}_e \end{bmatrix} = \begin{bmatrix} a_{11} & a_{12} \\ a_{21} & a_{22} \end{bmatrix} \begin{bmatrix} s_m \\ s_e \end{bmatrix} + \begin{bmatrix} (I - b_{rmT}b_{rsT})^{-1}(b_m - b_{rmT}b_{sG}) \\ 0 \end{bmatrix} F_m \tag{12.25}$$

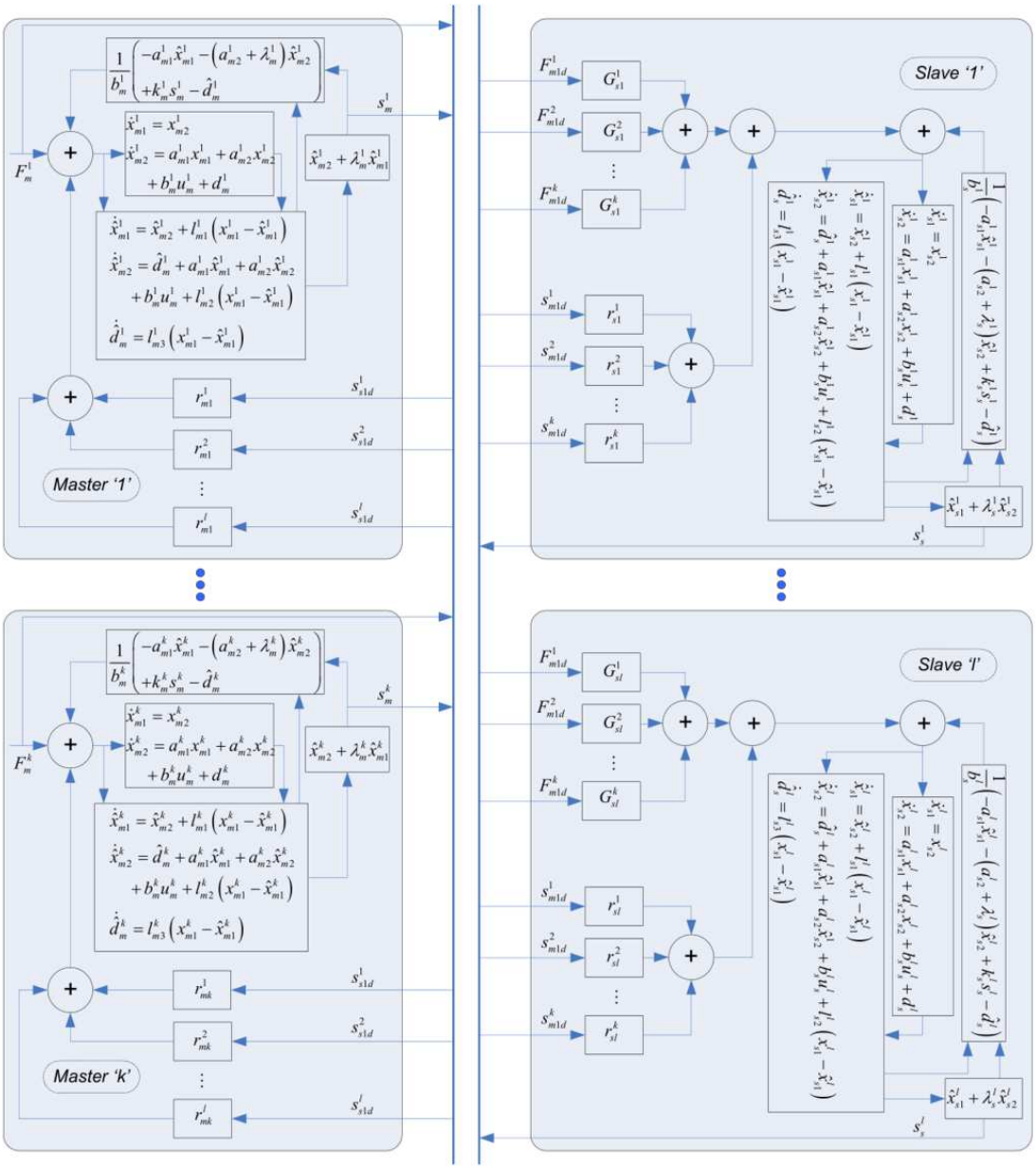

Figure 12.1: Detailed diagram of disturbance observer-based composite state convergence architecture

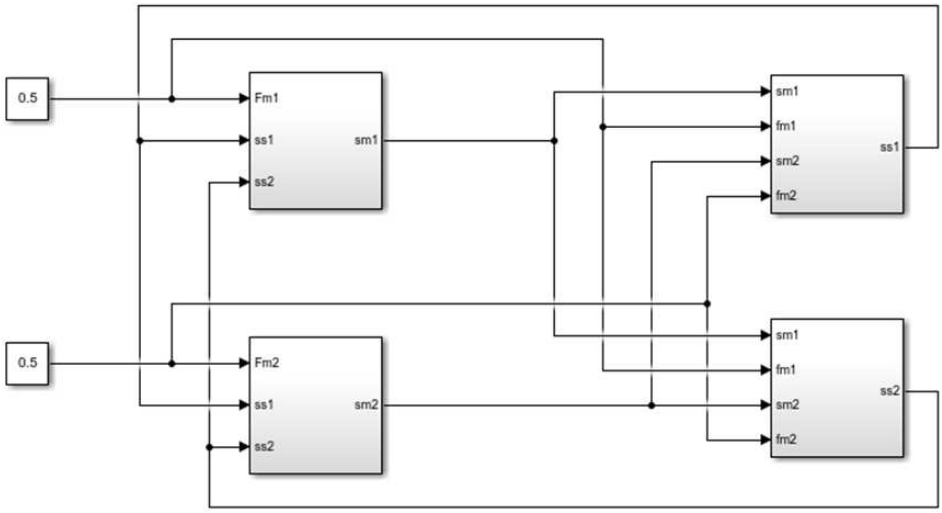

Figure 12.2: Wiring diagram of 2x2 composite state convergence architecture

where,

$$a_{11} = (I - b_{rmT}b_{rsT})^{-1}(k_m - b_{rmT}b_{rs} + b_{rm} - b_{rmT}k_s)$$
$$a_{12} = -(I - b_{rmT}b_{rsT})^{-1}(b_{rm} - b_{rmT}k_s)$$
$$a_{21} = 0$$
$$a_{22} = (I - b_{rmT}b_{rsT})^{-1}(k_s - b_{rsT}b_{rm}) - \alpha(I - b_{rmT}b_{rsT})^{-1}(b_{rm} - b_{rmT}k_s)$$

We now impose desired dynamic behavior onto this augmented system which results in the following additional design conditions:

$$(I - b_{rmT}b_{rsT})^{-1}(k_m - b_{rmT}b_{rs} + b_{rm} - b_{rmT}k_s) = -p \tag{12.26}$$

$$(I - b_{rmT}b_{rsT})^{-1}(k_s - b_{rsT}b_{rm}) - \alpha(I - b_{rmT}b_{rsT})^{-1}(b_{rm} - b_{rmT}k_s) = -q \tag{12.27}$$

The design conditions lead to the conclusion that composite errors converge to zero, implying that composite slave states converge to the weighted composite master states while their derivatives converge to zero. Based on this, we arrive at $x_{s2} + \lambda_s x_{s1} = \alpha(x_{m2} + \lambda_m x_{m1})$. In addition, closed loop analysis reveals that $x_{s2} + \lambda_s x_{s1} = \dot{s}_s, x_{m2} + \lambda_m x_{m1} = \dot{s}_m$. Therefore, velocity states converge to zero which implies $x_{s1} = \lambda_s^{-1}\alpha\lambda_m x_{m1}$. By assuming unity scaling factors, the convergence of slave positions to the weighted positions of master systems is ensured in the presence of uncertainties.

12.2 Simulation Results

The proposed enhanced composite state convergence scheme is simulated in MATLAB/Simulink environment on a 2x2 teleoperation system. The nominal parameters for the master and slave systems are given as:

$$\begin{aligned} a_m^1 &= \begin{bmatrix} 0 & 1 \\ 0 & -7.8572 \end{bmatrix}, b_m^1 = \begin{bmatrix} 0 \\ 0.3187 \end{bmatrix} \\ , a_m^2 &= \begin{bmatrix} 0 & 1 \\ 0 & -6.4286 \end{bmatrix}, b_m^2 = \begin{bmatrix} 0 \\ 0.2125 \end{bmatrix} \\ a_s^1 &= \begin{bmatrix} 0 & 1 \\ 0 & -7.500 \end{bmatrix}, b_s^1 = \begin{bmatrix} 0 \\ 0.3275 \end{bmatrix}, \\ a_s^2 &= \begin{bmatrix} 0 & 1 \\ 0 & -8.1250 \end{bmatrix}, b_s^2 = \begin{bmatrix} 0 \\ 0.3275 \end{bmatrix} \end{aligned} \tag{12.28}$$

In addition, slaves interact with environments having stiffness as $k_e^1 = k_e^1 = 20Nms/rad$. The closed loop poles of the augmented system are placed at $p = diag\,(2, 4)$, $q = diag\,(2, 10)$ and design conditions in Eq (12.23), Eq (12.24), Eq (12.26), Eq (12.27) are solved which yields the following controller and observer gains:

$$\begin{aligned} &g_{s1}^1 = 0.6813, g_{s1}^2 = 0.1947, g_{s2}^1 = 0.5840, g_{s2}^2 = 0.2595 \\ &k_m^1 = -4.6967, k_m^2 = -2.4294, k_s^1 = -1.4661, k_s^2 = -9.4077 \\ &r_{s1}^1 = -4.6281, r_{s1}^2 = 0.3438, r_{s2}^1 = 10.8245, r_{s2}^2 = 9.7045 \end{aligned} \tag{12.29}$$

$$\begin{aligned} L_{om}^1 &= \begin{bmatrix} 0.0082 & 0.2055 & 2.70 \end{bmatrix} \times 10^4, \\ L_{om}^2 &= \begin{bmatrix} 0.0084 & 0.2163 & 2.70 \end{bmatrix} \times 10^4 \\ L_{os}^1 &= \begin{bmatrix} 0.0083 & 0.2081 & 2.70 \end{bmatrix} \times 10^4, \\ L_{os}^2 &= \begin{bmatrix} 0.0082 & 0.2035 & 2.70 \end{bmatrix} \times 10^4 \end{aligned} \tag{12.30}$$

After computing the gains, we run simulations with the following plant parameters:

$$\begin{aligned} a_m^{1r} = a_m^{2r} &= \begin{bmatrix} 0 & 1 \\ 0 & -7.1429 \end{bmatrix}, b_m^{1r} = b_m^{2r} = \begin{bmatrix} 0 \\ 0.2656 \end{bmatrix} \\ a_s^{1r} = a_s^{2r} &= \begin{bmatrix} 0 & 1 \\ 0 & -6.25 \end{bmatrix}, b_s^{1r} = b_s^{2r} = \begin{bmatrix} 0 \\ 0.2729 \end{bmatrix} \end{aligned} \tag{12.31}$$

In Eq (12.31), superscript 'r' is added to denote real plant parameters, which differ up to 30% from the nominal parameters. The simulation results with constant operators' forces of 0.5N are depicted in Figure 12.3 and Figure 12.5. It can be seen that the composite reference is well-tracked by the composite slave systems, and the slave positions also converge to the composite reference, which is in line with the theoretical results.

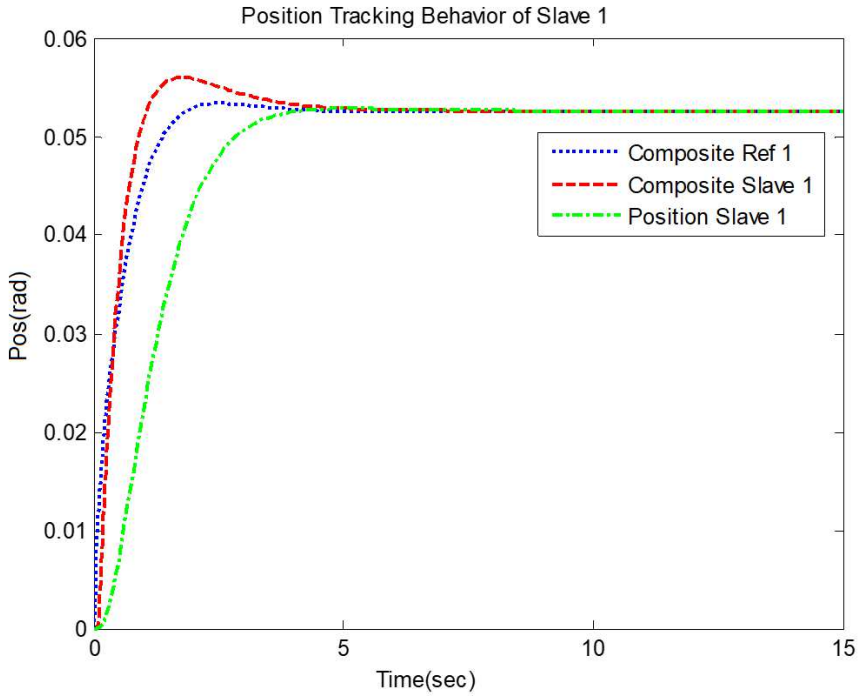

Figure 12.3: Reference tracking by first slave system

The proposed scheme is also compared with the existing composite state convergence scheme for the multilateral teleoperation system [110]. The existing composite state convergence scheme does not utilize disturbance observers. The same control gains are used to simulate both the proposed and existing schemes, while the former scheme employs observer gains as well. The uncertainty levels in the control input coefficients of both slaves are increased, and simulations are performed. The position tracking errors of the slaves are recorded in Figure 12.5 and Figure 12.6. It can be seen that the proposed scheme offers fast transient performance as compared to the existing scheme. In this way, the superiority of the proposed scheme is established over the existing one.

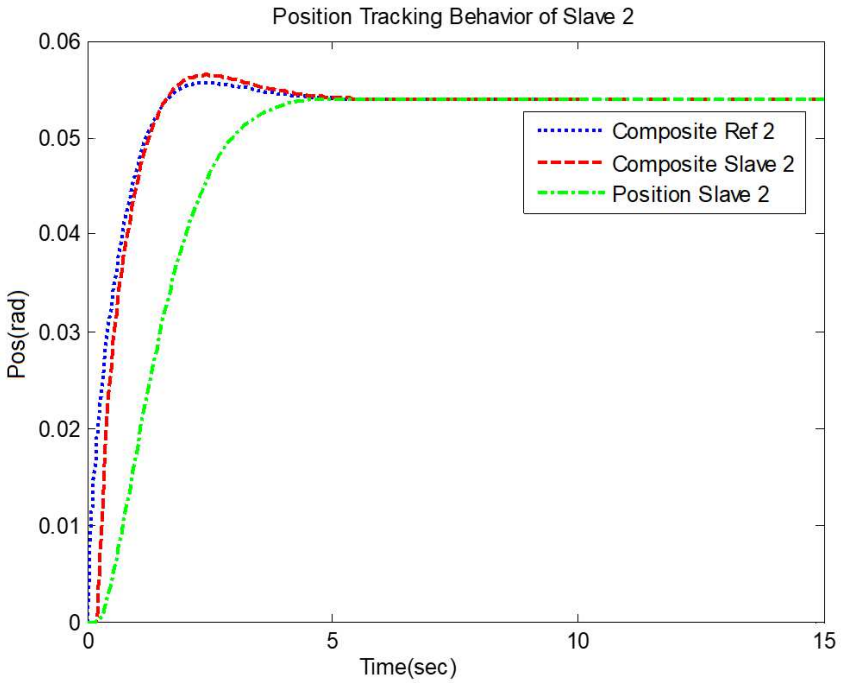

Figure 12.4: Reference tracking by second slave system

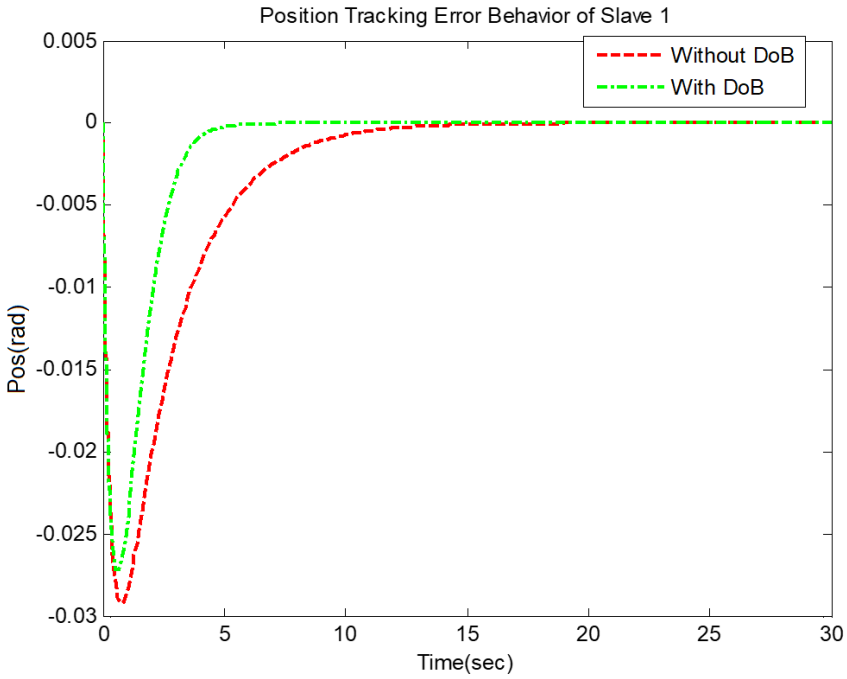

Figure 12.5: Tracking error for the first slave by the proposed and existing schemes

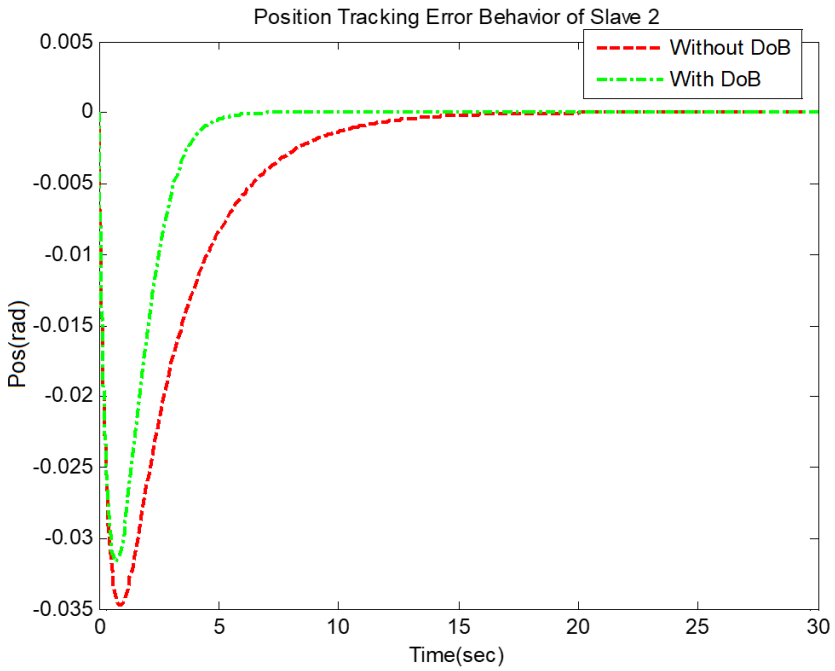

Figure 12.6: Tracking error for the second slave by the proposed and existing schemes

12.3 Experimental Results

The proposed scheme is verified through experimentation on three Qube servo-2 platforms which are arranged to form a 1x2 teleoperation system as shown in Figure 12.7. In order to determine controller and observer gains for the master and slave systems, the following nominal models are utilized:

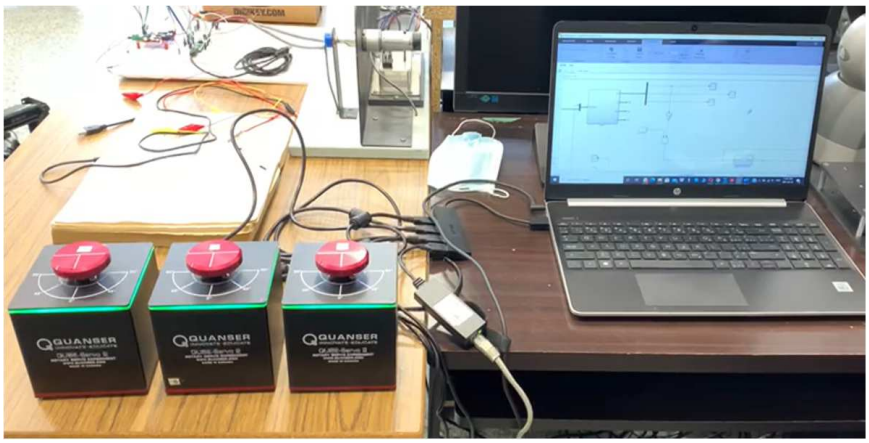

Figure 12.7: Experimental setup to test improved CSC architecture on multilateral teleoperation system

$$a_z^i = \begin{bmatrix} 0 & 1 \\ 0 & -6.67 \end{bmatrix}, b_z^i = \begin{bmatrix} 0 \\ 149.34 \end{bmatrix} \tag{12.32}$$

It is assumed that slaves are interacting with a soft environment having a stiffness of 1Nms/rad. It is further assumed that time delay between the master and first slave is 0.1s while it is 0.2s between the master and second slave. The closed loop poles are selected as $p = 27.4, q_1 = 10, q_2 = 40$ and design conditions are solved using MATLAB symbolic toolbox which yields the following control gains:

$$\begin{aligned} &k_m^1 = -180.025, k_s^1 = -8.445, k_s^2 = -17.938 \\ &G_{s1}^1 = 0.090, G_{s2}^1 = 0.1292 \\ &r_{s1}^1 = -0.0339, r_{s2}^1 = -0.0098 \end{aligned} \tag{12.33}$$

In order to compute the observer gains, we utilize the nominal models and place all the observer poles at 30 which yield the following master and slave observer gains:

$$L_{oz} = \begin{bmatrix} 0.0083 & 0.2144 & 2.70 \end{bmatrix} \times 10^4 \tag{12.34}$$

The teleoperation system is now set up in Simulink/QUARC environment such that the master system communicates its composite signal on the time-delayed channels to the two slave systems via two stream serves having IDs '0' ($udp://localhost:18000?peer='any'$) and '1' ($udp://localhost:18001?peer='any'$). In addition to the composite signal, the master system also sends the operator's force on the time-delayed channels to the slave systems via two stream serves to have IDs '2' ($udp://localhost:18002?peer='any'$) and '3' ($udp://localhost:18003?peer='any'$). In response, slave systems send their composite signals to the master system via stream clients having IDs '4' ($udp://localhost:18000$) and '6' ($udp://localhost:18001$). Slave systems also send force feedback to the master system using stream clients having IDs '5' ($udp://localhost:18002$) and '7' ($udp://localhost:18003$). The data received by stream servers is demultiplexed to read composite and force signals from the two slave systems. Two additional stream servers having IDs '10' ($udp://localhost:18004?peer='any'$) and '11' ($udp://localhost:18005?peer='any'$) are installed on the master side for the purpose of recording slave position signals. This also needs the deployment of two additional stream clients at the slave

sides with IDs '8' ($udp://localhost:18004$) and '9' ($udp://localhost:18005$).

During the experiment, the operator moves the master's servo-disk while slave-servo disks interact with their virtual environments. The operator starts experiencing a greater environmental force as he continues to increase the rotational angle of the servo disk. The experiment is run for 300 seconds, and the recorded results are displayed in Fig Figure 12.8 and Figure 12.9, Figure 12.10.

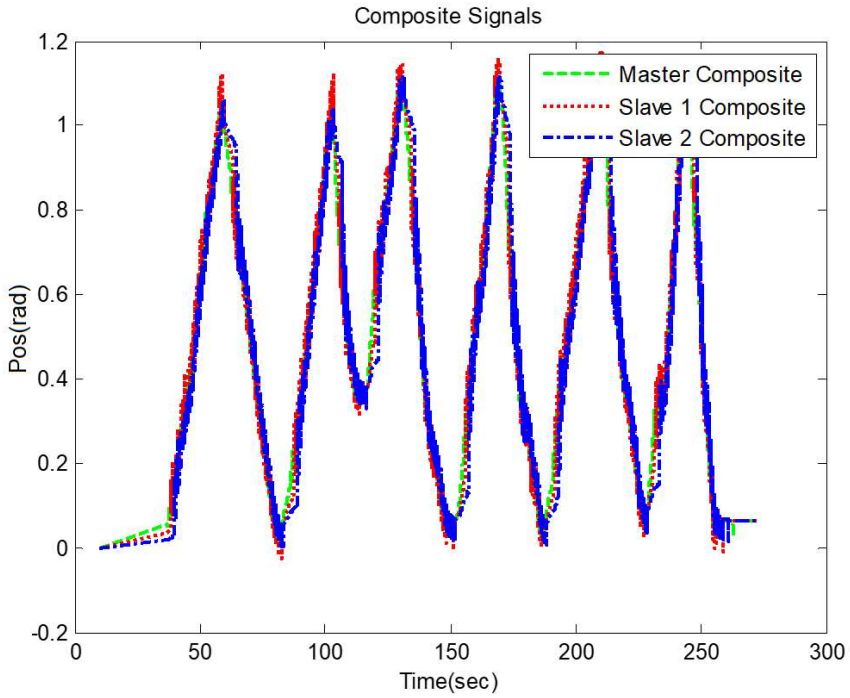

Figure 12.8: Composite states of 1x2 teleoperation system

It can be seen from Figure 12.8 that composite signals of the slave systems follow the master's composite signal. In theory, this should imply the convergence of position signals, which can be verified from Figure 12.9. In addition to position tracking, force reflection results in Figure 12.10 suggest that the proposed scheme can be used to design teleoperation systems.

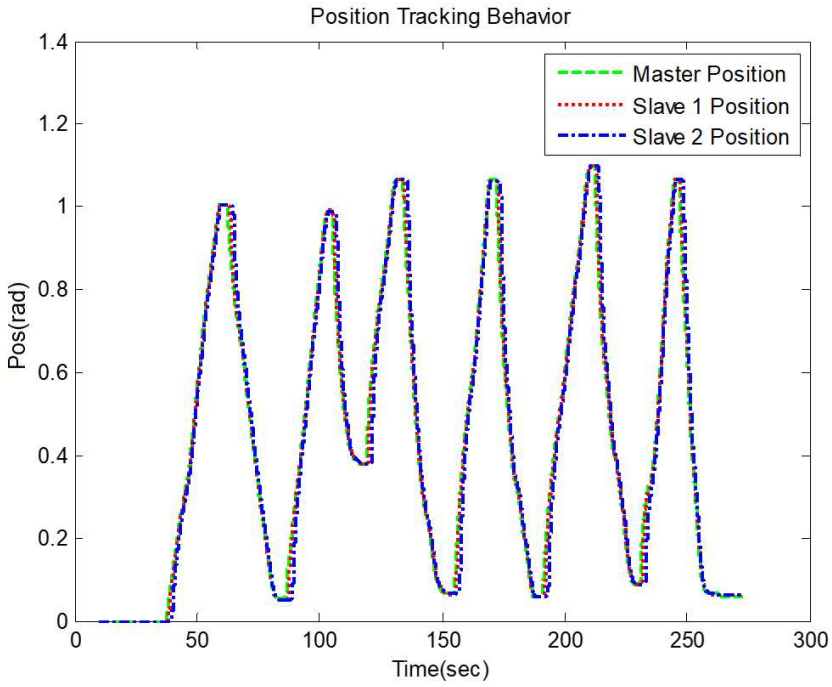

Figure 12.9: Position states of 1x2 teleoperation system

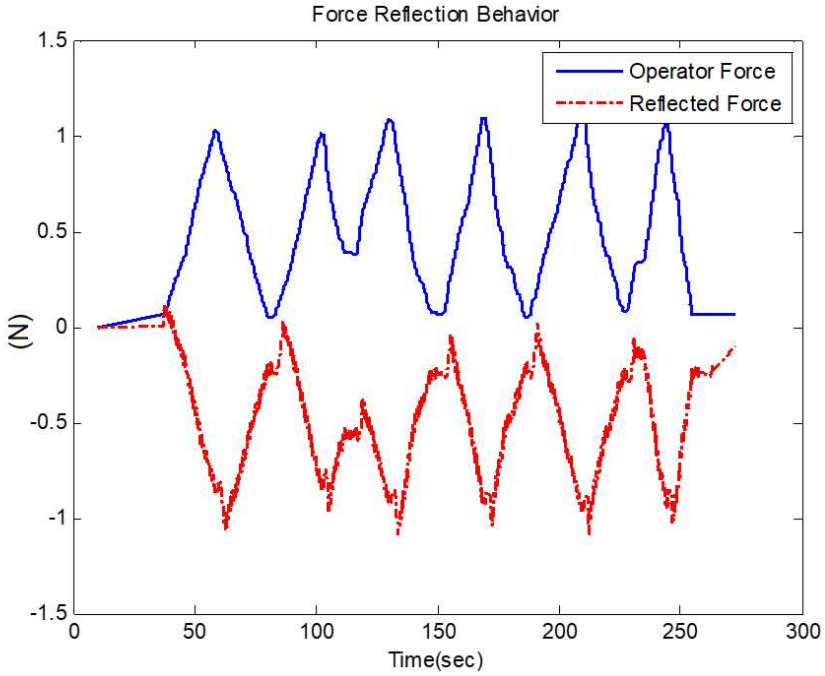

Figure 12.10: Force reflection behaviour of 1x2 teleoperation system

12.4 Conclusion

This chapter has proposed a disturbance observer-based scheme for controlling a multi-master, multi-slave teleoperation system through a composite state convergence methodology. At first, composite variables are constructed through estimated position and velocity states, and closed-loop composite master and composite slave systems are found. By augmenting the composite master and composite error systems and employing the method of state convergence, control gains, and observer gains are determined. The stability of the scheme is guaranteed under fixed-time delays. The proposed scheme is validated through simulations as well as experimentation in MATLAB/Simulink/QUARC environment by considering different arrangements of master and slave systems. Comparison with the existing scheme shows that the proposed scheme can indeed counter the effect of disturbances while ensuring the tracking of references by slave systems, which are set by the master systems. Future work involves designing force observers to eliminate the dependence of design procedures on environmental parameters.

Chapter 13

Conclusions and Future Work

13.1 Conclusions

This thesis presents modified versions of state convergence architecture for controlling bilateral and multilateral teleoperation systems. In addition, a novel composite state convergence architecture to reduce the complexity of existing state convergence architecture for both bilateral and multilateral teleoperation systems is presented. In the first part of the thesis, modifications in SC architecture have been proposed to address the shortcomings in the original SC architecture. The first modification is proposed to counter the effect of parametric uncertainties using disturbance observers. Secondly, a nonlinear disturbance observer is introduced to ensure large range operation of SC architecture based on TS fuzzy description of master and slave systems. The same extended state observer-based approach is used to develop state convergence architectures for multilateral teleoperation systems. The second part of the thesis discusses the novel composite state convergence scheme, which lowers the complexity by reducing the number of communication channels in the existing SC architecture for a bilateral teleoperation system. Furthermore, the CSC architecture is investigated with a feedback linearization scheme for non-linear bilateral teleoperation. Moreover, another enhancement is proposed in CSC architecture to counter parametric uncertainties through disturbance observers. The CSC architecture is also extended to a multilateral teleoperation framework with reduced communication channels to testify to its efficacy. In conclusion, the prominent features of the proposed control architectures are summarized in Table 13.1 based on certain criteria which include mainly the number of communication channels, variables transmitted over communication channels, number of design equations, model type, comparison with other architecture, the impact of time delay, position tracking behavior, state estimation and disturbance compensation, force reflection behavior, motion scaling feature, and extension to a multilateral teleoperation system. The comparison between the proposed architectures and their advantages and limitations is also stated in Table 13.1.

13.2 Future Work

1. In the future, potential research will be to estimate the parameters of the remote environments and consider those parameters in the control design. These parameters will be fed back to the master controller to improve a better contact sensation to the user in the presence of time delays. This approach to designing a controller will have direct access to the model of the remote environment rather than sending slave sensory data to the operator, which will eventually provide a better sense of telepresence for improved user feedback without any lag under communications delays.

2. There is a need to search for a new composite variable that could be transmitted over the communication channel to reduce the number of design variables. It will help in reducing the complexity of overall architecture.

3. There is room to update the method of state convergence with different safety limits keeping in view the workspace of manipulators for different applications.

4. Different variants of state convergence can be introduced to perform collaborative tasks such as multi-master/multi-slave (MM/MS) and single-master/multi-slave (SMMS).

5. Linear matrix inequalities (LMI) can be used to perform the stability analysis of the state convergence method for a multilateral teleoperation system.

6. Different optimization techniques can be used to compute the control gains for the state convergence method.

7. More rigorous analysis is required for the force-tracking behavior of the state convergence method.

Table 13.1: Proposed state convergence-based teleoperation control architectures during Ph.D.

Criteria	Enhanced SC Arch with Disturbance Observer	Improved SC Architecture with TS-Fuzzy Control	Composite SC Architecture	Composite SC Architecture for Nonlinear System	DoB-based Three-Channel Composite SC Architecture
Number of Comm channel	Five	Five	Three	Three	Three
Variables transmitted over Comm Channel	Operator's Force, Master Position, Master Velocity, Slave Position, Slave Velocity	Operator's Force, Master Position, Master Velocity, Slave Position, Slave Velocity	Operator's Force, Master Composite, Slave Composite	Operator's Force, Master Composite, Slave Composite	Operator's Force, Master Composite, Slave Composite
Number of Design equations	$5n + 3$	$3n + 1$	Four (independent of n)	Four (independent of n)	$5n + 3$
Model Type	n^{th} order SISO nonlinear system	n^{th} order SISO nonlinear system	n^{th} order SISO linear system	n^{th} order SISO nonlinear system	n^{th} order SISO nonlinear system
Comparison With Other Architectures	Radial basis function Neural Network (RBFNN) controller	No Fuzzy PDC with DOB technique exists with desired dynamic feature	Three-Channel Error Force Compensated (EFC) Control Scheme	Comparison is not carried out in this study	Genetically Optimized PD Based Error Force Compensated (EFC-PD) Controller
Impact of Time Delay	System is stable under small constant time delay by virtue of pole assignment	System is stable under small constant time delay by virtue of pole assignment	System is stable under small constant time delay by virtue of pole assignment	System is stable under small constant time delay by virtue of pole assignment	System is stable under small constant time delay by virtue of pole assignment

Criteria	Enhanced SC Arch with Disturbance Observer	Improved SC Architecture with TS-Fuzzy Control	Composite SC Architecture	Composite SC Architecture for Nonlinear System	DoB-based Three-Channel Composite SC Architecture
Position tracking behavior	Position tracking is established under constant operator's force	Position tracking is established under constant operator's force	Position tracking is established under constant operator's force	Position tracking is established under constant operator's force	Position tracking is established under constant operator's force
State Estimation and Disturbance Compensation	ESO is used to estimate the states and compensate for the disturbances on the master and slave sides	Nonlinear Disturbance Observer is used to estimate the states and compensate the disturbances on the master and slave sides	State estimators and disturbance compensators are not deployed	State estimators and disturbance compensators are not deployed	ESO is used to estimate the states and compensate the disturbances on the master and slave sides
Force Reflection behavior	Reaction force is displayed to the operator through a haptic device	Reaction force is displayed to the operator through a haptic device	Reaction force is displayed to the operator through a haptic device	Reaction force is displayed to the operator through a haptic device	Reaction force is displayed to the operator through a haptic device
Motion Scaling	Motion Scaling feature is not available	Motion Scaling feature is not available	Motion Scaling feature is available	Motion Scaling feature is available	Motion Scaling feature is not available

Criteria	Enhanced SC Arch with Disturbance Observer	Improved SC Architecture with TS-Fuzzy Control	Composite SC Architecture	Composite SC Architecture for Nonlinear System	DoB-based Three-Channel Composite SC Architecture
Extension to Multilateral System	Extension to multiple systems is carried out	Extension to multiple systems is not carried out	Extension to multiple systems is carried out	Extension to multiple systems is not carried out	Extension to multiple systems is carried out

Appendix A

State Convergence Design Equations

The solution of design conditions Eq (6.28) - Eq (6.31) yields the following control gains:

$$G_2 = \frac{b_m\left(Tq+1\right)}{b_s\left(Tp+2Tb_mr_m+T^2b_mpr_m+T^2b_mqr_m+1\right)} \tag{A.1}$$

$$k_m = -p - b_mr_m - Tpb_mr_m \tag{A.2}$$

$$k_s = \frac{-b_mpqr_mT^2 - pqT - q + b_mr_m}{Tp+2Tb_mr_m+T^2pb_mr_m+T^2qb_mr_m+1} \tag{A.3}$$

$$r_s = \frac{-p+q-b_mr_m-Tpb_mr_m}{b_s+Tpb_s+2Tb_sb_mr_m+T^2pb_sb_mr_m+T^2qb_sb_mr_m} \tag{A.4}$$

Appendix B

Stability of 2x2 and 1x3 Teleoperation Systems

Proposition 1 :

The closed loop composite master-error system of Eq (11.17) under the control gains found as a solution of Eq (11.19), Eq (11.20) is Hurwitz-stable if and only if there exists a symmetric positive definite matrix $P \in R^{(k+l)\times(k+l)}$ such that

$$\begin{bmatrix} P_{11} & P_{12} \\ P_{12}^T & P_{22} \end{bmatrix} > 0$$
$$\begin{bmatrix} \tilde{A}_{11} & \tilde{A}_{12} \\ \tilde{A}_{21} & \tilde{A}_{22} \end{bmatrix}^T \begin{bmatrix} P_{11} & P_{12} \\ P_{12}^T & P_{22} \end{bmatrix} + \begin{bmatrix} P_{11} & P_{12} \\ P_{12}^T & P_{22} \end{bmatrix}^T \begin{bmatrix} \tilde{A}_{11} & \tilde{A}_{12} \\ \tilde{A}_{21} & \tilde{A}_{22} \end{bmatrix} < 0 \tag{B.1}$$

The Hurwitz stability of composite master-error system Eq (11.17) implies the stability of master-error system as closed loop analysis yields$\dot{s}_z = \dot{x}_{z2} + \lambda_z x_{z2}\,(z = m, s)$. Therefore, the teleoperation system with small constant time delays of the communication channel remains stable as long as Eq (B.1) is satisfied.

We will investigate the stability of 2x2 and 1x3 teleoperation systems through the application of Eq (B.1) in section 11.3. By plugging the control gains of Eq (11.21) in Eq (11.17) and considering time delays, the system matrix of a composite master-error system of 2x2 teleoperation setup is obtained as:

$$[A = \begin{bmatrix} -8.1069 & 0.2066 & 0.7583 & 1.5217 \\ 3.0295 & -2.1322 & 0.8564 & 0.8796 \\ -12.9114 & 0.7136 & -3.4446 & 0.5139 \\ -5.0248 & 2.1746 & -1.6064 & -11.5093 \end{bmatrix} \tag{B.2}$$

The feasibility of LMI in Eq (B.1) yields the following symmetric positive definite matrix, which establishes the stability of a closed-loop teleoperation system:

$$P = \begin{bmatrix} 0.3062 & 0.0150 & -0.1533 & 0.0186 \\ 0.0150 & 0.3529 & 0.0575 & 0.0367 \\ -0.1533 & 0.0575 & 0.1693 & -0.0096 \\ 0.0186 & 0.0367 & -0.0096 & 0.0531 \end{bmatrix} \tag{B.3}$$

Now, let us analyze the stability of the 1x3 teleoperation setup. By substituting Eq (11.21) and time delay values in Eq (11.17), following system matrix is obtained:

$$A = \begin{bmatrix} -1.6160 & 0.5751 & 1.1244 & 3.0831 \\ 0.6857 & -6.5578 & -1.5904 & -4.3608 \\ 0.4994 & -0.7471 & -5.0551 & -4.0054 \\ 2.4295 & -1.4340 & -2.8037 & -16.7554 \end{bmatrix} \tag{B.4}$$

The solution of LMI in (B.1) yields the following symmetric positive definite matrix, and hence stability is verified under small time delays:

$$P = \begin{bmatrix} 0.5292 & 0.0215 & 0.0528 & 0.0799 \\ 0.0215 & 0.0908 & -0.0119 & -0.0132 \\ 0.0528 & -0.0119 & 0.1378 & -0.0182 \\ 0.0799 & -0.0132 & -0.0182 & 0.0544 \end{bmatrix} \tag{B.5}$$

Appendix C

Composite Master and Slave Systems for Multilateral Teleoperation Systems

$$
\begin{bmatrix} \dot{s}_m^1 \\ \dot{s}_m^2 \\ \vdots \\ \dot{s}_m^k \end{bmatrix} = \begin{bmatrix} k_m^1 & 0 & \cdots & 0 \\ 0 & k_m^2 & \cdots & 0 \\ & \vdots & & \\ 0 & 0 & \cdots & k_m^k \end{bmatrix} \begin{bmatrix} s_m^1 \\ s_m^2 \\ \vdots \\ s_m^k \end{bmatrix} + \begin{bmatrix} b_m^1 r_{m1}^1 & b_m^1 r_{m1}^2 & \cdots & b_m^1 r_{m1}^l \\ b_m^2 r_{m2}^1 & b_m^2 r_{m2}^2 & \cdots & b_m^2 r_{m2}^l \\ & \vdots & & \\ b_m^k r_{mk}^1 & b_m^k r_{mk}^2 & \cdots & b_m^k r_{mk}^l \end{bmatrix}
$$
$$
\begin{bmatrix} s_s^1 \\ s_s^2 \\ \vdots \\ s_s^l \end{bmatrix} - \begin{bmatrix} b_m^1 r_{m1}^1 T_{m1}^1 & b_m^1 r_{m1}^2 T_{m1}^2 & \cdots & b_m^1 r_{m1}^l T_{m1}^l \\ b_m^2 r_{m2}^1 T_{m2}^1 & b_m^2 r_{m2}^2 T_{m2}^2 & \cdots & b_m^2 r_{m2}^l T_{m2}^l \\ & \vdots & & \\ b_m^k r_{mk}^1 T_{mk}^1 & b_m^k r_{mk}^2 T_{mk}^1 & \cdots & b_m^k r_{mk}^l T_{mk}^l \end{bmatrix} \begin{bmatrix} \dot{s}_s^1 \\ \dot{s}_s^2 \\ \vdots \\ \dot{s}_s^l \end{bmatrix} + \tag{C.1}
$$
$$
\begin{bmatrix} b_m^1 & 0 & \cdots & 0 \\ 0 & b_m^2 & \cdots & 0 \\ & \vdots & & \\ 0 & 0 & \cdots & b_m^k \end{bmatrix} \begin{bmatrix} F_m^1 \\ F_m^2 \\ \vdots \\ F_m^k \end{bmatrix} + \begin{bmatrix} \xi_m^1 & 0 & \cdots & 0 \\ 0 & \xi_m^2 & \cdots & 0 \\ & \vdots & & \\ 0 & 0 & \cdots & \xi_m^k \end{bmatrix} \begin{bmatrix} e_m^1 \\ e_m^2 \\ \vdots \\ e_m^k \end{bmatrix}
$$

$$
\begin{bmatrix} \dot{s}_s^1 \\ \dot{s}_s^2 \\ \vdots \\ \dot{s}_s^l \end{bmatrix} = \begin{bmatrix} k_s^1 & 0 & \cdots & 0 \\ 0 & k_s^2 & \cdots & 0 \\ & \vdots & & \\ 0 & 0 & \cdots & k_s^l \end{bmatrix} \begin{bmatrix} s_s^1 \\ s_s^2 \\ \vdots \\ s_s^l \end{bmatrix} + \begin{bmatrix} b_s^1 r_{s1}^1 & b_s^1 r_{s1}^2 & \cdots & b_s^1 r_{s1}^k \\ b_s^2 r_{s2}^1 & b_s^2 r_{s2}^2 & \cdots & b_s^2 r_{s2}^k \\ & \vdots & & \\ b_s^l r_{sl}^1 & b_s^l r_{sl}^2 & \cdots & b_s^l r_{sl}^l \end{bmatrix}
$$
$$
\begin{bmatrix} s_m^1 \\ s_m^2 \\ \vdots \\ s_m^k \end{bmatrix} - \begin{bmatrix} b_s^1 r_{s1}^1 T_{s1}^1 & b_s^1 r_{s1}^2 T_{s1}^2 & \cdots & b_s^1 r_{s1}^k T_{s1}^k \\ b_s^2 r_{s2}^1 T_{s2}^1 & b_s^2 r_{s2}^2 T_{s2}^2 & \cdots & b_s^2 r_{s2}^k T_{s2}^k \\ & \vdots & & \\ b_s^l r_{sl}^1 T_{sl}^1 & b_s^l r_{sl}^2 T_{sl}^2 & \cdots & b_s^l r_{sl}^l T_{sl}^k \end{bmatrix} \begin{bmatrix} \dot{s}_m^1 \\ \dot{s}_m^2 \\ \vdots \\ \dot{s}_m^k \end{bmatrix} \tag{C.2}
$$
$$
+ \begin{bmatrix} b_s^1 G_{s1}^1 & b_s^1 G_{s1}^2 & \cdots & b_s^1 G_{s1}^k \\ b_s^2 G_{s2}^1 & b_s^2 G_{s2}^2 & \cdots & b_s^2 G_{s2}^k \\ & \vdots & & \\ b_s^l G_{sl}^1 & b_s^l G_{sl}^2 & \cdots & b_s^l G_{sl}^l \end{bmatrix} \begin{bmatrix} F_m^1 \\ F_m^2 \\ \vdots \\ F_m^k \end{bmatrix} + \begin{bmatrix} \xi_s^1 & 0 & \cdots & 0 \\ 0 & \xi_s^2 & \cdots & 0 \\ & \vdots & & \\ 0 & 0 & \cdots & \xi_s^k \end{bmatrix} \begin{bmatrix} e_s^1 \\ e_s^2 \\ \vdots \\ e_s^k \end{bmatrix}
$$

Appendix D

Author's Publications

Journal Publications

1. **M. U. Asad**, J. Gu, U. Farooq, Rajeeb Dey, Nabanita Adhikary, Rupak Datta and Chunqi Chang. Disturbance observer-based extended state convergence architecture for multilateral teleoperation system. ***International Journal of Robotics and Automation***, Vol. 37, No. 6, ACTA PRESS, Canada, 2023. **(IF: 1.042)** doi: 10.2316/J.2023.206-0712

2. **M. U. Asad**, J. Gu, U. Farooq, V. E. Balas, M. Balas, and G. Abbas. An improved composite state convergence scheme with disturbance compensation for multilateral teleoperation systems. ***Studies in Informatics and Control***, vol 31, pages 43–52, ICI Bucharest, 2022. **(IF: 1.649)** doi: 10.24846/v31i3y202204

3. **M. U. Asad**, J. Gu, U. Farooq, M. Balas, Z. Chen, K. K. Qureshi, G. Abbas, and C. Chang. Disturbance observer-supported fuzzy-model-based controller with application to bilateral teleoperation systems. ***Journal of Intelligent and Fuzzy Systems***, vol 43, pages 1911–1919. IOS Press, 2022. **(IF: 1.737)** doi: 10.3233/JIFS-219292

4. **M. U. Asad**, J. Gu, U. Farooq, R. Dey, V. E. Balas, and G. Abbas. Intelligent obstacle avoidance controller for qbot2. In 7th International Conference on Advances in Control and Optimization of Dynamical Systems (ACODS), ***ELSEVIER-IFAC-PapersOnLine***, vol 55, pages 120–125. 2022. **(IF: 1.132)** doi: 10.1016/j.ifacol.2022.04.020

5. **M. U. Asad**, J. Gu, U. Farooq, R. Dey, and V. E. Balas. Teleoperation of multi-degrees-of-freedom manipulator through composite state convergence scheme. In 7th International Conference on Advances in Control and Optimization of Dynamical Systems (ACODS), ***ELSEVIER-IFAC-PapersOnLine***, vol 55, pages 126–130. , 2022. **(IF: 1.132)** doi: 10.1016/j.ifacol.2022.04.021

6. **M. U. Asad**, J. Gu, U. Farooq, V. E. Balas, Z. Chen, C. Chang, and A. Hanif. Disturbance observer supported three-channel state convergence architecture for bilateral teleoperation systems. ***International Journal of Robotics and Automation***. ACTAPRESS Canada, 2021. **(IF: 1.042)** doi: 10.2316/J.2021.206-0411

7. **M. U. Asad**, J. Gu, U. Farooq, V. E. Balas, Z. Chen, C. Chang, and A. Hanif. A composite state convergence scheme for multilateral teleoperation systems. ***Studies in Informatics and Control***, vol 30, pages 33–42. ICI Bucharest, 2021. **(IF: 1.649)**. doi: 10.24846/v30i2y202103

8. **M. U. Asad**, U. Farooq, J. Gu, R. Liu, and V. E. Balas. A composite state convergence scheme for bilateral teleoperation systems. ***IEEE/CAA Journal of Automatica Sinica***, vol 6, pages 1166–1178. IEEE, 2019. **(IF: 11.80)**. doi: 10.1109/JAS.2019.1911690

9. **M. U. Asad**, U. Farooq, J. Gu, V. E. Balas, and M. Balas. Design of a Composite State Convergence Controller for a Nonlinear Telerobotic System. ***Acta Polytechnica Hungarica***, vol 16, pages 157–172. Obuda University, 2019. **(IF :1.806)** doi: 10.12700/APH.16.10.2019.10.10

10. **M. U. Asad**, U. Farooq, J. Gu, V. E. Balas, G. Abbas, M. Balas, and V. Muresan. An enhanced state convergence architecture incorporating disturbance observer for bilateral teleoperation systems. ***International Journal of Advanced Robotic Systems***, volume 16. SAGE Publications, 2019. **(IF: 1.714)** doi: 10.1177/17298814198800

11. R. Datta, R. Dey, N. Adhikari, **M. U. Asad**, and U. Farooq. H_∞ control for T–S fuzzy system via delayed state feedback: Application to two-link robotic system. In 7th International Conference on Advances in Control and Optimization of Dynamical Systems (ACODS), ***ELSEVIER-IFAC-PapersOnLine***, vol 55, pages 777–782. 2022. **(IF: 1.132)** doi: 10.1016/j.ifacol.2022.04.127

12. K. Cherfouh, J. Gu, U. Farooq, **M. U. Asad**, R. Dey, and V. E. Balas. Bilateral teleoperation control of a bipedal robot gait using a manipulator. In 7th International Conference on Advances in Control and Optimization of Dynamical Systems (ACODS), ***ELSEVIER-IFAC-PapersOnLine***, vol 55, pages 765–770. 2022. **(IF: 1.132)**. doi: 10.1016/j.ifacol.2022.04.125

13. M. Sabih, M. Umer, U. Farooq, J. Gu, M. Balas, **M. U. Asad**, K. K. Qureshi, I. A. Khan, G. Abbas. Image Processing Based Fault Classification in Power Systems with Classical and Intelligent Techniques. ***Journal of Intelligent and Fuzzy Systems***, vol 43, no. 2, page 1921 – 1932, IOS Press, 2022. **(IF: 1.737)** doi: 10.3233/JIFS-219293

14. G. Abbas,**M. U. Asad**, J. Gu, S. Alelyani, V. E. Balas, M. R. Hussain, U. Farooq, A. B. Awan, A. Raza, and C. Chang. Multivariable Unconstrained Pattern Search Method for Optimizing Digital PID Controllers Applied to Isolated Forward Converter. ***Energies***, vol 14, no. 1, page 77, 2021. **(IF: 3.004)**. doi: 10.3390/en14010077

15. U. Farooq, J. Gu, **M. U. Asad**, G. Abbas, and A. Hanif. Online identification of nonlinear systems using neo-fuzzy supported brain emotional learning network. ***Journal of Intelligent and Fuzzy Systems***, vol 38, page 6045–6051. IOS Press, 2020. **(IF: 1.737)** doi: 10.3233/JIFS-179689

16. U. Farooq, J. Gu, V. E. Balas, G. Abbas, **M. U. Asad**, and M. Balas. A hybrid time series forecasting model for disturbance storm time index using a competitive brain emotional neural network and neo-fuzzy neurons.***Acta Polytechnica Hungarica***, vol 16, pages 213–229. Obuda University, 2019. **(IF: 1.806)**. doi: 10.12700/APH.16.4.2019.4.11

17. A. Naveed, T. Izhar, G. Abbas, V. E. Balas, M. M. Balas, T. Lin, **M. U. Asad**, U. Farooq, and J. Gu. A Single-Phase Buck and Boost AC-to-AC Converter with Bipolar Voltage Gain: Analysis, Design, and Implementation. ***Energies, MDPI*** vol 12, no. 7, page 1376, 2019. **(IF: 3.004)**.doi: 10.3390/en12071376

18. T. Umair, G. Abbas, D. O. Glavan, V. E. Balas, U. Farooq, M. M. Balas, A. Raza, **M. U. Asad**, and J. Gu. Design of Three Phase Solid State Transformer Deployed within Multi-Stage Power Switching Converters. ***Applied Sciences, MDPI***, vol 9, no. 17, page 3545, 2019. **(IF: 2.679)** doi: 10.3390/app9173545

19. M. A. Shahid, G. Abbas, M. R. Hussain, **M. U. Asad**, U.Farooq, J. Gu, V. E. Balas, M. Uzair, A. B. Awan, and T. Yazdan. Artificial Intelligence-Based Controller for DC-DC Flyback Converter. ***Applied Sciences, MDPI***, vol 9, no. 23, page 5108, 2019. **(IF: 2.679)** doi: 10.3390/app9235108

20. G. Abbas, M. Q. Nazeer, V. E. Balas, T. Lin, M. M. Balas, **M. U. Asad**, A.

Raza, M. N. Shehzad, U. Farooq, and J. Gu. Derivative-Free Direct Search Optimization Method for Enhancing Performance of Analytical Design Approach-Based Digital Controller for Switching Regulator. ***Energies, MDPI***, vol 12, no. 11, page 2183, 2019. **(IF: 3.004)**. doi: 10.3390/en12112183

21. U. Farooq, **M. U. Asad**, J. Gu, G. Abbas, and V. E. Balas and. Design of a single-master/multi-slave nonlinear teleoperation system through state convergence with time-varying delay. ***Acta Polytechnica Hungarica***, vol 15, pages 55–82. Obuda University, 2018. **(IF: 1.806)** doi: 10.12700/APH.15.8.2018.8.3

22. U. Farooq, J. Gu, M. El-Hawary, **M. U. Asad**, G. Abbas, and J. Luo. A time-delayed multi-master-single-slave non-linear tele-robotic system through state convergence. ***IEEE Access***, vol 6, pages 5447–5459. IEEE, 2018. **(IF: 3.367)** doi: 10.1109/ACCESS.2017.2782178

23. G. Abbas, J. Gu, U. Farooq, M. I. Abid, A. Raza, **M. U. Asad**, V. E. Balas, and M. E. Balas. 2018. Optimized Digital Controllers for Switching-Mode DC-DC Step-Down Converter. ***Electronics, MDPI***, vol 7, no. 12, page 412, 2018. **(IF: 2.690)** doi: 10.3390/electronics7120412

Conference Publications

1. **M. U. Asad**, K. Qureshi, J. Gu, V. E. Balas, and U. Farooq. LMI-based stability analysis of state convergence architecture for bilateral teleoperation systems. In ***IEEE Canadian Conference on Electrical and Computer Engineering (CCECE)***, vol 55, pages 130–140. IEEE, 2022. doi: 10.1109/CCECE49351.2022.9918395

2. X. Zhang, J. Gu, **M. U. Asad**, U. Farooq, and G. Abbas. Beetle bee algorithm applied to trajectory tracking control of omni manipulator. In ***International Conference on Emerging Trends in Electrical, Control, and Telecomm Engineering (ETECTE)***, pages 1–5. IEEE, 2022. doi: 10.1109/ETECTE55893.2022.10007292

3. K. Cherfouh, J. Gu, U. Farooq, **M. U. Asad**, R. Dey, N. Adhikari, and C. Chang. Performance comparison between higher-order sliding mode and fixed boundary layer sliding mode controller for a 10-dof bipedal robot. In Communication and Control for Robotic Systems. Smart Innovation, Systems and Technologies, ***Springer***, vol 229, pages 45–62. Singapore, 2021. Book Chapter

4. N. Adhikary, R. Dey, **M. U. Asad**, J. Gu, U. Farooq, and R. Dutta. Adaptive robust control of tele-operated master-slave manipulators with communication delay. In Communication and Control for Robotic Systems. Smart Innovation, Systems and Technologies, ***Springer*** volume 229, page 123–140, Singapore, 2021. Book Chapter

5. A. Ali, A. Amjad, **M. U. Asad**, J. Gu, G Abaas, U. Farooq, V. E. Balas. Fuzzy Logic Based Control of Higher Order Dual Output Buck Converter, 9^{th} International Workshop on Soft Computing Applications, ***(SOFA)*** 27-29 NOV-2020 Arad, Romania.

6. K. Cherfouh, J. Gu, **M. U. Asad** and U. Farooq. Control of Robotic Manipulator using Optimized Neural Networks. 9^{th} International Workshop on Soft Computing Applications, ***(SOFA)*** 27-29 NOV-2020 Arad, Romania.

7. K. Cherfouh, E. W. Handerson, J. Gu, E. Scheme, M. U. Asad and U. Farooq. Robot Identification Using Modern Pattern Recognition Techniques. 9^{th} International Workshop on Soft Computing Applications, ***(SOFA)*** 27-29 NOV-2020 Arad, Romania.

8. A. Haroon, U. Farooq, J. Gu, A. Rahim, H. Siddique, I. Maryyam, K. K. Qureshi, **M. U. Asad**. Enhanced Functionality of Footing Machine through Deep Learning. 9^{th} International Workshop on Soft Computing Applications, ***(SOFA)*** 27-29 NOV-2020 Arad, Romania.

9. **M. U. Asad**, J. Gu, U. Farooq, and M. Balas V. E. Balas. Design of dual-master-dual-slave teleoperation system through state convergence. In ***IEEE 23rd International Conference on Intelligent Engineering Systems (INES)***, pages 000313–000318. IEEE, 2019.
doi: 10.1109/INES46365.2019.9109471

10. **M. U. Asad**, J. Gu, U. Farooq, R. Liu, V. E. Balas, and M. Balas. State convergence-based design of a single-master-multi-slave nonlinear teleoperation system. In ***IEEE 14th International Conference on Control and Automation (ICCA)***, pages 186–191. IEEE, 2018.
doi: 10.1109/ICCA.2018.8444228

Awards/Achievements During Ph.D.

1. Oral Award Third Prize in ***Electrical and Computer Engineering Graduate Conference, (ECEGC)*** 2018, Halifax, NS, Canada

2. Best Paper (Theory) Award in ***International Symposium of Control, Communication and Embedded System for Robotics (SOCCER)***, NIT Silchar, Assam, India, 2020.

3. Best Presenter Award in ***International Symposium of Control, Communication and Embedded System for Robotics (SOCCER)***, NIT Silchar, Assam, India, 2020.

4. Best Paper Award in ***Ninth International Workshop on Soft Computing Applications (SOFA)***, Arad, Romania, 2020.

5. Peer Oral Award Second Prize in ***Electrical and Computer Engineering Graduate Conference, (ECEGC)*** 2022, Halifax, NS, Canada

6. Became ***Engineer-in-Training (EIT)*** in the Province of Nova Scotia, Canada in April 2021.

7. Became ***Professional Engineer (P.Eng)*** in the Province of Nova Scotia, Canada in April 2023.

8. Elevation to the grade of ***IEEE Senior Member, USA*** on June 2023.

Bibliography

[1] C. Liu A. Albakri and P. Poignet. Stability and performance analysis of three-channel teleoperation control architectures for medical applications. In *Proc. IEEE/RSJ Int. Conf. Intell. Robot. and Syst.*, pages 456–462. IEEE, 2013.

[2] R. V. Patel M. Moallem A. Aziminejad, M. Tavakoli. Transparent time-delayed bilateral teleoperation using wave variables. *IEEE Transactions on Control Systems Technology*, 16(3):548–555, 2008.

[3] K. Razi A. Haddadi and K. Hashtrudi-Zaad. Operator dynamics consideration for less conservative coupled stability condition in bilateral teleoperation. *IEEE/ASME Transactions on Mechatronics*, 20(5):2463–2475, 2015.

[4] J. Amat A. Hernansanz and A. Casals. Virtual robot: A new teleoperation paradigm for minimally invasive robotic surgery. In *Proc. 4th IEEE RAS EMBS International Conference on Biomedical Robotics and Biomechatronics (BioRob), Rome*, pages 749–754. IEEE, 2012.

[5] B. Alvarez C. Fernandez J. M. F. Merono A. Iborra, J. A. Pastor. Robots in radioactive environments. *IEEE Robotics and Automation Magazine*, 10(4):12–22, 2003.

[6] P. J. Navarro J. M. Fernandez J. A. Pastor-Franco A. Iborra, B. Alvarez. Passive four-channel multilateral shared control architecture in teleoperationrobotized system for retrieving fallen objects within the reactor vessel of a nuclear power plant (pwr). In *Proc. IEEE Intl. Symposium on Industrial Electronics*, pages 529–534. IEEE, 2000.

[7] J. Till S. Chung D. C. Rucker A. L. Orekhov, C. B. Black. Analysis and validation of teleoperated surgical parallel continuum manipulator. *IEEE Robotics and Automation Letters*, 1(2):828–835, 2016.

[8] M. Tavakoli A. Mohammadi and H. J. Marquez. Control of nonlinear bilateral teleoperation systems subject to disturbances. In *Proc. 50th Conf. on Decision and Control*, pages 1765—-1770. IEEE, 2011.

[9] M. Tavakoli A. Mohammadi and H. J. Marquez. Disturbance observer based control of nonlinear haptic teleoperation systems. *IET Control Theory Appl.*, 5(17):2063—-2074, 2011.

[10] G. Murat A. Sherman and F. Tendick. Comparison of teleoperator control architectures for palpation task. In *IMECE Symp. on Haptic Interfaces for Virtual Environment and Teleoperator Systems*, 2000.

[11] J. J. Abbott and A. M. Okamura. Stable forbidden-region virtual fixtures for bilateral telemanipulation. *ASME J. Dynamic Systems, Measurement, and Control*, 128(1):53–64, 2006.

[12] Usman Ahmad and Ya-Jun Pan. A time domain passivity approach for asymmetric multilateral teleoperation system. *IEEE Access*, 6:519–531, 2018.

[13] Abdulrahman Albakri. *Haptic Teleoperation for Robotic-Assisted Surgery*. PhD thesis, Université Montpellier, December 2015.

[14] D. Jolly A.M. Jolly-Desodt and F. Wawak. Conception of a decision support system, and its interface: Application to a teleoperation system. *Acta Polytechnica Hungarica*, 12(2):107–117, 2002.

[15] R. J. Anderson and M. W. Spong. Bilateral control of teleoperators with time delay. *IEEE Transactions on Automatic Control*, 34(5):494–501, 1989.

[16] J. Artigas. Teleoperation for on-orbit servicing missions through the astra geostationary satellite. In *Proc. IEEE Aerospace Conference, Big Sky, MT*, pages 1–12. IEEE, 2016.

[17] Jordi Barrio, Jose Maria Azorin, Rafael Aracil, Manuel Ferre, Jose M. Sabater, and Nicolas M. Garcia. Experimental bilateral control by state convergence. In *2006 IEEE/RSJ International Conference on Intelligent Robots and Systems*, pages 1127–1132. IEEE, 2006.

[18] A. K. Bejczy and M. Handlykken. Generalization of bilateral force-reflecting control of manipulators. In *Proc. CISM-IFTOMM Symp. on Theory and Practice of Rob. and Manip.*, pages 300–312. IEEE, 1981.

[19] M. Bowthorpe and M. Tavakoli. Generalized predictive control of a surgical robot for beating-heart surgery under delayed and slowly-sampled ultrasound image data. *IEEE Robotics and Automation Letters*, 1(2):892–899, 2016.

[20] C. Spiten C. D. Pham and P. J. From. A control allocation approach to haptic control of underwater robots. In *Proc. IEEE International Workshop on Advanced Robotics and its Social Impacts (ARSO), Lyon*, pages 1–6. IEEE, 2015.

[21] C. R. Carignan and P. A. Olsson. Cooperative control of virtual objects over the internet using force-reflecting master arms. In *Proc. IEEE International Conference on Robotics and Automation*, pages 1221–1226. IEEE, 2004.

[22] Linping Chan, Yang Liu, Qingqing Huang, and Ping Wang. Robust adaptive observer-based predictive control for a non-linear delayed bilateral teleoperation system. *IEEE Access*, 10:52294–52305, 2022.

[23] Zheng Chen, Fanghao Huang, Wei Song, and Shiqiang Zhu. A novel wave-variable based time-delay compensated four-channel control design for multi-lateral teleoperation system. *IEEE Access*, 6:25506–25516.

[24] Zheng Chen, Fanghao Huang, Wei Song, and Shiqiang Zhu. A novel wave-variable based time-delay compensated four-channel control design for multi-lateral teleoperation system. *IEEE Access*, 6:25506–25516, 2018.

[25] H. Ching and W.J. Book. Internet-based bilateral teleoperation based on wave variable with adaptive predictor and direct driff control. *Trans. Journal of Dynamic Systems, Measurement and Control*, 128:86–93, 2006.

[26] H. Cho and J. Park. Stable bilateral teleoperation under a time delay using a robust impedance control. *Mechatronics*, 15(5):611—-625, 2005.

[27] Hyeonseok Choi, Ribin Balachandran, and Jee-Hwan Ryu. Chattering-free time domain passivity approach. *IEEE Transactions on Haptics*, 15(3):572–581, 2022.

[28] J.E. Colgate. Robust impedance shaping telemanipulation. *IEEE Tran. Rob. and Auto*, 9(4):374–384, 1993.

[29] L. Cragg and H. Hu. Application of mobile agents to robust teleoperation of internet robots in nuclear decommissioning. In *Proc. Intl. Conf. on Industrial Technology*, pages 1214–1219. IEEE, 2003.

[30] P. Lee S. Hong D. Kwon, J. Ryu. Design of a teleoperation controller for an underwater manipulator. In *Proc. Intl. Conf. on Robotics and Automation*, pages 3114–3119. IEEE, 2000.

[31] F. Zhang H. Du W. Li D. Nig, S. Sun and B. Zhang. Disturbance observer-based takagi-sugeno fuzzy control for an active seat suspension. *Mechanical Systems and Signal Processing*, 93:515–530, 2017.

[32] F. Naghdy D. Sun and H. Du. Enhancing flexibility of the dual-master-dual-slave multilateral teleoperation system. In *Proc. IEEE Conference on Control Applications (CCA)*, pages 300–305. IEEE, 2015.

[33] G. R. Duan and H. H. Yu. *LMIs in Control Systems: Analysis, Design and Applications*. CRC Press, 1 edition, 2013.

[34] O. J. Elle E. Naerum and B. Hannaford. The effect of interaction force estimation on performance in bilateral teleoperation. *IEEE Transactions on Haptics*, 5(2):160–171, 2012.

[35] Z. Chen F. Huang, W. Zhang. Rbfnn-based adaptive sliding mode control design for nonlinear bilateral teleoperation system under time-varying delays. *IEEE Access*, 7:11905–11912, 2019.

[36] Umar Farooq. *State Convergence Based Control of Teleoperation Systems*. PhD thesis, 2017.

[37] Umar Farooq, Jason Gu, Mohamed El-Hawary, Muhammad Usman Asad, and Ghulam Abbas. Fuzzy model based bilateral control design of nonlinear teleoperation system using method of state convergence. *IEEE Access*, 4:4119–4135, 2016.

[38] Umar Farooq, Jason Gu, Mohamed El-Hawary, Muhammad Usman Asad, and Jun Luo. An extended state convergence architecture for multilateral teleoperation systems. *IEEE Access*, 5:2063–2079, 2017.

[39] A. Fattouh and O. Sename. H-infinity-based impedance control of teleoperation systems with time delay. In *Proc. 5th IFAC Workshop on Time Delay Systems*, page 1–5. IEEE, 2003.

[40] H. Flemmer and J. Wikander. Transparency and stability analysis of a surgical teleoperator system. In *11th Symposium on Haptic Interfaces for Virtual Environment and Teleoperator Systems*, pages 382–389. IEEE, 2003.

[41] S. G. Loizou G. C. Karras and K. J. Kyriakopoulos. Semi-autonomous teleoperation of a non-holonomic underwater vehicle using a laser vision system: A visual-servoing switching control approach. In *Proc. 17th Mediterranean Conference on Control and Automation, Thessaloniki*, pages 797–802. IEEE, 2009.

[42] J. J. E. Slotine G. Niemeyer. Stable adaptive teleoperation. *IEEE Journal of Oceanic Engineering*, 16(1):152–162, 1991.

[43] R.C. Goertz and M. W. Thompson. Electronically controlled manipulator nucleonics. 12(11):46–47, 1954.

[44] A. A. Sarhan J. Akbari H. Amini, S. Rezaei and N. Mardi. Transparency improvement by external force estimation in a time-delayed nonlinear bilateral teleoperation system. *J. Dyn. Syst. Meas. Control*, 137(5), 2015.

[45] A. Kheddar H. Arioui and S. Mammar. A predictive wave-based approach for time delayed virtual environments haptics systems. In *Proc Intl. Workshop on Rob and Human Interactive Communication*, pages 134—-139. IEEE, 2002.

[46] T.I. Tsay H. Kazerooni and K. Hollerbach. A controller design framework for telerobotic systems. *IEEE Trans. on Trans. Cont. Sys. Tech*, 1(1):50–62, 1993.

[47] P. Falcon H. Tugal, J. Carrasco and A. Barreiro. Stability analysis of bilateral teleoperation with bounded and monotone environments via zames–falb multipliers. *IEEE Trans. on Control Syst. Technol*, 25(4):1331–1344, 2017.

[48] A. Haddadi and K. Hashtrudi-Zaad. Bounded-impedance absolute stability of bilateral teleoperation control systems. *IEEE Transactions on Haptics*, 3(1):15–27, 2010.

[49] Keyu Wu Hongliang Ren Haibo Yu, Liao Wu. Development of a multi-channel concentric tube robotic system with active vision for transnasal nasopharyngeal carcinoma procedures. *IEEE Robotics and Automation Letters*, 1(2):1172–1178, 2016.

[50] B. Hannaford and R.J. Anderson. Experimental and simulation of hard contact in force reflecting teleoperation. In *Proc. IEEE Int. conf. Rob. and Auto.*, pages 584–589. IEEE, 1988.

[51] Shuang Hao, Lingyan Hu, and Peter X. Liu. Sliding mode control for a surgical teleoperation system via a disturbance observer. *IEEE Access*, 7:43383–43393, 2019.

[52] K. Hashtrudi-Zaad and S. Salcudean. Analysis of control architectures for teleoperation systems with impedance/admittance master and slave manipulators. *The International Journal of Robotics Research*, 20(6):419–2001, 2001.

[53] K. Hashtrudi-Zaad and S. E. Salcudean. Transparency in time-delayed systems and the effect of local force feedback for transparent teleoperation. *IEEE Transactions on Robotics and Automation*, 18(1):108–114, 2002.

[54] K. Hashtrudi-Zaad and S.E. Salcudean. Adaptive transparent impedance reflecting teleoperation. In *Proc. IEEE Int. Conf. Robot. Auto*, pages 1369–1373. IEEE, 1996.

[55] K. Hastrudi-Zaad and S.E. Salcudean. On the use of local force feedback for transparent teleoperation. In *Proc. IEEE Int. Conf. Robot. and Auto.*, volume 3, pages 1863–1869. IEEE, 1999.

[56] Peter F Hokayem and Mark W Spong. Bilateral teleoperation: An historical survey. *Automatica*, 42(12):2035–2057, 2006.

[57] C. Hua and P. Liu. Delay-dependent stability criteria of teleoperation systems with asymmetric time-varying delays. *IEEE Trans. Robot*, 26(5):925–932, 2010.

[58] J. Huang and F. Lewis. Neural-network predictive control for nonlinear dynamic systems with time-delay. *IEEE Trans. on Neural Networks*, 14(2):377–389, 2003.

[59] M. Franken M. Steinbuch I. Font, S. Weiland and L. Rovers. Haptic feedback designs in teleoperation systems for minimal invasive surgery. In *Proc. IEEE*

International Conference on Systems, Man and Cybernetics, pages 2513–2518. IEEE, 2004.

[60] C. M. Pugh F. A. M-Ivaldi A. Karniel I. Nisky, A. Pressman. Perception and action in teleoperated needle insertion. *IEEE Transactions on Haptics*, 4(3):155–166, 2011.

[61] G. Hirzinger J. Artigas. A brief history of dlr's space telerobotics and force feedback teleoperation. *Acta Polytechnica Hungarica*, 13(1):239–249, 2016.

[62] H. B. Gilbert P. J. Swaney P. T. Russell K. D. Weaver R. J. Webster J. Burgner, D. C. Rucker. A telerobotic system for transnasal surgery. *IEEE/ASME Transactions on Mechatronics*, 19(3):996–1006, 2014.

[63] R. Aracil J. C. Tafur, C. García and R. Saltaren. Control of a teleoperation system by state convergence with variable time delay. In *Proc. 9th France-Japan 7th Europe-Asia Congress on and Research and Education in Mechatronics*, pages 40–47. IEEE, 2012.

[64] R. Aracil J. C. Tafur, C. García and R. Saltaren. Stability analysis of teleoperation system by state convergence with variable time delay. In *Proc. American Control Conference*, pages 5696–5701. IEEE, 2013.

[65] R. Aracil R. Saltaren J. C. Tafur, C. Garcia. Control of nonlinear teleoperation system by state convergence. In *Proc. IEEE International Conference on Control and Automation*, pages 489–494. IEEE, 2011.

[66] C. Liu J. Guo and P. Poignet. Enhanced position-force tracking of time-delayed teleoperation for robotic-assisted surgery. In *Proc. 37th Annual International Conference of the IEEE Engineering in Medicine and Biology Society (EMBC), Milan*, pages 4894–4897. IEEE, 2015.

[67] A. Rubio J. J. Gil, A. Avello and J. Florez. Stability analysis of a 1 dof haptic interface using the routh-hurwitz criterion. *IEEE Trans. on Cont. Sys. Tech*, 12(4):583–588, 2004.

[68] C. Perez N. M. Garcia J. M. Sabater J. M. Azorin, R. Aracil. "bilateral control architecture for telerobotics systems in unknown environments. In *Proc. Euro Haptics*, pages 13–22. IEEE, 2008.

[69] E. Ianez J. M. Azorin, J. A Berna. Nonlinear bilateral control of teleoperators by state convergence. In *Proc. European Control Conference (ECC), Budapest*, pages 2815–2820. IEEE, 2009.

[70] E. Iazez J. M. Azorin, J. A. Berna. Nonlinear bilateral control of teleoperators by state convergence. In *Proc. European Control Conference*, pages 2815–2820. IEEE, 2009.

[71] N. M. Garcia C. Perez J. M. Azorin, R. Aracil. Bilateral control of teleoperation systems through state convergence. In *Advances in Telerobotics*, volume 31, pages 271–288. Springer, Berlin, Heidelberg, 2007.

[72] R. Aracil M. Ferre J. M. Azorin, O. Reinoso. Control of teleoperators with communication time delay through state convergence. *Journal of Robotic Systems*, 21(4):167–182, 2004.

[73] R. Aracil M. Ferre J. M. Azorin, O. Reinoso. Generalized control method by state convergence for teleoperation systems with time delay. *Automatica*, 40(9):1575–1582, 2004.

[74] J. Yang J. Su, HW Chen. On relationship between time-domain and frequency-domain disturbance observers and its applications. *J Dyn Syst Measure Control*, 138(9), 2016.

[75] WH Chen J. Su. On relationship between time-domain and frequency-domain disturbance observers and its applications. *Automatica*, 93:550–553, 2018.

[76] P. Jia Z. Wang J. Yao, L. Wang. Development of a 7-function hydraulic underwater manipulator system. In *Proc. Intl. Conf. on Mechatronics and Automation*, pages 1202–1206. IEEE, 2009.

[77] M. A. Jordan and J. L. Bustamante. Guidance of underwater vehicles with cable tug perturbations under fixed and adaptive control systems. *IEEE Journal of Oceanic Engineering*, 33(4):579–598, 2008.

[78] J.Yan and S.E. Salcudean. Teleoperation controller design using h-infinity optimization with application to motion-scaling. *IEEE Trans. on cont. syst. tech.*, 4(3):244—-258, 1996.

[79] N. Pernalete K. A. Manocha and R. V. Dubey. Variable position mapping based assistance in teleoperation for nuclear cleanup. In *Proc. Intl. Conf. on Robotics and Automation*, pages 374–379. IEEE, 2001.

[80] R. D. Ellis K. Chintamani, A. Cao and A. K. Pandya. Improved telemanipulator navigation during display-control misalignments using augmented reality cuess. *IEEE Trans. Syst. Man Cybern*, 40:29–39, 2009.

[81] K. Ohnishi A. Hace K. Natori, T. Tsuji and K. Jezernik. Time-delay compensation by communication disturbance observer for bilateral teleoperation under time-varying delay. *IEEE Trans. Ind. Electron.*, 57(3):1050—-1062, 2010.

[82] Takahiro Kanno and Yasuyoshi Yokokohji. Multilateral teleoperation control over time-delayed computer networks using wave variables. In *Proc. IEEE Haptics Symposium*, pages 125–131. IEEE, 2012.

[83] Seiichiro Katsura, Toshiyuki Suzuyama, and Kiyoshi Ohishi. A realization of multilateral force feedback control for cooperative motion. *IEEE Transactions on Industrial Electronics*, 54(6):3298–3306, 2007.

[84] Yasunori Kawai, Taiga Takagi, and Takanori Miyoshi. Written communication system based on multilateral teleoperation using time-domain passivity control. In *2019 2nd International Conference on Communication Engineering and Technology (ICCET)*, pages 39–42. IEEE, 2019.

[85] Behzad Khademian and Keyvan Hashtrudi-Zaad. A four-channel multilateral shared control architecture for dual-user teleoperation systems. In *2007 IEEE/RSJ International Conference on Intelligent Robots and Systems*, pages 2660–2666.

[86] P. K. S. Tam L. K. Wong, F. H. F. Leung. Design of fuzzy logic controllers for takagi-sugeno fuzzy model based system with guaranteed performance. *International Journal of Approximate Reasoning*, 30:41–5, 2002.

[87] Y. Zhang L. Liu, G. Liu and D. Wang. A modified motion mapping method for haptic device-based space teleoperation. In *Proc. IEEE International Symposium on Robot and Human Interactive Communication, Edinburgh*, pages 449–453. IEEE, 2014.

[88] D. A. Lawrence. Stability and transparency in bilateral teleoperation. *IEEE Trans. on Robotics and Automation*, 9(5):624–637, 1993.

[89] D. Lee and M.W. Spong. Passive bilateral teleoperation with constant time delay. *IEEE Transactions on Robotics*, 22(2):269–281, 2006.

[90] V. Parra-Vega L.G. Garcia-Valdovinos and M.A. Arteaga. Higher-order sliding mode impedance bilateral teleoperation with robust state estimation under constant unknown time delay. In *Proc. IEEE/ASME Intl. Conf. on Advanced Inteli. Mechatr.*, pages 1293—1298. IEEE, 2005.

[91] V. Parra-Vega L.G. Garcia-Valdovinos and M.A. Arteaga. Observer-based higherorder sliding mode impedance control of bilateral teleoperation under constant unknown time delay. In *Proc. IEEE/RSJ Intl. Conf. on Intel. Rob. and Syst.*, pages 1692—1699. IEEE, 2006.

[92] V. Parra-Vega L.G. Garcia-Valdovinos and M.A. Arteaga. observer-based sliding mode impedance control of bilateral teleoperation under constant unknown time delay. *Robotics and Autonomous Systems*, 55(8):609–617, 2007.

[93] H. Li and K. Kawashima. Bilateral teleoperation with delayed force feedback using time domain passivity controller. *Robotics and Computer-Integrated Manufacturing*, 37:188–196, 2016.

[94] Wei Xiaoqian Zheng-Wenfeng Yang Bo Liu, Shan. A four-channel time domain passivity approach for bilateral teleoperator. In *2018 IEEE International Conference on Mechatronics and Automation (ICMA)*, pages 318–322.

[95] Yu Liu, Chuanzhi Zang, Yuqi Liu, and Peng Zeng. Model predictive control for nonlinear bilateral teleoperation systems with time delay. In *2022 41st Chinese Control Conference (CCC)*, pages 2651–2657. IEEE, 2022.

[96] L.J. Love and W.J. Book. force reflecting teleoperation with adaptive impedance control. *IEEE Transactions on systems, man, and cybernetics Part B: cybernetics*, 34(1):159–165, 2004.

[97] M. Ferre C. Garcia M. A. Artigas, R. Aracil. Bilateral adaptive control by state convergence in teleoperation systems. In *Proc. IEEE International Conference on Control Applications*, pages 548–553. IEEE, 2009.

[98] A. Á. García M. Bowthorpe and M. Tavakoli. Gpc-based teleoperation for delay compensation and disturbance rejection in image-guided beating-heart surgery. In *Proc. IEEE International Conference on Robotics and Automation (ICRA), Hong Kong*, pages 4875–4880. IEEE, 2014.

[99] H. Melouah M. Guiatni, A. Kheddar. Sliding mode bilateral control and four channels scheme control of a force reflecting master/slave teleoperator. In *IEEE International Conference Mechatronics and Automation*, volume 3, pages 1660–1665. IEEE, 2005.

[100] P. Pitakwatchara M. Mitsuishi, N. Sugita. Force-feedback augmentation modes in laparoscopic minimally invasive telesurgical system. *IEEE/ASME Transactions on Mechatronics*, 12(4):447–454, 2007.

[101] A. Tobergte P. Kotyczka C. Preusche A. Albu-Schaeffer M. Panzirsch, J. Artigas and G. Hirzinger. A peer-to-peer trilateral passivity controller for delayed collaborative teleoperation. In *Proc. EuroHaptics, Part I, LNCS 7282*, pages 395–406. IEEE, 2012.

[102] T. Jimenez M. Sanchez M. Serna, L. G. Valdovinos. Bilateral teleoperation of a commercial small-sized underwater vehicle for academic purposes. In *Proc. MTS/IEEE Oceans*, pages 1–5. IEEE, 2015.

[103] R. V. Patel M. Tavakoli, A. Aziminejad and M. Moallem. Enhanced transparency in haptics-based master-slave systems. In *Proc. American Control Conference*. IEEE, 2007.

[104] J. Gu G. Abbas R. Liu M. U.Asad, U. Farooq and V. E. Balas. A composite state convergence scheme for bilateral teleoperation systems. *IEEE/CAA J. Autom. Sinica*, 6(5):1166–1178, 2019.

[105] T. Hirabayashi M. Utsumi and M. Yoshie. Development for teleoperation underwater grasping system in unclear environment. In *Proc. International Symposium on Underwater Technology*, pages 349–353. IEEE, 2002.

[106] A. Fleischner M. Wilde, Z. K. Chua. Effects of multivantage point systems on the teleopertion of spacecraft docking. *IEEE Transactions on Human-Machine Systems*, 44(2):200–210, 2014.

[107] Y. Matsumoto, S. Katsura, and K. Ohnishi. An analysis and design of bilateral control based on disturbance observer. In *IEEE Intl. Conf. on Industrial Technology, 2003*, volume 2, pages 802–807 Vol.2. IEEE, 2003.

[108] Sarmad Mehrdad, Fei Liu, Minh Tu Pham, Arnaud Lelevé, and S. Farokh Atashzar. Review of advanced medical telerobots. *Applied Sciences*, 11(1):1–48, 2021.

[109] Alireza Mohammadi. *Disturbance Observer Design for Robotic and Telerobotic Systems*. PhD thesis, 09 2011.

[110] U Farooq V. E. Balas Z. Chen C. Chang A. Hanif M.U. Asad, J. Gu. A composite state convergence scheme for multilateral teleoperation systems. *Studies in Informatics and Control*, 30(2):33–42, 2002.

[111] S. Munir and W.J. Book. Wave-based teleoperation with prediction. In *Proc American Control Conf.*, volume 6, pages 4605–4611 vol.6. IEEE, 2001.

[112] S. Munir and W.J. Book. Internet-based teleoperation using wave variables with prediction. *IEEE/ASME Transactions on Mechatronics*, 7(2):124–133, 2002.

[113] R. Muradore and P. Fiorini. A review of bilateral teleoperation algorithms. *Acta Polytechnica Hungarica*, 13(1):191–208, 2016.

[114] K. Natori N. Iiyama and K. Ohnishi. Bilateral teleoperation under time-varying communication time delay considering contact with environment. *Electronics and Communications in Japan*, 92(7):38–46, 2009.

[115] M. Xia V. Gupta N. Kottenstette, M. J. McCourt and P. J. Antsaklis. On relationships among passivity, positive realness, and dissipativity in linear systems. *Automatica*, 50(4):1003–1016, 2014.

[116] A. K. Pandya N. P. Lucas and R. D. Ellis. Review of multi-robot taxonomy, trends, and applications for defense and space. *Unmanned Systems Technology XIV, SPIE Defense, Security, and Sensing*, 8387, 2012.

[117] E. Naerum and B. Hannaford. Global transparency analysis of the lawrence teleoperator architecture. In *Proc. IEEE Int. Conf. Robot. Auto*, pages 4344–4349. IEEE, 2009.

[118] L. Ni and D. W. L. Wang. A gain-switching control scheme for position-error-based bilateral teleoperation: Contact stability analysis and controller design. *International Journal of Robotics Research,*, 23(3):255–274, 2004.

[119] G. Niemeyer and J.-J. E. Slotine. Towards force-reflecting teleoperation over the internet. In *Proc. Int. Conf. Robot. Auto.* IEEE, 1998.

[120] NSHA. Robot-assisted surgery at the qeii nova scotia: Medtronic surgical robot for spinal surgeries, August 2022.

[121] J. Barrio M. Ferre R. Aracil P. G-Borras, P. G-Robledo. Technofusion remote handling laboratory: contributions to nuclear fusion facilities maintenance tasks. In *Proc. Intl. Conf. on Applied Robotics for the Power Industry*, pages 1–6. IEEE, 2010.

[122] V. Gupta M. J. McCourt Y. Wang P. Wu M. Xia H. Yu P. J. Antsaklis, B. Goodwine and F. Zhu. Control of cyber-physical systems using passivity and dissipativity-based methods. *European J. of Control*, 19(5):379–388, 2013.

[123] D. Mikolajewski L. Apiecionek D. Sl zak P. Prokopowicz, J. Czerniak. Theory and applications of ordered fuzzy numbers: A tribute to professor witold kosinski. In *Proc. Springer Nature*. Springer, 2017.

[124] J.H. Park and H.C. Cho. Sliding-mode-based impedance controller for bilateral teleoperation under varying time-delay. In *Proc. IEEE/RSJ Intl. Conf. Rob. and Auto.*, page 1025–1030. IEEE, 2001.

[125] Nicola Piccinelli and Riccardo Muradore. A passivity-based bilateral teleoperation architecture using distributed nonlinear model predictive control. In *2020 IEEE/RSJ International Conference on Intelligent Robots and Systems (IROS)*, pages 11466–11472. IEEE, 2020.

[126] H. Van Quang and J. H. Ryu. Stable multilateral teleoperation with time domain passivity approach. In *Proc. IEEE/RSJ International Conference on Intelligent Robots and Systems*, pages 5890–5895. IEEE, 2013.

[127] J. Zhao R. Hao, J. Wang and S. Wang. Observer-based robust control of 6-dof parallel electrical manipulator with fast friction estimation. *IEEE Trans. Autom. Sci. Eng.*, 13(3):1399–1408, 2016.

[128] K. Natori K. Ohnishi R. Kubo, N. Iiyama and H. Furukawa. Performance analysis of a three-channel control architecture for bilateral teleoperation with time delay. *IEEE Transactions on Industry Applications*, 127(12):1224–1230, 2007.

[129] W. Gu R. Wang, C. Xia and K. Li. Fuzzy singularly perturbed model and stability analysis of bilateral teleoperation system. *30th Chinese Control Conference*, pages 3664–3668, 2011.

[130] J. Rebelo and A. Schiele. Time domain passivity controller for 4-channel time delay bilateral teleoperation. *IEEE Transactions on Haptics*, 8(1):79–89, 2015.

[131] B. Rosa. Intuitive teleoperation of active catheters for endovascular surgery. In *Proc. IEEE/RSJ International Conference on Intelligent Robots and Systems (IROS), Hamburg*, pages 2617–2624. IEEE, 2015.

[132] Jee-Hwan Ryu, Jordi Artigas, and Carsten Preusche. A passive bilateral control scheme for a teleoperator with time-varying communication delay. *Mechatronics*, 20(7):812–823, 2010. Special Issue on Design and Control Methodologies in Telerobotics.

[133] Jee-Hwan Ryu, Quang Ha-Van, and Aghil Jafari. Multilateral teleoperation over communication time delay using the time-domain passivity approach. *IEEE Transactions on Control Systems Technology*, 28(6):2705–2712, 2020.

[134] D. Stipanovic S. Deka and T. Kesavadas. Stable bilateral teleoperation with bounded control. *IEEE Trans. Control Syst. Technol*, 27(6):2351–2360, 2019.

[135] W.-H. Zhu S. E. Salcudean, M. Zhu and K. Hashtrudi-Zaad. Transparent bilateral teleoperation under position and rate control. *Int. J. Robot. Res*, 19:1185–1202, 2000.

[136] A.K. Pandya S. Eslamian, L. A. Reisner. Development and evaluation of an autonomous camera control algorithm on the da vinci surgical system. *Int J Med Robot*, 16(2):29–39, 2020.

[137] H. Momeni S. Ganjefar and F. Janabi-Sharifi. Teleoperation systems design using augmented wave-variables and smith predictor method for reducing time-delay effect. In *Proc Symposium on Intelligent Control*, pages 333—-338. IEEE, 2002.

[138] A. E. Saddik S. Islam, P. X. Liu and Y. B. Yang. Bilateral control of teleoperation systems with time delay. *IEEE/ASME Trans. Mechatronics*, 20(1):155–159, 2015.

[139] B. J. Buckham S. Soylu, F. Firmani and R. P. Podhorodeski. Comprehensive underwater vehicle-manipulator system teleoperation. In *Proc. MTS/IEEE OCEANS, Seattle, WA*, pages 1–8. IEEE, 2010.

[140] K. Natori S. Susa and K. Ohnishi. Three-channel micro-macro bilateral control system with scaling of control gains. In *Proc. IEEE Int. Conf. Indus. Electr.*, pages 2598–2603. IEEE, 2008.

[141] Y. Jia S. Wang, B. Xu and Y. Liu. Real-time mobile robot teleoperation over ip networks based on predictive control. pages 2091—-2096. IEEE, 2007.

[142] S. Tafazoli S.P. DiMaio S.E. Salcudean, K. Hashtrudi-Zaad and C. Reboulet. Bilateral matched impedance teleoperation with application to excavator control. control systems. *IEEE*, 1999:29–37, 2004.

[143] O. Sename. H-infinity control of a teleoperation drive-by-wire system with communication time-delay. In *Proc. Conf. on Control and Automation*. IEEE, 2006.

[144] J. Sheng and M.W. Spong. Model predictive control for bilateral teleoperation systems with time delays. In *Canadian Conference on Electrical and Computer Engineering 2004 (IEEE Cat. No.04CH37513)*, volume 4, pages 1877–1880 Vol.4. IEEE, 2004.

[145] A.C. Smith and K. Hashtrudi-Zaad. Smith predictor type control architectures for time delayed teleoperation. *The International Journal of Robotics Research*, 25(8):797–818, 2006.

[146] C. Smith and H. Christensen. A minimum jerk predictor for teleoperation with variable time delay. In *Proc IEEE/RSJ Intl. Inteli. Rob. and Syst.*, pages 5621—-5627. IEEE, 2009.

[147] S. S.N.F. Nahri, S. Du and B.J. Van Wyk. A review on haptic bilateral teleoperation systems. *J Intell Robot Syst*, 104(13), 2022.

[148] Da Sun, Qianfang Liao, Xiaoyi Gu, Changsheng Li, and Hongliang Ren. Multilateral teleoperation with new cooperative structure based on reconfigurable robots and type-2 fuzzy logic. *IEEE Transactions on Cybernetics*, 49(8):2845–2859, 2019.

[149] Da Sun, Fazel Naghdy, and Haiping Du. Wave-variable-based passivity control of four-channel nonlinear bilateral teleoperation system under time delays. *IEEE/ASME Transactions on Mechatronics*, 21(1):238–253, 2016.

[150] Da Sun, Fazel Naghdy, and Haiping Du. Neural network-based passivity control of teleoperation system under time-varying delays. *IEEE Transactions on Cybernetics*, 47(7):1666–1680, 2017.

[151] T. Doi M. Oda T. Yoshikawa T. Imaida, Y. Yokokohji. Ground-space bilateral teleoperation of ets-vii robot arm by direct bilateral coupling under 7-s time delay condition. *IEEE Transactions on Robotics and Automation*, 20(3):499–511, 2004.

[152] X. X. Huang T. J. Hu and Q. Tan. Active disturbance rejection controller for space teleoperation. In *Proc. International Conference on Automatic Control and Artificial Intelligence (ACAI 2012), Xiamen*, pages 334–337. IEEE, 2012.

[153] Huang Fanghao Chen Zheng Wang Tao Gu Jason Zhu Shiqiang Tang, Jianzhong. Disturbance-observer-based sliding mode control design for nonlinear bilateral teleoperation system with four-channel architecture. *IEEE Access*, PP:1–1, 05 2019.

[154] Jianzhong Tang, Fanghao Huang, Zheng Chen, Tao Wang, Jason Gu, and Shiqiang Zhu. Disturbance-observer-based sliding mode control design for nonlinear bilateral teleoperation system with four-channel architecture. *IEEE Access*, 7:72672–72683, 2019.

[155] Yuan Tangqing, Zheng Min, and Zhang Ke. Control of multilateral teleoperation system based on the generalized wave variables. In *37th Chinese Control Conference (CCC)*, pages 132–136. IEEE, 2018.

[156] L.Kovacs andZ.Benyo T.Haidegger, B.Benyo. Force sensing and force control for surgical robots. In *IFAC Proceeding*, volume 42, pages 401–406. IFAC, 2009.

[157] U. Tumerdem. Three-channel control architecture for multilateral teleoperation under time delay. *Turkish Journal of Electrical Engineering Computer Sciences*, 27(1):120–138, 2019.

[158] Uğur Tümerdem. A study on the l2 stability and transparency of three channel control architectures in bilateral teleoperation under time delays. *International Journal of Advances in Engineering and Pure Sciences*, 33(3):455–466, 2021.

[159] M. El-Hawary M. U. Asad U. Farooq, J. Gu and J. Luo. An extended state convergence architecture for multilateral teleoperation systems. *IEEE Access*, 5:2063–2079, 2017.

[160] M. El-Hawary M. U. Asad G. Abbas U. Farooq, J. Gu. Fuzzy model based bilateral control design of nonlinear tele-operation system using method of state convergence. *IEEE Access*, 4:4119–4135, 2016.

[161] M. El-Hawary V.E. Balas M.U. Asad U. Farooq, J. Gu and G. Abbas. Fuzzy model-based design of a transparent controller for a time delayed bilateral teleoperation system through state convergence. *Acta Polytechnica Hungarica*, 14(8):7–26, 2017.

[162] H. Kawabe M. Kinami Y. Tsumaki M. Uchiyama M. Oda T. Doi W. K. Yoon, T. Goshozono. Model-based space robot teleoperation of ets-vii manipulator. *IEEE Transactions on Robotics and Automation*, 20(3):602–612, 2004.

[163] J. Zhang W. Liu and L. Gao. Fuzzy impedance and sliding mode bilateral control in underwater ratio teleoperation based on observer. In *Proc. OCEANS, Shanghai*, pages 1–7. IEEE, 2016.

[164] G. Wenjin L. Kehua W. Ruiqi, X. Changjun. Fuzzy singularly perturbed model and stability analysis of bilateral teleoperation system. In *Proc. Chinese Control Conference*, pages 3664–3668. IEEE, 2011.

[165] Gao Zhitao Peng Fangyu Chen Chen Tang Xiaowei Wang, Kunyu and Zhiwei Liu. Four-channel sliding mode control for haptic teleoperation system with disturbance in contact with adaptive stiffness environments. In *2022 41st Chinese Control Conference (CCC)*, pages 3852–3857.

[166] Ting Wang, Zhenxing Sun, Aiguo Song, Pengwen Xiong, and Peter X. Liu. Sliding mode impedance control for dual hand master single slave teleoperation systems. *IEEE Transactions on Intelligent Transportation Systems*, 23(12):25500–25508, 2022.

[167] Yuji Wang, Fuchun Sun, Huaping Liu, and Zidi Li. Passive four-channel multilateral shared control architecture in teleoperation. In *9th IEEE Intl. Conf. on Cognitive Informatics (ICCI'10)*, pages 851–858. IEEE, 2010.

[168] W.J. Wilson X. Liu and X. Fan. Pose reflecting teleoperation using wave variables with wave prediction. In *Proc IEEE Intl. Mechatronics Automation*, pages 1642—-1647. IEEE, 2005.

[169] J. Yan X. P. Guan X. Yang, C. C. Hua. A new master-slave torque design for teleoperation system by t-s fuzzy approach. *IEEE Transactions on Control Systems Technology*, 23(4):1611–1619, 2015.

[170] Xiao Xu, Sili Chen, and Eckehard Steinbach. Model-mediated teleoperation for movable objects: Dynamics modeling and packet rate reduction. page 1–6. IEEE Press, 2015.

[171] Xiao Xu, Burak Cizmeci, Clemens Schuwerk, and Eckehard Steinbach. Model-mediated teleoperation: Toward stable and transparent teleoperation systems. *IEEE Access*, 4:425–449, 2016.

[172] M. Meng Y. Pan, J. Gu and J. Jayachandran. Bilateral teleoperation of robotic systems with predictive control. In *IEEE International Conference on Robotics and Automation*, pages 1651–1656. IEEE, 2007.

[173] A. A. Goldenberg Y. Strassberg and J. K. Mills. A new control scheme for bilateral teleoperating systems: Lyapunov stability analysis. In *Proc. Int. Conf. Robot. Auto*, pages 837–838. IEEE, 1992.

[174] A.A. Goldenberg Y. Strassberg and J.K. Mills. Stability analysis of a bilateral teleoperation system. *Trans. AME Jour. Dyn. Sys. Meas. and Cont.*, 115:419–425, 1993.

[175] H. Changchun Y. Yana and G. Xinping. Adaptive prescribed performance control for nonlinear networked teleoperation system under time delay. In *Proc. 33rd Chinese Control Conference*, pages 5608–5613. IEEE, 2014.

[176] Y. Wang Y. Yuan and L. Guo. Force reflecting control for bilateral teleoperation system under time-varying delays. *IEEE Trans. Ind. Informat*, 15(2):1162–1172, 2019.

[177] Yongqiang Ye, Ya-Jun Pan, and Trent Hilliard. Bilateral teleoperation with time-varying delay: A communication channel passification approach. *IEEE/ASME Transactions on Mechatronics*, 18(4):1431–1434, 2013.

[178] C. Canudas de Wite Y.J. Pan and O. Sename. A new predictive approach for bilateral teleoperation with applications to drive-by-wire systems. *IEEE Transactions on robotics*, 22(6):1146–1162, 2006.

[179] D. Yoerger and J. J. Slotine. Supervisory control architecture for underwater teleoperation. In *Proc. IEEE International Conference on Robotics and Automation*, pages 2068–2073. IEEE, 1987.

[180] K. Yoshida and T. Namerikawa. Stability and tracking properties in predictive control with adaptation for bilateral teleoperation. In *Proc American Control Conference*, page 1323–1328. IEEE, 2009.

[181] Laihong Hu Zidi Li Yuji Wang, Fuchun Sun and Huaping Liu. Space teleoperation with large time delay based on vision feedback and virtual reality. In *Proc. IEEE/ASME International Conference on Advanced Intelligent Mechatronics, Singapore*, pages 1200–1205. IEEE, 2009.

[182] Q. Tan Z. Shi, X. Huang and T. Hu. Fractional-order pid control method for space teleoperation. In *Proc. IEEE International Conference on Multimedia Big Data, Beijing*, pages 216–219. IEEE, 2015.

[183] D. Zhai and Y. Xia. A novel switching-based control framework for improved task performance in teleoperation system with asymmetric time-varying delays. *IEEE Trans. Cybern*, 48(2):625–638, 2018.

[184] Di-Hua Zhai and Yuanqing Xia. Adaptive fuzzy control of multilateral asymmetric teleoperation for coordinated multiple mobile manipulators. *IEEE Transactions on Fuzzy Systems*, 24(1):57–70, 2016.

[185] J. Zhang. Development of a virtual platform for telepresence control of an underwater manipulator mounted on a submersible vehicle. *IEEE Transactions on Industrial Electronics*, 64(2):1716–1727, 2017.

[186] Jinhui Zhang, Xinwei Liu, Yuanqing Xia, Zhiqiang Zuo, and Yijing Wang. Disturbance observer-based integral sliding-mode control for systems with mismatched disturbances. *IEEE Transactions on Industrial Electronics*, 63(11):7040–7048, 2016.

[187] Zhenhua Zhao, Jun Yang, Shihua Li, and Wen-Hua Chen. Composite nonlinear bilateral control for teleoperation systems with external disturbances. *IEEE/CAA Journal of Automatica Sinica*, 6(5):1220–1229, 2019.

[188] Jiayi Zhu and Wail Gueaieb. Adaptive fuzzy logic control for time-delayed bilateral teleoperation. In *Autonomous and Intelligent Systems*, pages 106–115. Springer Berlin Heidelberg, 2012.

[189] W-H. Zhu and S.E. Salcudean. Stability analysis of a bilateral teleoperation system. In *Proc. Proc. IEEE Int. conf. Rob. and Auto.*, pages 231–237. IEEE, 1999.